7 nicotinic acetylcholine receptors at the glutamatergic synapse

Hammond, Victoria

Award date:
2014

Awarding institution:
University of Bath

α7 nicotinic acetylcholine receptors at the glutamatergic synapse

Victoria J. Hammond

Thesis submitted for the degree of Doctor of Philosophy

University of Bath

Department of Biology and Biochemistry

August 2014

Signed on behalf of the Faculty of Science: ……

Dated: ……

Abstract

Nicotinic acetylcholine receptor (nAChR) activation is neuroprotective and nicotine is a cognitive enhancer. Loss of nAChRs, deposition of tau neurofibrillary tangles, cleavage of amyloid precursor protein (APP) and inflammation are well documented in the pathogenesis of Alzheimer's disease (AD). Sequential cleavage of APP by β- and γ-secretase enzymes generates soluble Aβ peptides, with oligomeric forms of Aβ implicated in both the control of synaptic excitability and dysregulation of synaptic transmission and induction of neuronal death in AD. Aβ production is inhibited by calcium-dependent recruitment of α-secretase, as exemplified by activation of N-methyl-D-aspartate receptors (NMDAR). All neurodegenerative diseases are associated with inflammation, arising from altered homeostasis of the innate immune system, resulting in heightened activation of immune cells and induction of a pro-inflammatory environment. Stimulation of the α7 subtype of nAChR is anti-inflammatory and also enhances cognition and promotes neuronal survival. This work addressed the hypotheses that stimulation of highly calcium-permeable α7nAChR inhibits Aβ production by promoting α-secretase-mediated processing of APP and also modulates inflammatory cellular behaviour of microglia. Thus, this study assessed the role of α7nAChR at glutamatergic synapses, through probing effects on APP processing and phagocytosis in primary cortical neurons and microglia, respectively. Primary cortical neurons expressed functional α7nAChR and glutamate receptors, and through a number of experimental approaches, including immunoblotting and a cleavage reporter assay, results indicated α7nAChR activation with the α7nAChR-selective agonist PNU-282987 and positive allosteric modulator PNU-120596 had no effect on APP and Tau, in contrast to NMDAR activation that significantly modulated these proteins. Data suggest low expression of α7nAChR, coupled with distinct localisation of presynaptic α7nAChR and postsynaptic APP could explain the lack of effect. In addition, primary microglia were highly responsive to lipopolysaccharide and possessed functional α7nAChR that coupled to ERK phosphorylation. Microglial α7nAChR activation promoted neuroprotective phagocytic behaviour, in agreement with the 'cholinergic anti-inflammatory pathway'. This study supports the hypothesis that α7nAChR are modulators of anti-inflammatory behaviour, thus α7nAChR-selective ligands are viable candidates for the treatment of AD and promoting cognitive enhancement.

Table of Contents

Abstract **2**

List of Figures **7**

List of Tables **8**

List of Abbreviations **9**

Acknowledgements **12**

1. Introduction **14**

1.1 Cholinergic signalling within the central nervous system **14**

1.2 Nicotinic acetylcholine receptors **14**

1.3 nAChR function **16**

1.4 nAChR diversity **18**

1.4.1 Neuronal nAChR subtypes 19

1.4.2 The α7 subtype of nAChR 21

1.4.2.1 α7nAChR expression and distribution 22

1.4.2.2 Expression of α7nAChR within CNS cell types 23

1.4.2.3 α7nAChR physiological functions 23

1.5 nAChR pharmacology **29**

1.5.1 Modulators of nAChR and effects on cognitive function 33

1.5.1.1 α7nAChR-selective agonists 35

1.5.1.2 α7nAChR-selective PAMs 35

1.6 The cholinergic hypothesis of Alzheimer's disease **35**

1.6.1 Alzheimer's disease and age-related cognitive decline 36

1.7 Amyloid cascade hypothesis **37**

1.8 Amyloid precursor protein **40**

1.8.1 Physiological functions of APP 40

1.8.2 APP processing 41

1.8.2.1 Regulation of APP processing by secretases 42

1.8.2.2 Activity-dependent regulation of APP processing 46

1.9 Targeting α7nAChR in Alzheimer's disease **54**

1.9.1 AChE inhibitors 55

1.10 Hypotheses and aims **56**

2.1 Materials 58

2.2 Methods 63

2.2.1 Primary cortical neuron cell culture 63

2.2.2 Primary cortical glial cell culture 63

2.2.3 Primary microglia purification 64

2.2.4 Immunocytochemistry 64

2.2.4.1 Immunocytochemistry staining 64

2.2.4.2 Image acquisition 65

2.2.5 Fluorescent labelling of α7nAChR 65

2.2.6 Intracellular calcium microfluorimetry imaging 65

2.2.7 SDS-PAGE and Western blotting 66

2.2.7.1 Sample preparation for SDS-PAGE 66

2.2.7.2 Tris-Glycine SDS-PAGE 66

2.2.7.3 Western blotting 67

2.2.7.4 Protein detection 67

2.2.7.5 Analysis of protein densitometry 67

2.2.8 APP C-terminal fragment Western blotting 68

2.2.8.1 APP-CTF sample preparation 68

2.2.8.2 Tris-Tricine SDS-PAGE 68

2.2.8.3 Western blotting for APP-CTFs 68

2.2.9 Synaptosome preparation and treatment 69

2.2.9.1 Tissue preparation 69

2.2.9.2 Percoll gradient preparation 69

2.2.9.3 Synaptosome preparation and purification 70

2.2.9.4 Synaptosome drug treatments 70

2.2.10 APP-Gal4 cleavage luciferase reporter assay 71

2.2.11 Egr-1 transcription luciferase reporter assay 71

2.2.12 Microglial bead uptake assay 72

2.2.13 Statistical analyses 72

3.1 Introduction 74

3.2 Results 76

3.2.1 Primary cortical cultures display a neuronal phenotype and express neuron-specific proteins 76

3.2.2 Primary cortical neurons express postsynaptic AMPAR that couple to calcium influx 76
3.2.3 Neuronal AMPAR are functional and couple to ERK phosphorylation 79
3.2.4 Neuronal NMDAR couple to cellular activation and ERK phosphorylation 81
3.2.5 Primary cortical neurons express calcium-permeable α7 nicotinic acetylcholine receptors 85
3.2.6 Neuronal nAChR couple to ERK phosphorylation 86
3.2.7 α7nAChR-activation has no effect on Egr-1 promoter-driven luciferase expression..... 91
3.3 Discussion 93
3.3.1 Primary cortical neurons express functional glutamate receptors... 93
3.3.2 Primary cortical neurons express functional calcium-permeable α7nAChR..... 94
3.3.3 Primary cortical neuronal α7nAChR couple to ERK phosphorylation without effecting ERK-dependent transcription 94
3.3.3 Summary 96
4.1 Introduction 98
4.2 Results 100
4.2.1 APP is predominantly expressed at postsynaptic sites in primary cortical neurons 100
4.2.2. Primary cortical neurons express putative α-secretase enzymes, ADAM-10 and ADAM-17 100
4.2.3 NMDAR activation reduces levels of full-length APP 103
4.2.4 α7nAChR activation has no effect on full-length APP levels 103
4.2.5 Isolation and activation of presynaptic α7nAChR has no effect on full-length APP levels..... 106
4.2.6 α7nAChR activation has no effect on APP-CTF production..... 109
4.2.7 α7nAChR activation has no effect on β-/γ-secretase activity 113
4.2.8 α7AChR stimulation does not modulate full length Tau..... 115
4.3 Discussion 118
4.3.1 α7nAChR activation does not modulate APP processing 118

4.3.2 NMDAR activation promoted non-amyloidogenic APP processing 119
4.3.3 Non-amyloidogenic APP processing is not guaranteed following activity-dependent ERK phosphorylation 120
4.3.4 Summary 121

5.1 Introduction 123
5.1.1 α7nAChR and modulation of microglial function 123

5.2 Results 126
5.2.1 Primary cortical glia mature *in vitro,* with microglia adopting a basal 'resting' phenotype 126
5.2.2 Microglia are purified from a mixed glial population through mild trypsin incubation 126
5.2.3 Purified microglia are free from astrocytic contaminants and display microglia-specific protein expression 129
5.2.4 Primary microglia adopt a reactive 'activated' phenotype following exposure to LPS 129
5.2.5 Primary microglia are functional and express α7nAChR that couple to ERK phosphorylation 132
5.2.6 α7nAChR activation promotes microglial phagocytosis 134

5.3 Discussion 137
5.3.1 Trypsinisation of a primary cortical mixed glial population gives rise to pure microglia 137
5.3.2 Primary cortical microglia are responsive and express functional α7nAChR 138
5.3.3 Primary cortical microglia are a good model system to study inflammatory cell phagocytic behaviour 139
5.3.4 Summary 139

6. Discussion 142
6.1 α7nAChR-dependent regulation of APP processing 142
6.2 α7nAChR-dependent modulation of microglial behaviour 145
6.3 Future work 150
6.4 Conclusion 151

References 152

List of Figures

Chapter 1

Figure 1.1: Cholinergic signalling pathways in the rodent brain. ……15
Figure 1.2: nAChR physiology and structural components. ……17
Figure 1.3: Putative vertebrate nAChR subunit combinations. ……..20
Figure 1.4: Schematic of the MAPK signalling cascade ……..26
Figure 1.5: The electrophysiological distinction between type I/II positive allosteric modulators (PAMs) of α7nAChR. ……..34
Figure 1.6: The amyloid cascade hypothesis. ……..39
Figure 1.7: Amyloid precursor protein (APP) processing. ……...43
Figure 1.8: Schematic highlighting APP processing, Aβ production and secretion are closely related to neuronal activity and modulate neuronal survival. ……...50

Chapter 3

Figure 3.1: Cortical neurons display a classical neuronal phenotype and express neuron-specific proteins. ……77
Figure 3.2: Cortical neurons express postsynaptic and functional AMPAR. ……78
Figure 3.3: AMPA-induced ERK phosphorylation is time-dependent. ……..80
Figure 3.4: AMPAR-induced ERK phosphorylation is MEK-dependent. ……..82
Figure 3.5: NMDA-induced cellular activation is time-dependent. ……..83
Figure 3.6: NMDA-induced ERK phosphorylation is NMDAR- and MEK-dependent. ……84
Figure 3.7: Primary cortical neurons express functional calcium-permeable α7nAChR. ……87
Figure 3.8: nAChR couple to cellular activation and ERK phosphorylation. ……90
Figure 3.9: Figure 3.9: Activation of α7nAChR does not stimulate ERK-dependent transcription of Egr-1 in primary cortical neurons. ……..92

Chapter 4

Figure 4.1: APP is mainly trafficked to postsynaptic neuronal compartments. ……...101
Figure 4.2: Primary cortical neurons express putative α-secretase proteins ADAM-10 and ADAM-17. ……..……102

Figure 4.3: NMDAR activation induces cleavage of APP. ……104
Figure 4.4: α7nAChR activation does not affect APP levels. ……...105
Figure 4.5: Density gradient centrifugation produces viable synaptosomes with functional presynaptic α7nAChR. ……..107
Figure 4.6: NMDAR-stimulation increases time-dependent APP processing, whilst α7nAChR-stimulation has no effect over basal CTF production. ……111
Figure 4.7: α7nAChR activation does not affect APP-Gal4 cleavage in a luciferase reporter assay measuring γ-secretase-mediated APP processing. ……..114
Figure 4.8: NMDAR-stimulation induces concentration-dependent Tau cleavage and/or dephosphorylation, whilst α7nAChR-stimulation has no effect on Tau. ……117

Chapter 5

Figure 5.1: Morphological assessment of primary cortical mixed glia over time *in vitro.* ……...…127
Figure 5.2: Purification of microglia from a mixed glial population. ……128
Figure 5.3: Purified primary microglia are free of astrocytic contaminants and express microglia-specific markers. ……..130
Figure 5.4: LPS exposure of primary microglia induces a reactive phenotype. ……131
Figure 5.5: Cellular activation and stimulation of α7nAChR couples to ERK phosphorylation in 28-50 DIV primary microglia. ……..133
Figure 5.6: LPS-activated and α7nAChR-stimulated microglia display increased phagocytic behaviour. ……..…..136

Chapter 6

Figure 6.1: Schematic of α7nAChR at the glutamatergic synapse. ……..……147

List of Tables

Table 1.1: nAChR-interacting ligands, nAChR-subtype selectivity and pharmacological effects. ……30
Table 2.1: Pharmacological compounds used to assess α7nAChR at the glutamatergic synapse *in vitro.* ……59
Table 2.2: Antibodies used for Western blotting and immunocytochemistry. ……..61

List of Abbreviations

5-HT	5-Hydroxytryptamine
ACh	Acetylcholine
AChE	Acetylcholinesterase
AD	Alzheimer's disease
ADAM	A disintegrin and metalloproteinase
AICD	Amyloid intracellular domain
Akt	Protein kinase B
AM	Acetoxymethyl ester
AMPA	α-Amino-3-hydroxy-5-methyl-4-isoxazolepropionic acid
AMPAR	α-Amino-3-hydroxy-5-methyl-4-isoxazolepropionic acid receptor
ANOVA	Analysis of variance
APH-1	Anterior pharynx defective-1
APLP	Amyloid precursor like protein
ApoE	Apolipoprotein E
APP	Amyloid precursor protein
Aβ	Amyloid-β peptide
BACE	β-site APP cleaving enzyme
BDNF	Brain-derived neurotrophic factor
BFC	Basal forebrain complex
BSA	Bovine serum albumin
CA1	Cornu Ammonis area 1
Ca^{2+}	Calcium ions
CaMK	Calmodulin kinase
CD11b	Cluster of differentiation molecule 11B
ChT	Choline reuptake transporters
CICR	Calcium-induced calcium release
CO_2	Carbon dioxide
CREB	CRE-binding protein
CSF	Cerebrospinal fluid
CTF	C-terminal fragment
DAPI	4',6-Diamidino-2-phenylindole
DHβE	Dihydro-β-erythroidine

DIV	Days *in vitro*
DMEM	Dulbecco's modified Eagle's medium
DMSO	Dimethyl sulphoxide
DNA	Deoxyribonucleic acid
DUSPs	Dual-specificity phosphatases
ECL	Enhanced chemiluminescence
EDTA	Ethylenediaminetetraacetic acid
Egr-1	Early growth response gene-1
EGTA	Ethylene glycol tetraacetic acid
ERK	Extracellular signal-regulated kinase
GABA	γ-Amino butyric acid
GABAR	γ-Amino butyric acid receptor
GFAP	Glial fibrillary acidic protein
GSK-3β	Glycogen synthase kinase 3β
GTP	Guanosine-5'-triphosphate
HEPES	N-2-Hydroxyethylpiperazine-N-2-ethane sulfonic acid
HRP	Horseradish peroxidase
IL	Interleukin
IP_3	Inositol (1,4,5)-trisphosphate
JAK2	Janus kinase 2
JNK	C-Jun N-terminal kinase
KCl	Potassium chloride
LDT	Laterodorsal tegmental areas
LPS	Lipopolysaccharide
LTD	Long-term depression
LTP	Long-term potentiation
mAChR	Muscarinic acetylcholine receptor
MAP	Microtubule associated protein
MAPK	Mitogen activated protein kinase
MEK	Mitogen activated ERK kinase
Mg^{2+}	Magnesium ions
mGluR	Metabotropic glutamate receptor
MLA	Methyllycaconitine
nAChR	Nicotinic acetylcholine receptor

NaCl	Sodium chloride
NFT	Neurofibrillary tangle
NMDA	N-Methyl-D-aspartic acid
NMDAR	N-Methyl-D-aspartic acid receptor
NMJ	Neuromuscular junction
PAM	Positive allosteric modulator
PBS	Phosphate-buffered saline
PEN-2	Presenilin enhancer-2
pERK	Phosphorylated ERK
pfu	Plaque forming units
PI3K	Phosphatidylinositol 3-kinase
PKC	Protein kinase C
PPT	Pedunculopontine
PS	Presenilin
PSD	Postsynaptic density
PVDF	Polyvinylidene difluoride
RIPA	Radioimmunoprecipitation assay
sAPPα	Soluble APPα ectodomain
SD	Standard deviation
SDS	Sodium dodecyl sulphate
SDS-PAGE	Sodium dodecyl sulphate polyacrylamide gel electrophoresis
SEM	Standard error of the mean
TBS	Tris-buffered saline
TBS-T	Tris-buffered saline with Tween-20
TEMED	Tetramethylethylenediamine
TIMP	Tissue inhibitors of metalloproteases
TM	Transmembrane
TNFα	Tumour necrosis factor-α
TTX	Tetrodotoxin
UAS	Upstream activating sequence
VAChT	Vesicular acetylcholine transporter
α7nAChR	α7-subtype of nicotinic acetylcholine receptor
αBTX	α-bungarotoxin
αBTX-488	α-bungarotoxin conjugated to Alexa Fluor-488

Acknowledgements

This is a major milestone: my sincerest gratitude to all who made this possible.

The greatest of thanks go to my two fantastic supervisors, **Dr Rob Williams** and **Prof Sue Wonnacott**. Without being exposed to your immense knowledge and passion, I would never have fallen in love with APP and nicotinic receptors. Rob, your honesty and support have provided a fantastic, fun and friendly environment in which to spend my Ph.D.; and of course the Halloween pink monkey tale shall forever be legendary. Sue, your unfathomable knowledge is awe-inspiring and I feel truly blessed to have been involved in your work. Both of you have challenged and pushed me to ensure I have got the most out of this experience.

Bath has been more than my home over the last 8 years; many of the relationships I have formed will last forever. Most notably, to **Matt**, I owe my journey deeper into science to you. I should have known you were the one when you patiently taught me basic mathematics over weekends in the physics laser lab. Thanks to you, Geoff, Fred and Jim *et al*., I have known for some time what I was getting myself into; except I've not come out of academia with an unrelenting love of ABBA… Secondly, to my lab mate **Carla**- your happy outlook and endless energy made every weekday genuinely brilliant fun, even if you are so very messy in the lab.

To past and present members of the office (including **Gail, Tülay, Chris, Joe** and my undergraduate minions, to name but a few), thank you for the baklava, cuppas and in-jokes. To those of you I leave behind, I am insisting the office traditions carry on. Full commitment to office parties is a prerequisite: fancy dress is not optional. Ever.

Outside of the lab, I blame **Roxy** for weekday cocktail-induced hangovers, which impaired my Western blotting capabilities on more than a few occasions. To **Alison**, my oldest and dearest friend, you have provided me with hilarious distractions from science; I can't wait to re-read the last 15 years of your diaries when we're old and wrinkly. Nonetheless both your friendships have helped me through the whirlwind of the last 4 years, thanks for being there for me: I'll get the next round of drinks.

Finally I'd like to thank my parents, **Jayne** and **Shaun**, for having unwavering faith in me. Your support and advice has always been faultless. Yow bin bostin' ay ya!

Chapter 1

1. General Introduction

1. Introduction

1.1 Cholinergic signalling within the central nervous system

Acetylcholine (ACh) modulates a wide array of physiological processes within both the peripheral nervous system and the central nervous system (CNS). CNS roles of ACh include modulation of reward, pain, memory and cognition (reviewed by Miwa *et al*., 2011). An early pharmacological approach enabled identification of distinct acetylcholine receptor subtypes, namely muscarinic and nicotinic receptors, after observing the plant alkaloids muscarine and nicotine mimicked some of the actions of ACh. The identification of these pharmacologically distinct receptors resulted in the classification of two functionally unrelated receptor groups, muscarinic acetylcholine receptors (mAChR) and nicotinic acetylcholine receptors (nAChR), with nAChR being the focus of this thesis. ACh is generated by the enzyme choline acetyltransferase, which catalyses the formation of ACh from acetyl-CoA and choline. Conversely, ACh is rapidly broken down by acetylcholinesterase (AChE), which enables choline reuptake into neurons for conversion back to ACh, allowing precise temporal and spatial regulation of signalling (Brady *et al*., 2012). Regions of dense cholinergic activity within the brain and peripheral nervous system have been mapped through biochemical detection of choline acetyltransferase, AChE, choline reuptake transporters (ChT) and vesicular acetylcholine transporters (VAChT). The major cholinergic projection pathways (in the rodent CNS) are indicated in figure 1.1. Of particular importance, with respect to this thesis, are the neurons projecting from the basal forebrain complex (BFC), which send axons to the hippocampus, limbic cortex, olfactory bulb, amygdala and neocortex. The cholinergic projections from the BFC to the neocortex, hippocampus and limbic cortex degenerate in Alzheimer's disease (AD) (Whitehouse *et al*., 1982), as discussed below (section 1.6), which gives rise to the clinical symptoms of memory loss, personality alterations and declined cognitive performance.

1.2 Nicotinic acetylcholine receptors

nAChR were the first identified from the muscle endplate of electric ray, eel and *Torpedo* from the *Electrophorus* family. The presence of nAChR was also observed within mammalian skeletal muscle, where they are found highly concentrated at the neuromuscular junction (NMJ). Muscle nAChR have been extensively studied and

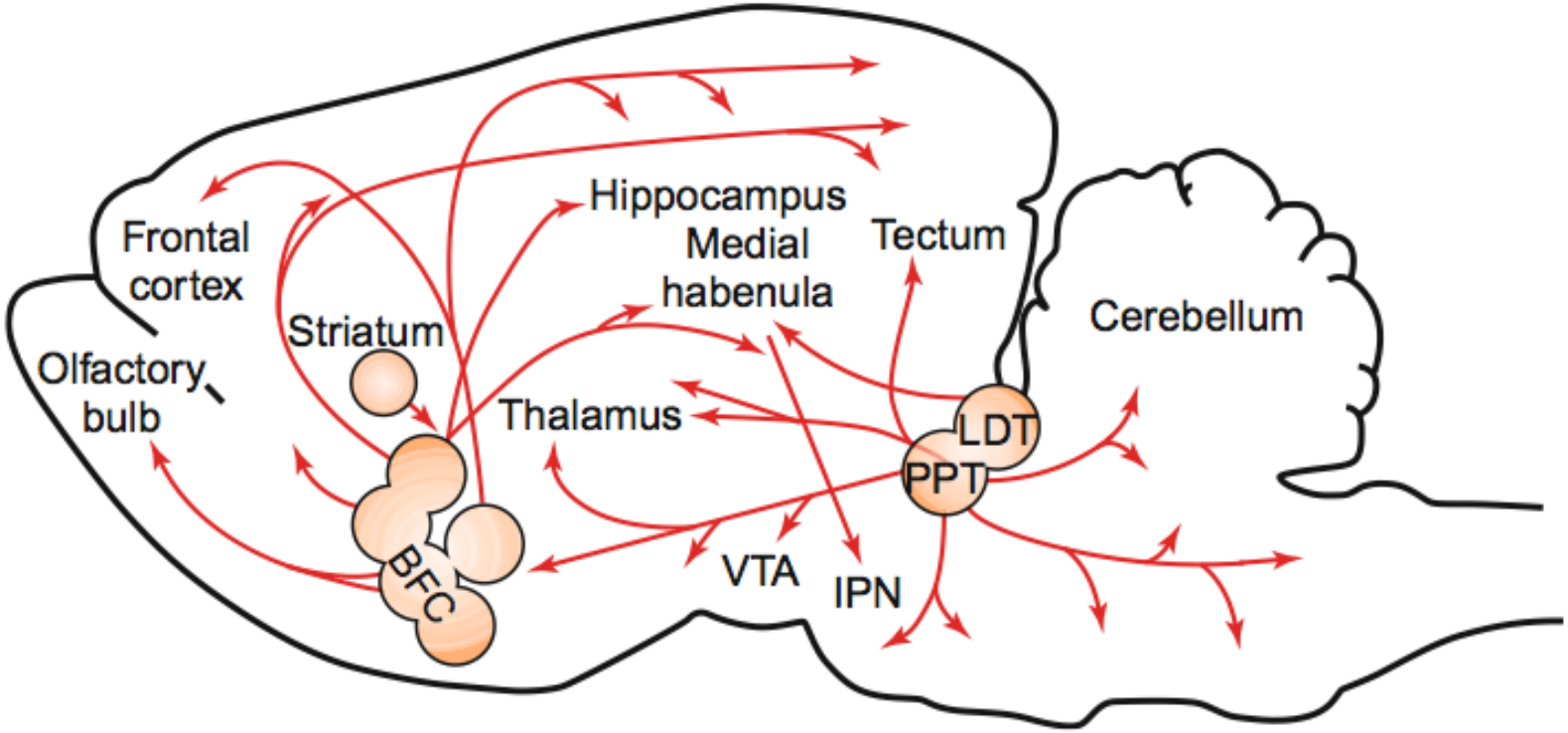

Figure 1.1: Cholinergic signalling pathways in the rodent brain. The basal forebrain (BFC) provides the major cholinergic output projections to the cortex and hippocampus. Acetylcholine signalling (red arrows) into the hippocampus and cortex enhances plasticity and learning. The pedunculopontine (PPT) and laterodorsal tegmental areas (LDT) innervate the brain stem and midbrain, whilst cholinergic interneurons are found within the striatum (taken from Brady *et al*., 2012).

well characterised, and more recently the structurally analogous neuronal nAChR have been the focus of significant research efforts. Muscle nAChR were the first neurotransmitter receptors identified (Nachmansohn, 1966) and are the prototypical receptor within the Cys loop family of pentameric ligand-gated ion channels. The Cys loop family comprises nAChR, $GABA_A$, $GABA_C$, glycine, $5\text{-}HT_3$ receptors and invertebrate glutamate-, histamine- and 5-HT-gated chloride channels (Changeux, 2013a). The extracellular N-terminus of each receptor subunit contains a 15-residue disulphide bonded 'Cys loop', providing the defining feature of this ligand-gated ion channel family of receptors, purported to be involved in channel opening, following agonist binding, figure 1.2A.

In the ~50 years since their identification (Changeux, 2012), nAChR have been extensively studied by pharmacology, electrophysiology, biochemistry, molecular biology, structural biology and cellular biology techniques. As discussed below (section 1.4) using a pharmacological approach, identification of distinct nAChR subtypes was possible, thanks to subtype-selective ligands. Such, subtype-selective ligands have been developed to target nAChR, in order to investigate a number of human diseases. Biochemistry and molecular biology enabled identification of endogenous neurotransmitter interaction sites within nAChR, through mutagenesis screens, figure 1.2B. Electrophysiology has enabled a detailed understanding of nAChR responses to exogenous ligands and endogenous neurotransmitters. nAChR were the first receptors to have channel currents and kinetics studied and the era of structural biology has begun to elucidate the detailed molecular composition and functional regions of nAChR, and specifically how nAChR-ligand interactions modulate receptor behaviour (Unwin, 2005). Finally, cellular biology has begun to investigate downstream cellular signalling events, following nAChR activation (Dajas-Bailador and Wonnacott, 2004).

1.3 nAChR function

Thanks to a number of structural studies (Brejc *et al*., 2001; Karlin, 2002; Samson *et al*., 2002; Miyazawa *et al*., 2003; Unwin, 2005; Sine and Engel, 2006; Li *et al*., 2011), we now have a greater understanding of Cys loop receptor functionality, from the stages of neurotransmitter binding, communication between binding site and the channel barrier, and opening and closing of the channel modulating ion passage, in turn affecting membrane potential. For all Cys loop family members, at least two agonist molecules are required for channel opening and receptor activation.

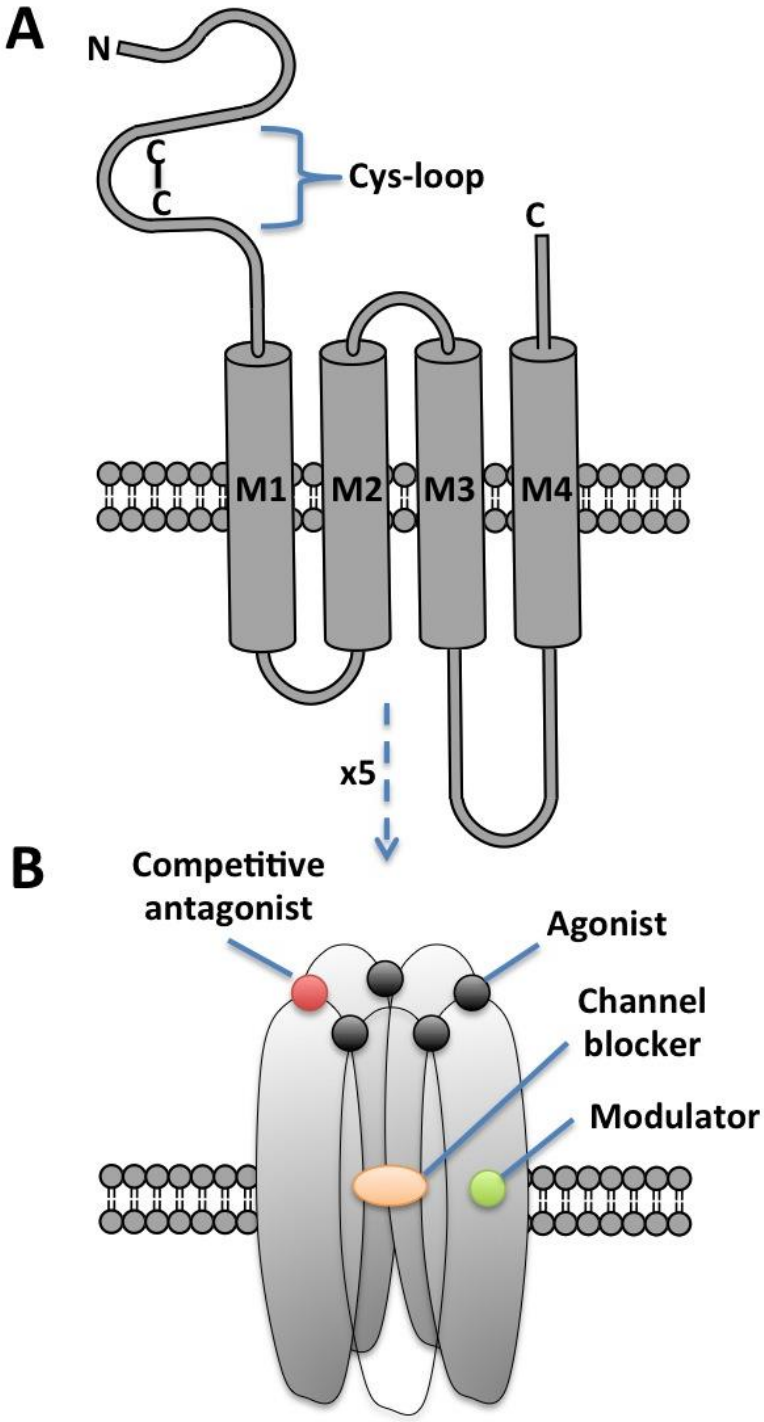

Figure 1.2: nAChR physiology and structural components. A: Orientation of a single nAChR subunit within the plasma membrane. B: Schematic of an assembled homomeric nAChR composed of five α7-subunits arranged around a central pore, lined by M2. Each principle agonist binding site is derived from three loops of the entire extracellular N-terminal domain of an α-subunit and three loops from an adjacent complementary subunit. Notional sites of nAChR-interacting drugs are indicated, either on extracellular or luminal domains of the receptor.

Upon agonist binding, the channel opens following an allosteric transition and agonist remains bound, due to its high affinity for an open-state receptor. In the open state, an influx of Na^+ and Ca^{2+} ions is permitted, alongside efflux of K^+ ions. The kinetics of channel opening are rapid, with the time between agonist binding and channel opening measured as tens of microseconds (Sine and Engel, 2006). In the transition from closed to open state, the second transmembrane segment (M2 domain) of each subunit acts as a barrier to ion passage, which following agonist binding undergoes a rotation to widen the channel pore by 3Å, enabling transient ion passage. In the open state, the residues flanking M2 act as an ion selectivity filter. Coupled with this, the presence of a ring of negatively charged residues within the internal channel vestibule contributes to cation selectivity (Li *et al*., 2011). Naturally occurring mutations within nAChR subunits and other Cys loop receptor family members can lead to reduced function receptors and result in a number of disease-causing conditions, termed channelopathies. The presence of bound agonist does not guarantee channel opening and receptor activation, as nAChR are subject to rapid desensitisation, a period in which the receptor is non-conducting following agonist-induced activation. Primary hippocampal neurons exhibit desensitisation periods of ~1 second (Dani *et al*., 2000) and desensitisation is entirely overcome by 15-30 seconds (Frazier *et al*., 1998a, 1998b). Alternatively, blockade of nAChR activation can arise from antagonist binding. Structural studies have enabled mechanistic insight into competitive nAChR antagonists, which bind within the agonist binding pocket (Samson *et al*., 2002), blocking the entrance of agonist and thus preventing channel opening and receptor activation.

1.4 nAChR diversity

The (limited) diversity of muscle nAChR subtypes, has been appreciated for over 60 years but extensive diversity amongst neuronal nAChR was only accepted ~20 years ago, following sequencing, cloning, exogenous oocyte expression and examining nAChR pharmacology using subtype-selective antagonists (Marks *et al*., 1986; Chen and Patrick, 1997; Wu and Lukas, 2011). Partially cross-linking nAChR from electric eel revealed a pentameric structure. Each of the five subunits combine to form a functional ion channel, spanning the plasma membrane, enabling the inward passage of Ca^{2+} and Na^+ ions and efflux of K^+ ions. The five subunits comprising muscle nAChR are known to be composed of up to five different proteins, termed $\alpha 1$, $\beta 1$, γ, δ and ε. Through gel separation, the relative subunit stoichiometry for muscle nAChR

was determined as $\alpha1_2\beta1_1\delta_1(\gamma/\varepsilon)_1$, where γ and ε are foetal and adult expressed muscle nAChR subunits, respectively (Changeux, 2013a). In contrast, 9 neuronal nAChR subunits have been identified to date, designated $\alpha2$-$\alpha7$ and $\beta2$-$\beta4$, figure 1.3. In addition, an $\alpha8$ subunit has been identified in avian species and $\alpha9$-$\alpha10$ in mammalian non-CNS tissues. In both muscle and neuronal nAChR, ligand binding occurs at the interface between an α- and an adjacent complementary (either α- or β-) subunit (Sauguet *et al*., 2013). Mutagenesis of single residues within the N-terminus of the α-subunit has revealed four crucial aromatic residues that constitute the agonist binding site. These residues (Tyr^{93}, Trp^{149}, Tyr^{190} and Tyr^{198}), coupled with two adjacent cysteine residues (Cys^{192} and Cys^{193}) constitute the principle binding site of a nAChR, with the adjacent subunit (β-strand rich, containing $Trp^{55/57}$) termed the complementary site (Sine and Engel, 2006; Li *et al*., 2011). The presence of differing nAChR subunits at the complementary site alters the affinity of nAChR ligands, giving rise to the agonist affinity variations between nAChR subtypes (Andersen *et al*., 2011).

1.4.1 Neuronal nAChR subtypes

Each of the above listed α-subunits (except $\alpha5$, which lacks Tyr^{190}) is capable of acting as the principle agonist binding site. Conversely, β-subunits lack the agonist binding site, but instead contain the complementary site (with the exception of the $\beta3$ subunit). Thus, α- and β-subunit conformations can form complementary pairs and constitute functional heteropentameric nAChR. In addition, $\alpha7$-$\alpha9$ subunits can form functional homomeric receptors that lack β-subunits. Homomeric α-subunit expression results in the formation of both the principle and complementary binding sites, which are capable of binding up to five agonist molecules per receptor (Rayes *et al*., 2009), with enhanced agonist sensitivity and Ca^{2+} permeability over heteromeric nAChR (Andersen *et al*., 2011, 2013). As a result, the potential number of receptor subunit combinations is huge, and there exists a large diversity of naturally expressed nAChR subtypes (Wu and Lukas, 2011), named according to their subunit composition, figure 1.3. Following successful efforts to sequence, clone and express neuronal nAChR subunits (Boulter *et al*., 1987; Heinemann *et al*., 1990; Séguéla *et al*., 1993), the distinction between muscle, neuronal and ganglionic nAChR pharmacology began to be appreciated, along with the breadth of receptor subtypes. The differential affinity of nicotine for populations of nAChR was further

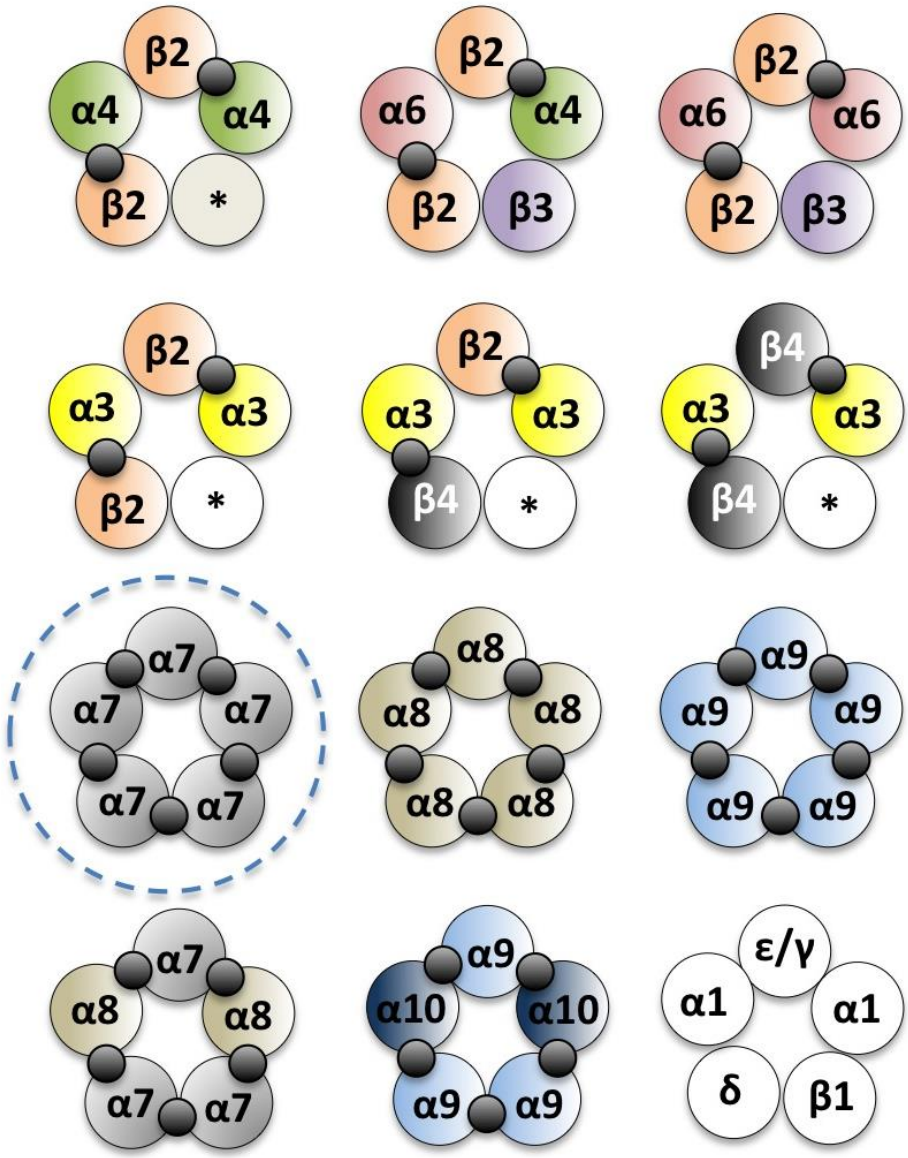

Figure 1.3: Putative vertebrate nAChR subunit combinations. Reported subunit combinations reveals vast heterogeneity of nAChR subunit stoichiometry. Black circles indicate putative agonist binding sites between principle and complementary binding sites. Vertebrate neuronal (α2-α8 and β2-β4) and mammalian non-CNS (α9-α10) nAChR subunits are coloured, whilst muscle nAChR subunits (α1, β1, δ, ε and γ) are white. The α7nAChR subtype (circled) is the focus of this thesis.

evidence for expression of a host of neuronal nAChR subtypes, as determined by subunit combinations. Accordingly, the $\alpha4\beta2$ nAChR subtype possesses a high affinity for nicotine, and accounts for >90% of [^{3}H]-nicotine binding within brain material, with $\alpha7$nAChR making up the remainder, with a minimal contribution from other nAChR subtypes. Native $\alpha4\beta2$ receptors exhibit an $(\alpha4)_2(\beta2)_3$ stoichiometry, containing the minimum required two agonist binding sites. In contrast, exogenous expression of an $(\alpha4)_3(\beta2)_2$ nAChR conformation reduced ACh affinity but enhanced Ca^{2+} permeability, reminiscent of homomeric α-subunit expression properties (Andersen *et al*., 2011, 2013). The most phylogenetically ancient $\alpha7$nAChR forms a homopentamer ligand-gated ion channel, with $\alpha4\beta2$* and $\alpha7$nAChR exhibiting complementary distributions across the mammalian CNS.

1.4.2 The $\alpha7$ subtype of nAChR

Initial work comparing the nAChR within the muscle and brain highlighted a striking difference between muscle and neuronal nAChR. All muscle nAChR (which bound nicotine) bind the 74 amino acid 8kDa α-neurotoxin, α-bungarotoxin (αBTX), which renders the nAChR silent. In contrast, within the brain, only the low affinity nicotine-binding nAChR bind αBTX. αBTX is now known to be an $\alpha7$nAChR-selective antagonist (Chen and Patrick, 1997), binding to the α-subunit agonist binding pocket (Samson *et al*., 2002) to stop access of the agonist molecule.

$\alpha7$nAChR are distinguished from other nAChR subtypes due to their unique pharmacological properties, most notably their high permeability to calcium (Séguéla *et al*., 1993; Dajas-Bailador and Wonnacott, 2004; Fucile, 2004), rapid desensitisation kinetics (Williams *et al*., 2012) and low open state probability (Pesti *et al*., 2014). The $\alpha7$nAChR has the highest fractional Ca^{2+} current (Fucile, 2004), being the highest reported for ligand-gated ion channels and is equal to NMDA-type glutamate receptors (Dajas-Bailador and Wonnacott, 2004). Desensitisation of $\alpha7$nAChR is more likely to occur following saturating agonist binding to the principle binding sites, with maximal receptor activation occurring with 1-2 bound agonist molecules (Williams *et al*., 2011a, 2012) or with 3 agonist molecules bound at non-consecutive binding sites (Rayes *et al*., 2009).

Following $\alpha7$nAChR activation increased intracellular Ca^{2+} concentration can be produced through a number of means. Firstly, Ca^{2+} influx can occur directly through the Ca^{2+}-permeable nAChR ion channel. Secondly, nAChR-mediated cellular

depolarization, as a result of Na^+ influx, also activates voltage-operated calcium channels (Barrantes *et al*., 1995a), significantly increasing the influx of Ca^{2+} ions. Thirdly, α7nAChR activation induces calcium-induced calcium release (CICR) from endoplasmic reticulum calcium stores, via ryanodine receptors (Dajas-Bailador and Wonnacott, 2004). Finally, α7nAChR-mediated Ca^{2+}-induced activation of the inositol (1,4,5)-trisphosphate (IP_3) receptor within the endoplasmic reticulum results in further release of Ca^{2+} from intracellular stores, which is purported to be ryanodine receptor-dependent. Thanks to the strong increase in intracellular calcium following α7nAChR activation, a range of signalling cascades and cellular processes are facilitated (Dajas-Bailador and Wonnacott, 2004). As populations of α7nAChR have differential spatial distribution across the CNS and are capable of increasing intracellular Ca^{2+} by a number of means, the diversity of nAChR-induced calcium-dependent cellular processes is vast (Berg and Conroy, 2002) and is subject to intense research efforts.

1.4.2.1 α7nAChR expression and distribution

In situ hybridization, radio-ligand binding and immunolabelling studies have enabled extensive analyses of nAChR expression throughout the CNS (Marks *et al*., 1986; Breese *et al*., 1997; Lewis and Picciotto, 2013) and across human brain aging (Perry *et al*., 2000). The α7nAChR subtype is of particular interest due to its relatively high expression within discrete brain regions associated with cognition, learning and memory. α7nAChR are highly expressed within the hippocampus (Fabian-Fine *et al*., 2001; Ji *et al*., 2001; Kawai *et al*., 2002), cortex (Lubin *et al*., 1999; Metherate, 2004; Poorthuis *et al*., 2013) and ventral tegmental area (Mansvelder and Mcgehee, 2000; Mansvelder *et al*., 2009). The α7nAChR expressed within these brain regions are well documented as being involved in attention, learning and memory and reward processes, respectively. Thus, targeting α7nAChR within these brain regions has been the focus of intense research efforts to treat cognitive disorders, ranging from schizophrenia to mild cognitive impairment and Alzheimer's disease (AD) (Wallace and Porter, 2011), as discussed below (section 1.9).

1.4.2.2 Expression of α7nAChR within CNS cell types

Within native CNS tissue, α7nAChR are expressed across a number of brain regions by neurons (Ji *et al*., 2001; Charpantier *et al*., 2005; Wu and Lukas, 2011; Poorthuis *et al*., 2013), astrocytes (Teaktong *et al*., 2003; Poisik *et al*., 2008; Duffy *et al*., 2011; Wang *et al*., 2013) and microglia (Shytle *et al*., 2004; Thomsen and Mikkelsen, 2012; Parada *et al*., 2013; Morioka *et al*., 2014). α7nAChR have also been extensively studied in mammalian CNS cell lines (Nakayama *et al*., 2002; El Kouhen *et al*., 2009), primary neurons (Dajas-Bailador *et al*., 2002; Brown and Wonnacott, 2014) and through exogenous expression of α7nAChR (and non-α7 nAChR subtypes) in *Xenopus* oocytes (Charpantier *et al*., 2005; Williams *et al*., 2011a). α7nAChR have also been documented within non-CNS cell types (Sharma and Vijayaraghavan, 2002; Wessler and Kirkpatrick, 2008). The most intensively studied non-CNS cell type is macrophages (Lu *et al*., 2014), due to α7nAChR's reported role as an inhibitor of inflammation (Wang *et al*., 2003; Cui and Li, 2010; Bencherif *et al*., 2011), in line with their purported function of reducing pro-inflammatory cytokine release from microglia (Giunta *et al*., 2004; Lu *et al*., 2014; section 1.4.2.3.2).

1.4.2.3 α7nAChR physiological functions

Neuronal α7nAChR are expressed at presynaptic, perisynaptic, somatodendritic and extrasynaptic sites. Their function within the CNS is broadly to modulate synaptic function and plasticity (Gray *et al*., 1996; Lozada *et al*., 2012; Pesti *et al*., 2014), underlying their role in cognition (Hurst *et al*., 2013). The majority of studies have focused on the presynaptic population of α7nAChR and their role in modulating calcium-dependent release of neurotransmitters (Wonnacott, 1997; Wonnacott *et al*., 2006), such as aspartate (Rousseau *et al*., 2005) dopamine (Grilli *et al*., 2012), GABA (Alkondon *et al*., 1997) and glutamate (Gray *et al*., 1996; Dickinson *et al*., 2008; Gomez-Varela and Berg, 2013). For example, in the hippocampus, where some of the highest levels of α7nAChR are expressed presynaptically on mossy fibres, the α7nAChR modulate release of the major excitatory neurotransmitter glutamate. As a result of enhanced glutamate release, increased numbers of α-amino-3-hydroxy-5-methyl-4-isoxazolepropionic acid (AMPA)- and N-methyl-D-aspartate (NMDA)-type glutamate receptors are trafficked to the postsynaptic membrane; increasing the potential to enhance synapse strength and long-term potentiation (LTP, Lin *et al*.,

2010; Halff *et al*., 2014), and thus α7nAChR can modulate synaptic plasticity, learning and memory. Conversely, the postsynaptic population of α7nAChR (mostly found at extrasynaptic sites) are best known for their role in generating excitatory responses. As α7nAChR are capable of being (weakly) activated by choline, the ubiquitously present precursor to ACh, it has also been suggested α7nAChR evolved to undertake slower signalling and alternative physiological roles, as well as rapid neurotransmission (Papke, 2014). The physiological levels of choline at pyramidal neurons of the CA1 region of the hippocampus (estimated to be ~10μM, Kalappa *et al*., 2010) were used to assess α7nAChR activation, revealing persistent activation of α7nAChR (Kalappa *et al*., 2010) and thus emphasizing the potential of α7nAChR modulators as cognitive enhancers.

1.4.2.3.1 α7nAChR in cognition, learning and memory

α7nAChR activation selectively promotes glutamatergic synapse formation in development, as determined by examination of glutamatergic synapse number in α7nAChR knock-out mice (Lozada *et al*., 2012). Furthermore, α7nAChR maintain and modulate glutamate release probability. A pool of presynaptic α7nAChR, within primary hippocampal neurons, was shown to transition from mobile and freely diffusible to synaptically constrained (via PSD-95 and CAST/ELKS association), which in turn increased the capacity for neurotransmitter release by enhancing the size of the readily releasable pool of vesicles (Gomez-Varela and Berg, 2013). Following enhanced glutamate release, α7nAChR activation also indirectly modulates glutamate receptor trafficking (Lin *et al*., 2010) to the postsynaptic membrane, promoting synapse maintenance and synaptic plasticity (Gomez-Varela and Berg, 2013). α7nAChR activity-dependent regulation of glutamate release results in long-term consequences, such as changes in gene expression, regulation of gene transcription, namely immediate-early genes, which in turn activate the MAPK pathway and subsequent activation of CREB (Berg and Conroy, 2002) and section 1.4.2.3.1.1. As α7nAChR are highly expressed in brain regions associated with cognition, such as the hippocampus and cortex, they are capable of inducing long-lasting synaptic changes that act as the cellular basis for learning and memory (Newhouse *et al*., 2004; Lendvai *et al*., 2013; Yang *et al*., 2013). Depletion of ACh signalling to the prefrontal cortex significantly impairs working memory (Croxson *et*

al., 2011), whilst chronic α7nAChR-selective agonist treatment of aged AD model mice restored cognition (Medeiros *et al*., 2014).

1.4.2.3.1.1 α7nAChR signalling in cognition, learning and memory

The specific downstream cellular events following nAChR activation have not been fully defined, owing to a lack of subtype-selective antagonists. In recent years the effects of nicotine and selective α7nAChR activation and cellular transduction have been mapped to phosphatidylinositol 3-kinase (PI3K, Kihara *et al*., 2004) and protein kinase B (Akt) via Janus Kinase 2 (JAK2, Shaw *et al*., 2002) and extracellular signal-related kinase (ERK, Steiner *et al*., 2007; Dickinson *et al*., 2008; El Kouhen *et al*., 2009) phosphorylation as part of the mitogen-activated protein kinase (MAPK) pathway. The central signalling cascade implicated in learning and memory processes is the MAPK pathway, physiologically targeted by neurotrophins binding a cell surface receptor-linked tyrosine kinase (such as TrkB) and a number of ionotropic and metabotropic receptors. Upon ligand binding, receptor activation, dimerization and autophosphorylation results, and a downstream phosphorylation signalling cascade initiates. Receptor-docking proteins (SOS and GRB2) activate GTP-bound Ras, which activates a central three-tiered core signalling module beginning with Raf, which in turn activates and phosphorylates MEK, figure 1.4. Activation of the serine/threonine-selective protein kinase MEK results in rapid but reversible ERK1/2 isoform phosphorylation at both a serine and threonine residue (Ferrell and Bhatt, 1997). ERK1/2 activation results in a number of signalling events, which can broadly be attributed to cytoplasm-specific and nucleus-specific ERK targets. Within the cytoplasm, phospho-ERK1/2 act on components of the MAPK pathway (such as destabilization of the receptor docking SOS-GRB2 complex and ERK dephosphorylation enzyme activation) to serve as a negative feedback regulator of further ERK phosphorylation and hyperactivation. Within the nucleus, phospho-ERK activates numerous pro-survival transcription factors and subsequent transcription and translation of pro-survival and cell cycle genes and proteins, such as CREB (Bitner *et al*., 2007) and Akt (Nakayama *et al*., 2002). α7nAChR-mediated ERK activation (Cui and Li, 2010) has also been observed in microglia, with subsequent PI3K-, Akt- and JAK-mediated cell survival (Bencherif *et al*., 2011). There exists a balance between ERK phosphorylation by kinase enzymes and dephosphorylation by phosphatase enzymes. Dual-specificity phosphatases (DUSPs) serve to dephosphorylate ERK1/2 at both serine and threonine residues

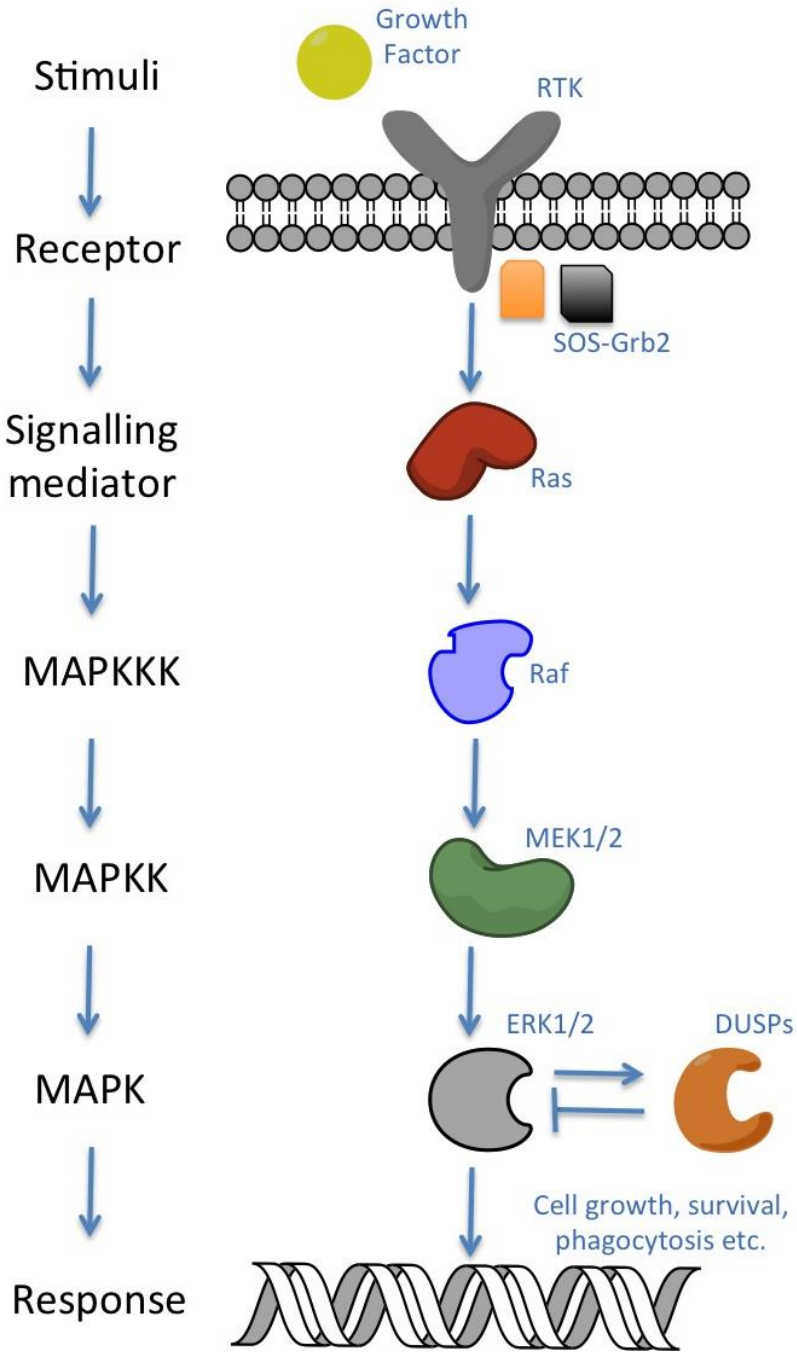

Figure 1.4: Schematic of the MAPK signalling cascade. Physiological activation of a receptor-linked tyrosine kinase (RTK) by growth factors results in receptor dimerization and autophosphorylation. Receptor-docking proteins (SOS and GRB2) activate GTP-bound Ras, which activates Raf, which in turn activates and phosphorylates MEK. Activation of MEK results in rapid but reversible ERK1/2 phosphorylation and activation, resulting in a number of signalling events, including activation of pro-survival transcription factors and cell cycle genes. As a negative feedback loop, phospho-ERK1/2 acts to destabilise the SOS-GRB2 complex and activate dual-specificity phosphatases (DUSPs), which dephosphorylate and inactivate ERK1/2.

and regulate MAPK signal transduction cascades (Caunt and Keyse, 2013). Activation of α7nAChR stimulates MEK-dependent ERK phosphorylation in neurons (Dajas-Bailador *et al*., 2002; Bitner *et al*., 2007; Steiner *et al*., 2007; Dickinson *et al*., 2008; El Kouhen *et al*., 2009), astrocytes (Koyama *et al*., 2004) and microglia (Giunta *et al*., 2004), in response to a number of ligands. The resultant MAPK signalling results in cell survival, cell division, and in a neuronal context: axon growth (Nordman *et al*., 2014), LTP (Schafe *et al*., 2008) and memory consolidation (Schafe *et al*., 2000). Phosphorylated ERK is increased in the hippocampus following memory consolidation and pharmacological antagonism of MEK prevents ERK phosphorylation and concomitant blockade in long-term memory formation (Bitner *et al*., 2007). The emerging role of phospho-ERK in cognition, learning and memory is only now becoming more apparent, with the development of more sensitive molecular, biochemical and imaging tools (Sweatt, 2004).

1.4.2.3.2 α7nAChR and CNS inflammation

All CNS degenerative diseases are associated with inflammation (Shytle *et al*., 2004). The cholinergic anti-inflammatory pathway modifies the immune system, through immune cells, such as macrophages (in the peripheral nervous system) and microglia (in the CNS). α7nAChR are essential regulators of cholinergic anti-inflammatory pathway (Wang *et al*., 2003), controlling the innate immune response to prevent excessive inflammation. Macrophage pro-inflammatory TNFα cytokine release is negatively regulated by ACh signalling to the vagus nerve, with enhanced TNFα release in α7nAChR knock-out mice (Wang *et al*., 2003).

Microglia are intrinsic immune cells of the brain, derived from erythromyeloid precursor lineage (Kierdorf *et al*., 2013; Prinz and Priller, 2014). Microglia are highly ramified cells, with motile processes, termed ‘resting’ microglia. Resting microglia constantly survey their environment and are the first cells to respond to any changes, by transforming into an amoeboid morphology and becoming ‘activated’. Activated microglia can proliferate, secrete cytokines, reactive oxygen species and phagocytose damaged cells and debris (Pocock and Kettenmann, 2007). Macrophages and microglia are activated by lipopolysaccharide (LPS), found on the outer membrane of Gram-negative bacteria. LPS exposure triggers synthesis of inflammatory mediators, such as TNFα and interleukin-1β (IL-1β), along with regulatory cytokines, such as IL-12. Diffusible inflammatory mediators activate large numbers of immune cells, amplifying the immune response, which produce large

quantities of pro-inflammatory cytokines, such as TNFα, IL-1, IL-6, IL-12 and IL-18 (Bencherif *et al*., 2011) resulting in neurodegeneration (Bodea *et al*., 2014). Microglia not only express chemokine and cytokine receptors, but have more recently been shown to respond to neurotransmitters via expression of neurotransmitter receptors (reviewed by Pocock and Kettenmann, 2007). Activation of microglial neurotransmitter receptors can be protective or inflammatory, depending on the receptor class. For example, activation of ionotropic AMPA-type glutamate receptors is pro-inflammatory, enhancing TNFα release, whereas metabotropic glutamate receptors can be either protective or inflammatory (via activation of type III or type II, respectively). Activation of G-protein coupled purinergic P2Y receptors is neuroprotective, enhancing microglial motility, migration and phagocytosis. α7nAChR expression on glial cells has not been well studied, as the focus on α7nAChR's cognitive enhancing effects have historically remained on the neuronal population within the CNS. However, as α7nAChR flux calcium, which is the basis for glial cell excitability (Parri *et al*., 2011), the question of whether α7nAChR can modulate glial cell behaviour remains largely unanswered. However, the few studies of nAChR in microglia show sole expression of the α7-subtype; and its activation is anti-inflammatory and neuroprotective. Activation of microglial α7nAChR enhanced neuroprotective gene expression (Parada *et al*., 2013), reduced LPS-induced TNFα release (Shytle *et al*., 2004), reduced IFN-γ mediated pro-inflammatory cell activation (Giunta *et al*., 2004), enhanced GLAST/EAAT1 expression (Morioka *et al*., 2014), reducing glutamate-mediated neuronal excitotoxicity and enhanced macrophage phagocytosis of bacteria in infected mice (Sitapara *et al*., 2014). Furthermore, the anti-inflammatory effects of macrophages can be attenuated by αBTX application (Ulloa, 2005). The anti-inflammatory nature of α7nAChR activation can also be attributed to reduced inflammasome activation. The inflammasome is a multi-molecular complex that orchestrates the activation of pro-inflammatory caspase-1 and IL-1β and IL-18 release. Bacteria-mediated macrophage activation prime microglia to activate the NLRP3 inflammasome (Lee *et al*., 2013). The activated NLRP3 inflammasome is released as an extracellular particle to signal and amplify an immune response (Baroja-Mazo *et al*., 2014). Knock-out of the NLRP-3 inflammasome reduced caspase-1 activation and IL release, whilst enhancing microglial phagocytosis (Heneka *et al*., 2013). Recent data has shown α7nAChR activation inhibits NLRP3 inflammasome activation by preventing mitochondrial DNA

release (Lu *et al*., 2014). Thus activation of microglial neurotransmitter receptors (especially α7nAChR) and their subsequent downstream signalling cascades may be a key strategy in controlling inflammatory cell behaviour, with the potential to regulate inflammation within the CNS for the treatment of inflammatory neurodegenerative diseases (Bencherif *et al*., 2011).

1.5 nAChR pharmacology

As nAChR (particularly the α7 subtype) are involved in a vast range of cellular processes and are implicated in cognitive function; compounds that modulate nAChR have been the focus of significant research efforts in a bid to improve cognition and also combat neurological decline. Table 1.1 lists neuronal nAChR-selective ligands, grouped into agonists, antagonists and modulators. Agonists activate nAChR to bring about a biological response, whereas antagonists block agonist-mediated responses, by binding to orthosteric or allosteric sites on the receptors. Modulators encompass all nAChR-binding ligands that exert alternative effects to agonism and antagonism of nAChR. Allosteric modulators of nAChR have been developed to modulate native nAChR in cognitive disease states, such as schizophrenia and Alzheimer's disease, where nAChR-mediated processes are reduced (Timmermann *et al*., 2007; Taly *et al*., 2009; Williams *et al*., 2011b). Positive allosteric modulators (PAMs) have been grouped into two classes, type I and type II PAMs (Grønlien *et al*., 2007), as determined by their apparent peak current profile and type II PAMs can reactivate nAChR following receptor desensitisation (Bertrand and Gopalakrishnan, 2007; Changeux, 2013b; Uteshev, 2014), figure 1.5. PAMs bind to nAChR at sites distinct from the agonist binding (orthosteric) site (Barron *et al*., 2009) and enhance receptor gating in the presence of agonists. PNU-120596 dramatically enhances the channel open time (daCosta *et al*., 2011; Williams *et al*., 2012) and also enables α7nAChR to overcome desensitisation and receptor silencing (Papke *et al*., 2009; Szabo *et al*., 2014). Non-desensitising α7nAChR-selective agonists have also recently been reported in the literature (Gill *et al*., 2011) and exhibit potential in neurological conditions where endogenous neurotransmitter levels are reduced.

Throughout this thesis, the α7nAChR-selective type II PAM PNU-120596 (Table 1.1; (Hurst *et al*., 2005; Grønlien *et al*., 2007) was used in combination with the α7nAChR-selective agonist PNU-282987

Drug	nAChR-isoform selectivity	Comment(s)	Reference(s)
Agonists			
A-85380	$\alpha4\beta2$*-selective	Analog of (±)-Epibatidine, with lower binding to non-$\alpha4\beta2$ nAChR.	Sullivan *et al*, 1996
5-iodo-A-85380	$\alpha4\beta2$*-selective	Iodinated variant of A-85380, shows improved selectivity for $\beta2$-containing nAChR.	Mukhin *et al*, 2000, Rousseau *et al*, 2005
Acetylcholine	All mAChR and nAChR subtypes	Susceptible to hydrolysis and requires the presence of AChE inhibitor.	Williams *et al*, 2011
AR-R17779	$\alpha7$-selective	100-fold greater potency for binding to $\alpha7$nAChR than $\alpha4\beta2$nAChR. Binding potency K_i: 0.2μM, EC_{50}: 10-20μM.	Mullen at al, 2000
Choline	Weak agonist at $\alpha7$ Partial agonist at $\alpha3\beta4$	Weak agonist, 10-fold lower potency than ACh. Binding potency K_i: 2mM, EC_{50}: 0.4-1.6mM.	Alkondon *et al*, 1997; Kalappa *et al*, 2010
Compound A	$\alpha7$-selective agonist	Potent and selective agonist. Binding potency K_i: 40nM, EC_{50}: 14nM-0.95μM.	Ondrejcak *et al*, 2012
(-)-Cotinine	$\alpha4\beta2$*-selective agonist $\alpha7$-selective antagonist	Metabolite of nicotine, with lower potency.	Vainio *et al*, 2001
(-)-Cytisine	$\alpha4\beta2$*-selective partial agonist	Isolated from *leguminosae* plant family. Full efficacy for the $\beta4$ subunit. Binding potency K_i: 1nM.	Marotta *et al*, 2014
(±)-Epibatidine	Highly potent agonist at heteromeric nAChR	Isolated from Amazonian frog skin.	Rousseau *et al*, 2005
EVP-6124	Partial agonist at $\alpha7$	Acts as an agonist as well as potentiating ACh-evoked responses.	Prickaerts *et al*, 2012
GTS-21	Partial agonist at $\alpha7$ Very weak partial agonist at $\alpha4\beta2$ Strong antagonist at $\alpha4\beta2$	Elicits only 30% of an ACh-evoked $\alpha7$nAChR maximum response. Binding potency K_i: 0.2-0.5μM, EC_{50}: 6-26μM.	Sitapara *et al*, 2014
(-)-Nicotine	All nAChR subtypes	Higher affinity for $\alpha4\beta2$* over $\alpha7$. Prolonged nicotine-binding induces a reversible desensitisation state.	Wonnacott *et al*, 2005

PNU-282987	α7-selective	Selective and potent. Weak activity at 5-HT receptors. Binding potency K_i: 26nM, EC_{50}: 14nM-128nM.	Bodnar *et al*, 2005; Hajos *et al*, 2005; Barrio *et al*, 2010
RJR 2403	α4β2*-selective agonist	EC_{50}: 26nM.	Bencherif *et al*, 1996
Sazetidine-A	α4β2* desensitising agent α7 agonist and desensitising agent	Originally thought to have no effect on nAChR activation. EC_{50}: 4.2μM.	Xiao *et al*, 2006; Brown and Wonnacott, 2014; Marotta *et al*, 2014
SSR180711	α7-selective partial agonist	Elicits 30-50% of an ACh-evoked α7nAChR maximum response. Binding potency K_i: 20nM, EC_{50}: 1-4μM.	Biton *et al*, 2006; Pichat *et al*, 2006
TC 2559	α4β2-selective partial agonist	Selective for $(\alpha4)_2(\beta2)_3$ stoichiometry. Low efficacy. EC_{50}: 200nM.	Bencherif *et al*, 2000
Antagonists			
α-bungarotoxin (αBTX)	Homomeric α7-, α8-, α9-selective competitive antagonist	Polypeptide toxin from snake venom. Interacts with α-subunit. Binding potency K_i: 0.5-1nM, IC_{50}: 1-100nM.	Samson *et al*, 2002
Aβ peptide	α7-selective antagonist	Selective to the $A\beta_{42}$ form. Binds competitively IC_{50}: 5pM and inhibits non-competitively at 1-100nM.	Wang *et al*, 2000; Liu *et al*, 2001; Pettit *et al*, 2001; Grassi *et al*, 2003
Dihydro-β-erythroidine (DHβE)	Competitive neuronal non-α7 antagonist	Isolated from *Erythrina* seeds. More potent at α4β2 and α3β2 and 50-fold less potent at α3β4 and α7 in oocytes. In neurons, DHβE only blocked α4β2*.	Harvey *et al*, 1996; Alkondon and Albuquerque, 1993
Mecamylamine	Non-competitive non-selective antagonist Weak NMDAR antagonist	α7 less sensitive then heteromeric nAChR (mecamylamine only blocks ~70% of a αBTX block). Saturating concentrations inhibit NMDAR. IC_{50}: 0.1-1μM.	Chavez-Noriega *et al*, 1997; Ridley *et al*, 2002; Sharma and Vijayaraghavan, 2003
Methyllycaconitine (MLA)	Potent α7 competitive antagonist Relatively potent at α9, α9/10 and α6β2*	Isolated from *Delphinium sp*. Discriminates between muscle and α7nAChR. Binding potency K_i: 1nM, IC_{50}: 10-200nM.	Ward *et al*, 1990; Drasdo *et al*, 1992; Mogg *et al*, 2002

MK-801	Potent NMDAR antagonist Weak open nAChR channel blocker	IC_{50} at nAChR: 15μM.	Ramoa *et al*, 1990; Briggs and McKenna, 1996; Buisson and Bertrand, 1998
Modulators			
Galantamine	AChE inhibitor Potentiates nAChR responses	Isolated from the common snowdrop. Modest potentiation of ACh-evoked currents (30%) and increases intracellular calcium at low concentrations, above which reverts to a nAChR antagonist. Approved for use in treatment of mild to moderate AD.	Dajas-Bailador *et al*, 2003; Smulders *et al*, 2005; Arias *et al*, 2005
5-hydroxyindole	Potentiates α7	5-HT metabolite, Type I PAM: increases ACh potency and efficacy without effect on desensitisation. EC_{50}: 2.5mM.	Zwart *et al*, 2002; Timmermann *et al*, 2007
JNJ-1930942	α7-selective positive allosteric modulator No effect at α4β2, α3β4 or 5-HT_3R	No agonist properties at α7. Type I PAM: enhances recovery but does not prevent desensitisation. EC_{50}: 1.9μM	Dinklo *et al*, 2010
LY2087101	Potent potentiator of α7 and α4β2	Avoids potentiation of α3β4 nAChR hence removes undesirable *in vivo* side effects. EC_{50}: 4.2μM.	De Filippi *et al*, 2010
PNU-120596	α7-selective positive allosteric modulator No effect on α4β2, α3β4 or α9α10	Type II PAM. No agonist properties at α7. Prolongs and increases agonist-evoked currents. No effect on ion-selectivity or unitary conductance. Reactivates desensitized α7nAChRs. Binds to α7nAChR within α-helical transmembrane regions. Capable of cognitive enhancement *in vivo*. EC_{50}: 200nM	Hurst *et al*, 2005; Gronlien *et al*, 2007; Timmermann *et al*, 2007; Young *et al*, 2008; Barron *et al*, 2009; Da Costa *et al*, 2011; Sitzia *et al*, 2012; Williams *et al*, 2012; Szabo *et al*, 2014

Table 1.1: nAChR-interacting ligands, nAChR-subtype selectivity and pharmacological effects. Selected notable neuronal nAChR ligands grouped into agonists, antagonists and positive allosteric modulators (PAMs), with key references of characterisation included.

(Bodnar *et al*., 2005; Hajos *et al*., 2005; del Barrio *et al*., 2011) to reveal the activity of native α7nAChR, in order to examine the biological role of α7nAChR at the glutamatergic synapse.

1.5.1 Modulators of nAChR and effects on cognitive function

Presynaptic α7nAChR-mediated glutamate release at hippocampal synapses is known to contribute to development of synaptic plasticity (Mansvelder and Mcgehee, 2000; Huang *et al*., 2010), and is modulated by inhibitory GABA signalling inputs (Alkondon *et al*., 1997). Due to the high expression level of α7nAChR within the hippocampus (Dani and Bertrand, 2007) and the nicotinic deficits observed in pathological conditions (section 1.6.1), α7nAChR are implicated in various neurological and cognitive disorders. In support of this, α7nAChR gene knockout studies showed impaired learning and memory (Marubio and Changeux, 2000; Dineley *et al*., 2002b; Young *et al*., 2007). The depolarisation contributed by α7nAChRs helps to relieve the magnesium block of postsynaptic NMDA-type glutamate receptors (NMDAR) (Kenney and Gould, 2008; Yang *et al*., 2013; Cheng and Yakel, 2014) and enhance probability of LTP induction. Hence, a loss of hippocampal and cortical ACh signalling through α7nAChRs in aging or pathological acceleration of aging is of significant detriment, and is thought to be a major contributing factor underlying age-related memory decline (Bierer *et al*., 1995) and loss of working memory (Croxson *et al*., 2011). Many years of research (Mansvelder and Mcgehee, 2000; Miwa *et al*., 2011) has shown in both animals and humans, that nicotine can paradoxically, both improve and impair cognitive performance (Newhouse *et al*., 2004). Nicotine-induced cognitive enhancement is generally observed in subjects exhibiting sub-optimal cognitive performance, such as those with age-related cognitive decline or Alzheimer's disease (AD). Contrastingly, nicotinic stimulation impairs cognitive performance in those performing at a near-optimal level (Newhouse *et al*., 2004). However, the mechanism of nicotine-induced improvements in cognition is unknown. To this end, an array of pharmacological compounds (namely agonists, positive allosteric modulators (PAMs) and AChE inhibitors) have been developed to selectively enhance physiological α7nAChR activity, in favour of α7nAChR activation-induced cognitive enhancement (Table 1.1, reviewed by Wallace and Porter, 2011), without the undesirable side effects of ACh and nicotine-mediated pan-mAChR and nAChR activation, respectively.

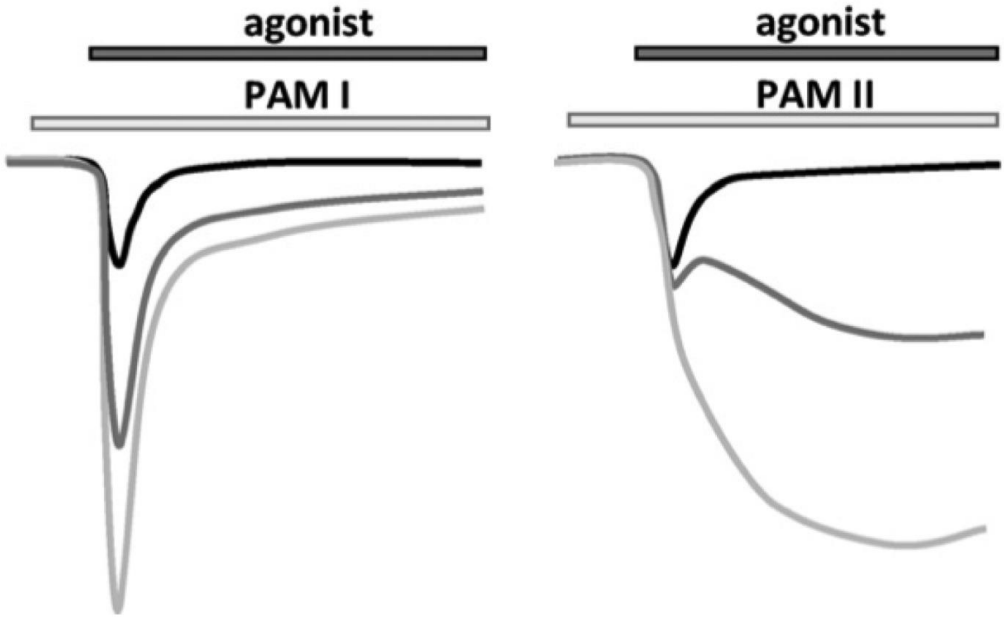

Figure 1.5: The electrophysiological distinction between type I/II positive allosteric modulators (PAMs) of α7nAChR. Type I and type II PAM-potentiated signals (grey traces) produce different peak current profiles following agonist-mediated (black traces) receptor activation (adapted from Lendvai *et al*., 2013). Type II PAMs prevent receptor desensitisation and allow increased mean channel open time.

1.5.1.1 α7nAChR-selective agonists

Agonists acting at nAChR exhibit inverted U-shaped dose response curves, attributed to the rapid desensitisation of nAChR (particularly the α7 subtype), thus resulting in a dose-limiting loss of effect (Picciotto, 2003; Wallace and Porter, 2011), when applied in the absence of type II PAMs. Development of orthosteric agonists has been intense, however, the homology of nAChR with other members of the Cys-loop ligand-gated ion channel family has resulted in few wholly α7nAChR-selective compounds. The few α7nAChR-selective agonists have been shown to improve deficits in sensory gating in schizophrenia (Toyohara and Hashimoto, 2010), enhance cognition in humans and animals (Levin and Rezvani, 2000), mild cognitive impairment and AD mouse models (Medeiros *et al*., 2014), enhance attention (Levin, 2013), episodic memory (Wallace and Porter, 2011) and working memory (Lendvai *et al*., 2013). Conversely, α7nAChR-selective antagonists, such as MLA (Table 1.1) impair cognition in animal behavioural models (Wallace and Porter, 2011). Thus enhanced activation of native α7nAChR is widely regarded as an attractive strategy in cognitively impaired disease states.

1.5.1.2 α7nAChR-selective PAMs

Type II PAMs are more favourable clinical molecules, over type I PAMs, as they prevent or overcome nAChR desensitisation (Grønlien *et al*., 2007), but may introduce the risk of excitotoxicity (Ng *et al*., 2007; Hu *et al*., 2009a). PAMs serve to enhance small α7nAChR stimuli and thus heighten them above the receptor activation threshold, leading to cellular activation and concomitant cell survival. PAMs allow enhancement of endogenous agonist effect and have shown promise in models of sensory gating deficits and paradigms of altered cholinergic tone (Wallace and Porter, 2011). Many of the AChE inhibitors also act as α7nAChR-selective PAMs (Dajas-Bailador *et al*., 2003) to further boost cholinergic signalling.

1.6 The cholinergic hypothesis of Alzheimer's disease

The cholinergic hypothesis (Perry, 1986) postulates that cholinergic neurodegeneration within the basal forebrain induces the cognitive decline observed in AD (Coyle *et al*., 1983). This neurodegeneration within the basal forebrain leads to reduced cholinergic neurotransmission and resultant losses of presynaptic terminals

in the cortex and hippocampus (Pettit *et al*., 2001). Studies showed a marked reduction in acetylcholine synthesis and breakdown within post-mortem AD patient cortex and hippocampal tissue, by measuring choline acetyltransferase and acetylcholinesterase activity, respectively (Bartus *et al*., 1982; Whitehouse *et al*., 1982). Furthermore, reduced uptake of the acetylcholine precursor, choline (Apelt *et al*., 2002), reduced acetylcholine release (Francis *et al*., 1999) and reduced levels of nAChR in AD brains (Martin-Ruiz *et al*., 2002) further reinforced this hypothesis. Hence following this theory, acetylcholinesterase inhibitors (section 1.9.1) were adopted as therapeutic treatments for AD. These findings, when coupled with the central role of acetylcholine in memory and cognition implicate dysregulation of acetylcholine release and nAChR signalling in the pathogenesis of AD, and reinforce the central role of cholinergic function in healthy cognitive aging.

1.6.1 Alzheimer's disease and age-related cognitive decline

Dementia affects approximately 30-40 million people worldwide with numbers projected to rise to 115 million by 2050 (Alzheimer's Society, 2014), due to the world's aging population. The most common cause of dementia is AD. AD is characterised by progressive memory loss with age, due to specific vulnerability of the neurons within the hippocampus and cortex associated with memory formation and storage, with pathology beginning in and spreading from the entorhinal cortex (Khan *et al*., 2013). It is these brain regions that show the pathological signs of AD, including extracellular plaques, composed of Aβ peptide and intracellular neurofibrillary tangles (NFT), composed of hyperphosphorylated Tau (Walsh and Selkoe, 2007). Subsequently, the hippocampus and cortex exhibit synapse loss and neuronal cell death (Wei *et al*., 2010), leading to the impaired cognition and behavioural changes observed in AD (Näslund *et al*., 2000). Throughout physiological aging, the brain accrues extracellular plaques of Aβ peptides (Walsh *et al*., 2002; Walsh and Selkoe, 2007). These plaques are observed to a greater degree in AD patient brains (La Joie *et al*., 2012), but whether they play a primary role in initiating, or secondary role in mediating cholinergic dysfunction in both aging and AD is controversial (Kenney and Gould, 2008; Knowles *et al*., 2014). Cholinergic axon loss has been shown to be more pronounced in the vicinity of Aβ plaques in aged humans, primates and AD patients (Shah *et al*., 2010). Soluble and oligomeric Aβ peptide species have been shown to modulate synaptic plasticity and LTP (Walsh *et al*., 2002; Wang *et al*., 2002; Cleary *et al*., 2005; Abramov *et al*., 2009), as well as cholinergic synapse dysfunction

(Shankar *et al*., 2007; Innocent *et al*., 2010; Fowler *et al*., 2014). Aβ dimerisation, oligomerisation and differential species formation may precede deposition of insoluble Aβ plaques (Schliebs and Arendt, 2011; Larson and Lesné, 2012). Aβ may exert its cholinergic neurotoxic effects through interactions with α7nAChR (Wang *et al*., 2000a, 2000b; Parri and Dineley, 2010; Tong *et al*., 2011; Liu *et al*., 2013) but conversely, cholinergic signalling has also been shown to be neuroprotective against Aβ toxicity (Liu *et al*., 2001; Lahiri *et al*., 2002; Mousavi and Hellström-Lindahl, 2009; Nie *et al*., 2010). Thus, understanding the mechanism leading to Aβ-induced neurodegeneration of the neurons within the hippocampus and cortex is central to aging-induced cognitive decline and AD, and the fundamental process underlying this is the cleavage of amyloid precursor protein (APP) to yield Aβ peptides. The amyloid cascade hypothesis posits that the Aβ peptides, derived from APP holoprotein, are the root cause of AD.

1.7 Amyloid cascade hypothesis

The essence of the amyloid cascade hypothesis is that increased Aβ production (especially the $A\beta_{42}$ species, over $A\beta_{40}$) or reduced Aβ clearance causes AD. Accumulation of Aβ results in aggregation and plaque formation, which initiates a cascade of cellular events ultimately resulting in cell death. The amyloid cascade hypothesis was suggested ~20 years ago (Hardy and Allsop, 1991; Hardy and Selkoe, 2010), with genetic and biochemical data supporting the hypothesis although some researchers believe that Aβ is one factor and not the sole cause of AD (Pimplikar *et al*., 2010).

Of the millions of AD sufferers worldwide, less than 1% exists as 'familial' cases, caused by autosomal dominant mutation(s) in either APP or presenilin (PS-1/ PS-2) genes (Price and Sisodia, 1998; Hardy and Selkoe, 2002). Presenilin 1 and 2 make up the catalytic core of γ-secretase (De Strooper, 2003; Selkoe and Wolfe, 2007), which cleaves APP to yield Aβ species; with familial presenilin mutations favouring the secretase-mediated production of the longer 42-residue Aβ form. APP mutations occur near the site of secretase cleavage and serve to enhance total Aβ levels and the $A\beta_{42}$:$A\beta_{40}$ ratio. $A\beta_{42}$ is more prone to aggregation and plaque formation (Meisl *et al*., 2014). Familial AD typically affects patients at 40-50 years of age, whereas symptoms of sporadic AD occur after 65 years of age. These two forms of AD present with similar neurological and pathological hallmarks and are thus thought to be

identical or at least highly analogous diseases. Whilst mutations in APP or presenilin potentially cause AD, Tau NFT load more closely correlates with disease severity and cognitive decline correlates with hippocampal volume (Ong *et al*., 2014). Whilst the presence of amyloid plaques (composed of Aβ) and NFT (composed of Tau) are considered to be the defining hallmarks of AD, these aggregates are increasingly recognised as not being the neurotoxic species underlying cell death in AD. As more research has been undertaken into the amyloid cascade hypothesis, the central toxic species has been revised, from Aβ plaques to a multi-faceted neurotoxic insult (Oddo *et al*., 2006), including NFT, environmental factors and soluble Aβ species, which have been isolated from cell culture medium (Walsh and Selkoe, 2007), AD brain extracts (Shankar *et al*., 2007) and AD mouse models (Lesné *et al*., 2006); but this remains controversial as the exact toxic nature of the Aβ species is yet to be resolved, figure 1.6. Aβ plaques are no longer purported to be the toxic species, after they were shown to be present in cognitively normal people (Nordberg, 2008), lacking in AD patients (Terry *et al*., 1991), the non-correlative relationship between plaque load and disease progression (Ong *et al*., 2014) and a number of animal models showing cognitive impairment prior to plaque deposition (Lesné *et al*., 2006). Nonetheless, the majority of modern pharmacological intervention strategies for AD have focussed on amyloid-based therapeutic approaches, aiming to lower Aβ production, in accordance with mechanisms postulated through the amyloid cascade hypothesis. A number of pharmacological compounds have been developed to target toxic Aβ species, namely β- and γ-secretase inhibition (Zhou *et al*., 2011), inhibition of Aβ aggregation (McKoy *et al*., 2012), Aβ immunisation (Schenk *et al*., 1999) and enhancing amyloid degradation (Walker *et al*., 2013); each of which has had minimal success in the clinic (Karran *et al*., 2011). However, given the emerging evidence highlighting Aβ-mediated NFT formation and the strong correlation between NFT deposition and cognitive decline, this suggests amyloid-targeting mechanisms may have some future scope, inhibiting Aβ as an upstream modulator of Tau modification (namely hyperphosphorylation), further validating the amyloid cascade hypothesis and placing it at the crux of on-going research into the basic mechanistic biology of AD.

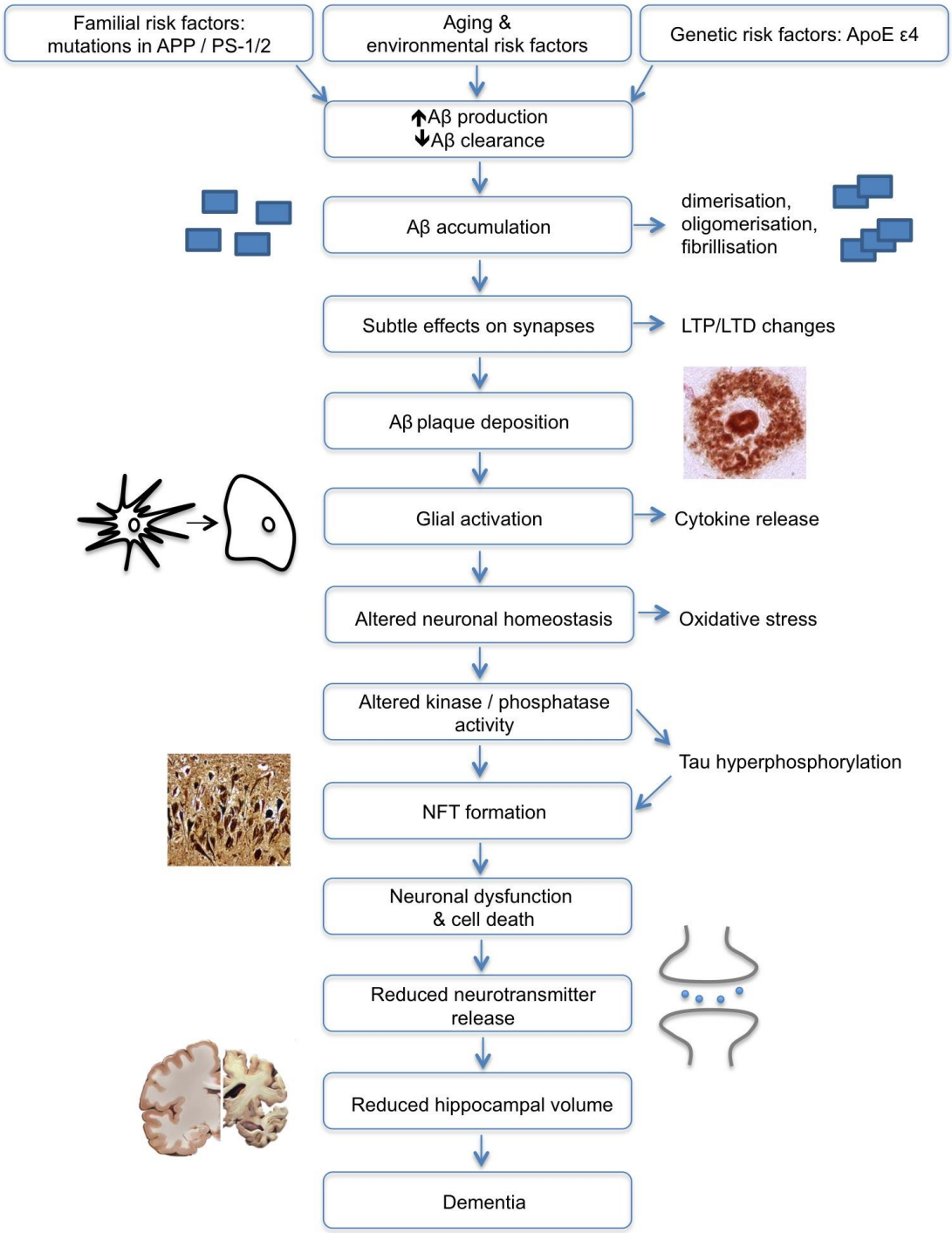

Figure 1.6: The amyloid cascade hypothesis. According to the amyloid cascade hypothesis, the causative event in AD pathogenesis is an imbalance between Aβ production and clearance. Various Aβ species can directly inhibit hippocampal LTP and impair synaptic function, in addition to the inflammatory and oxidative stress caused by Aβ plaques. As a result, Tau hyperphosphorylation and subsequent NFT formation impairs neuronal and synaptic function, resulting in neuronal death, neurotransmitter deficits and cognitive decline before the symptomatic onset of dementia.

1.8 Amyloid precursor protein

APP is found in the plasma membrane as a type I transmembrane glycoprotein (Hardy and Selkoe, 2002). There are three major isoforms, APP_{770}, APP_{751} and APP_{695}. APP_{695} is the major isoform localised to the brain, where it is found in a mature O- and N-glycosylated state. APP_{695} is the major isoform in mouse primary cortical neurons (Hoey *et al*., 2009), whilst primary astrocytes and microglia express all three isoforms of APP (Haass *et al*., 1991), where APP is found densely localised to the Golgi and endoplasmic reticulum (Palacios *et al*., 1992).

APP interacts with a number of cell-surface localised proteins but its role in both development and the mature brain is yet to be elucidated. Analysis of APP's *in vivo* physiological function is made difficult by its proteolytic cleavage, to yield various peptides with their own functions. Furthermore, APP is part of a highly conserved family with overlapping and redundant functions (Müller and Zheng, 2012). APP is a member of a gene family including APL-1 in *Caenorhabditis elegans*, APPL in *Drosophila*, appa and appb in zebrafish and APLP1 and APLP2 (along with APP) in mammals. APP family proteins are composed of highly conserved regions, and interestingly, the extracellular and juxtamembrane regions are divergent across the family, with Aβ being specific to APP (Müller and Zheng, 2012). The family is subject to posttranslational modifications, such as N- and O-glycosylation, sialyation, and phosphorylation at many intracellular C-terminal sites by GSK-3β (Rockenstein *et al*., 2007). The exact role of APP phosphorylation is unknown, but is the subject of intense study. Hypothesised functions include regulation of APP secretion (Caporaso *et al*., 1992), neuronal sensitivity to trophic signalling (Matrone *et al*., 2011), regulation of APP's interaction with adaptor and signalling proteins (Schettini *et al*., 2010) and as an iron-export ferroxidase (Duce *et al*., 2011). The phosphorylation state-mediated regulation of APP processing remains a topic of considerable debate (Sano *et al*., 2006; Barbagallo *et al*., 2010; Matrone *et al*., 2011) and its *in vivo* relevance is only beginning to be revealed. APP is particularly highly expressed in neurons, where it is localised to the cell body, axons and dendrites (Back *et al*., 2007; Hoe *et al*., 2009; Hoey *et al*., 2009, 2013).

1.8.1 Physiological functions of APP

Despite a wealth of data on Aβ and its production, the physiological role of APP remains an enigma (Hoe *et al*., 2009). Much of the data on APP comes from knock-

out studies, complemented by cellular *in vitro* studies (Müller and Zheng, 2012). Complete knock-out of APP produced viable and fertile mice, but with 20% reduced body mass and 10% reduced brain weight (Zheng *et al*., 1995), consistent with *in vitro* data showing APP mediates neurogenesis, synaptic adhesion and axonal pathfinding (Sosa *et al*., 2013; Wang *et al*., 2014). The mice also showed increased levels of metal deposition, consistent with recent data highlighting APP and its cleavage product sAPPα as being involved in iron efflux (Duce *et al*., 2011; McCarthy *et al*., 2014). Furthermore, knock-out mice were hypersensitive to kainate-induced seizures, and impaired performance in learning and spatial memory tasks, associated with a defect in LTP, consistent with a role for APP in mediating the balance of neuronal excitation (Zhang *et al*., 2013). Finally, knock-out mice displayed reduced grip strength, consistent with APP's hypothesised role in directing the formation of the neuromuscular junction early in development (Zheng *et al*., 1995). Combinatorial knock-out of APP family members (APP/APLP) is postnatal lethal, revealing defects in glutamatergic synaptic transmission (Schrenk-Siemens *et al*., 2008) and reinforcing the role of APP in mature synapse formation and synaptic transmission.

In contrast, APP cleavage products have been extensively studied, and extracellular soluble forms of APP (particularly sAPPα) have been shown to act as neurotrophins, regulating axon pruning and degeneration (Copanaki *et al*., 2010) through binding to the death receptor DR6 under stress (Nikolaev *et al*., 2009; Kallop *et al*., 2014). sAPPα is able to rescue the APP knock-out phenotypes of anatomical, behavioural and electrophysiological defects (Ring *et al*., 2007), reinforcing the important physiological function of APP and its cleavage products. The AICD produced from γ-secretase cleavage of APP-CTFs regulates gene expression (Pardossi-Piquard and Checler, 2012), following its stabilisation by Fe65 (Kimberly *et al*., 2001) and translocation to the nucleus; where AICD forms a transcriptionally active complex with Fe65 and Tip60 (Cao and Südhof, 2001). Understanding the physiological processing of APP may provide a more in depth insight into the fundamental role of APP and its cleavage products.

1.8.2 APP processing

Processing of APP produces the Aβ peptide which appears to be central to the pathogenesis of AD. Only a small quantity of mature APP is cleaved, however its half-life is predicted to be ~10 min (De Strooper and Annaert, 2000), indicating a highly dynamic regulation. There are two principal APP processing pathways, the pro-

amyloidogenic pathway, leading to Aβ formation and the non-amyloidogenic pathway, preventing Aβ formation, figure 1.7. The principle proteolytic cleavage of APP, under basal homeostatic conditions is via the non-amyloidogenic pathway, with initial APP cleavage performed by an α-secretase (Buxbaum *et al*., 1998). α-secretase cleaves APP between Lys16 and Leu17 residues, cutting APP within the Aβ peptide sequence (Sisodia *et al*., 1999), preventing the formation of the amyloid plaque-forming peptide. α-secretase action yields extracellular sAPPα and an 83-residue CTF-α (also known as C83). Intracellular CTF-α is subsequently cleaved by intra-membrane γ-secretase, to give rise to intracellular p3 and AICD, figure 1.7.

Conversely, pro-amyloidogenic APP processing produces the Aβ peptide by the consecutive action of β- and γ-secretase (Lichtenthaler and Haass, 2004). β-secretase cleaves APP at the N-terminus of the Aβ sequence, producing a large ectodomain peptide, CTF-β or C99, which is cleaved by γ-secretase to give rise to intracellular AICD and Aβ, which has been found to be secreted into plasma and CSF (Cirrito *et al*., 2003). Distinct sites of γ-secretase action on CTF-β yield a number of potentially neurotoxic Aβ species (Hartmann *et al*., 1997; Lesné *et al*., 2006). There is conflicting evidence to show α-/β-secretase activity act in competition or reciprocally with one another. Some studies indicate BACE-1 inhibition does not enhance α-secretase activity and sAPPα release (Kim *et al*., 2008; Dobrowolska *et al*., 2014) and others reporting the converse (Postina *et al*., 2004; Fukumoto *et al*., 2010; Zhang *et al*., 2010; May *et al*., 2011) with enhanced sAPPα production following reduced BACE-1 expression. Similarly, a number of studies report increased α-secretase activity results in reduced β-secretase activity and Aβ formation (Lichtenthaler and Haass, 2004; Hiraoka *et al*., 2007). However, this relationship may depend on cell type and subcellular localisation of both secretase enzymes and APP substrate.

1.8.2.1 Regulation of APP processing by secretases

1.8.2.1.1 α-secretase

Putative α-secretases (ADAM-9, ADAM-10 and ADAM-17) are members of the ADAM (a disintegrin and metalloproteinase) family and are each type I transmembrane proteins. Of the three putative α-secretase enzymes, ADAM-10 and

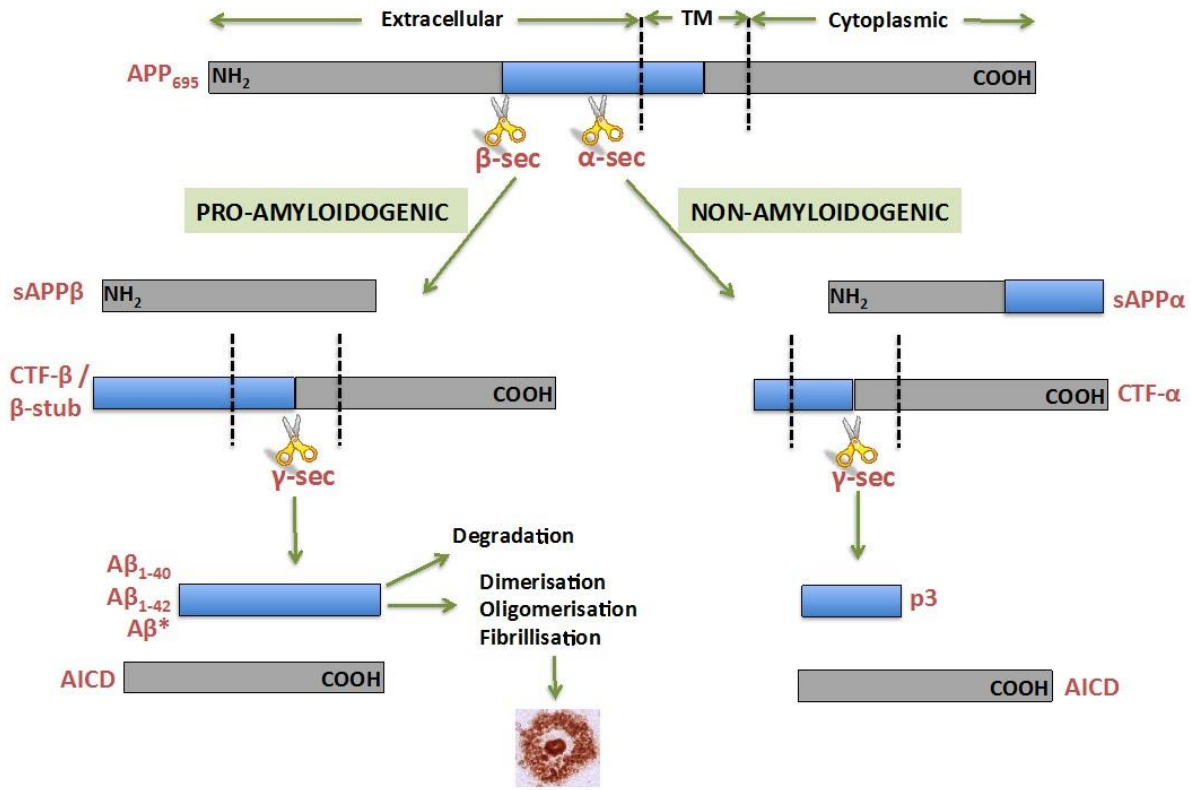

Figure 1.7: Amyloid precursor protein (APP) processing. Initial cleavage of APP occurs in the extracellular region of the peptide by either α- or β-secretase to release soluble APP fragments (sAPP) and intracellular C-terminal fragments (CTF). Membrane embedded γ-secretase subsequently carries out a second cleavage of APP within the transmembrane (TM) region of the CTF peptide. Cleavage of CTF-α by γ-secretase within the non-amyloidogenic pathway (right hand side), gives rise to APP intracellular cytoplasmic domain (AICD) and p3 fragments. Pro-amyloidogenic cleavage (left hand side) of APP gives rise to CTF-β that is cleaved by γ-secretase to yield AICD and various putative Aβ species, dependent on the residue of γ-secretase action. Aβ peptides can subsequently be degraded by neprilysin or dimerise, oligomerise and form fibrils, which are deposited as extracellular plaques.

ADAM-17 are the best characterised, whilst knock-out of ADAM-9 had no effect on APP processing and sAPPα generation, suggesting it is not a constitutive α-secretase and can be compensated for by other ADAMs (Kuhn *et al*., 2010). Under normal conditions, constitutive α-secretase processing is carried out by the zinc metalloproteinase ADAM-10 (Kuhn *et al*., 2010), which is localised to the cell surface and Golgi apparatus. Overexpression of ADAM-10 enhances non-amyloidogenic APP cleavage and knock-down completely suppressed α-cleavage (Kuhn *et al*., 2010) and results in enhanced Aβ plaque deposition (Postina *et al*., 2004). Rare ADAM-10 mutations exist in the population, but have been shown to have no role in sporadic AD onset (Cai *et al*., 2012) but in transgenic mice can enhance Aβ production through chaperone dysfunction (Suh *et al*., 2013; Vassar, 2013). ADAM-17 cleaves APP (as well as TNFα, amongst other notable cytokine and growth factor substrates) in a PKC-dependent process (Nitsch *et al*., 1992) and knock-out of ADAM-17 produced defective PKC-mediated sAPPα secretion, suggesting ADAM-17 is a regulated and stimulatory α-secretase (Buxbaum *et al*., 1998) in both primary neurons and cell lines (Zhang *et al*., 2011). The pharmacological broad-spectrum matrix metalloproteinase inhibitor TAPI-1 blocks the *in vitro* shedding of α-secretase cleaved cell surface proteins by both constitutive and stimulated ADAMs (Slack *et al*., 2001). *In vivo*, ADAM-10 is regulated by endogenous secreted TIMP-1 and TIMP-3 matrix metalloproteinase inhibitors (Postina, 2012; Vingtdeux and Marambaud, 2012).

1.8.2.1.2 β-secretase

Only one β-secretase has been identified in neurons and is known to be the sole enzyme responsible for pro-amyloidogenic APP processing, known as BACE-1. β-site APP cleaving enzyme (BACE-1) is a type I integral transmembrane protein and is an aspartyl protease (Cole and Vassar, 2007). BACE-1 functions optimally at low pH, hence is found in endosomes and the Golgi apparatus (Vassar, 1999), and whose activity is required for *Drosophila* glial cell survival (Bolkan *et al*., 2012). The BACE-1 homolog BACE-2 is expressed as the APP cleaving β-secretase in astrocytes (Bettegazzi *et al*., 2011), which cleaves APP within the Aβ peptide, analogous to α-secretase (Farzan *et al*., 2000). Under physiological conditions APP and BACE-1 are spatially segregated (Das *et al*., 2013) in neurons, with APP and BACE-1 localised to the trans-Golgi and recycling endosomes, respectively. BACE-1 overexpression shifts the subcellular localisation of APP, suggesting cleavage of the APP substrate and Aβ

formation are tightly controlled and depend on secretase availability (Lee *et al*., 2005). BACE-1 cleavage is the rate-limiting step in Aβ production (Vassar, 2004) and is an important therapeutic target, as BACE-1 knock-out removes both Aβ production and CTF-β generation, which has also been reported as a toxic species (Lahiri *et al*., 2006; Lauritzen *et al*., 2012) and reduces Aβ plaque pathology (Cai *et al*., 2001). BACE-1 knock-out mice display severe defects in hippocampal CA1 mossy fibre synapses, due to defective ryanodine receptor-mediated intracellular calcium release, which can be rescued by nicotine-mediated activation of α7nAChR that restores LTP (Wang *et al*., 2010a). BACE-1 knock-out mice are viable and fertile, but exhibit behavioural, pain sensitivity and muscle defects (Cheret *et al*., 2013) as a result of an accumulation of other BACE-1 substrates, such as Notch (Brou *et al*., 2000), neuregulin-1 and the β2 subunit of voltage-gated sodium channels.

1.8.2.1.3 γ-secretase

The intra-membrane cleavage of both α- and β-CTFs by γ-secretase gives rise to p3 and Aβ peptides, respectively. CTFs generated by α-/β-secretase cleavage of APP are difficult to detect due to a very short half-life (Kuhn *et al*., 2010) as a result of their high affinity to γ-secretase and subsequent rapid hydrolysis. The hydrophobic nature of the plasma membrane makes γ-secretase cleavage controversial, as peptide bond hydrolysis typically requires a water molecule (Haass *et al*., 2012).

γ-secretase exists as a high molecular weight complex, composed of a number of components: presenilin-1/-2, nicastrin, anterior pharynx-defective-1 (APH-1) and presenilin enhancer-2 (PEN-2). Each component is necessary for γ-secretase activity. Either of the presenilin (PS) isoforms (PS-1 and PS-2) can make up the transmembrane catalytic core of γ-secretase (Xia *et al*., 1998). PEN-2 regulates presenilin maturation, whilst nicastrin is a scaffold protein within the complex, acting as the size-selective substrate receptor (Xie *et al*., 2014) and implicated in intracellular calcium homeostasis and synaptic plasticity (Lee *et al*., 2014). APH-1 acts to stabilise nicastrin during formation of the γ-secretase complex (Zhang *et al*., 2011; Haass *et al*., 2012).

There exist a number of intra-membrane γ-secretase substrates, with 91 known to date (Haapasalo and Kovacs, 2011), with the most notable being APP and Notch. The huge variety of cellular processes regulated by PS-substrates makes targeting γ-secretase for therapeutic intervention in AD an enormous challenge (Wolfe, 2012).

Designing inhibitors capable of selectively targeting γ-secretase-mediated Aβ production remains a challenge in intelligent drug design (Haapasalo and Kovacs, 2011). The spatial separation of specific substrates across various subcellular membranous organelles may make targeting specific populations of presenilin-containing γ-secretase complexes easier (Jeon *et al*., 2013; Mizutari *et al*., 2013).

γ-secretase can cleave CTF-β within the plasma membrane to give rise to Aβ peptides ranging from 38-43 amino acids in length (Zhang *et al*., 2012). The predominant γ-secretase cleavage gives rise to the $A\beta_{40}$ isoform, but (as discussed above) mutations within PS-1 and PS-2 are a major cause of familial AD (Sisodia *et al*., 1999), with the majority of PS mutations altering γ-secretase action to favour formation of the aggregation-prone $A\beta_{42}$ isoform (Page *et al*., 2008). Selective loss of presenilins at presynaptic sites within neurons of the hippocampus impairs activity-dependent neurotransmitter release (Pratt *et al*., 2011), due to depleted endoplasmic reticulum calcium stores (Zhang *et al*., 2009) in a ryanodine receptor-mediated fashion (Oulès *et al*., 2012; Wu *et al*., 2013), resulting in impaired LTP induction. Thus, γ-secretase and its components play a vital role in a number of cellular processes and which probably accounts for the adverse effects observed both *in vivo* and *in vitro* following γ-secretase inhibition or knock-out (Wang *et al*., 2004; Selkoe and Wolfe, 2007).

1.8.2.2 Activity-dependent regulation of APP processing

APP processing and thus generation of Aβ is closely related to excitatory neuronal activity (Kamenetz *et al*., 2003; Cirrito *et al*., 2005, 2008; Tampellini *et al*., 2009; Tampellini and Gouras, 2010; Bero *et al*., 2011; Walker and Jucker, 2011). However, determining the precise relationship of APP, its proteolytic by-products and functional neuronal excitation is yet to be completely elucidated. Neuronal activity has been shown to modulate formation and secretion of Aβ in a number of cellular models, such as CNS cell lines, primary neurons, organotypic brain slices and *in vivo* using plasma and CSF microdialysis. Electrical depolarisation of synapses has been shown to both enhance pro-amyloidogenic APP cleavage and Aβ production (Kamenetz *et al*., 2003; Cirrito *et al*., 2005; Schroeder and Koo, 2005; Bero *et al*., 2011; Walker and Jucker, 2011) and conversely also promote non-amyloidogenic cleavage and reduce Aβ (Buxbaum *et al*., 1992; Nitsch *et al*., 1992; Hoey *et al*., 2009, 2013; Tampellini *et al*., 2009; Tampellini and Gouras, 2010; Cisse *et al*., 2011).

Recent data has attempted to clarify the opposing synaptic regulation of Aβ production by neuronal activity (Verges *et al*., 2011). Thus, it appears that neuronal electrical hyperexcitability is detrimental to synapses as a result of excessive neuronal activity, which enhances Aβ production and its progressive accumulation. For example, Aβ-mediated synaptic depression was observed in hippocampal slices, and the enhanced CTF-β production was reversed by blocking sustained neuronal activity with TTX or by blocking NMDAR with high Mg^{2+} application, and Aβ/CTF-β production was enhanced by ($GABA_A$ channel blocker) picrotoxin application. Reciprocally, hippocampal slices over expressing APP showed Aβ-mediated reductions in excitatory synaptic transmission in an NMDAR activity-dependent fashion (Kamenetz *et al*., 2003), suggesting a negative feedback loop to keep neuronal hyperactivity under control. The synaptic depression observed from hyperactivity-dependent Aβ production could contribute to the cognitive decline observed in AD. Furthermore, epileptiform electrical stimulation of afferent axons leading into the hippocampus and concomitant real-time *in vivo* microdialysis sampling of ISF showed a 30% increase in Aβ over a 1 h time period, which was reversed by TTX perfusion (Cirrito *et al*., 2005). Similarly, neuronal hyperexcitability is observed in transgenic models of AD (Palop *et al*., 2007; Busche *et al*., 2008), and increased Aβ deposition is observed in human epilepsy (Mackenzie and Miller, 1994), suggesting neuronal hyperexcitation could promote enhanced Aβ release and deposition. Excessive electrical depolarisation of cortical and hippocampal neurons increases presynaptic glutamate release, resulting in activation of both the synaptic and extrasynaptic population of ionotropic glutamate receptors. More subtle activation of neurons will induce release of physiological concentrations of glutamate, solely acting at the synaptic ionotropic glutamate receptor population (section 1.8.2.2.1). Activation of these distinct ionotropic glutamate receptor populations may give rise to the differential APP processing effects, further discussed below, and figure 1.8. Following more 'subtle' neuronal signalling, under more physiological conditions, synaptic activation reduced intraneuronal Aβ and protected synapses from Aβ-mediated synaptic changes and PSD-95 loss. Physiological synaptic activity has been shown to promote Aβ degradation by neprilysin and also enhanced APP trafficking to synapses (Tampellini *et al*., 2009), away from sites of BACE-1 activity.

Under normal conditions, the physiological concentration of Aβ species in the CSF is very low, within the picomolar range (1,500pM and 200pM for $Aβ_{40}$ and $Aβ_{42}$,

respectively (Puzzo and Arancio, 2013)), even after activity-dependent release of Aβ (Cirrito *et al*., 2003), and is not neurotoxic at these low concentrations. However, the rising concentration of Aβ in the extracellular space will no doubt play a role in the aggregation state of Aβ and thus its eventual toxicity (Schroeder and Koo, 2005). Nonetheless, exogenous application of picomolar concentrations of Aβ monomers and oligomers has been shown to enhance LTP and synaptic plasticity in hippocampal brain slices and boost both reference and contextual fear memory *in vivo* (Puzzo *et al*., 2008). In humans, the protective nature of cognitive activity has been shown by the correlation between higher educational level and reduced incidence of AD (Stern, 2006). This is further reinforced by environmental enrichment of transgenic AD model mice displaying reduced Aβ plaque load (Lazarov *et al*., 2005) and the fact that cognitively normal humans also secrete Aβ into the CSF. Thus, the notion that cognitive activity may or may not be protective is still somewhat controversial; due to conflicting data indicating neuronal depolarisation can paradoxically both increase and decrease Aβ level (Verges *et al*., 2011). Many of these contradictory findings will vary depending on the model system and especially the experimental conditions of promoting neuronal activity, through either electrical, synaptic or ion channel-mediated activation (Bordji *et al*., 2011).

A number of receptor and ion channel populations have been shown to selectively mediate activity-dependent non-amyloidogenic APP processing, including ionotropic glutamate receptors, metabotropic glutamate receptors, muscarinic and nicotinic acetylcholine receptors and other ligand-gated ion channels, and their associated literature shall be reviewed below.

1.8.2.2.1 Ionotropic glutamate receptors and APP processing

Ionotropic glutamate receptors are important in learning and memory, due to their role in mediating a large part of the postsynaptic calcium influx into neurons (Grienberger and Konnerth, 2012). NMDAR activation exhibits contrasting effects *in vivo*, with over activation being implicated in excitotoxicity, whilst physiological signalling through NMDAR is neuroprotective and plays a role in synaptic plasticity and neurotrophic processes (Hardingham, 2006). In recent years, uncovering the molecular mechanisms behind the reciprocal effects of NMDAR activation have identified two distinct pools of NMDAR, synaptic and extrasynaptic, which may explain the contradictory relationship between NMDAR activation and both cell survival and death. Synaptic NMDAR activation is neuroprotective (Léveillé *et al*., 2008; Hoey *et*

al., 2009; Bordji *et al*., 2010), whereas extrasynaptic NMDAR initiate neuronal death and neurodegeneration (Léveillé *et al*., 2008; Bordji *et al*., 2010; Talantova *et al*., 2013; Parsons and Raymond, 2014; Rush and Buisson, 2014). Selective NR2A-containing synaptic NMDAR activation reduced Aβ production whilst NR2B-containing extrasynaptic NMDAR activation increased Aβ release (Bordji *et al*., 2010), and hence is a promising therapeutic target. Accordingly, the NMDAR antagonist memantine (an approved therapeutic agent for the treatment of AD) has been shown to selectively block extrasynaptic NMDAR (Léveillé *et al*., 2008; Xia *et al*., 2010), with no effect on the remaining synaptic activity (Lipton, 2007) and confers a beneficial effect in AD patients. Memantine is a non-competitive open channel NMDAR blocker that only comes into effect in pathological conditions, to prevent prolonged channel opening of the extrasynaptic population of NMDAR (Lipton, 2007; Bordji *et al*., 2011) resulting in excitotoxicity and cell death. Aβ-induced down-regulation of synaptic NMDAR expression acts to further disrupt the balance between pro-survival and apoptotic cell signalling (Snyder *et al*., 2005). Thus, the relationship between prolonged extrasynaptic NMDAR activation and Aβ production is clear, whilst the mechanism behind synaptic NMDAR signalling and reduced Aβ production is yet to be fully elucidated, figure 1.8. The high calcium permeability of NMDAR (and also AMPAR) contributes to their ability to participate in induction of LTP and modulate synaptic plasticity. The calcium influx is also required for glutamate receptor-mediated APP processing (Hoey *et al*., 2009, 2013). In primary hippocampal neurons, activation of synaptic NMDAR promoted upregulation of transcription (Wan *et al*., 2012) and protein trafficking of the α-secretase ADAM-10 to the postsynaptic membrane (Marcello *et al*., 2007), where APP is predominantly localised (Hoey *et al*., 2009, 2013). Both synaptic NMDAR and AMPAR activation increases non-amyloidogenic APP processing, with reduced β-secretase cleavage of APP, reduced Aβ production and enhanced sAPPα and CTF-α production in primary cortical neurons (Hoey *et al*., 2009, 2013). Similarly,

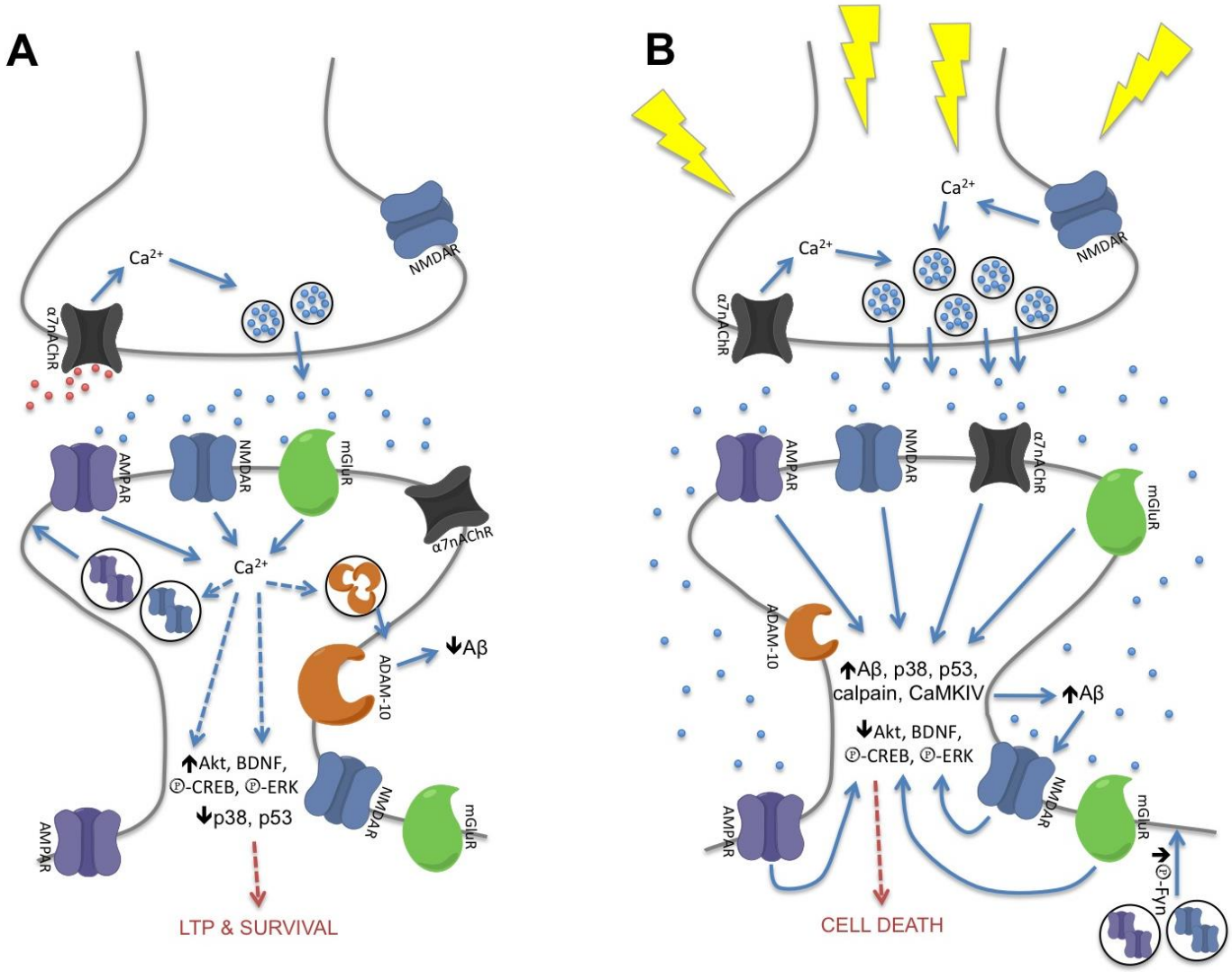
A
Ca2+
NMDAR
α7nAChR
AMPAR
NMDAR
mGluR
α7nAChR
Ca2+
ADAM-10
↓Aβ
↑Akt, BDNF,
Ⓟ-CREB, Ⓟ-ERK
↓p38, p53
AMPAR
NMDAR
mGluR
LTP & SURVIVAL
B
Ca2+
Ca2+
NMDAR
α7nAChR
AMPAR
NMDAR
α7nAChR
mGluR
ADAM-10
↑Aβ, p38, p53,
calpain, CaMKIV
↑Aβ
↓Akt, BDNF,
Ⓟ-CREB, Ⓟ-ERK
AMPAR
NMDAR
mGluR
→Ⓟ-Fyn
CELL DEATH

Figure 1.8: Schematic highlighting APP processing, Aβ production and secretion are closely related to neuronal activity and modulate neuronal survival. A: Subtle signalling through α7nAChR (grey) induces physiological concentrations of glutamate release (blue dots) throughout the cortex (Gray *et al*., 1996), which acts at synaptic receptor populations (NMDAR (blue), AMPAR (purple), mGluR (green)). Activation of synaptic receptors enhances non-amyloidogenic APP processing, through ERK-dependent ADAM-10 (orange) activation (Hoey *et al*., 2009; Verges *et al*., 2011), ERK-dependent ADAM-10 trafficking (Marcello *et al*., 2007; Wan *et al*., 2012), enhanced Aβ degradation and spatial separation of APP from BACE-1, whilst also reducing pro-amyloidogenic APP processing by BACE-1 (Tampellini *et al*., 2009). Synaptic receptor activation enhances pro-survival signalling cascades, through PI3K Akt, and CREB phosphorylation resulting in increased BDNF transcription (Léveillé *et al*., 2008). B: Neuronal hyperexcitability is detrimental to synapses through activation of extrasynaptic receptor populations, which increases pro-amyloidogenic APP processing, Aβ release, CTF-β production (Bordji *et al*., 2010) and pro-apoptotic signalling cascades through p38 MAPK and p53 (Parsons and Raymond, 2014). Extrasynaptic receptor activation is targeted by the clinically approved drug memantine (Lipton, 2007) for the treatment of AD.

selective activation of NMDAR (not AMPAR or metabotropic glutamate receptors) induced activity-dependent ADAM-10-mediated cleavage of nectin-1 and ectodomain shedding (Kim *et al*., 2010a). Upregulation of α-secretase expression and activity is ERK-dependent (Marcello *et al*., 2007; Wan *et al*., 2012), suggesting an ERK-dependent mechanism for non-amyloidogenic APP processing. Thus, the high relative calcium permeability and MAPK/ERK signalling through α7nAChR makes them a logical candidate for being putative APP processing modulators.

1.8.2.2.2 Neuronal α7nAChR and APP processing

Initial studies focussed on the effect of muscarinic acetylcholine receptors (section 1.8.2.2.3), with subsequent research highlighting the effect of nAChR activation on APP processing, however this has mostly been restricted to cell lines and through nAChR activation with the non-selective agonist nicotine. Many *in vitro* studies have highlighted the protective effect of nAChR activation, especially the α7 subtype, against Aβ-induced neurotoxicity (Zamani *et al*., 1997; Kihara *et al*., 2001; Shimohama and Kihara, 2001; Picciotto and Zoli, 2008; Yu *et al*., 2011) and also nicotine-induced sAPPα release (Kim *et al*., 1997; Lahiri *et al*., 2002; Mousavi and Hellström-Lindahl, 2009; Nie *et al*., 2010). Chronic treatment with nicotine for 6 weeks *in vivo,* following Aβ infusion, reduced CSF Aβ levels and BACE-1 protein levels in the hippocampus, whilst preventing Aβ-induced synaptic transmission defects and Aβ-mediated reduction in nAChR subunit expression (Srivareerat *et al*., 2011). Accordingly, when APP overexpressing AD transgenic mice were crossed with α7nAChR knock-out mice, enhanced cognitive decline was observed, with a dramatic loss in hippocampal neuron number and reduced brain volume, versus APP transgenic mice alone (Hernandez and Dineley, 2012). Furthermore, nicotine treatment of α7nAChR-expressing cell lines reduced Aβ release (Nie *et al*., 2010) and lowered Aβ plaque deposition (Nordberg *et al*., 2002) and soluble Aβ species (Hellström-Lindahl *et al*., 2004; Hedberg *et al*., 2008) in AD transgenic mice. Aβ has also been shown to modulate nAChR signalling, through directly binding to the α7 subtype of nAChR (Wang *et al*., 2000a, 2000b, 2009; Dineley *et al*., 2002a; Parri and Dineley, 2010; Nery *et al*., 2013), with implications in enhanced tau phosphorylation (Wang *et al*., 2010b), aberrant cell signalling (Dineley *et al*., 2001) and synaptic dysfunction (Hu *et al*., 2007).

1.8.2.2.3 Other cell surface receptors and APP processing

Modulation of APP processing by cell surface receptors was first demonstrated for M1 and M3 muscarinic acetylcholine receptors (mAChR), with the M2 and M4 subtypes displaying no effect (Nitsch *et al*., 1992). mAChR activation increased sAPP release and numerous subsequent studies confirmed this to be robust and reproducible (Haring *et al*., 1998; Davis *et al*., 2010; Cisse *et al*., 2011; Fisher, 2012). Activation of mAChR in both neuronal and glial cell lines induced a dose-dependent release of sAPP that was blocked by TTX (Buxbaum *et al*., 1992; Nitsch *et al*., 1992), and was PKC-dependent (Nitsch *et al*., 1992; Caputi *et al*., 1997). Furthermore, knock-out of M1 mAChR increased amyloid pathology, with enhanced Aβ production and reduced sAPPα secretion, both in vivo and in primary neurons (Davis *et al*., 2010). AChE inhibitors serve to boost endogenous ACh levels in the CNS and along with mAChR-selective PAMs, enhance and prolong mAChR activation (Fisher, 2012), enhancing cognition, similar to nAChR activation. Thus, targeting cholinergic signalling is an attractive a therapeutic target in AD, as both nAChR and mAChR activation exerts beneficial effects both *in vivo* and *in vitro*.

The purinergic P2X7 receptor, a non-selective ATP-gated cation channel is expressed in hippocampal neurons and glial cells, has been shown to mediate non-amyloidogenic APP processing, with enhanced sAPPα release, in a calcium influx-, ERK- and JNK-dependent manner (Delarasse *et al*., 2011). Furthermore, the G-protein coupled nucleotide receptor P2Y2 has been shown to similarly enhance ADAM-10/-17-mediated sAPPα release in a PKC- and ERK-dependent manner (Camden *et al*., 2005).

Metabotropic glutamate receptors have been shown, similar to ionotropic glutamate receptors, to possess contradictory effects on Aβ production, through both reducing and enhancing pro-amyloidogenic APP processing, Aβ production and release from synapses. Non-amyloidogenic APP processing was upregulated following mGluR activation in primary hippocampal neurons and a non-CNS cell line (Lee *et al*., 1995), however a bi-phasic effect of mGluR activation has been observed, with up to 50μM glutamate application to cortical brain slices promoting non-amyloidogenic APP processing, whilst higher doses produced negligible effect on sAPP release (Kirazov *et al*., 1997). In contrast, KCl-induced depolarisation of cortical synaptosomes has also been shown to induce sustained Aβ release, as well as α-, β- and γ-secretase activation (Kim *et al*., 2010b).

The similarities existing between receptor- and ion channel-mediated non-amyloidogenic APP processing subtype indicate α7nAChR are endowed with equally similar properties and are a viable target in the treatment of AD.

1.9 Targeting α7nAChR in Alzheimer's disease

Neuronal α7nAChR promote both direct and indirect activity-dependent neuroprotective mechanisms and are thus critical for maintenance of neuronal integrity within the CNS. Stimulation of α7nAChR has been proposed to reduce pro-amyloidogenic APP processing, enhance non-amyloidogenic APP processing and to attenuate Aβ-mediated toxicity. Exploiting these putative properties of α7nAChR to either delay AD onset or to treat the disease at later stages is the crux of a number of potential therapeutic avenues that are currently being explored by drug discovery. The α7-selective agonist A-582941 was used in the treatment of 3xTg-AD transgenic mice (expressing mutated PS-1 and double mutated APP), displaying robust AD pathology and cognitive deficits. Long-term α7nAChR activation restored cognition in the mice, as judged by novel object recognition, Morris water maze task and contextual fear conditioning, but had no effect on AD pathology (Medeiros *et al*., 2014),

The reported interaction between Aβ and α7nAChR has been the subject of intense research (Parri and Dineley, 2010), with data showing Aβ binding with high affinity (Wang *et al*., 2000a, 2000b; Dineley *et al*., 2001; Nagele *et al*., 2002) to the agonist binding site of α7nAChR (Nery *et al*., 2013); which when dissociated can restore α7nAChR- and also NMDAR-evoked currents (Dineley *et al*., 2002a; Wang *et al*., 2009), likely via restoring α7nAChR-mediated glutamate release. This remains controversial as Aβ-mediated toxicity has also been reported to occur through Aβ binding to receptor-dense lipid rafts (Rushworth and Hooper, 2011; Rushworth *et al*., 2013) and not to α7nAChR directly (Small *et al*., 2007). Aβ-induced α7nAChR inactivation results in LTD, excitotoxicity, neuron death and eventual cognitive decline. Thus, targeting both reduced Aβ-α7nAChR interaction and prolonged physiological α7nAChR activation, through Aβ-α7nAChR dissociating compounds, α7nAChR-selective agonists, PAMs and AChE inhibitors is an on going pharmaceutical strategy to enhance cognition and delay the onset of AD (Maelicke, 2000; Parri and Dineley, 2010; Parri *et al*., 2011).

1.9.1 AChE inhibitors

A long-standing mechanism for enhancing cholinergic transmission has been to selectively target and inhibit the hydrolysis of ACh by the serine hydrolase enzyme acetylcholinesterase (AChE), which acts to breakdown ACh at a rate of one molecule per 100μsec (Miwa *et al*., 2011). AChE inhibitors affect both nicotinic and muscarinic receptor function, as they boost levels and prolong action of the endogenous neurotransmitter ACh throughout the CNS. A number of AChE inhibitors have been approved for human clinical use (donepezil, galantamine and rivastigmine), for the treatment of AD. These compounds are the major class of drugs showing clinical efficacy, capable of retarding AD progression by 6-12 months. In AD cholinergic signalling from the basal forebrain degenerates, resulting in a loss of projections to the higher functioning centres of the brain (namely, the hippocampus and cortex) and subsequent cognitive decline and memory deficits (section 1.6). The reversible and non-competitive AChE inhibitor donepezil has shown cognitive enhancement properties and delayed deposition of AD-hallmark amyloid (Aβ) plaques (Colović *et al*., 2013) and reduced tau hyperphosphorylation (Noh *et al*., 2013). Donepezil has been further reported to exert homeostatic neuroprotective effects, by reducing microglial inflammatory cytokine release (Giunta *et al*., 2004; Hwang *et al*., 2010). In clinical trials the competitive, rapidly reversible, AChE inhibitor galantamine improved attention (Galvin *et al*., 2008) and has further been shown to block Aβ-induced glutamate excitotoxicity (Kihara *et al*., 2004) and boost Aβ clearance by microglia (Takata *et al*., 2010), another central mechanism in AD pathogenesis. Galantamine is known to further boost cholinergic signalling by acting as an α7nAChR-selective PAM (Maelicke *et al*., 2001; Dajas-Bailador *et al*., 2003). Rivastigmine acts at both AChE and the pseudocholinesterase butrylcholinesterase to enhance the endogenous level and temporal effect of ACh, and has been reported to lower Aβ levels in degenerating primary neurons (Bailey *et al*., 2011). Rivastigmine is approved for the treatment of both AD and Parkinson's disease (Colović *et al*., 2013). Boosting cholinergic signalling is a widely used treatment in a number of neurological disorders. This stems from attempts to recover a loss of ACh signalling, following a wealth of evidence indicating cholinergic dysfunction in the early stages of AD onset, termed the cholinergic hypothesis of AD.

1.10 Hypotheses and aims

The **hypotheses** of this thesis were that:

1. α7nAChR activation would enhance non-amyloidogenic APP processing in an ERK-dependent manner in primary cortical neurons and

2. α7nAChR activation would modulate inflammatory cellular behaviour of primary cortical microglia.

To investigate these hypotheses, specific **aims** were outlined:

1. To characterise the primary cortical neuronal and microglial model systems

2. To assess the α7nAChR-mediated contribution to APP processing, using an α7nAChR-selective agonist and PAM, in primary cortical neurons

3. To determine the α7nAChR contribution to inflammatory cell behaviour using α7nAChR-selective agonist and PAM, in primary cortical microglia.

Chapter 2

2. Materials and Methods

2.1 Materials

All bench chemicals were purchased from Sigma Aldrich, unless otherwise stated. All pharmacological compounds were purchased from Tocris, unless otherwise stated and were made up as 1000x concentrated stock solutions in either purified water or DMSO for long-term storage at -20°C. Compounds were added directly into culture medium to achieve a working concentration, unless otherwise stated, refer to Table 2.1 for all pharmacological compounds. All tissue culture reagents were purchased from Invitrogen, Paisley, UK. For primary and secondary antibody working concentrations and suppliers, as used in Western blotting and/or immunocytochemistry, refer to Table 2.2. A custom-made (Eurogentec) rabbit polyclonal antibody CT20 raised against the C-terminus of human APP (residues 676-695: NGYENPTYKFFEQMQN) was optimised and used for both Western blotting and immunocytochemistry.

Compound	Supplier	Stock concentration	Working concentration	Solvent	Information
α-bungarotoxin (αBTX)	Tocris	100μM	100nM	dH_2O	Irreversible α7nAChR antagonist
α-bungarotoxin Alexa Fluor-488 (αBTX-488)	Invitrogen	100μM	100nM	dH_2O	Irreversible α7nAChR antagonist conjugated to AlexaFluor-488
AMPA	Tocris	10mM	50μM	dH_2O	Selective agonist of AMPA-type glutamate receptors
β-secretase inhibitor (BSI)	Calbiochem	10mM	10μM	dH_2O	Peptide inhibitor sequence: H-Lys-Thr-Glu-Glu-Ile-Ser-Glu-Val-Asn-Stat-Val-Ala-Glu-Phe-OH
Choline bitartrate	Sigma Aldrich	30mM	3mM	Neurobasal medium	Weak α7nAChR-selective agonist
DAPT	Sigma Aldrich	10mM	10μM	DMSO	γ-secretase inhibitor
Dynasore	Gift from Dr Paul Whitley (Bath)	50mM	100μM	DMSO	Dynamin inhibitor, blocks endocytosis
Ethylene glycol tetraacetic acid (EGTA)	Sigma Aldrich	0.25M	2.5mM	dH_2O	Free calcium chelator
Lipopolysaccharide (LPS)	Sigma Aldrich	1mg/ml	100ng/ml	DMEM-F12 medium	Prototypical endotoxin purified from gram-negative bacteria
(-)-Nicotine hydrogen tartrate	Sigma Aldrich	10mM	10μM	Neurobasal medium	Broad nAChR agonist
MK-801	Tocris	2.5mM	2.5μM	dH_2O	Selective open channel NMDA receptor antagonist
NMDA	Tocris	10mM	50μM	dH_2O	Selective NMDA-type glutamate receptor agonist
PNU-120596	Tocris	10mM	10μM	DMSO	Selective type II positive allosteric modulator of α7nAChR
PNU-282987	Tocris	100mM	10μM	DMSO	Potent and selective agonist of α7nAChR

TAPI-1	Enzo Life Sciences	10mM	50μM	DMSO	Broad spectrum TACE and metalloprotease inhibitor
Tetrodotoxin (TTX)	Tocris	1mM	1μM	dH_2O	Potent neurotoxin, blocks voltage-gated sodium channels
U0126	Tocris	5mM	5μM	DMSO	MEK inhibitor

Table 2.1: Pharmacological compounds used to assess α7nAChR at the glutamatergic synapse *in vitro.*

Target	Supplier	Species	Working concentration		Information
			Western blot	ICC	
ADAM10	Sigma Aldrich	Rabbit	Not used	1:1,000 N/A	Raised against C-terminal residues 732-748 of human ADAM10
ADAM17	Chemicon	Rabbit	Not used	1:400 2.5µg/ml	Raised against residues 807-823 of human ADAM17
AlexaFluor-488/546	Invitrogen	Goat	Not used	1:1,000 2.0µg/ml	Goat anti-mouse/rabbit IgG secondary antibody used for immunofluorescence
APP	Eurogentec	Rabbit	1:2,000 1:5,000 (CTF blots)	1:1,500 N/A	Custom made, raised against C-terminal residues 680-695 of human APP_{695}
APP	Alpha Diagnostics	Mouse	Not used	1:100 10µg/ml	Raised against the N-terminus of APP (clone 13-M)
β-tubulin	Chemicon	Mouse	1:5,000 N/A	Not used	Used as a loading control for Western blotting
CD11b	Serotec	Mouse	Not used	1:1000 1.0µg/ml	Recognises cluster of differentiation molecule 11B, used as a specific marker for microglia
ERK2	Santa Cruz	Rabbit	1:5,000 0.4ng/ml	Not used	Recognises both phosphorylated and un-phosphorylated ERK2
ppERK1/2	Cell Signalling Technologies	Rabbit	1:1,000 N/A	Not used	Recognises individually or dually phosphorylated ERK1 and ERK2 at Thr202 and Tyr204 (ERK1) or Thr185 and Tyr187 (ERK2)
GFAP	Dako	Rabbit	Not used	1:10,000 0.1µg/ml	Recognises glial fibrillary acidic protein, used as a specific marker of astrocytes
GluA1	Millipore	Rabbit	Not used	1:500 N/A	Recognises GluA1-containing AMPA receptors. Raised against the cytoplasmic domain of GluA1
GluA2	Millipore	Rabbit	Not used	1:300 N/A	Recognises GluA2-containing AMPA receptors. No cross-reactivity with GluA1, GluA3 or GluA4
HRP-conjugated	Millipore	Goat	1:2,500 0.8µg/ml	Not used	Goat anti-mouse/rabbit-HRP secondary antibody used for Western blotting chemiluminescence
MAP-2	Chemicon	Rabbit	Not used	1:1,000 N/A	Recognises all MAP-2 isoforms (MAP2A, MAP2B, MAP2C and MAP2D)
PSD-95	Millipore	Mouse	1:500 N/A	1:500 N/A	Anchoring protein located at the postsynaptic density (PSD)

Synaptophysin	Sigma Aldrich	Mouse	1:500 N/A	1:200 N/A	Pre-synaptic marker. Clone SVP-38
Tau-1	Chemicon	Mouse	1:2,000 5.0µg/ml	1:500 2.0µg/ml	Recognises all species of Tau

Table 2.2: Antibodies used for Western blotting and immunocytochemistry (ICC).

2.2 Methods

2.2.1 Primary cortical neuron cell culture

All animal work was carried out in accordance with UK Home Office guidelines. Pregnant CD1 mice were sacrificed by cervical dislocation following a schedule 1 procedure. Primary cortical neurons were produced from mouse embryos at embryonic day 15-16. Embryonic brains were dissected and cortices dissociated in phosphate buffered saline (PBS) (Mg^{2+} and Ca^{2+}-free, pH 7.4) supplemented with 33mM glucose, using a heat-inactivated foetal bovine serum-coated fire-polished pipette. Subsequently, cells were centrifuged at 1,800 x g for 5 min and resuspended in Neurobasal medium, without phenol red and supplemented with B-27, 2mM glutamine, 100µg/ml streptomycin and 60µg/ml penicillin. During cortical dissection, care was taken to remove the striatum and meninges; these cultures also contained hippocampus precursor cells and hence are not 100% pure cortical neurons. Cells were plated (at 600,000 cells/ml for Western blotting or 300,000 cells/ml for all other uses) onto plastic Nunc multiwell (6- or 12- well) dishes coated with 20µg/ml poly-D-lysine and maintained for up to 18 days *in vitro* (DIV) in an incubator kept at 37°C with 5% CO_2. Morphological assessment of cell viability was made by phase contrast microscopy. Cells were visualised with a Nikon Eclipse TS100 microscope and phase contrast images taken using a Nikon Coolpix 5000 camera.

2.2.2 Primary cortical glial cell culture

All animal work was carried out in accordance with UK Home Office guidelines. Newborn P0-P2 CD1 mouse pups were sacrificed by cervical dislocation following a schedule 1 procedure. Cortices were dissected from brains in cold Mg^{2+} and Ca^{2+}-free PBS supplemented with 33mM glucose. During cortical dissection, care was taken to remove the striatum and meninges and resulting cortical sections were minced before centrifugation at 200 x g for 3 min. Cells were resuspended in warm 0.25% Trypsin-EDTA and incubated for 15 min in a 37°C 100rpm shaking water bath. Trypsinisation was halted with addition of 0.5ml DNase I (7,500 units in PBS) plus DMEM/F12 medium supplemented with HEPES, 10% heat-inactivated foetal bovine serum, 2mM glutamine, 100µg/ml streptomycin and 60µg/ml penicillin and mixed by inversion and pipetted to a single cell suspension (as per Saura *et al*., 2003), before

centrifugation at 200 x g for 7 min. Cells were resuspended in DMEM-F12 supplemented with HEPES, 10% heat-inactivated foetal bovine serum, 2mM glutamine, 100µg/ml streptomycin and 60µg/ml penicillin and were filtered with a 100µm mesh cell strainer (Fisher) and brought to a final density of 300,000 cells/ml. Full media changes were done to the primary mixed glial cultures (microglia and astrocytes) at 5 DIV and every subsequent 7 d until 4-6 weeks *in vitro* when confluency was reached.

2.2.3 Primary microglia purification

Removal of contaminating astrocytes from microglia was carried out 24 h prior to experimental use. Conditioned medium was removed and kept at 37°C whilst cells were incubated in 0.0625% Trypsin-EDTA in DMEM-F12 supplemented with HEPES, 2mM glutamine, 100µg/ml streptomycin and 60µg/ml penicillin for 15-25 min at 37°C. Multiwell plates were knocked every 5 min to aid complete astrocyte layer detachment and Trypsin activity halted with DMEM-F12 supplemented with 10% heat-inactivated foetal bovine serum, HEPES, 2mM glutamine, 100µg/ml streptomycin and 60µg/ml penicillin. Medium and astrocytes were aspirated and conditioned medium replaced onto microglia, maintained in an incubator kept at 37°C with 5% CO_2.

2.2.4 Immunocytochemistry

2.2.4.1 Immunocytochemistry staining

Visualisation of specific proteins of interest was carried out by immunocytochemistry on primary cells grown on 20µg/ml poly-D-lysine coated 13mm round glass coverslips in Nunc 12-well plates and used following 5-10 DIV. Cells were washed in fresh culture medium before fixation with 4% paraformaldehyde in PBS for 20 min at room temperature, washed with PBS three times. Non-specific primary antibody blocking was performed using 10% bovine serum albumin (BSA) in PBS (supplemented with 0.1% Triton X-100 for intracellular epitopes) for 30 min at room temperature. Primary antibodies were incubated overnight at 4°C in antibody buffer (3% BSA (with 0.1% Triton X-100 for intracellular epitopes) in PBS) on a rocking platform. Cells were washed three times with PBS before 1 h incubation with Alexa-Fluor conjugated secondary antibodies (1:1,000, Molecular Probes) in antibody buffer at room temperature. Finally, cells were washed with PBS three times and incubated with

DAPI (600nM, Invitrogen) for 10-30 min before coverslips were mounted onto glass slides using Mowiol.

2.2.4.2 Image acquisition

Immunofluorescence labelled cells were visualised using a Zeiss 510 META confocal laser-scanning microscope at either 40x or 63x. Images were analysed using Zeiss Image Browser software and ImageJ (NIH). Scale bars were applied following calibration of microscope-captured image size to relative image resolution.

2.2.5 Fluorescent labelling of α7nAChR

For α7 nicotinic acetylcholine receptor (α7nAChR) visualisation, live cells were incubated at 37°C with 100nM Alexa Fluor-488 conjugated α-bungarotoxin (αBTX-488, Invitrogen) for 45 min and subsequently washed in warm PBS (Kawai *et al*., 2002). The most commonly used primary antibodies directed to α7nAChR are unsuitable as they have shown immunoreactivity in α7nAChR knock out transgenic mice (Herber *et al*., 2004). Non-specific αBTX-488 binding was assessed by 10 min pre-incubation with 1mM nicotine or 5μM α-bungarotoxin. Cells were fixed with 4% paraformaldehyde in PBS for 20 min at room temperature and washed with PBS three times and incubated with DAPI (600nM, Invitrogen) for 10-30 min. For subsequent immunofluorescence antibody labelling, cells were subjected to the immunocytochemistry protocol listed above, following the fixation stage. Coverslips were mounted onto glass slides using Mowiol and visualised using a Zeiss 510 META confocal laser-scanning microscope at either 40x or 63x. Images were analysed using Zeiss Image Browser software and ImageJ (NIH).

2.2.6 Intracellular calcium microfluorimetry imaging

Measurement of calcium ion influx into primary cortical neurons was carried out using the ratiometric calcium chelator and fluorescent indicator Fura-2-acetoxymethyl ester (AM). Primary cortical neurons were grown on glass coverslips for 7 DIV and dye loaded for 45 min at 37°C. 5μM Fura-2 AM was incubated in combination with 0.02% Pluronic F-127 (Invitrogen) in assay buffer (140mM sodium chloride, 5mM potassium chloride, 1mM magnesium chloride, 1.8mM calcium chloride, 10mM glucose and 5mM HEPES in distilled water at pH 7.4). Following dye incubation, cells were washed in assay buffer and coverslips applied to the Concord microscope-based live imaging

platform (Perkin Elmer, UK) and maintained at 37°C with a constant supply of assay buffer (rate of 5ml/min) supplemented with 1μM TTX (Tocris) to limit background action potential spectral noise. Following baseline image recording, drugs were applied (in assay buffer) to the neurons by microperfusion, followed by a washout period with assay buffer. Fields of view with 30-40 cells were captured live every ~1 sec by dynamic video imaging and Fura-2 AM excited at 340 and 380nm wavelengths (SpectroMaster I), with emission detected at 510nm (Ultrapix PDCI low light CCD camera). Analyses of emission spectra were performed using Ultraview Concord software (Perkin Elmer, UK) and F340:380nm ratios plotted in Graphpad Prism 6. Values expressed are mean F340:380nm ± SD or SEM.

2.2.7 SDS-PAGE and Western blotting

2.2.7.1 Sample preparation for SDS-PAGE

After 5-18 DIV primary cells (neurons or microglia) were treated with drugs as indicated in figure legends. Cells were subsequently washed with ice-cold PBS (Mg^{2+} and Ca^{2+}-free, pH 7.4), lysed in 200μl RIPA buffer (50mM Tris, 150mM NaCl, 1% NP40, 0.5% sodium deoxycholate, 0.1% SDS, in dH_2O at pH 7.4) containing Complete Protease and Phosphatase Inhibitor Cocktails (Roche) and kept on ice for 45-60 min. Samples were scraped into Eppendorf tubes and centrifuged at 2,000 x g for 2 min before dilution of the supernatant in sample boiling buffer (62.5mM Tris, pH 6.8, 2% SDS, 5% 2-mercaptoethanol, 10% glycerol and 0.0025% bromophenol blue) before boiling for 5 min. Samples were stored at -20°C until required for Tris-Glycine SDS-PAGE.

2.2.7.2 Tris-Glycine SDS-PAGE

Tris-Glycine polyacrylamide resolving gels (8-12%) were prepared (375mM Tris (pH 8.8), 0.1% SDS, 8-12% acrylamide, 0.5mg/ml ammonium persulphate and 0.06% TEMED) and overlaid with 4% Tris-Glycine stacking gels (125mM Tris (pH 6.8), 0.1% SDS, 4% acrylamide, 0.5mg/ml ammonium persulphate, 0.06% TEMED) and stored at 4°C in SDS-PAGE running buffer (25mM Tris, 0.192M glycine and 0.01% SDS, National Diagnostics) for 24-48 h before use. Cell lysates were resolved by SDS-PAGE at 140V for ~1 h, alongside a See Blue protein molecular weight ladder (Invitrogen) in SDS-PAGE running buffer.

2.2.7.3 Western blotting

Acrylamide gel proteins were transferred onto 0.45µm nitrocellulose membranes (GE Healthcare) using a semi-dry transfer immunoblotting apparatus (Hoefer SemiPhor) at 1.5mA/cm^2 for 1 h. Nitrocellulose membranes were pre-soaked in distilled water before equilibration in blotting buffer (20% methanol plus SDS-PAGE running buffer), with Whatman filter papers equilibrated in blotting buffer placed either side of the gel and membrane. Non-specific antibody binding to membranes was blocked using 5% milk powder in TBS (20mM Tris, 150mM NaCl, pH 7.4) for 60 min. Membranes were rinsed quickly in TBS-T (20mM Tris, 150mM NaCl, 0.5% Tween-20, pH 7.4) before incubation with primary antibody in TBS-T and 1% milk powder overnight at 4°C on a rocking platform. Subsequent removal of unbound primary antibody occurred through quickly rinsing membranes once and subsequently three times for 5 min in TBS-T before 1 h incubation with a HRP-conjugated secondary antibody (1:2,500, Millipore) in TBS-T and 1% milk powder. Membranes were again washed three times for 5 min in TBS-T and finally once with TBS before protein band detection.

2.2.7.4 Protein detection

Primary and secondary antibody-incubated membranes were exposed to standard ECL reagent (GE Healthcare) for 1 min according to manufacturer's instructions. Blots were exposed to Hyperfilm ECL (GE Healthcare) in an autoradiography film cassette in the dark, and developed by X-ray film processor (OPTIMAX). Alternatively, ECL-exposed membranes were imaged by a Fusion SL (Vilber Lourmat) chemiluminescence camera and digital images captured directly for analysis.

2.2.7.5 Analysis of protein densitometry

Densitometry quantification of bands on Hyperfilm-exposed blots was carried out after scanning films (Epson V700 scanner) at a resolution of 1200 dots/inch (dpi) and mean background optical density (OD) of bands interpolated from an OD calibration curve, calculated from an OD step tablet using ImageJ software (NIH). Fusion SL acquired digital images were analysed with FUSION software (Vilber Lourmat). Mean OD data were expressed relative to a loading control ± SEM and were subjected to statistical analysis in GraphPad Prism 6 software.

2.2.8 APP C-terminal fragment Western blotting

To assess the modulation of APP processing, intermediate APP_{695} cleavage products (C-terminal fragments (CTF)) analyses was carried out by Tris-Tricine SDS-PAGE.

2.2.8.1 APP-CTF sample preparation

After 10-18 DIV neurons were treated with drugs as described in figure legends. Neurons were subsequently washed with ice cold PBS (Mg^{2+} and Ca^{2+}-free, pH 7.4), lysed in sample boiling buffer for 30-60 min (62.5mM Tris pH 6.8, 2% SDS, 5% 2-mercaptoethanol, 10% glycerol and 0.0025% bromophenol blue) and scraped into Eppendorf tubes. Samples were centrifuged at 2,000 x g for 5 min before boiling for 5 min.

2.2.8.2 Tris-Tricine SDS-PAGE

Tris-Tricine polyacrylamide resolving gels (16.5%) were prepared (1M Tris (pH 8.45), 16.5% acrylamide, 0.5mg/ml ammonium persulphate and 0.06% TEMED) and overlaid with 4% Tris-Tricine stacking gels (1M Tris (pH 8.45), 4% acrylamide, 0.5mg/ml ammonium persulphate, 0.06% TEMED) and stored at 4°C in SDS-PAGE running buffer (25mM Tris, 0.192M glycine and 0.01% SDS, National Diagnostics) for 24 h before use. Lysates were resolved by gel electrophoresis at a constant 105V using a defined inner/cathode gel tank buffer (100mM Tris, 100mM Tricine, 0.1% SDS pH 8.2) and outer/anode tank buffer (0.2M Tris pH 8.9) and run for 3-4 h, alongside a See Blue protein molecular weight ladder, until adequate separation of the low molecular weight ladder bands was reached.

2.2.8.3 Western blotting for APP-CTFs

Tris-Tricine gel-resolved samples were transferred to 0.2µm PVDF membranes (Millipore) using semi-dry transfer at 1.5mA/cm^2 for 1 h. PVDF membrane was pre-soaked in methanol before equilibration in CTF blotting buffer (20% methanol plus SDS-free running buffer, 25mM Tris and 0.192M glycine, National Diagnostics) with Whatman filter papers equilibrated in CTF blotting buffer placed either side of the gel and membrane. Non-specific antibody binding was blocked using 4% ECL Advance (GE Healthcare) blocking powder in TBS (20mM Tris, 150mM NaCl, pH 7.4) for 1 h. Membranes were rinsed three times for 20 min in TBS-T (20mM Tris, 150mM NaCl, 0.5% Tween-20, pH 7.4) before incubation with primary antibody in TBS-T and 4%

ECL Advance blocking powder overnight at 4°C on a rocking platform. Removal of unbound primary antibody followed through quickly rinsing membranes once and subsequently 3 times for 20 min in TBS-T before 1 h incubation with a HRP-conjugated secondary antibody (1:150,000, Millipore) in TBS-T and 4% ECL Advance blocking powder. Membranes were again washed at least 4 times for 20 min in TBS-T and finally once with TBS before exposure to ECL Advance reagent (GE Healthcare) for 1 min according to manufacturer's instructions. Blots were exposed to Hyperfilm ECL (GE Healthcare) and developed for densitometry quantification using ImageJ software (NIH), as detailed above.

2.2.9 Synaptosome preparation and treatment

Synaptosomes are a useful tool for studying nerve terminals, free of axons and postsynaptic connections. Synaptosomes are resealed nerve terminals, and closely resemble functional nerve terminals found *in vivo*.

2.2.9.1 Tissue preparation

All animal work was carried out in accordance with UK Home Office guidelines. Adult CD1 mice were sacrificed by cervical dislocation following a schedule 1 procedure. Cortices were rapidly dissected, washed in isotonic homogenisation buffer (0.32M sucrose, 1mM EDTA, 5mM Tris, 0.25mM DTT, pH 7.4), before being weighed and homogenised in 10% w/v homogenisation buffer. All brain material was carefully stored on ice for the duration of the preparation and centrifuges and rotors cooled to 4°C in advance. The crude homogenate was centrifuged at 1000 x g for 10 min in polycarbonate tubes and the S1 supernatant diluted 1.5x in homogenisation buffer before being flowed onto the top of a discontinuous Percoll gradient.

2.2.9.2 Percoll gradient preparation

Discontinuous Percoll gradients were used to separate and purify organelles, including synaptosomes, by their differential density (as per Dunkley *et al*., 2008). Percoll slurry was filtered through 0.45μm syringe filter units (Millipore) before diluting in gradient buffer (1.28M sucrose, 4mM EDTA, 20mM Tris, 0.1mM DTT, pH 7.4) to produce 3%, 10%, 15% and 23% (w/v) Percoll gradient buffers. 2ml of each gradient buffer was flowed, using a peristaltic pump (Gilson Minipuls 2), at a rate of 0.5ml/min, through a 12 gauge needle constantly placed at the top of the meniscus whilst

touching the wall of an angled polycarbonate tube, to minimise Percoll layer disruption. Percoll gradient buffers of 15%, 10% and 3% were sequentially layered onto the bottom 23% Percoll gradient buffer to create the discontinuous gradient required for density gradient centrifugation of mouse brain material. Gradients were made 15-20 h before use and carefully stored on ice at 4°C until S1 supernatants were prepared.

2.2.9.3 Synaptosome preparation and purification

S1-layered Percoll gradients were centrifuged at 31,000 x g for exactly 5 min (excluding acceleration and deceleration times) with rotor breaking disabled, thus ensuring optimal interface separation. Fractions 3 and 4 (synaptosomes plus membranes and pure synaptosomes, respectively) were pooled to increase yield. Synaptosomes were diluted at least 4-fold with ice-cold sucrose/EDTA buffer (0.32M sucrose, 1mM EDTA, 5mM Tris, pH 7.4) before centrifugation at 20,000 x g for 30 min at 4°C to remove Percoll. The synaptosomal pellet was carefully resuspended (using a fire-polished glass pipette) in 1-2ml physiological buffer (118mM sodium chloride, 2.4mM potassium chloride, 1.2mM magnesium chloride, 1.2mM sodium dihydrogen orthophosphate 1-hydrate, 2.4mM calcium chloride 2-hydrate, 20mM HEPES, 10mM glucose, pH 7.4) before a final spin at 18,000 x g for 10 min and the pellet of viable synaptosomes resuspended in a required volume (typically 0.5-1ml) of physiological buffer and subjected to Bradford protein assay.

2.2.9.4 Synaptosome drug treatments

Synaptosomes (at 2-3mg/ml protein concentration) were incubated in a water bath at 37°C for 10 min pre-treatment with vehicle or 10μM PNU-120596, before a 30 min vehicle or agonist (10μM PNU-282987 or 50μM NMDA) treatment. Following drug treatments, synaptosomes were spun at 10,000 x g for 5 min before addition of lysis buffer to the pellet (0.5% Triton X-100, 150mM sodium chloride, 10mM HEPES, complete protease and phosphatase inhibitor tablets (Roche), pH 7.4) and sample boiling buffer (62.5mM Tris pH 6.8, 2% SDS, 5% 2-mercaptoethanol, 10% glycerol and 0.0025% bromophenol blue) before boiling for 5 min. Denatured synaptosome samples were stored at -20°C until required for SDS-PAGE and Western blotting, as detailed above.

2.2.10 APP-Gal4 cleavage luciferase reporter assay

To study APP cleavage using a high-sensitivity molecular gene reporter assay, primary neurons (following 5 DIV) were transfected with 0.5μg APP_{695}-Gal4 fusion construct, 0.5μg pC1-CMV-Fe65 construct, 0.5μg pFR-Luciferase construct (firefly luciferase gene from *Photinus pyralis*) and 0.5μg phRL-*Renilla* construct (luciferase gene from *Renilla reniformis*) using Lipofectamine 2000 (0.5μl/well; Invitrogen). Transfection mixes were made up in OptiMEM I medium (Invitrogen) 25 min in advance of application onto neurons. 10μM DAPT was added 30 min prior to transfection mix and left for 24 h in a 37°C incubator before application of drugs. Following 6 h 10μM PNU-120596 and 10μM PNU-282987 drug treatments neurons were lysed for 15 min with Glo Lysis Buffer (Promega) and Dual-Glo luciferase activity measured using a FluorBMG microplate luminometer, according to the manufacturer's instructions. Firefly luciferase reporter activity was normalised to constitutive *Renilla* luciferase activity to control for transfection rate efficiency between repeat conditions and expressed as fold change of vehicle-treated control. Following APP_{695}-Gal4 cleavage by β-secretase, APP-CTF-Gal4 is produced, which is further cleaved by γ-secretase, giving rise to AICD-Gal4. AICD-Gal4 binds to the upstream activating sequence (UAS) of Firefly/*Renilla* luciferase DNA and promotes its transcription within transfected primary cortical neurons. Subsequent translation of luminescent luciferase peptide is detected through the Dual-Glo luciferase assay (Promega). A schematic of the luciferase APP cleavage reporter assay can be found in figure 4.7.

2.2.11 Egr-1 transcription luciferase reporter assay

$1x10^5$ plaque forming units (pfu)/ml Ad5-Egr1-luciferase plasmid was transduced into primary cortical neurons at 6-7 DIV in 24 well plates. For transduction, conditioned media was removed from the neurons and fresh media containing viral particles was added to the cells and incubated at 37°C for 3 h. Media was then removed and original conditioned media replaced onto the neurons. Neurons were subsequently treated as detailed in figure legends. 6 h post-treatment, media was removed from the cells and cells lysed in Glo Lysis Buffer (Promega) and incubated at room temperature whilst rocking for 15 min. Lysed cells were transferred to a white 96-well plate and Dual Glo substrate was added, the plate was incubated in the dark for 10 min followed by

measurement using a FluorBMG microplate luminometer. Luciferase activity was expressed as fold change of vehicle-treated control.

2.2.12 Microglial bead uptake assay

To observe microglial phagocytic activity, purified primary microglia were cultured on 20μg/ml poly-D-lysine coated 13mm round coverslips. Latex (amino-modified polystyrene) 1.0μm beads with fluorescent green-yellow tag (excitation/emission: 470/540nm) were used as quantifiable phagocytosis targets. Drugs were added, as indicated in figure legends, to a 0.5μl/ml bead stock solution of PBS supplemented with 0.1% bovine serum albumin (BSA), and were incubated on the microglia for 2 h at 37°C. Following a 2 h bead ± drug incubation, cells were washed 3 times with ice cold PBS (Mg^{2+} and Ca^{2+}-free, pH 7.4) and fixed with warm 4% paraformaldehyde in PBS for 20 min at room temperature. Following fixation, cells were washed a further three times with PBS, nuclei counter-stained with 600nM DAPI and coverslips mounted onto glass slides using Mowiol for fluorescence microscopy. Cells were examined under a Zeiss 510 META confocal laser-scanning microscope at 20x magnification. Z-stack images indicated beads were engulfed by cells and not merely surface-bound. Numbers of ingested beads were counted manually and used to determine mean bead uptake across randomly selected fields of view containing 40+ cells.

2.2.13 Statistical analyses

Mean data ± SEM/SD were graphed and analysed using GraphPad Prism 6 software. Data were analysed using one-way ANOVA with Bonferroni post-test and considered statistically significant when $p<0.05$. Levels of significance between indicated conditions were: * = $p<0.05$, ** = $p<0.01$, *** = $p<0.005$, **** = $p<0.001$.

Chapter 3

3. Characterisation of α7nAChR at the glutamatergic synapse

3.1 Introduction

Glutamatergic synapse development is an essential and fundamental part of brain development, requiring communication between major excitatory and inhibitory receptor types, namely, N-methyl-D-aspartic acid (NMDA), α-amino-3-hydroxy-5-methyl-4-isoxazolepropionic acid (AMPA) and gamma-aminobutyric acid ($GABA_A$) receptors (Wang and Kriegstein, 2008). Synaptic activity is required for synapse formation, and in the developing synapse initial activity is mediated by NMDA receptors (NMDAR) (Durand *et al*., 1996; Wu *et al*., 1996). Immature neurons initially lack surface-expressed AMPA receptors (AMPAR), and the NMDAR pore is blocked by Mg^{2+} ions, rendering synapses silent until maturation occurs. During postnatal development, ACh signalling from the basal forebrain activates cortical presynaptic α7nAChR, which regulate glutamate release. Glutamate release subsequently activates postsynaptic NR2B-containing NMDAR, the activation of which contributes to enhanced insertion of AMPAR into the postsynaptic membrane (Metherate, 2004).

The importance of cholinergic input into the cortex has been reinforced by selective cholinergic input depletion in primates, through immunotoxin exposure. Cholinergic pathway-depleted monkeys retained episodic memory and decision-making capability, but displayed severely impaired working memory (Croxson *et al*., 2011), consistent with the cholinergic hypothesis of AD (Bartus *et al*., 1982; Perry, 1986; Francis *et al*., 1999) and the key role of ACh signalling to the cortex. The role of presynaptic α7nAChR in modulating cortical postsynaptic receptor function has largely focussed on neurotransmitter release, with α7nAChR playing a homeostatic role in modulating the subtleties of glutamate release at the glutamatergic synapse (Huang *et al*., 2010; Gomez-Varela and Berg, 2013; Cheng and Yakel, 2014), postsynaptic glutamate receptor expression (Wang *et al*., 2013), cell survival, neuronal plasticity, LTP and learning and memory (Zolles *et al*., 2009).

Much of what we currently understand about α7nAChR function comes from electrophysiology studies of overexpressing cell lines and exogenous receptor expression in *Xenopus* oocytes. Such data have paved the way for our in-depth understanding of the molecular and structural functionality of nAChR, but lack the physiological relevance and insight into downstream cellular signalling, following α7nAChR activation. Thus, the results described in this chapter are from experiments

utilising primary mouse cortical neurons as a model system for studying α7nAChR activity at glutamatergic synapses.

This chapter aims to thoroughly characterise this model system, first with respect to the expression and function of ionotropic glutamate receptors (GluR) before probing the expression and concomitant functionality of α7nAChR *in vitro*.

3.2 Results

3.2.1 Primary cortical cultures display a neuronal phenotype and express neuron-specific proteins

Initial characterisation of primary mouse cortical neuron cultures from e15-16 CD1 mice following 5 days in vitro (DIV) appeared neuronal under phase contrast microscopy, with extensive dendrites and axonal projections from the cell body (figure 3.1A). To further validate these cells were neuronal, the distribution of neuron-specific proteins Tau and MAP-2 was examined by fluorescence immunocytochemistry. Tau is known to be most abundant in axons, but can also be localised to somatodendritic compartments (Morris *et al*., 2011). MAP-2 is mainly expressed in neurons, where it is found specifically localised to dendrites; but is also expressed in oligodendrocytes (Dehmelt and Halpain, 2004). Double immunofluorescence showed distinct (non-colocalised) subcellular localisation of these proteins, revealing axonal Tau and dendritic MAP-2 (figure 3.1B) consistent with the expected neuronal phenotype of these cultures. Further immunocytochemistry with an anti-GFAP antibody showed minimal glial contamination suggesting cultures were 95-99% neuronal (data not shown).

3.2.2 Primary cortical neurons express postsynaptic AMPAR that couple to calcium influx

To initially determine whether the primary cortical neurons possessed the cellular components expected within glutamatergic synapses, 7 DIV neurons were used to assess expression and distribution of α-amino-3-hydroxy-5-methyl-4-isoxazolepropionic acid (AMPA)-type glutamate receptor (AMPAR) subunits, GluA1 and GluA2. Immunofluorescence labelling of the cortical neurons revealed widespread expression of GluA1 (figure 3.2Ai) and GluA2 (figure 3.2Bi) throughout both the cell body and projections of neurons, consistent with the glutamatergic nature of the model system. Double immunofluorescence labelling of the AMPAR subunits with the nerve terminal marker synaptophysin revealed little colocalisation of either GluA1 or GluA2 with synaptophysin (figure 3.2Aii and 3.2Bii, respectively). However, GluA1 and GluA2 expression extensively colocalised with the postsynaptic marker PSD-95 (figure 3.2Aiii and 3.2Biii, respectively), indicating AMPAR are predominantly postsynaptic in primary cortical neurons, in accordance

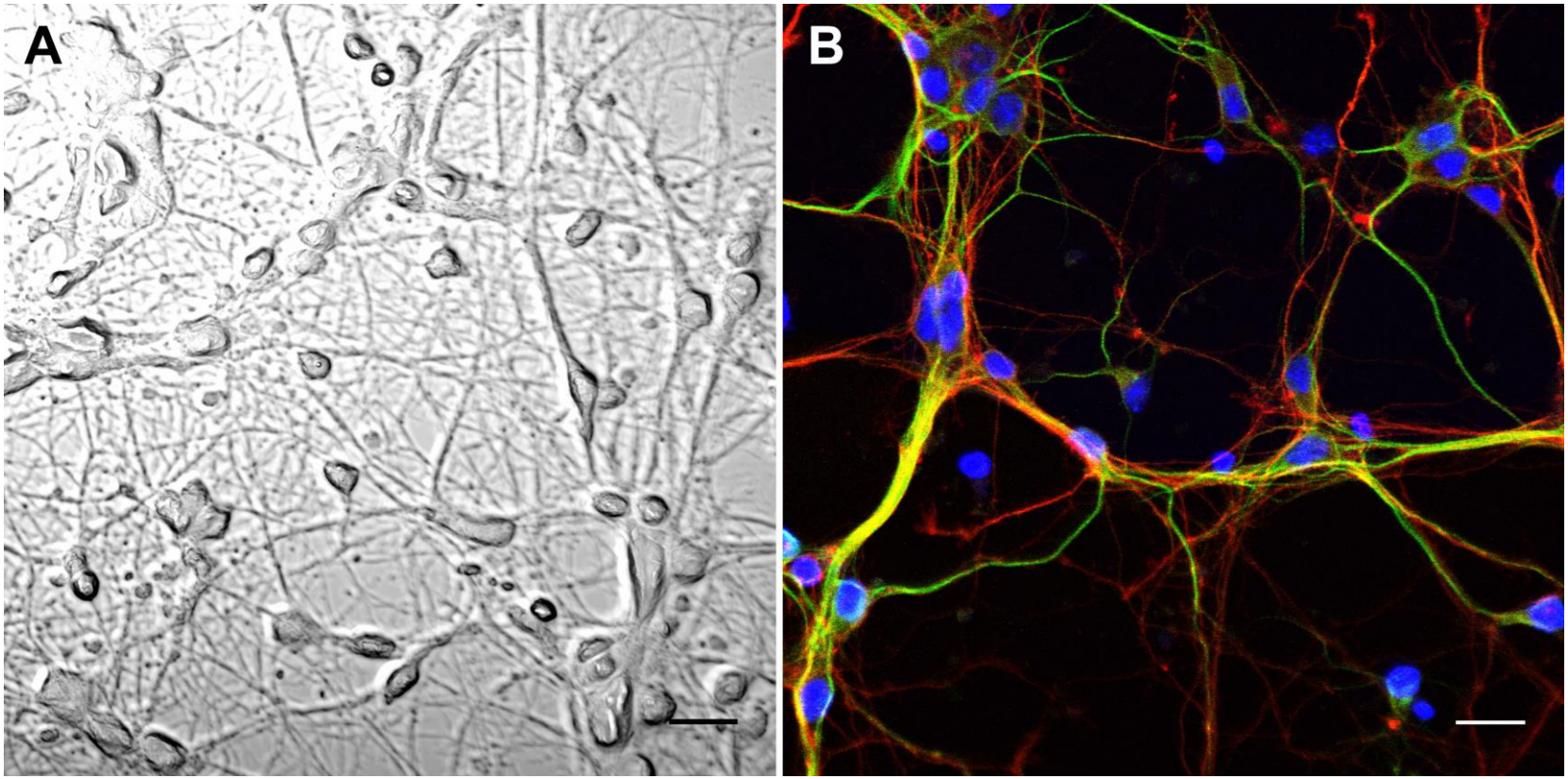

Figure 3.1: Cortical neurons display a classical neuronal phenotype and express neuron-specific proteins. A: Phase contrast imaging of primary cortical neurons at 5 DIV and 40x magnification. Classical morphological features of neurons are observed, with networks of axons and dendrites extending from cell bodies. B: Neuron-specific immunofluorescence labelling of primary cortical neurons at 5 DIV at 40x magnification. Double immunostaining for the axonal marker Tau (red) and dendritic marker MAP-2 (green) reveals distinct subcellular localisation of the proteins. Nuclei are counterstained with DAPI (blue). Scale bars indicate 20μm.

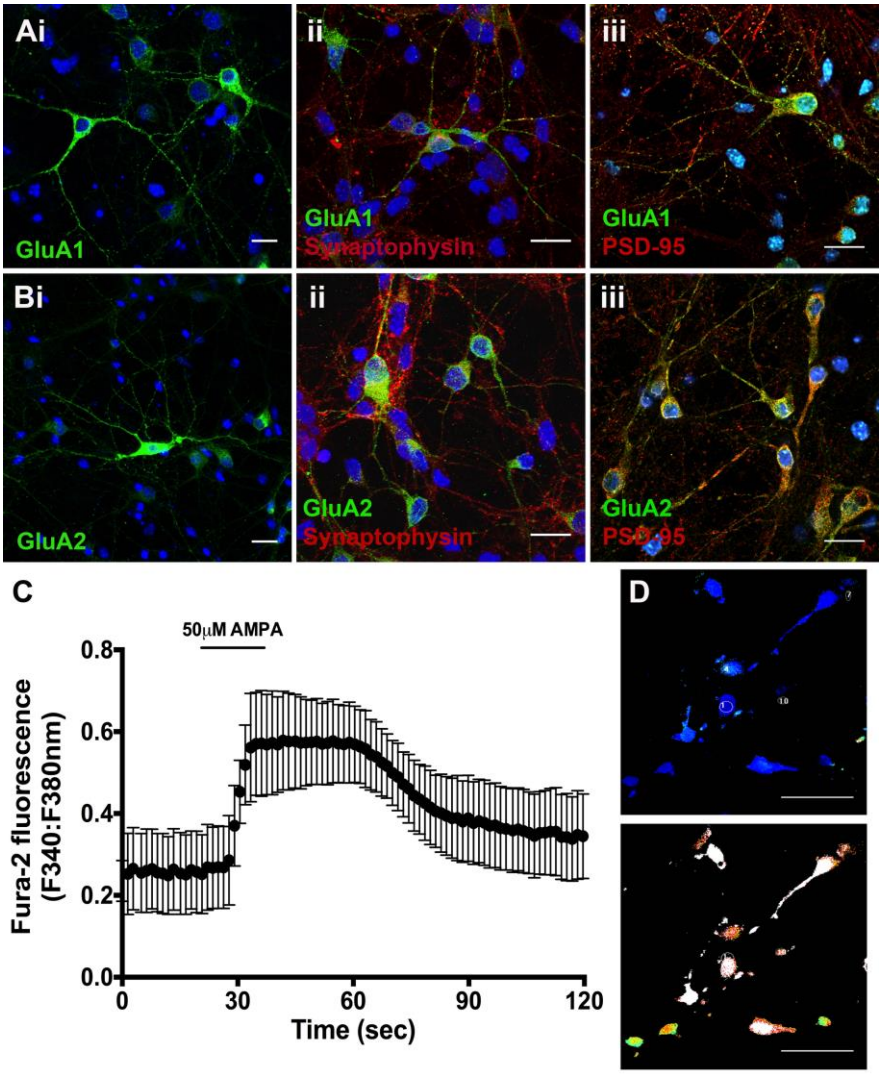

Figure 3.2: Cortical neurons express postsynaptic and functional AMPAR. A: AMPAR GluA1 subunit-specific immunofluorescence of 7 DIV primary cortical neurons shows GluA1 (Ai, green) is expressed throughout the cell body and neuronal projections. Double staining with nerve terminal synaptophysin (Aii, red) reveals little overlap but a strong postsynaptic colocalisation of AMPAR with PSD-95 (iii, red). B: Similarly, GluA2 immunofluorescence (Bi, green) reveals widespread (~90%) neuronal expression, minimal nerve terminal expression (Bii) with no overlap with synaptophysin (red) and strong postsynaptic expression (Biii, colocalisation with PSD-95, red). GluA staining reveals 80-90% of the neuronal population express AMPAR. A-B scale bars indicate 20μm. C: Fura-2 AM microfluorimetry ratiometric trace reveals an AMPA-induced increase in intracellular calcium, across all n=11 cells, mean F340:380nm ±SD. Neurons were microperfused with assay buffer before a 20 sec pulse of 50μM AMPA (indicated by black line). Cells were imaged every ~1 sec by dynamic video imaging to capture live pseudocoloured images. D: Representative pseudocoloured images of baseline intracellular calcium influx (top) and maximal AMPA-induced calcium influx at 50 sec (bottom) are shown. Microfluorimetry scale bars indicate 100μm.

with previous studies both *in vitro* (Lozada *et al*., 2012) and *in vivo* (Ehrlich and Malinow, 2004). The subunit composition of AMPAR determines the level of calcium ion permeability, and so to establish the calcium permeability properties of the primary cortical neurons, AMPA-mediated changes in intracellular calcium were probed, using a chemical calcium indicator FURA-2 AM and single cells visualised live by dual-emission microfluorimetry. As AMPA-induced calcium fluxes in neurons can be indirect, as result of the opening of voltage-dependent calcium channels, all microfluorimetry recordings were undertaken or performed in the presence of 1μM tetrodotoxin (TTX). Initial baseline recordings (0 to 20 sec) indicated little, if any, spontaneous action potential firing in the primary cultures (figure 3.2C), with no visible fluorescence change observed across the field of view (figure 3.2D, top). 50μM AMPA application for 20 sec induced a rapid increase in intracellular calcium, with the F340:380nm ratio recorded adopting a classical trace, as observed across many previous studies (Rainey-Smith *et al*., 2010; Hoey *et al*., 2013). The observation of rapid and strong intracellular calcium influx was reinforced by dynamic video imaging-captured images showing increased fluorescence intensity (blue/green to orange/white) within pseudocoloured images (figure 3.2D, bottom). These data suggest that widespread AMPAR expression in cultured cortical neurons enables calcium influx through calcium-permeable postsynaptic AMPAR.

3.2.3 Neuronal AMPAR are functional and couple to ERK phosphorylation

Having demonstrated glutamatergic components of the primary cortical neurons, through probing the expression and calcium-permeability of GluA1/2-composed AMPAR, AMPA-mediated neuronal activity was further assessed by examining modulation of a known downstream effector of AMPAR activation, ERK phosphorylation. 5-10 DIV neurons were treated with 50μM AMPA for up to 1 h, and lysates immunoblotted for dual-phosphorylated (Thr202 and Tyr204) active pERK2 and total ERK2. AMPAR activation caused a robust and significant ~2-fold increase in ERK2 phosphorylation, as rapidly as 3 min and was sustained over 15 min of AMPA treatment (figure 3.3). Over a longer AMPA treatment time course (30-60 min), the variation in AMPA-mediated ERK phosphorylation increased, likely due to AMPAR desensitisation, activity of ERK phosphatases and natural biological variation of the neurons between cultures. The AMPA-mediated change in pERK2 density was not due to varied levels of protein loaded into gels, as no change was

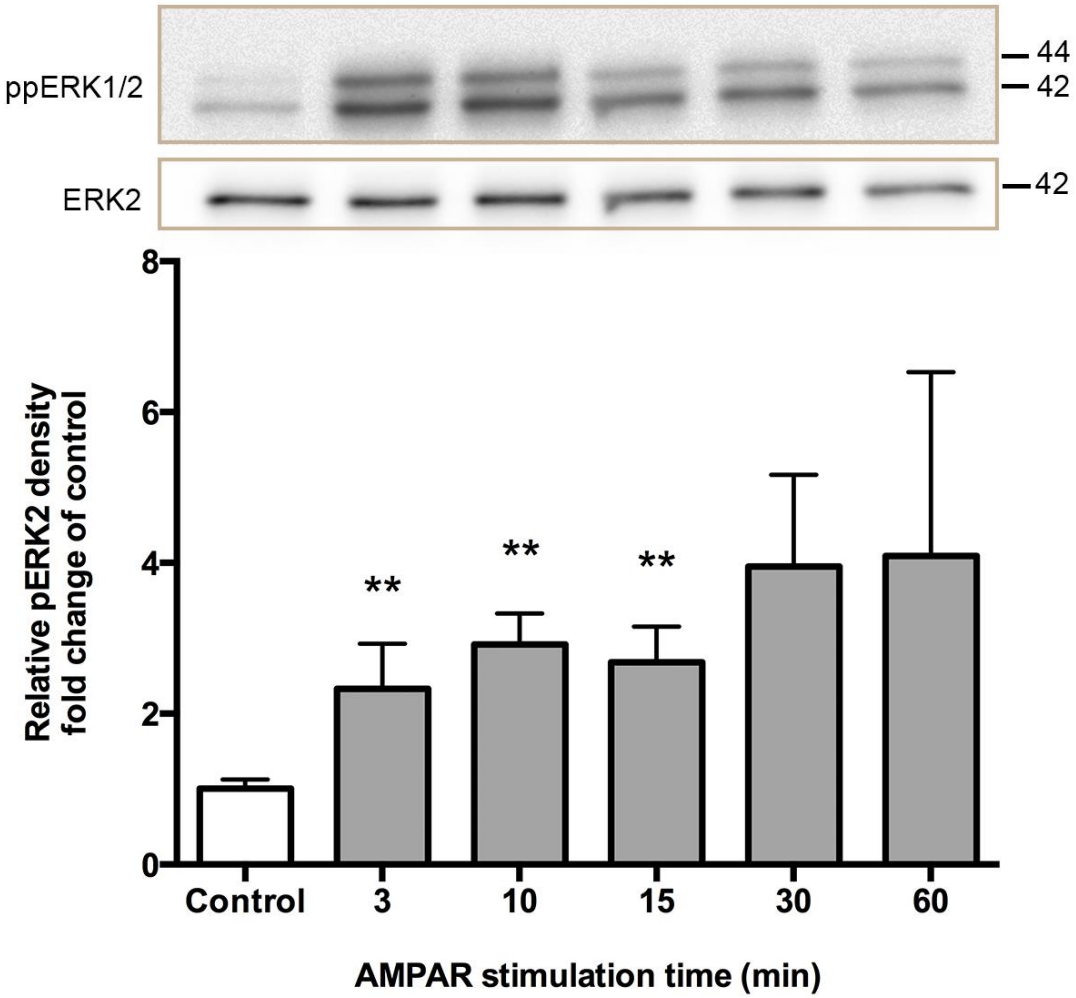

Figure 3.3: AMPA-induced ERK phosphorylation is time-dependent. 50μM AMPA treatment of 5-10 DIV primary cortical neurons induces rapid ERK phosphorylation. Neurons were treated with vehicle (control) or 50μM AMPA for 3, 10, 15, 30 or 60 min, followed by immunoblotting lysates with antibodies to dual phosphorylated ERK (ppERK) and total ERK2. Protein band densitometry quantification was expressed as the ratio of pERK2 to total ERK2 and indicates a significant time-dependent elevation in MAP kinase (ERK) activation. Data expressed as mean fold change of control pERK2:ERK2 ratio ± SEM, n=3 independent experiments, with representative ppERK1/2 and ERK2 blots shown. ** indicates $p<0.01$, control (white bar) vs AMPA (grey bars) subjected to one-way ANOVA with Bonferroni post-test.

total ERK2 levels was observed (figure 3.3). In order to establish the selectivity of AMPAR -dependent ERK phosphorylation, primary cortical neurons were pre-treated for 10 min with the MEK inhibitor U0126 (5μM), before application of 50μM AMPA for 3 min, observed to induce significant ERK phosphorylation (figure 3.3). Application of U0126 abolished baseline ERK phosphorylation levels (figure 3.4), indicating a tonic level of cellular activity in the primary neuronal cultures. U0126 also significantly abolished AMPA-induced ERK phosphorylation, indicating AMPAR signal to ERK in a classical MEK-dependent manner.

3.2.4 Neuronal NMDAR couple to cellular activation and ERK phosphorylation

To further establish the functional nature of the synapses present in the primary cortical neuron model system, assessment of the functionality of NMDA receptors (NMDAR) was carried out. As glutamatergic synapse development, maturation and plasticity is controlled by NMDAR, displaying the functionality of these receptors *in vitro* was essential. 5-10 DIV neurons were subjected to 50μM NMDA treatment for up to 1 h, and lysates immunoblotted for dual-phosphorylated (Thr202 and Tyr204) active pERK2 and total ERK2. NMDAR activation caused a rapid and significant ~9-fold increase in ERK2 phosphorylation, over vehicle treated control samples (figure 3.5). Over a time course of 1 h, ERK phosphorylation was significantly elevated following acute (3-10 min) periods of stimulation, with phosphorylation status returning to baseline levels over longer periods of treatment (15-60 min), in agreement with previously published findings from NMDAR-mediated ERK activation time course analyses in primary hippocampal neurons (Sala *et al*., 2000). Again, the NMDA-mediated change in pERK2 density was not due to varied levels of protein loaded into gels, as no change was observed in total ERK2 levels (figure 3.5).

To establish the selectivity of the NMDAR activation-dependent ERK phosphorylation, neurons were pre-treated for 10 min with either the NMDAR-selective antagonist MK801 (2.5μM) or the MEK inhibitor U0126 (5μM), before application of 50μM NMDA for the maximal ERK activation time of 3 min (figure 3.6). Application of MK801 alone had no effect on basal levels of ERK phosphorylation, indicating the tonic signalling activity in the cultures was mediated by another receptor population, most likely being AMPAR. MK801-mediated inhibition of NMDAR currents significantly abolished NMDAR-mediated ERK phosphorylation,

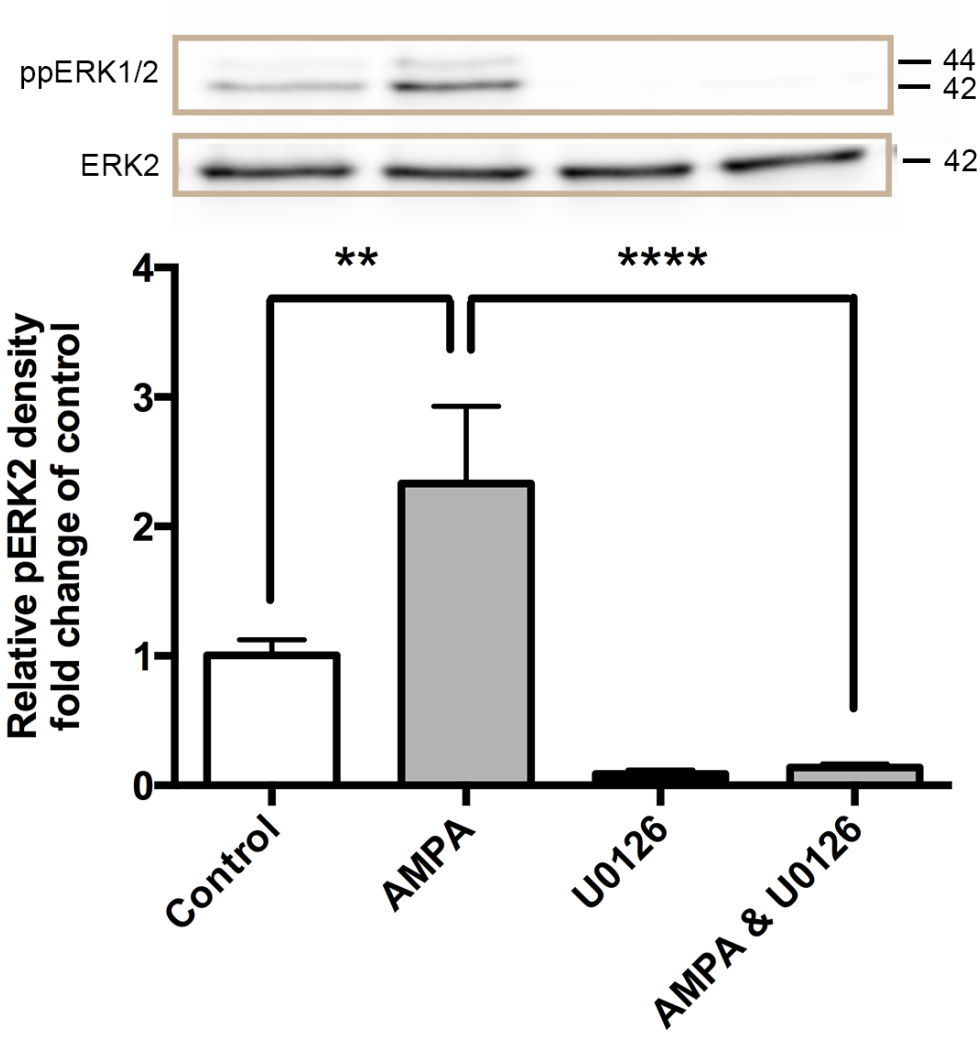

Figure 3.4: AMPAR-induced ERK phosphorylation is MEK-dependent. The selective MEK inhibitor U0126 blocks AMPA-mediated ERK phosphorylation. 5-10 DIV primary cortical neurons were treated with vehicle (control), U0126 (5μM, 10 min pre-treatment) or AMPA (50μM) alone or in the presence of U0126 for 3 min, followed by imunoblotting lysates with antibodies to dual phosphorylated ERK1/2 (ppERK) and total ERK2. Protein band densitometry quantification was expressed as the ratio of pERK2 to total ERK2 and indicates a significant AMPA-dependent elevation in MAP kinase (ERK) activation, selectively blocked by U0126. Data expressed as mean fold change of control pERK2:ERK2 ratio ± SEM, n=3 independent experiments, with representative ppERK1/2 and ERK2 blots shown. ** indicates $p<0.01$, **** indicates $p<0.001$, control (white bar) vs AMPA ± U0126 (grey bars) subjected to one-way ANOVA with Bonferroni post-test.

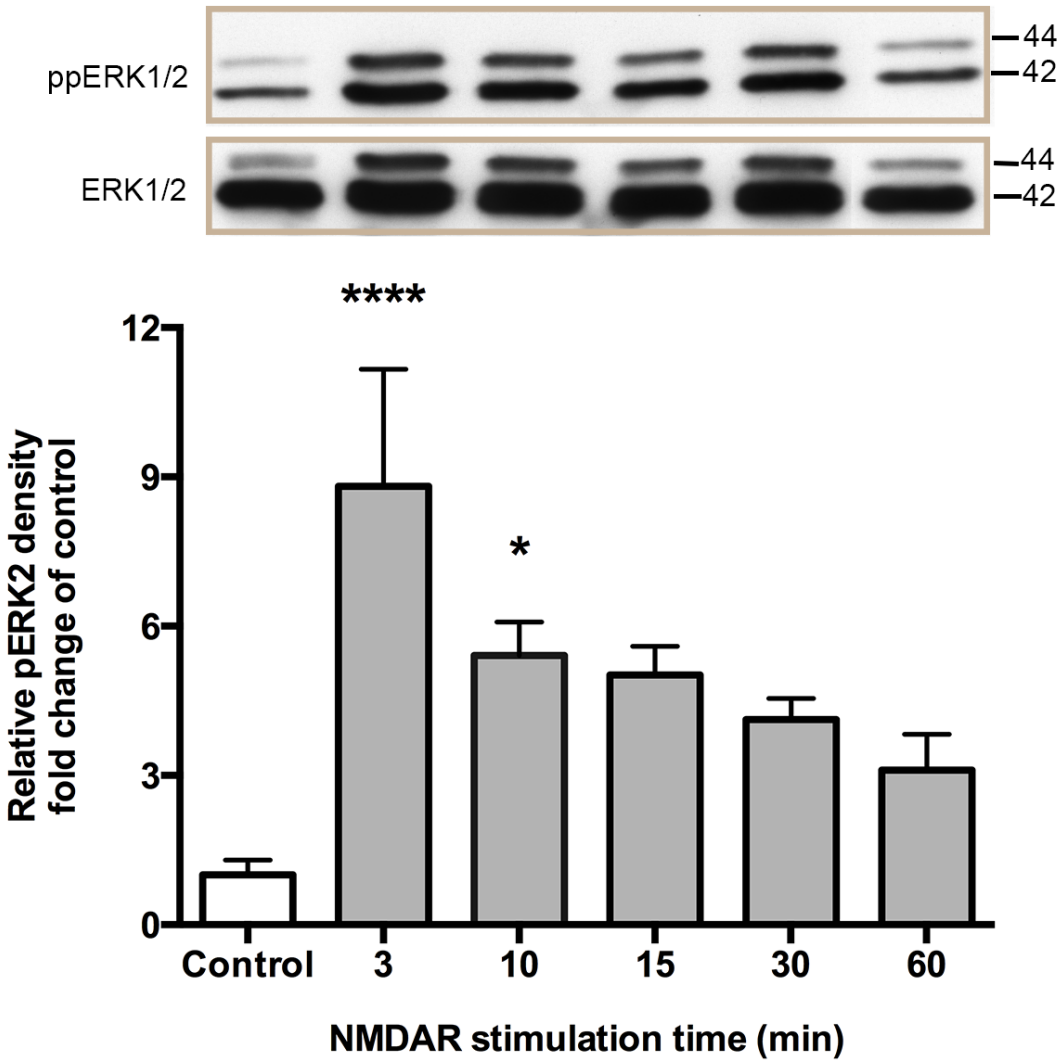

Figure 3.5: NMDA-induced cellular activation is time-dependent. 50μM NMDA treatment of 5-10 DIV primary cortical neurons induces rapid ERK phosphorylation. Neurons were treated with vehicle (control) or 50μM NMDA for 3, 10, 15, 30 or 60 min, followed by immunoblotting lysates with antibodies to dual phosphorylated ERK (ppERK) and total ERK2. Protein band densitometry quantification was expressed as the ratio of pERK2 to total ERK2 and indicates a significant time-dependent elevation in MAP kinase (ERK) activation. Data expressed as mean fold change of control pERK2:ERK2 ratio ± SEM, n=3 independent experiments, with representative ppERK1/2 and ERK2 blots shown. ** indicates $p<0.01$, control (white bar) vs NMDA (grey bars) subjected to one-way ANOVA with Bonferroni post-test.

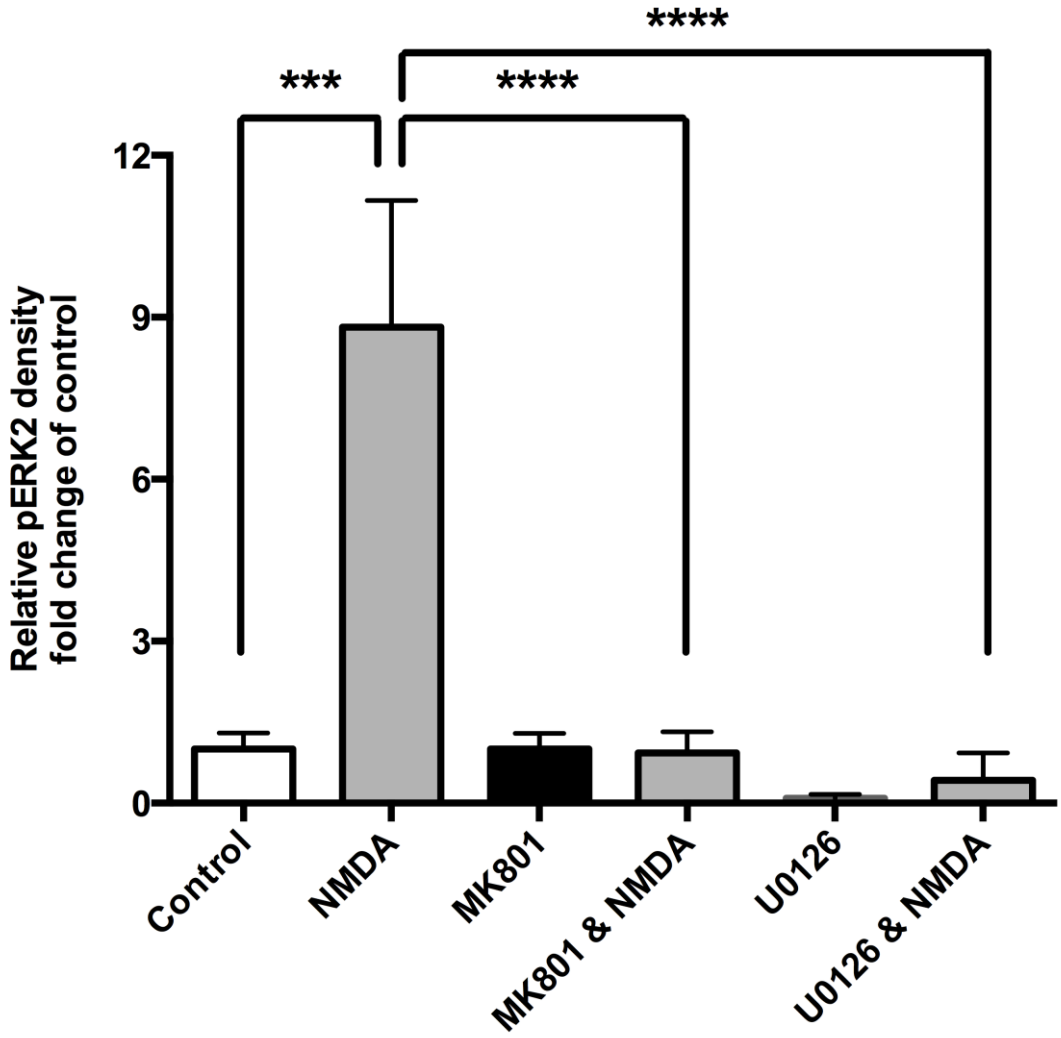

Figure 3.6: NMDA-induced ERK phosphorylation is NMDAR- and MEK-dependent. The selective NMDAR antagonist MK801 and the MEK inhibitor U0126 blocks NMDA-mediated ERK phosphorylation. 5-10 DIV primary cortical neurons were treated with vehicle (control), MK801 (2.5μM, 10 min pre-treatment), U0126 (5μM, 10 min pre-treatment) or NMDA (50μM) alone or in the presence of MK801 or U0126 for 3 min, followed by immunoblotting lysates with antibodies to dual phosphorylated ERK1/2 and total ERK2. Protein band densitometry quantification was expressed as the ratio of pERK2 to total ERK2 and indicates a significant NMDA-dependent elevation in MAP kinase (ERK) activation, selectively blocked by MK801 and U0126. Data expressed as mean fold change of control pERK2:ERK2 ratio ± SEM, n=3 independent experiments, with representative ppERK1/2 and ERK2 blots shown. *** indicates $p<0.005$, **** indicates $p<0.001$, control (white bar) vs NMDA ± MK801/U0126 (grey bars) subjected to one-way ANOVA with Bonferroni post-test.

returning pERK to baseline level, reinforcing the selectivity of NMDAR-mediated cellular activation. U0126 abolished both baseline ERK phosphorylation (figure 3.6) and 50μM NMDA-induced ERK phosphorylation, indicating NMDAR signal to ERK in a classical MEK-dependent manner.

3.2.5 Primary cortical neurons express calcium-permeable α7 nicotinic acetylcholine receptors

In order to assess α7nAChR expression, primary cortical neurons were incubated with the α7nAChR-selective antagonist α-bungarotoxin (αBTX), labelled with a fluorescent AlexaFluor-488 tag (αBTX-488) to enable direct visualisation. The 74 amino acid 8kDa α-neurotoxin extracted from snake venom, αBTX, has been shown to bind to the agonist-binding pocket of nAChR α-subunits (Samson *et al*., 2002). The antagonist binds with high affinity to α7nAChRs (Chen and Patrick, 1997) and thus acts as a useful tool to study α7nAChR expression and pharmacology. Staining intact live primary cortical neurons with αBTX-488 yielded a subpopulation of fluorescently labelled cells, possessing the classical morphological phenotype of neurons (figure 3.7A). Parallel visualisation of all cell nuclei counterstained with DAPI revealed ~10-15% were fluorescently labelled with αBTX-488. The observed staining appeared selective for α7nAChRs as the fluorescence signal was blocked by pre-incubation with an excess of nicotine (1mM) before application of αBTX-488 (figure 3.7B), in accordance with other studies (Kawai *et al*., 2002; Chang and Fischbach, 2006; Shelukhina *et al*., 2009).

Upon establishing primary cortical neurons expressed α7nAChR, investigation into the functionality of these receptors was subsequently undertaken. As nAChR-mediated influx of calcium ions is known to influence a variety of cellular processes, from neurotransmitter release to postulated mechanisms of learning and memory, characterisation of the *in vitro* nAChR functionality was essential. α7nAChRs are distinguished from other nAChRs by their high relative permeability to calcium (Dajas-Bailador and Wonnacott, 2004), so in order to probe α7nAChR calcium permeability, the calcium-sensitive chemical indicator FURA-2 AM was used in dual emission microfluorimetry live imaging of primary cortical neurons.

As calcium fluxes in neurons can be indirect, such as through other voltage-gated calcium channels, all microfluorimetry recordings were done in the presence of 1μM tetrodotoxin (TTX). Prior to agonist treatment, the neurons were microperfused for 3

min with the positive allosteric modulator (PAM) PNU-120596 (10μM). Initial baseline recordings (0 to 40 sec) indicated little, if any, spontaneous action potential firing in the primary cultures (figure 3.7C), with no visible fluorescence change observed across the field of view (figure 3.7D, top), confirming PNU-120596 (10μM) application does not directly activate α7nAChRs. Subsequent PNU-282987 (3μM) agonist application for 20 sec induced a rapid increase in intracellular calcium, as observed from the recorded F340:380nm ratio trace (figure 3.7C). The observation of rapid intracellular calcium influx was reinforced by dynamic video imaging-captured images showing increased fluorescence intensity, as a surrogate marker of calcium ion influx (blue to light blue), within a number of cells within pseudocoloured images (figure 3.7D, bottom).

3.2.6 Neuronal nAChR couple to ERK phosphorylation

To further establish the nature of the nicotinic acetylcholine receptors (nAChR) present in the primary cortical neuron model system, assessment of their functionality was carried out. 5-10 DIV neurons were treated with the non-selective nAChR agonist nicotine (10μM) for up to 30 min, in the presence of 10μM PNU-120596, and lysates immunoblotted for dual-phosphorylated (Thr202 and Tyr204) active pERK2 and total ERK2. Nicotine-induced nAChR activation caused a rapid and significant ~2.5-fold increase in ERK2 phosphorylation, over vehicle treated control samples (figure 3.8A). Over the time course of 30 min, ERK phosphorylation was significantly elevated across all periods of stimulation, in agreement with previously published findings from nicotine-treatment of primary cortical neurons (Steiner *et al*., 2007). The nicotine-mediated change in pERK2 density was not due to varied levels of protein loaded into gels, as no change was observed in total ERK2 levels (figure 3.8A). To establish the relative α7- and non-α7nAChR component of nicotine-induced ERK phosphorylation, nicotine was applied to the cortical neurons for the maximal ERK activation time of 3 min, in the absence of the α7nAChR-selective PAM PNU-120596. 3 min nicotine treatment did not significantly increase ERK phosphorylation above vehicle treated (control) samples (figure 3.8B), but a slight increase was observed, and can be attributed to the expression of rapidly desensitising α7- and α3β4 nAChR subtypes (Fenster *et al*., 1997) predominantly expressed in cortical neurons (Alkondon *et al*., 2007). Incubation with10μM PNU-120596 alone had no effect on cellular activation; with no observed

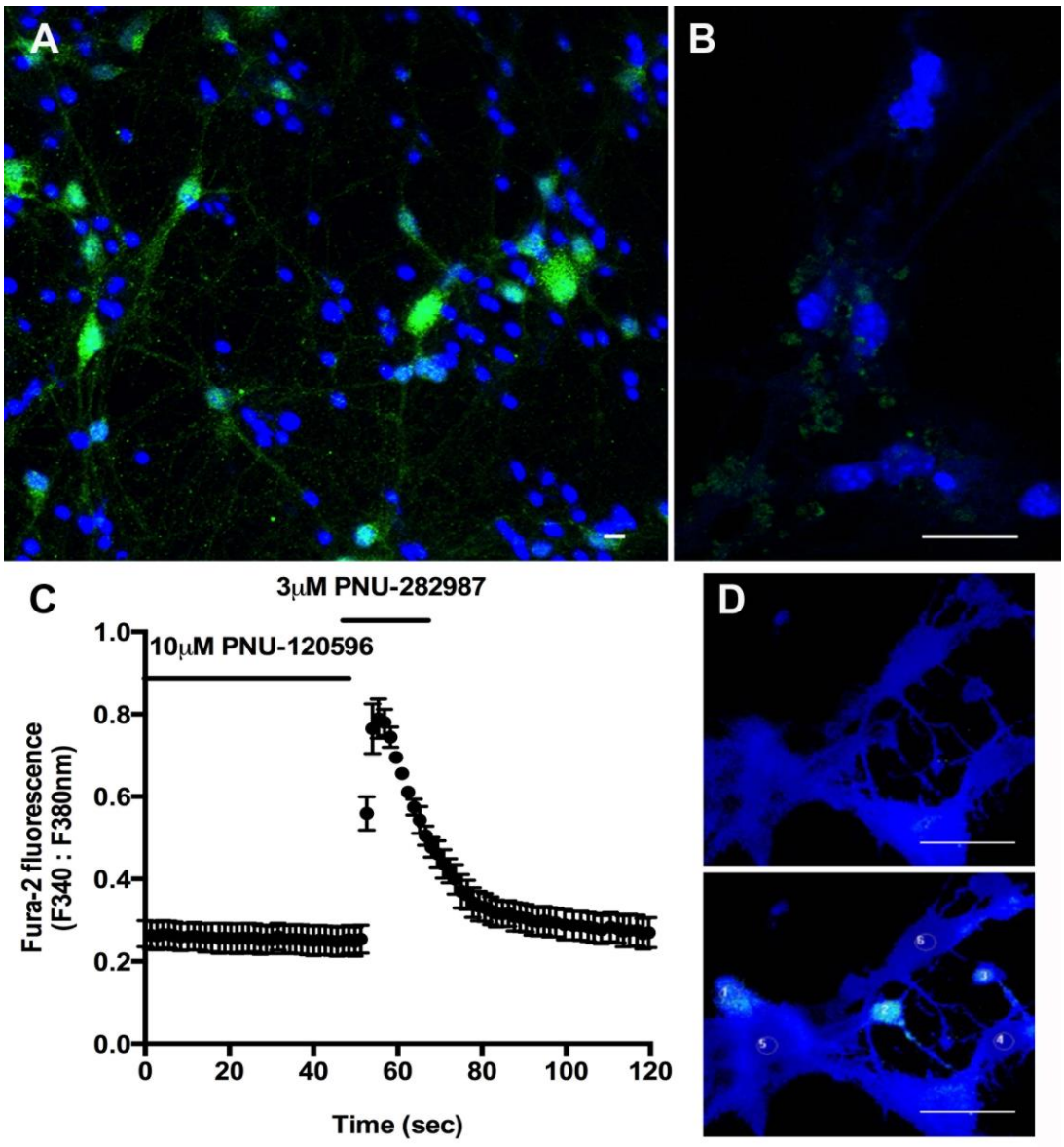

Figure 3.7: Primary cortical neurons express functional calcium-permeable α7nAChR. A: Imaging of α7nAChR using 100nM AlexaFluor-488 labelled α-bungarotoxin (green) of 5 DIV neurons reveals ~10-15% of neurons express α7nAChR. B: To assess specificity of α7nAChR:α-bungarotoxin labelling, neurons were pre-incubated with an excess of the broad nAChR agonist nicotine (1mM) to probe non-specific α-bungarotoxin labelling. Nicotine pre-incubation blocked all fluorescent labelling of α7nAChR, confirming specificity of α-bungarotoxin AlexaFluor-488 labelling. Fluorescence images scale bars indicate 20μm. C: Fura-2 AM microfluorimetry ratiometric F340:380nm trace reveals an α7nAChR activation-induced increase in intracellular calcium, n=3 cells, mean F340:380nm ± SEM. Neurons were microperfused with assay buffer before a 3 min incubation with 10μM PNU-120596 and subsequent 20 sec pulse of 10μM PNU-282987 (indicated by black lines). Cells were imaged every ~1 sec by live dynamic video imaging to capture pseudocoloured images. D: Representative pseudocoloured images of baseline intracellular calcium influx (top) and maximal α7nAChR activation-induced calcium influx at 60 sec (bottom) are shown. Microfluorimetry scale bars indicate 100μm.

change in ERK phosphorylation indicating the PAM requires the presence of agonist to activate α7nAChRs. The negligible PNU-120596 effect on ERK activation suggested that there was little if any tonic acetylcholine release in the cultures, which in the presence of a PAM could activate nAChRs. When pre-treatment (10min, 10μM) with PNU-120596 was combined with a 3 min nicotine (10μM) application, a significant increase in ERK phosphorylation was again observed (figure 3.8B), reinforcing the benefit of using PNU-120596, to enhance and unmask α7nAChR-activation-dependent signals *in vitro*. To determine the specificity of the PNU-120596-potentiated nicotine-induced increase in ERK phosphorylation, primary cortical neurons were incubated with the α7nAChR-selective antagonist αBTX (100nM). αBTX had no effect on basal levels of ERK phosphorylation (figure 3.8B); indicating no acetylcholine-mediated tonic signalling was present within these cultures. Cells were pre-treated for 10 min with αBTX (100nM), before application of 10μM PNU-120596 for a further 10 min, prior to 3 min nicotine treatment (figure 3.8B). αBTX-mediated inhibition of α7nAChR significantly inhibited α7nAChR-induced ERK phosphorylation, returning phospho-ERK to baseline level, reinforcing the specificity of PNU-120596-mediated potentiation of α7nAChR in nicotine-induced ERK phosphorylation.

Nicotine is a weak and non-selective agonist of nAChR, typically binding to the α4β2 nAChR subtype with significantly higher affinity (40-1000x) than at α7nAChR (Jensen *et al*., 2003) and significantly (10-100x) lower functional potency than other nAChR isoforms (Gopalakrishnan *et al*., 1995; Eaton *et al*., 2003). Thus to selectively investigate the effects of α7nAChR, without other nAChR isoforms confounding analyses, the α7nAChR-selective agonist PNU-282987 was used (Bodnar *et al*., 2005; Hajos *et al*., 2005; del Barrio *et al*., 2011), in combination with PNU-120596.

5-7 DIV neurons were treated with PNU-120596 (10μM, 10 min pre-incubation) and PNU-282987 (10μM) for up to 1 h, and lysates immunoblotted for dual-phosphorylated (Thr202 and Tyr204) active pERK2 and total ERK2. α7nAChR activation caused a rapid and significant ~3-fold increase in ERK2 phosphorylation, over vehicle treated control samples (figure 3.8C). Over a time course of 1 h, ERK phosphorylation was significantly elevated following acute (3 min) stimulation, with phosphorylation status returning to baseline levels over longer periods of treatment (10-60 min). The α7nAChR-mediated change in pERK2 was not due to varied levels of protein loaded into gels, as no change was observed in total ERK2 levels (figure 3.8C). No clear

effect was observed with 10μM PNU-282987 beyond an acute (3 min) treatment time. This cannot be attributed to α7nAChR desensitisation, due the presence of the PAM PNU-120596, which is known to reduce receptor desensitisation and to greatly prolong agonist-evoked cellular responses (Hurst *et al*., 2005), but instead can be likely ascribed to phosphatase-mediated deactivation of ERK. The agonist activity of PNU-282987 has previously been shown to more than double the frequency of synaptic activity, when compared to nicotine (Hajos *et al*., 2005), however, when comparing the relative effect of nicotine and PNU-282987 in the presence of PNU-120596, on ERK phosphorylation, no significant difference in peak ERK phosphorylation level was observed (figure 3.8A and B versus figure 3.8C and D). To determine the specificity of the PNU-282987-induced increase in ERK phosphorylation, via α7nAChR activation, primary cortical neurons were incubated with either the α7nAChR-selective antagonist αBTX (100nM), the MEK inhibitor U0126 (5μM) or the free calcium chelator EGTA (2.5mM), alone or before application of (PNU-120596 and) PNU-282987 for the maximal ERK activation time of 3 min. αBTX pre-treatment had no effect on basal levels of ERK phosphorylation (figure 3.8D). Application of αBTX (100nM), before PNU-120596 (10μM), prior to 3 min PNU-282987 agonist treatment (figure 3.8D) significantly attenuated PNU-282987-induced ERK phosphorylation, returning pERK to baseline level. U0126-mediated MEK inhibition abolished baseline ERK phosphorylation (figure 3.8D) and also PNU-282987-induced ERK phosphorylation. Finally, to investigate the extracellular calcium-dependence of the α7nAChR-mediated ERK activation, EGTA was applied in excess (2.5mM) to the cortical neurons. EGTA alone had no effect on baseline ERK phosphorylation, indicating extracellular calcium does not maintain basal ERK levels. Chelation of extracellular calcium with EGTA prevented an increase in α7nAChR-mediated pERK, following stimulation with PNU-282987 (figure 3.8D). When taken together, these data suggest that α7nAChR-mediated calcium influx stimulates robust MEK-dependent ERK phosphorylation in cultured cortical neurons

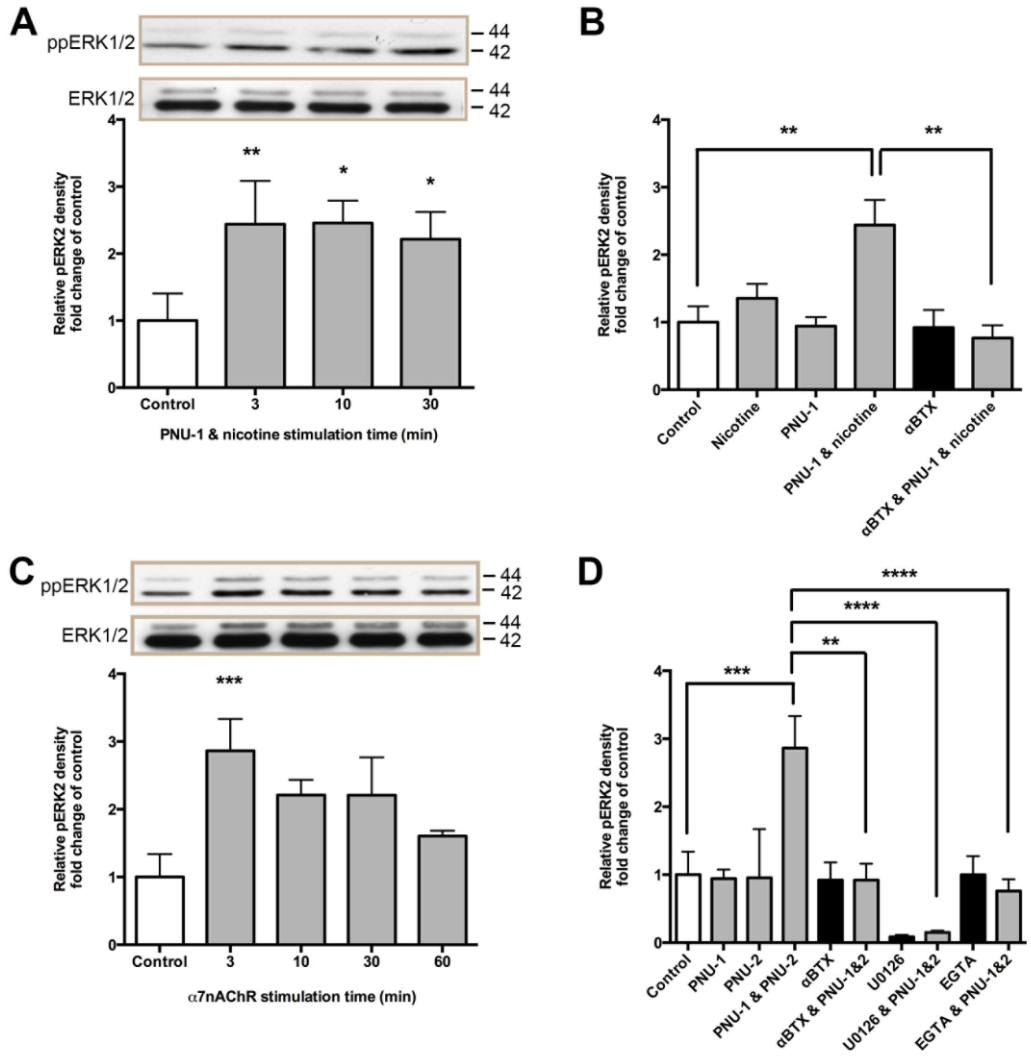

Figure 3.8: nAChR couple to cellular activation and ERK phosphorylation. A: Nicotine treatment (in the presence of PNU-120596) induces rapid time-dependent sustained ERK phosphorylation. B: Nicotine-induced ERK phosphorylation requires the presence of the α7nAChR-selective PAM PNU-120596 and is selectively blocked by the α7nAChR antagonist αBTX. C: PNU-282987 treatment (in the presence of PNU-120596) induces rapid but non-sustained ERK phosphorylation. D: Agonist-mediated ERK phosphorylation is blocked by αBTX, the MEK-inhibitor U0126 and the extracellular calcium chelator EGTA. 5-10 DIV primary cortical neurons were treated with vehicle (control) or agonist (10μM nicotine/PNU-282987) for 3, 10, 15, 30 or 60 min, following 10 min pre-treatment with 10μM PNU-120596 and/or 20 min pre-treatment with antagonist or signalling inhibitors (100nM αBTX, 5μM U0126 or 2.5mM EGTA) followed by immunoblotting lysates with antibodies to dual phosphorylated ppERK1/2 and total ERK2. Protein band densitometry quantification was expressed as the ratio of pERK2 to total ERK2. Data expressed as mean fold change of control pERK2:ERK2 ratio ± SEM, n=3 independent experiments, with representative ppERK1/2 and ERK2 blots shown. * indicates $p<0.05$, ** $p<0.01$, *** $p<0.005$, control (white bar) vs agonist/PAM treatment (grey bars) or antagonist/inhibitor (black bars) subjected to one-way ANOVA with Bonferroni post-test.

3.2.7 α7nAChR-activation has no effect on Egr-1 promoter-driven luciferase expression

Assessment of the levels of pERK protein as a marker of ERK activity is a commonly used measure of cellular activation. However, analyses of α7nAChR activation-induced changes in pERK1/2 protein levels do not give an indication as to whether α7nAChR stimulation can recruit ERK-driven gene transcription, a known mediator of long-term cellular processes, such as cell survival, learning and memory and memory consolidation. Given the proposed distinct spatial distribution of α7nAChR populations, being presynaptic and/or postsynaptic, the ability of α7nAChR to drive effective transcriptional changes within the nucleus of primary neurons is unknown. Given the relatively insensitive technique of immunoblotting, coupled with the low expression level of α7nAChR observed in primary cortical neurons, a highly sensitive viral transduction method was used to further probe α7nAChR activation-mediated network effects *in vitro*. Primary neurons (at 6-7 DIV) were transduced with an Ad5-Egr-1 reporter plasmid, to measure ERK-dependent transcription of early growth response gene-1 (Egr-1), as measured by luciferase readout. Following transduction, neurons were treated with BDNF (50ng/ml), U0126 (5μM), PNU-120596 (10μM), PNU-282987 (10μM) or αBTX (100nM) for 6 h. A 6 h treatment time was required to allow sufficient detectable transcription of the Egr-1 gene product (Dr Carla Cox, personal communication and unpublished data). BDNF treatment induced a significant 2-fold increase in Egr-1-mediated luciferase expression (figure 3.9), which was blocked by pre-treatment with the selective MEK inhibitor U0126. Neither the α7nAChR-selective PAM PNU-120596 nor the agonist PNU-282987 had a significant effect on Egr-1 transcription of the entire neuronal population, either alone or in combination (figure 3.9). Inhibition of α7nAChR with αBTX had no effect on basal levels of Egr-1 transcription. This suggests that despite stimulating ERK phosphorylation chronic α7nAChR activation does not modulate transcription of the ERK target gene Egr-1.

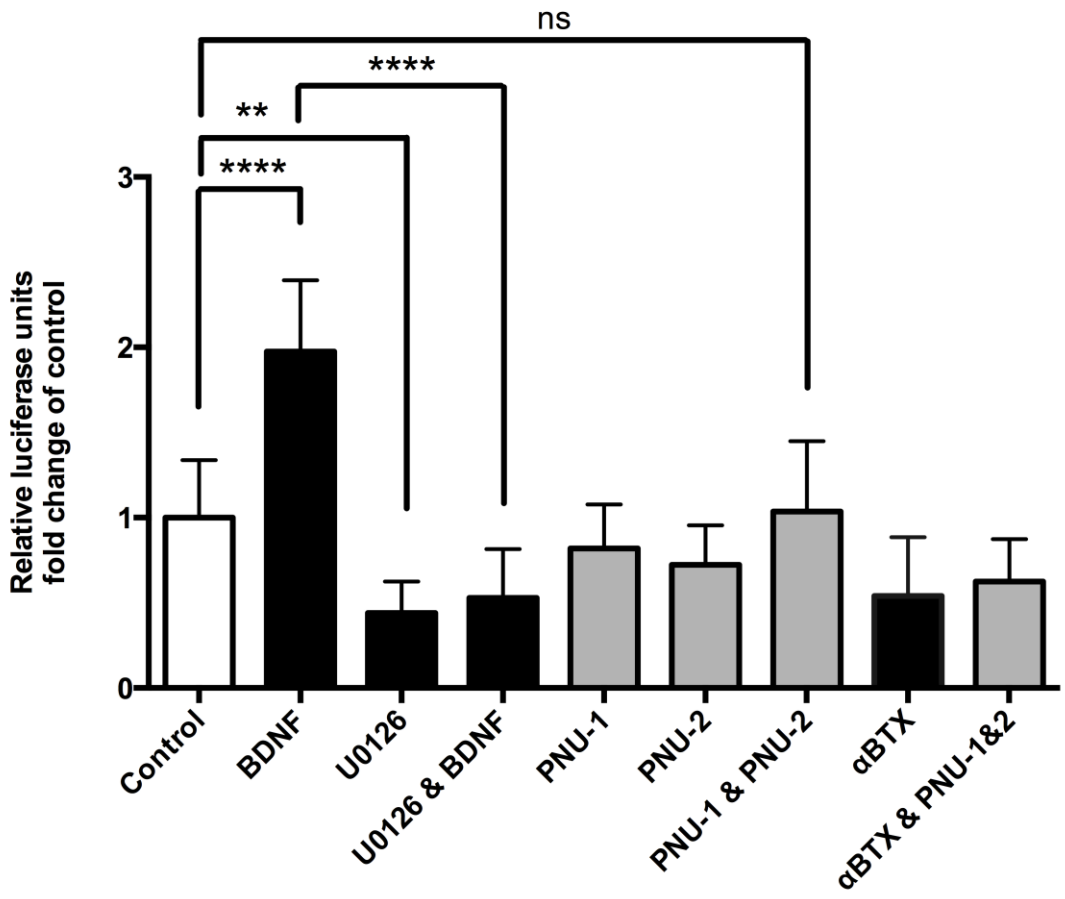

Figure 3.9: Activation of α7nAChR does not stimulate ERK-dependent transcription of Egr-1 in primary cortical neurons. 6 DIV primary cortical neurons were transduced with an Ad5-Egr1-luciferase plasmid. Neurons were treated with vehicle (control), BDNF (50ng/ml), U0126 (5μM), PNU-120596 (10μM), PNU-282987 (10μM) or αBTX (100nM) for 6 h. Luciferase activity was measured post drug treatments and is expressed as mean fold change of control ± SEM (n=8-12 individually transduced wells across 3 independent experiments, ns indicates not statistically significant, ** $p<0.01$, **** $p<0.001$, control (white bar) vs BDNF/U0126 (black bars) or PNUs (grey bars), subjected to one-way ANOVA with Bonferroni post-test.

3.3 Discussion

The aim of this chapter was to characterise primary cortical neurons to determine their suitability as a model system for studying α7nAChR signalling at the glutamatergic synapse. Accordingly, this chapter has shown primary cortical neurons express functional glutamate receptors (NMDAR and calcium-permeable AMPAR) that couple to cellular activation (ERK phosphorylation). Furthermore, detailed characterisation was undertaken to demonstrate the presence of functional calcium-permeable α7nAChR, which couple to ERK activation, but play no role in modulating ERK-mediated gene transcription.

3.3.1 Primary cortical neurons express functional glutamate receptors

Initial results, using phase contrast imaging and immunofluorescence with neuron-specific markers, showed that the primary cortical neuron model system possessed a neuronal phenotype. Furthermore, GluA-subunit immunofluorescence coupled with dual-emission microfluorimetry highlighted postsynaptic expression and functionality of calcium-permeable AMPAR, in accordance with previous literature (Rainey-Smith *et al*., 2010; Hoey *et al*., 2013). The widespread expression of AMPAR in primary cortical neurons was estimated as ~90%, in accordance with AMPAR expression in primary motor neurons (Damme, 2002) and primary cortical neurons (Hoey *et al*., 2013). Furthermore, following 5-10 DIV, AMPAR and NMDAR were coupled to ERK phosphorylation as previously demonstrated (Sala *et al*., 2000; Ivanov *et al*., 2006; Domercq *et al*., 2011). AMPAR- and NMDAR-mediated ERK phosphorylation was time-dependent and MEK-dependent, with rapid kinetics of activation, peaking at 2-5 and 5-10 min following treatment with NMDA (Sala *et al*., 2000) and AMPA (Domercq *et al*., 2011), respectively. Within the CNS, glutamate activates NMDAR, AMPAR and kainate receptors, which results in increases in intracellular calcium: a process that is a critical regulator of gene expression and long-term cell survival responses. Results described here show functionality of glutamate receptors in primary cortical neurons, reinforcing the use of these cells as an appropriate model system for the study of the glutamatergic synapse.

3.3.2 Primary cortical neurons express functional calcium-permeable α7nAChR

Using the α7nAChR-selective PAM PNU-120596, a clear α7nAChR activation effect was observed, through blocking receptor desensitisation (Hurst *et al*., 2005). Treatment of primary cortical neurons with the PAM and α7nAChR-selective agonist PNU-282987 enabled detection and measurement of a clear α7nAChR-mediated influx of calcium into a small population of αBTX-488-positive (10-15%) primary cortical neurons, as measured by dual-emission microfluorimetry calcium imaging (in accordance with Hu *et al*., 2009; Brown and Wonnacott, 2014). Previous literature has shown α7nAChR radiolabelling and immunoreactivity within primary neurons increases over time in culture, correlating with synapse formation and maturation (Samuel *et al*., 1997). When α7nAChR expression is compared to AMPAR expression and functionality, these data suggest a much lower expression level of α7nAChR than AMPAR in cultured primary cortical neurons. Immunofluorescence imaging of GluA1/2-containing AMPAR and FURA-2 AM microfluorimetry indicated widespread (~90%) AMPAR expression. Conversely, fluorescent αBTX-488 labelling of α7nAChR and FURA-2 AM dual-emission microfluorimetry indicated a modest (10-15%) cortical α7nAChR expression, in accordance with previously published findings (Liu *et al*., 2001; Poorthuis *et al*., 2013; Brown and Wonnacott, 2014; Genzen *et al*., 2014). As such, these results indicate a lower expression level of α7nAChR in a more representative and physiological model system than cell lines, which are currently favoured by many research groups. α7nAChR expression level may play a role in the differences and discrepancies observed between nAChR studies undertaken in cell lines, overexpressing transgenic mouse models and primary CNS tissues.

3.3.3 Primary cortical neuronal α7nAChR couple to ERK phosphorylation without effecting ERK-dependent transcription

Few studies have examined α7nAChR-mediated downstream signalling cascades, specifically ERK phosphorylation. Historically, this has arisen due to a lack of sensitive detection methods, owing to the rapid kinetics of activation and desensitisation of α7nAChR and also the relatively new emergence of α7nAChR-subtype selective ligands. Recent studies have highlighted both nicotine- and α7nAChR-selective

agonist-mediated ERK phosphorylation in primary cortical neurons, SH-SY5Y cells and PC12 cells. Accordingly, a similar kinetic was observed between PAM-potentiated PNU-282987-mediated ERK phosphorylation in PC12 cells (El Kouhen *et al*., 2009), with ERK phosphorylation peaking at 3-7 min, and also in nicotine-treated SH-SY5Y cells and primary cortical neurons, with ERK phosphorylation peaking rapidly between 1-5 min (Dajas-Bailador *et al*., 2002; Steiner *et al*., 2007). Similarly, the data presented here highlight a rapid 3 min maximal kinetic of ERK phosphorylation, mediated by PNU-120596-potentiated nicotine- and PNU-282987-mediated α7nAChR activation, which were blocked by αBTX and was both MEK- and extracellular calcium-dependent. Thus, these data presented in this chapter reinforce the published literature and combine distinct observations between nicotine and α7nAChR-selective ligands in a physiological cellular model.

Furthermore, data presented here highlight for the first time, that α7nAChR activation only couples to transient ERK phosphorylation and not ERK-dependent gene transcription. A limited number of studies have reported nAChR activation leads to *c-Fos* gene expression (Greenberg *et al*., 1986) following secondary activation of L-type voltage-dependent calcium channels. Neuronal activity-dependent gene transcription has been well documented for NMDAR and AMPAR, with ionotropic glutamate receptor activation tightly coupled to gene expression (West and Greenberg, 2011). So, why is this not the case for α7nAChR, which are also highly calcium-permeable? This may be a result of both the spatial localisation of presynaptic α7nAChR, with only postsynaptic receptors (such as NMDAR and AMPAR) capable of modulating transcription (Mokin and Keifer, 2005; Mittelbronn *et al*., 2009), or the low α7nAChR expression level observed in primary cortical neurons. Previous reports conform to this hypothesis, with *in vivo* data showing gene expression changes require neuronal signalling above a threshold level, met by a balance between the number of excitatory and inhibitory input signals (Mann and Paulsen, 2007). Overexpression of α7nAChR in cell lines is capable of prolonged and sustained ERK phosphorylation (Utsugisawa *et al*., 2002) and gene transcription, including the Egr-1 gene (Dunckley and Lukas, 2003). Conversely, data presented here show natively expressed α7nAChR are not able to bring about effects on gene transcription, but instead play a modulatory role in transiently activating intracellular (MAPK) signalling cascades.

3.3.3 Summary

Using a combination of an α7nAChR-selective PAM and agonist, this chapter highlights the activation of native α7nAChR within well-characterised primary cortical glutamatergic synapses induced rapid and robust ERK phosphorylation, in accordance with the published literature, but showed no effect on ERK transcription.

Chapter 4

4. α7nAChR-dependent regulation of APP processing

4.1 Introduction

There is a strong link between cholinergic signalling (at both muscarinic and nicotinic receptors) and APP metabolism (Hellström-Lindahl, 2000; Fisher, 2012) and section 1.8.2.2). A number of studies in cell lines have demonstrated that α7nAChR activation, with nicotine enhances sAPPα release (Kim *et al*., 1997; Lahiri *et al*., 2002; Mousavi and Hellström-Lindahl, 2009; Nie *et al*., 2010), inhibits soluble Aβ production (Hellström-Lindahl *et al*., 2004; Hedberg *et al*., 2008) and reduces Aβ plaque levels *in vivo* (Nordberg *et al*., 2002; Nie *et al*., 2010). These effects, which might be due to an α7nAChR-mediated reduction in BACE-1 protein levels, prevent Aβ-induced synaptic transmission defects and neurotoxicity (Zamani *et al*., 1997; Shimohama and Kihara, 2001; Picciotto and Zoli, 2008; Yu *et al*., 2011). Despite this body of evidence, the ability of α7nAChR to couple to APP processing in neurons has not been thoroughly investigated.

As reviewed in section 1.8.2.2, NMDAR activation can potentially exhibit contrasting effects on APP processing. Hyperactivation and stimulation of extrasynaptic NMDAR is implicated in excitotoxicity, enhanced pro-amyloidogenic APP processing and Aβ production, resulting in neurodegeneration (Hardingham *et al*., 2002; Léveillé *et al*., 2008; Bordji *et al*., 2010, 2011; Talantova *et al*., 2013; Parsons and Raymond, 2014; Rush and Buisson, 2014). In contrast, physiological signalling through synaptic NMDAR enhances non-amyloidogenic APP processing and is neuroprotective, playing a role in synaptic plasticity and neurotrophic processes (Hardingham *et al*., 2002; Léveillé *et al*., 2008; Hoey *et al*., 2009; Bordji *et al*., 2010). Ionotropic glutamate receptor-mediated non-amyloidogenic APP processing has been strongly linked to ERK phosphorylation (Verges *et al*., 2011; Wan *et al*., 2012; Hoey *et al*., 2013), with AMPAR activation-induced ERK phosphorylation following the same kinetic as APP processing (Hoey *et al*., 2013). Generally, the MAPK pathway has been shown to regulate neuron activity-dependent APP processing (Mills *et al*., 1997; Desdouits-Magnen *et al*., 1998) and enhanced α-secretase activity (Cisse *et al*., 2011), reinforcing the potential of α7nAChR to directly mediate non-amyloidogenic APP processing, given the data presented in Chapter 3, showing α7nAChR-induced ERK activation.

Furthermore, given the well-characterised capacity for presynaptic α7nAChR-mediated glutamate release (section 1.4.2.3), activation of this receptor population

may indirectly enhance non-amyloidogenic APP processing, via activation of synaptic ionotropic glutamate receptors, as well as directly through α7nAChR-mediated calcium influx and ERK-1/2 phosphorylation. As such, reduced glutamate signalling (by tetanus toxin application to primary hippocampal neurons) has been shown to increase α7nAChR dwell time at the nerve terminal. Accordingly, cell-surface immobilised α7nAChR enhanced the likelihood of glutamate release by increasing the size of the readily releasable pool of glutamate-containing vesicles (Gomez-Varela and Berg, 2013), thus reinforcing the potential for nerve terminal α7nAChR to modulate APP processing indirectly, through α7nAChR-induced glutamate release and postsynaptic glutamate receptor activation.

Given the calcium-permeability properties and activation-induced ERK phosphorylation of both ionotropic glutamate receptors and α7nAChR, this indicates α7nAChR are endowed with equal properties, and potentially capable of directly mediating non-amyloidogenic APP processing, or also indirectly via α7nAChR-mediated glutamate release and subsequent NMDAR/AMPAR activation. Therefore, the results described in this chapter aim to probe the *in vitro* APP processing functionality of α7nAChR natively expressed by primary cortical neurons, and compared to a known non-amyloidogenic APP processing-modulator, NMDAR. Through investigating whether α7nAChR couple to APP processing in primary cortical neurons, via a direct or indirect mechanism, secondary to NMDAR activation and calcium influx, will provide a new mechanistic insight into the physiological control of APP processing at the glutamatergic synapse and reinforce our understanding of the beneficial effect of targeting α7nAChR with agonists and PAMs, with a view to regaining control of Aβ production in aging and neurodegeneration.

4.2 Results

4.2.1 APP is predominantly expressed at postsynaptic sites in primary cortical neurons

Under basal homeostatic conditions, APP has been shown to be equally distributed across axonal and somatodendritic compartments of neurons (Back *et al*., 2007), but is most extensively expressed postsynaptically (Hoe *et al*., 2009; Hoey *et al*., 2009, 2013). To establish the expression and distribution of APP within our own primary cortical cultures, neurons at 5-7 DIV were used to examine physiological expression of endogenous APP holoprotein. APP immunofluorescence, using a custom-made primary antibody raised against the C-terminus of human APP, revealed widespread intracellular expression (figure 4.1A), with APP found throughout the cell body and neuronal projections. Double immunofluorescence of APP with the nerve terminal marker synaptophysin revealed little colocalisation (figure 4.1B). However, APP extensively colocalised with the postsynaptic marker PSD-95 (figure 4.1C), indicating APP is predominantly postsynaptic in primary cortical neurons, in accordance with previous studies.

4.2.2. Primary cortical neurons express putative α-secretase enzymes, ADAM-10 and ADAM-17

To assess the capability of this model system to undergo non-amyloidogenic cleavage of APP, the expression of the constitutive α-secretase ADAM-10 and stimulated α-secretase ADAM-17 was established. To probe whether the primary cortical neurons express the putative α-secretase proteins, commercially available primary antibodies were used in fluorescence immunostaining to investigate the expression and trafficking of ADAM-10 and ADAM-17. Under non-stimulated conditions, both ADAM-10/-17 were expressed (figure 4.2) throughout neurons. Double immunostaining of both ADAM-10 (figure 4.2A) and ADAM-17 (figure 4.2B) with the postsynaptic marker PSD-95 revealed notable, but not total overlap, indicating ADAM-10 and ADAM-17 are both trafficked postsynaptically. This data is in accordance with previous biochemical and immunolabelling studies, which highlights ADAM-10 is enriched postsynaptically and shows punctate expression on PSD-95-positive spine-like structures (Marcello *et al*., 2007).

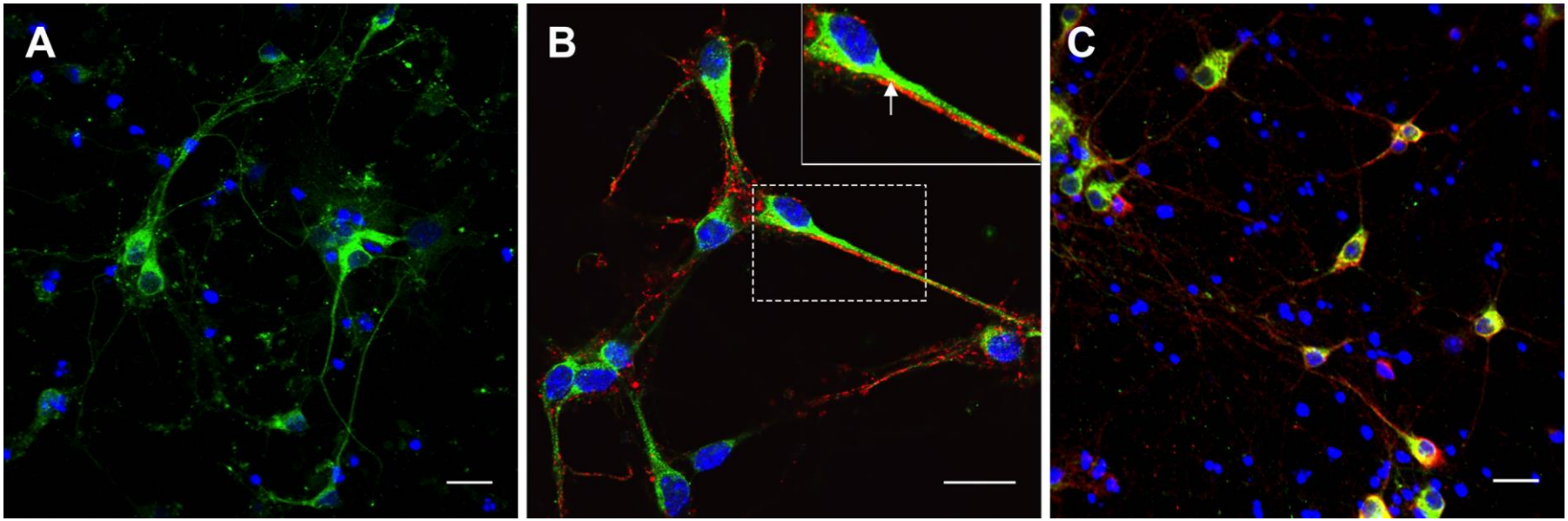

Figure 4.1: APP is mainly trafficked to postsynaptic neuronal compartments. A: Single immunofluorescence staining of 5-10 DIV primary cortical neurons reveals APP (green) is expressed throughout the cell body and neuronal projections. B: Double labelling of APP (green) with the presynaptic marker synaptophysin (red) indicates little colocalisation. Higher magnification (inset) of the indicated (dashed box) region suggests very little overlap between APP and synaptophysin (arrow). C: Double labelling of APP (green) with the postsynaptic marker PSD-95 (red) revealed extensive colocalisation, indicating APP is mainly postsynaptically expressed. All nuclei were counter stained with DAPI (blue) and scale bars show 20μm.

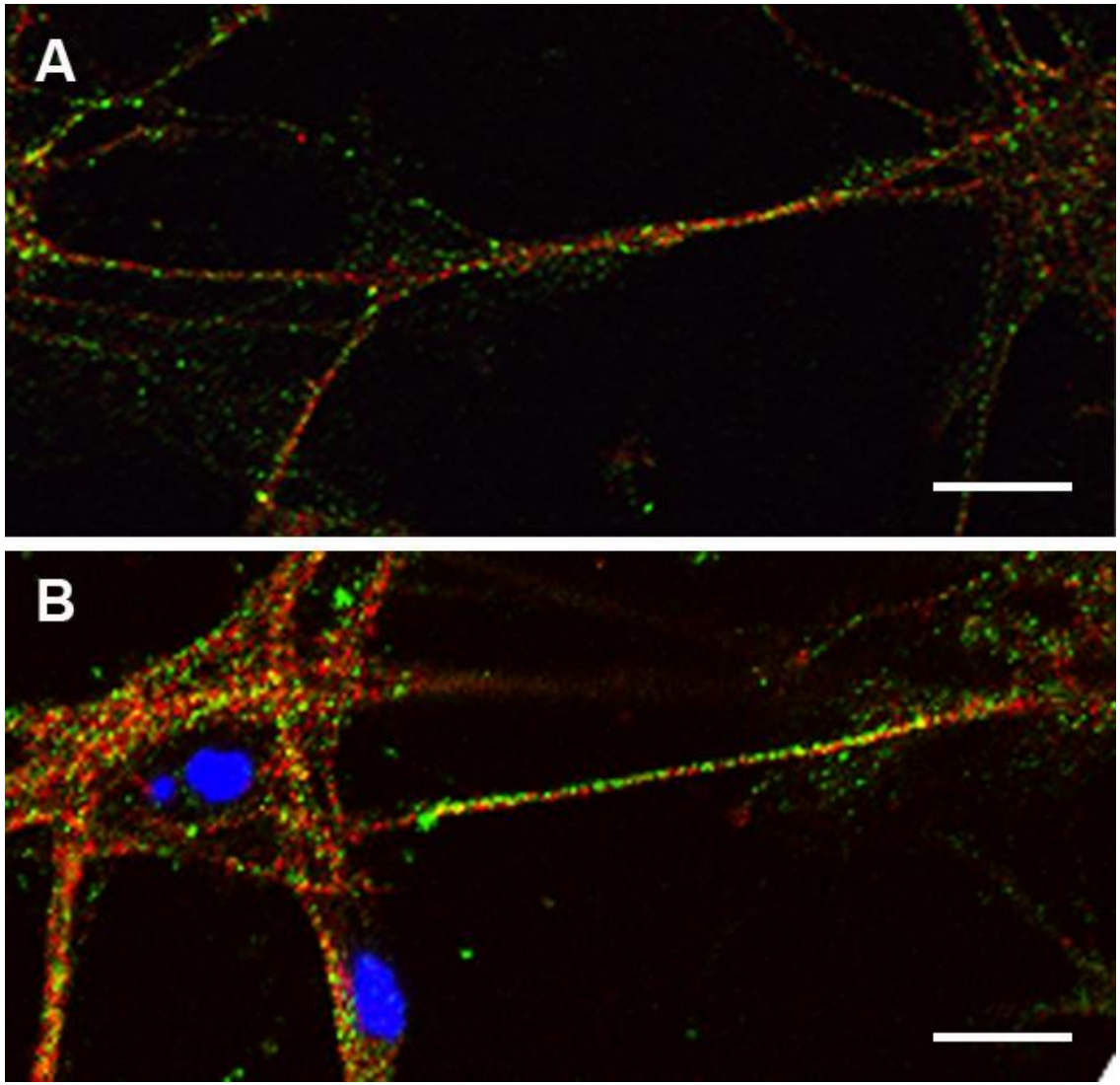

Figure 4.2: Primary cortical neurons express putative α-secretase proteins ADAM-10 and ADAM-17. A: Double immunofluorescence staining of 7 DIV primary cortical neurons reveals ADAM-10 (red) shows punctate expression throughout the neurons and is partly colocalised with the postsynaptic marker PSD-95 (green). B: Double immunofluorescence staining of 7 DIV primary cortical neurons reveals ADAM-17 (red) punctate expression throughout the neurons and is partly colocalised with the postsynaptic marker PSD-95 (green). Nuclei were counter stained with DAPI and scale bars represent 20μm.

4.2.3 NMDAR activation reduces levels of full-length APP

Having demonstrated expression of APP and two of secretase enzymes within primary cortical neurons, the kinetics of APP processing was investigated, first using a known APP processing enhancer, NMDA (Hoey *et al*., 2009; Hu *et al*., 2009b; Bordji *et al*., 2010; Verges *et al*., 2011). Neurons were treated with 50μM NMDA for up to 2 h and lysates immunoblotted using a custom-made primary antibody raised against the C-terminus of human APP and a loading control house keeping protein β-tubulin. Over the 2 h time course, NMDAR activation induced a time-dependent reduction in full-length APP_{695} holoprotein, reaching significance at 1 h and a maximal ~60% reduction in APP level by 2 h (figure 4.3), in accordance with reports (Hoey *et al*., 2009, 2013). A reduction in full-length APP is indicative of secretase-mediated cleavage of the holoprotein. The NMDA-mediated change in APP density was not due to varied levels of protein loaded into gels, as no change was observed in β-tubulin levels (figure 4.3) and was not due to cellular toxicity, as measured by MTT and LDH assays (data not shown).

4.2.4 α7nAChR activation has no effect on full-length APP levels

Upon establishing that endogenous APP undergoes NMDAR-dependent cleavage, the potential for α7nAChR to similarly couple to APP cleavage was investigated. Activation of α7nAChR has been reported to induce non-amyloidogenic cleavage of APP, (Kim *et al*., 1997; Hellström-Lindahl, 2000; Lahiri *et al*., 2002; Xiu *et al*., 2005; Mousavi and Hellström-Lindahl, 2009; Nie *et al*., 2010) in immortalised cell lines but this has not been tested in differentiated neurons. Therefore, to establish whether this effect is also observed in primary cortical neurons, cells were treated with the α7nAChR-selective agonist PNU-282987 (10μM), following a 10 min pre-incubation with the α7-PAM 10μM PNU-120596 for up to 2 h and lysates immunoblotted for full-length APP and a loading control house keeping protein β-tubulin. Over the 2 h time course α7nAChR activation had no effect on the overall levels of APP_{695}, relative to the β-tubulin loading control (figure 4.4). Further detailed analysis of the immunoblots revealed no change to the high molecular weight form of APP, known to be glycosylated mature APP, which is typically the first pool of APP to be cleaved by secretase enzymes acting at the plasma membrane (Hoey *et al*., 2009, 2013).

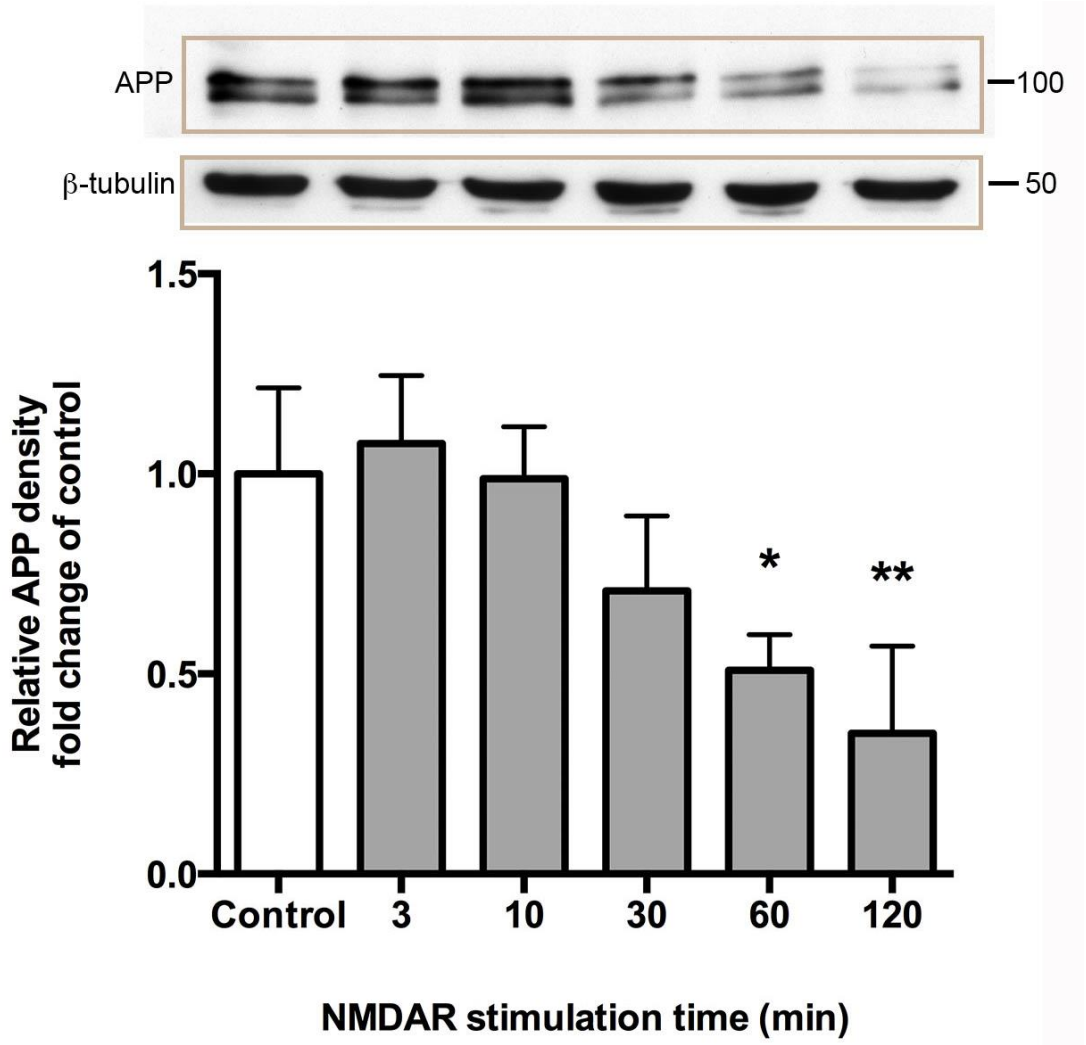

Figure 4.3: NMDAR activation induces cleavage of APP. 5-10 DIV primary cortical neurons were treated with vehicle (control) or 50μM NMDA for either 3, 10, 30, 60 or 120 min followed by immunoblotting for endogenous full-length APP_{695} and the loading control β-tubulin. Data expressed as relative mean fold change of control APP:β-tubulin ratio ± SEM, n=3 independent experiments. * indicates $p<0.05$ and ** $p<0.01$, control (white bar) vs NMDA treatment (grey bars) subjected to one-way ANOVA with Bonferroni post-test.

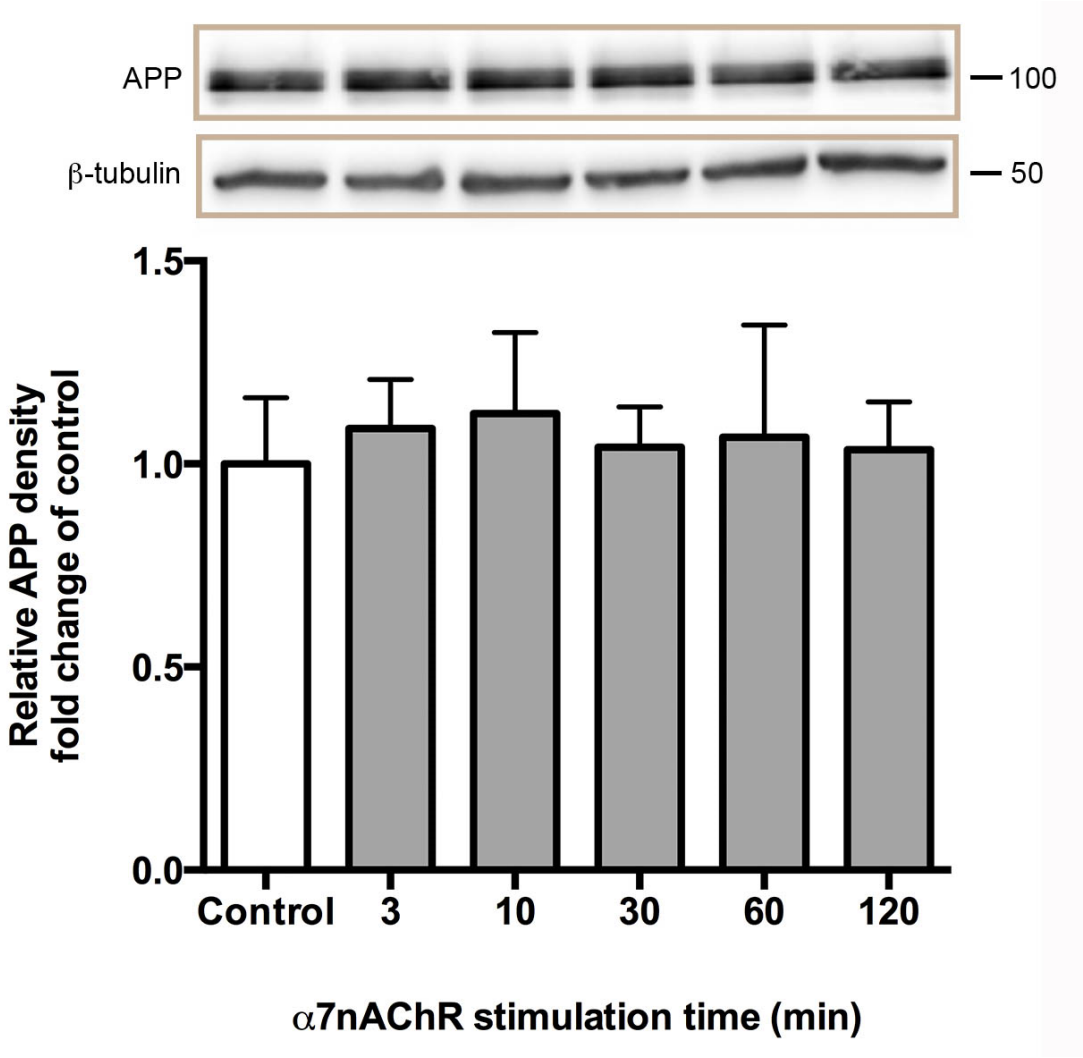

Figure 4.4: α7nAChR activation does not affect APP levels. 5-10 DIV primary cortical neurons were treated with vehicle (control) or 10 min pre-treatment with PNU-120596 prior to 10μM PNU-282987 for either 3, 10, 30, 60 or 120 min followed by immunoblotting for endogenous full-length APP_{695} and the loading control β-tubulin. Data expressed as relative mean fold change of control APP:β-tubulin ratio ± SEM, n=3 independent experiments. No significant difference over control (white bar) vs PNU-1/2 treatment (grey bars) was observed, as subjected to one-way ANOVA with Bonferroni post-test.

4.2.5 Isolation and activation of presynaptic α7nAChR has no effect on full-length APP levels

Given the distribution of α7nAChR at both presynaptic and postsynaptic sites, probing the functionality of these receptor populations individually requires separation of the distinct bodies of receptors. Given the relatively low number of α7nAChR within glutamatergic synapses (~10-15% cells, as stated in Section 3.2.5), combined with the low-sensitivity of whole cell lysate immunoblotting, a synaptosome approach was adopted to purify and concentrate mature cortical presynaptic α7nAChR and thereby assess APP densitometry, following receptor activation. Using Percoll density gradient centrifugation, whole adult mouse brain homogenates were separated into four distinct fractions (F1-F4, figure 4.5), where F3 is enriched with synaptosomes and membranes and F4 is enriched with pure synaptosomes (Dunkley *et al*., 2008). F3 and F4 were pooled to ensure sufficient viable synaptosomal material, which was subjected to vehicle, 50μM NMDA or 10μM PNU-282987 treatment (following a 10μM PNU-120596 10 min pre-treatment) for 30 min at 37°C. Following drug treatments, synaptosomes were lysed and denatured for immunoblotting. Through Western blotting, synaptosomes were assessed for expression of the nerve terminal/presynaptic marker synaptophysin, the postsynaptic marker PSD-95, dual-phosphorylated (Thr202 and Tyr204) active pERK2 and total ERK2, APP_{695} and a loading control of β-tubulin. Analysis of the immunoblotting bands revealed the purity of the synaptosome preparation and hence its validity for use in presynaptic assays. Lysates were positive for the presynaptic marker synaptophysin and negative for the postsynaptic marker PSD-95, figure 4.5 top two panels, which were unchanged following either NMDA- or PNU-1/2-treatment. Furthermore, the level of protein loaded across gel lanes was identical, as judged by β-tubulin (figure 4.5 fifth panel), and further suggested no toxicity or viability issues as a result of drug treatment. Furthermore, following 30 min NMDAR activation, a very minor increase in phospho-ERK levels was observed over basal (figure 4.5 third panel), which can be attributed to either very minimal contamination of the synaptosomes with some postsynaptic density and thus native NMDAR, or the presence of functional presynaptic NMDAR, which remains a highly controversial topic (Berg *et al*., 2013). In contrast to NMDA-treatment, 30 min α7nAChR activation resulted in a large increase in ERK phosphorylation, reinforcing the well-documented presence of functional presynaptic α7nAChR, which when

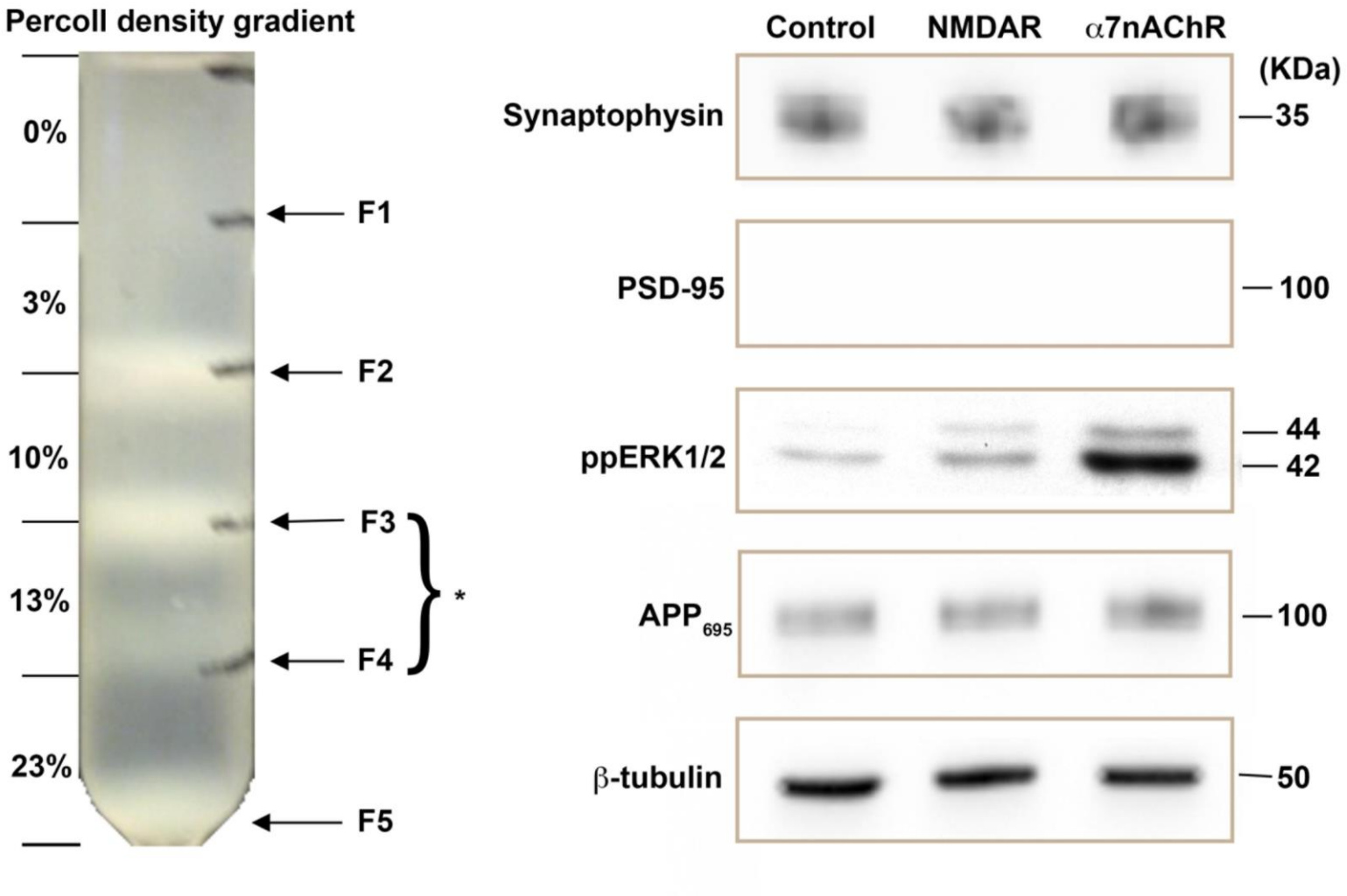
Percoll density gradient
0%
3%
10%
13%
23%
F1
F2
F3
F4
F5
*
Control
NMDAR
α7nAChR
(KDa)
Synaptophysin
35
PSD-95
100
ppERK1/2
44
42
APP695
100
β-tubulin
50

Figure 4.5: Density gradient centrifugation produces viable synaptosomes with functional presynaptic α7nAChR. Homogenised brain supernatant was applied atop a discontinuous Percoll density gradient. Five subcellular fractions (F1-F5) were produced, with the photograph identifying typical (white) gradient bands post-centrifugation. Small membranous material in F1; myelin, membranes and vesicles in F2; synaptosomes and membrane vesicles in F3; purified synaptosomes in F4 and extrasynaptosomal mitochondria in F5. Experimental synaptosomes were obtained from pooling F3 and F4 (*) and resuspending in isotonic physiological buffer before drug treatments. Synaptosomes were equilibrated at 37°C for 10 min (the duration of PNU-12596 pre-treatment, where required) and subsequently treated with vehicle (control), 50μM NMDA or 10μM PNU-282987 for 30 min before denaturing and lysates prepared for Western blot analyses. Typical immunoblots show purified synaptosomes positive for the nerve terminal marker synaptophysin and negative for the postsynaptic marker PSD-95. Activation of α7nAChR significantly increased ERK phosphorylation, unlike NMDAR activation, with no effect on either full-length APP or the loading control β-tubulin.

activated couple to the downstream activation of ERK (Dineley *et al*., 2001; Bitner *et al*., 2007; Steiner *et al*., 2007; Dickinson *et al*., 2008; El Kouhen *et al*., 2009). Purified presynaptic nerve terminals yielded low APP levels, relative to whole cell lysates, further reinforcing the mainly postsynaptic expression of APP, in accordance with Marcello *et al*., 2007. As detailed above, NMDAR activation induces robust APP processing in primary cortical neuronal whole cell lysates; however, in synaptosomes, NMDA treatment had no effect on APP holoprotein levels (figure 4.5 fourth panel). Also despite the isolation and activation of functional presynaptic α7nAChR, no effect on presynaptic APP levels was observed (figure 4.5 fourth panel), further reinforcing the lack of a measurable α7nAChR-mediated effect on APP processing in mature rodent cortex, as well as primary cortical neurons.

4.2.6 α7nAChR activation has no effect on APP-CTF production

In neurons, the constitutive cleavage of APP under basal/homeostatic conditions is carried out by an α-secretase enzyme (Kuhn *et al*., 2010) likely to be ADAM-9 (Koike *et al*., 1999), ADAM-10 (Lammich *et al*., 1999) or ADAM-17 (Slack *et al*., 2001), and results in the production of a C-terminal fragment (CTF), termed C83, along with soluble APP-α (sAPPα). Alternatively, under pathological conditions or following APP endocytosis (Cirrito *et al*., 2008), APP is cleaved by a β-secretase enzyme (BACE-1), and produces the CTF, termed C99, and soluble APP-β (sAPPβ) (Buxbaum *et al*., 1998). CTFs (8-12kDa) can be phosphorylated at Thr668 and Tyr682 (Sano *et al*., 2006; Barbagallo *et al*., 2010; Matrone *et al*., 2011), which may regulate APP processing (Barbagallo *et al*., 2010) and APP interaction with adaptor proteins (Schettini *et al*., 2010), however the definitive physiological role of CTF phosphorylation is yet to be determined. Following CTF production from APP_{695}, by α-/β-secretase, subsequent cleavage occurs by the transmembrane γ-secretase complex (Selkoe and Wolfe, 2007) to yield the APP intracellular cellular domain (AICD) and either Aβ (initial β-secretase cleavage) or p3 fragment (initial α-secretase cleavage). Thus, in order to further assess the potential for α7nAChR-mediated APP processing, APP-CTF profiles were analysed, to gain a more sensitive readout of APP cleavage by α-/β-secretase following α7nAChR activation. Using 16.5% Tris-Tricine SDS-PAGE, primary cortical neuron lysates were immunoblotted using a custom-made primary antibody raised against the C-terminus of human APP to probe the CTF profile. To characterise the profile of CTF bands, commercially available inhibitors

were used to target each secretase enzyme family individually (through TAPI-1-, BSI-, or DAPT-mediated inhibition of α-/β-/γ-secretase, respectively) to modulate the relative levels of α- and β-CTFs. Primary cortical neurons were subjected to vehicle, 50μM TAPI-1, 10μM BSI, or 10μM DAPT for 3 h, and the CTF profile compared to 1 h 10μM PNU-1/2 treatment and 20 min 50μM NMDA treatment, figure 4.6A. Under vehicle-treated (control) conditions, primary cortical neurons predominantly produced C83 α-CTFs under basal conditions (* lower molecular weight bands), in accordance with previously investigated APP-CTF profiles and constitutive α-secretase activity in primary neurons (Hoey *et al*., 2009, 2013; Kuhn *et al*., 2010). Inhibition of α-secretase with 50μM TAPI-1 (α) appeared to have little effect on C99 β-CTF production, likely due to the broad-spectrum profile of the peptide-based inhibitor and it's relatively low efficacy at ADAMs. Conversely, inhibition of β-secretase with 10μM β-secretase inhibitor (β) shifted the CTF profile to reflect enhanced α-secretase-mediated APP processing, with increased density of lower molecular weight α-CTF bands, as expected. Inhibition of γ-secretase with 10μM DAPT induced accumulation of CTFs, as they could no longer subsequently be cleaved to yield AICD and Aβ/p3 peptides. Thus the initial characterisation of CTF profiles in primary neurons mirrored that of previously published literature (Hoey *et al*., 2009, 2013; Kuhn *et al*., 2010) and the effects of α7nAChR activation could therefore be compared to NMDA treatment which enhances α-CTF production (Hoey *et al*., 2009; Tampellini *et al*., 2009; Bordji *et al*., 2010; Verges *et al*., 2011; Wan *et al*., 2012). Neurons were treated with 10μM PNU-120596 and 10μM PNU-282987 for 1 h and lysates analysed for their CTF profile, alongside the secretase inhibitors (figure 4.6A). α7nAChR activation for 1 h produced no change in CTF profile over control, indicating α7nAChR has no effect on α-secretase activity. Conversely, 20 min 50μM NMDA-treated samples mirrored the CTF profile of β-secretase inhibition, with increased α-CTF bands as a result of enhanced α-secretase activity (figure 4.6A). Previous studies have shown a time-dependent NMDAR-mediated enhancement of α-secretase-mediated APP processing, thus a time course of 50μM NMDA treatment was performed to establish the optimal time for α-CTF production (figure 4.6B). Neurons were treated with vehicle (control) or 50μM NMDA for up to 2 h, and lysates immunoblotted for APP-CTFs. NMDAR-stimulation produced a time-dependent increase in α-CTF

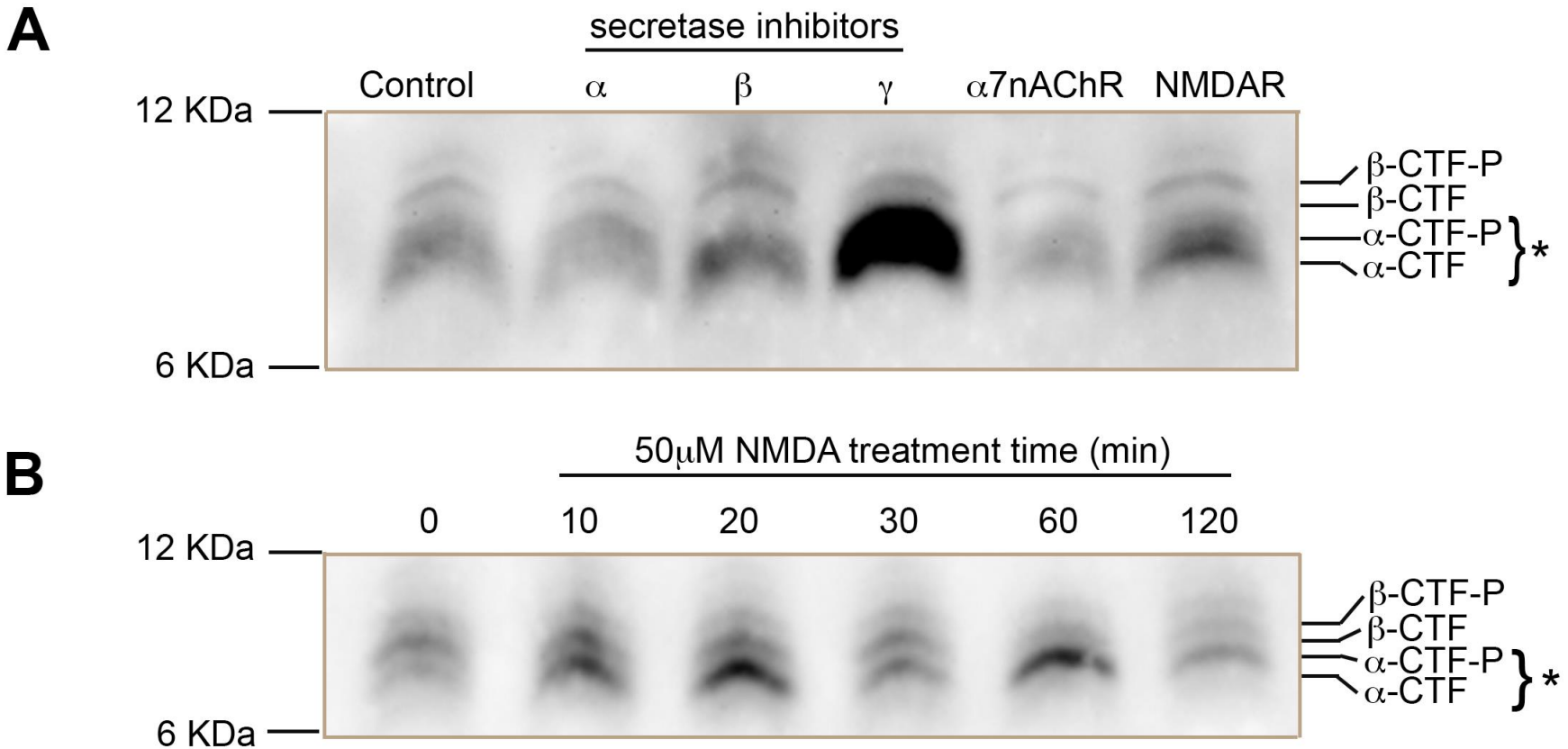
A
secretase inhibitors
Control
α
β
γ
α7nAChR
NMDAR
12 KDa
6 KDa
β-CTF-P
β-CTF
α-CTF-P
α-CTF
*
B
50μM NMDA treatment time (min)
0
10
20
30
60
120
12 KDa
6 KDa
β-CTF-P
β-CTF
α-CTF-P
α-CTF
*

Figure 4.6: NMDAR-stimulation increases time-dependent APP processing, whilst α7nAChR-stimulation has no effect over basal CTF production. A: APP C-terminal fragment (CTF) profiles under secretase enzyme activity-modulating conditions. Vehicle-treated (control) samples predominantly produced α-CTFs under basal conditions (* bottom bands), whilst inhibition of α-secretase with 50μM TAPI-1 (α), appeared to modestly modulate β-CTF production and inhibition of β-secretase with 10μM β-secretase inhibitor (β) shifted the CTF profile to reflect enhanced α-secretase-mediated APP processing, with increased α-CTF. Conversely, inhibition of γ-secretase with 10μM DAPT induced accumulation of CTFs, as they can no longer subsequently be degraded. Samples with activated α7nAChR (following PNU-120596 and PNU-282987 treatment) showed no change in CTF profile from control and 50μM NMDA-treated samples mirrored the CTF profile of β-secretase inhibition, with increased α-CTF bands. B: NMDAR-stimulation increases time-dependent non-amyloidogenic APP processing. NMDAR activation with 50μM NMDA increased α-CTF bands (* bottom bands), peaking around 20 min and returning to baseline by 2 h**.**

bands (* lower molecular weight bands, figure 4.6B), peaking around 20 min and returning to baseline by 2 h. Thus confirming primary cortical neurons are capable of stimulated non-amyloidogenic APP processing following NMDAR activation, but not α7nAChR activation.

4.2.7 α7nAChR activation has no effect on β-/γ-secretase activity

An APP-Gal4 gene reporter assay that can be used to very sensitively measure regulated APP processing has been previously described (Hoey *et al*., 2009, 2013; Cox *et al*., 2014). The assay requires transfection of primary cortical neurons with four plasmids: pRC-APP-Gal4, encoding full-length human APP_{695} fused to the yeast transcription factor Gal4 (APP-Gal4) via a glycine linker; pC1-CMV-Fe65; pFR-luciferase, encoding the Firefly luciferase gene and pRL-TKRenilla, encoding the constitutively expressed *Renilla* luciferase gene. Upon chemical transfection of primary neurons, APP-Gal4 is trafficked to the plasma membrane as an endogenous type I glycoprotein. Following secretase-mediated cleavage of APP-Gal4, AICD-Gal4 is released into the cytoplasm where it is bound directly by Fe65 and promotes AICD stabilisation (Kimberly *et al*., 2001). Upon translocation to the nucleus, AICD-Gal4 can bind to the promoter of the Firefly luciferase gene promoter of the pFR-luciferase plasmid and induce transcription of the Firefly luciferase gene. Both constitutive *Renilla* and APP cleavage-mediated Firefly luciferase gene expression is detected utilising a commercial luminescence assay kit (Section 2.2.10) and quantified Firefly luciferase data expressed as a ratio of *Renilla* luciferase expression, to account for differences in transfection efficiency between primary neurons. This sensitive molecular tool has been extensively characterised in mouse primary cortical neurons (Hoey *et al*., 2009; Cox *et al*., 2014) and has been validated as a preferential readout of pro-amyloidogenic β-γ-secretase-mediated APP processing. This APP cleavage luciferase assay was utilised to further probe the potential of α7nAChR-mediated APP processing, in response to α7nAChR activation and compared to γ-secretase inhibition using a pharmacological inhibitor, DAPT. Following 24 h 10μM DAPT treatment, a ~70% reduction in APP-Gal4-dependent luciferase gene expression was found relative to (vehicle-treated) control, indicating the assay was indeed a readout of γ-secretase-mediated APP processing. No significant effect over basal luciferase expression was observed following 6 h α7nAChR activation, by 10μM PNU-120596 and PNU-

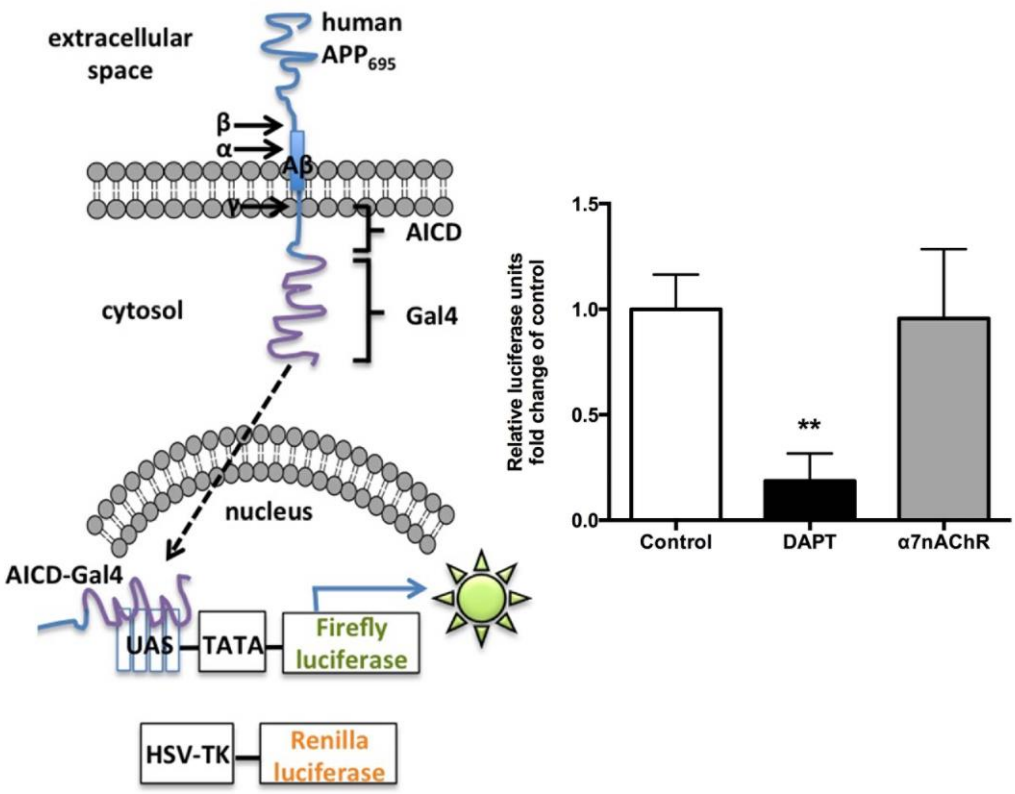

Figure 4.7: α7nAChR activation does not affect APP-Gal4 cleavage in a luciferase reporter assay measuring γ-secretase-mediated APP processing. Human APP_{695} fused to the yeast transcription factor Gal4 (APP-Gal4) is cleaved by endogenous γ-secretase, following β-secretase cleavage, to yield AICD-Gal4. AICD-Gal4 binds to the UAS and TATA box of the promoter of the Firefly luciferase plasmid and drives transcription of the luciferase reporter gene. Firefly luciferase signals are normalised to independently transfected *Renilla* luciferase plasmid signals, to account for transfection efficiency. 5 DIV primary cortical neurons were transfected with pRC-APP-Gal4, pC1-CMV-Fe65, pFR-Luciferase and pRL-TKRenilla plasmids and treated with either vehicle, γ-secretase inhibitor DAPT (10μM) for 24 h or PNU-120596 and PNU-282987 (both 10μM) for 6 h, before Dual-Glo and Stop-and-Glo luciferase activity measurement. DAPT treatment blocked γ-secretase-mediated APP processing, whilst α7nAChR activation had no effect on APP processing. Data expressed as mean fold change of control Firefly:*Renilla* luciferase activity ratio ± SEM, n=3 independent experiments, with 6 internal repeats for each independent experiment. ** indicates $p<0.01$, control (white bar) vs DAPT (black bar) subjected to one-way ANOVA with Bonferroni post-test.

282987 treatment. Thus, α7nAChR activation does not modulate α-/γ or β-/γ-secretase activity and therefore α7nAChR do not modulate APP processing in cultured cortical neurons. In contrast, NMDAR and AMPAR activation-suppressed β-γ-secretase-mediated cleavage of APP, as measured by APP cleavage luciferase assay, has been previously reported by our lab (Hoey *et al*., 2009, 2013; Cox *et al*., 2014). This APP cleavage luciferase assay further reinforces the data observed in figures 4.4-4.6; indicating α7nAChR activation has no effect on secretase-mediated APP cleavage, as detected by APP_{695} and CTF cleavage product immunoblotting.

4.2.8 α7AChR stimulation does not modulate full length Tau

Neuronal activity is known to regulate APP processing (section 1.8.2.2); similarly, very recent emerging evidence suggests neuronal activity may also control Tau release (Pooler *et al*., 2013; Yamada *et al*., 2014) before its subsequent conformation switch (Nakamura *et al*., 2012), aggregation, seeding and pathological spread (de Calignon *et al*., 2012; Jucker and Walker, 2013) from cell-to-cell as a prion-like entity (Nakamura *et al*., 2012; Sanders *et al*., 2014) before inducing neurodegeneration (Lewis *et al*., 2001; Lei *et al*., 2012). The microtubule-stabilising protein Tau is the major constituent of neurofibrillary tangle (NTF) deposits, the hallmark of tauopathies. Aβ exacerbates tau NFT formation, and tau mediates Aβ toxicity thus understanding the interplay between neuronal activity, activation of postsynaptic receptors and Aβ-induced Tau/NFT toxicity at synapses is crucial (Ittner *et al*., 2010). As the relationship between activity-dependent Tau and Aβ production, aggregation and tangle/plaque formation is coming to the fore; we reasoned activation of α7nAChR might play a role in the activity-dependent regulation of Tau phenotypes. Unpublished data from our lab strongly suggests NMDAR activation can induce re-localisation of Tau (data not shown) from the axon to dendrites (in accordance with Frandemiche *et al*., 2014). Furthermore, NMDAR activation-induced cleavage and/or dephosphorylation of Tau is evident, which may give rise to the distinct early-stage Tau strains involved in propagation of Tau pathology (Sanders *et al*., 2014). These effects are all strongly calcium dependent and given α7nAChR-mediate glutamate release to potentially act on NMDAR and AMPAR, it seemed reasonable to hypothesise that α7nAChR activation might modulate Tau. To this end, the effect of α7nAChR activation on Tau protein phenotype was examined, and compared with NMDAR activation. To prevent α7nAChR desensitisation, neurons were treated with 10μM PNU-120596 for 10 min

prior to a 1 h agonist treatment of PNU-282987 across a range of concentrations (300nM-30μM) and compared to the dose-dependent effect of 1 h NMDA treatment (1-100μM). Lysates were immunoblotted for Tau (figure 4.8) and the resultant molecular weight profiles analysed. Activation of NMDAR for 1 h induced the formation of lower molecular weight bands with 10-100μM NMDA, as a result of cleavage and/or dephosphorylation of Tau isoforms. The NMDA treatment was not excitotoxic, and the same protein concentration was loaded across the gel, and no change in β-tubulin loading control band profile was observed (figure 4.8A). In contrast, activation of α7nAChR with doses as high as 30μM PNU-282987 showed no effect on Tau or β-tubulin (figure 4.8B). PNU-282987 was restricted to a maximal dose of 30μM as higher concentrations activate non-α7nAChR (del Barrio *et al*., 2011). Therefore, activation of α7nAChR has no effect on either of the two key AD hallmarks, APP and Tau, whereas NMDAR promote both non-amyloidogenic APP processing and activity-dependent modulation of Tau.

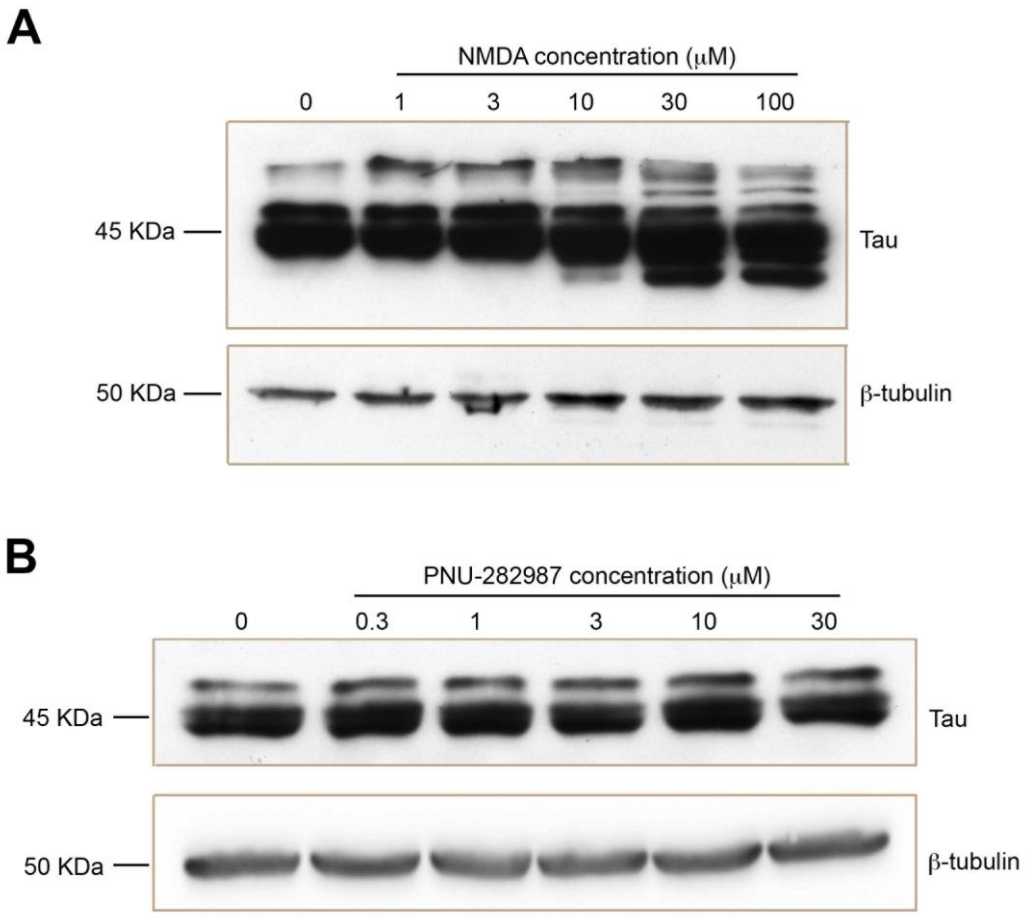

Figure 4.8: NMDAR-stimulation induces concentration-dependent Tau cleavage and/or dephosphorylation, whilst α7nAChR-stimulation has no effect on Tau. A: 5-10 DIV primary cortical neurons were treated with vehicle (control, 0μM) or 1, 3, 10, 30 or 10μM NMDA for either 1 h followed by immunoblotting for endogenous full length Tau and the loading control β-tubulin. Concentration-dependent (10-100μM) NMDA treatment revealed the appearance of lower molecular weight Tau bands. B: 5-10 DIV primary cortical neurons were treated with vehicle (control, 0μM) or 0.3, 1, 3, 10 or 30μM PNU-282987 for 1 h following 10 min 10μM PNU-120596 pre-treatment, followed by immunoblotting for endogenous full length Tau and the loading control β-tubulin. Sustained α7nAChR activation had no effect on Tau protein profile, over control.

4.3 Discussion

The aim of this results chapter was to assess the α7nAChR-mediated contribution to APP processing, with the hypothesis that α7nAChR activation in primary cortical neurons would directly enhance non-amyloidogenic APP processing in an ERK-dependent manner, or indirectly via α7nAChR-mediated glutamate release and concomitant activation of postsynaptic glutamate receptors. Accordingly, this chapter has shown primary cortical neurons express predominantly postsynaptic APP, along with the putative α-secretases ADAM-10 and ADAM-17; but that α7nAChR-specific activation had no effect on whole cell APP levels, presynaptic APP levels, CTF production, β-/γ-secretase activity or full length Tau levels, when compared to NMDAR activation.

4.3.1 α7nAChR activation does not modulate APP processing

α7nAChR-mediated cellular activation with PNU-282987, in the presence of the PAM PNU-120596, is insufficient to promote non-amyloidogenic APP processing, as α7nAChR activation had no effect on full-length APP protein levels or APP cleavage product CTF levels. Given the limitations of low sensitivity biochemical immunoblotting, the highly sensitive measurement of β-γ-secretase-regulated APP processing by APP cleavage luciferase assay was used to validate the lack of α7nAChR effect. Again, α7nAChR activation showed no effect on β-γ-secretase activity-dependent production of Gal4-AICD, reinforcing the negligible effect on APP processing. Conversely, the majority of studies have shown the non-selective nAChR agonist nicotine enhances non-amyloidogenic sAPPα release from neuron-like cell lines (Kim *et al*., 1997; Lahiri *et al*., 2002; Mousavi and Hellström-Lindahl, 2009; Nie *et al*., 2010). This discrepancy may have arisen due to the cell lines expressing high levels of α7- and non-α7 nAChR, which are capable of coupling to non-amyloidogenic APP processing via nAChR-mediated calcium-influx. In contrast, the low physiological expression level of α7nAChR within the primary cortical neurons, coupled with the spatial separation of presynaptic α7nAChR being segregated from the large pool of postsynaptic APP may explain the opposing findings. Nonetheless, using synaptosomes, this study shows α7nAChR activation cannot couple directly to APP processing at the presynaptic nerve terminal. Furthermore, the lack of α7nAChR-mediated non-amyloidogenic processing is in agreement with the *in vivo* use of the

α7-selective agonist A-582941, in the treatment of 3xTg-AD transgenic mice, which display robust AD pathology and cognitive deficits. A-582941-mediated α7nAChR activation had no effect on AD pathology (Medeiros *et al*., 2014), in accordance with native physiological α7nAChR having no effect on APP processing and thus plaque deposition.

Furthermore, published data from α7nAChR-expressing SH-SY5Y and PC12 cell lines (Hellström-Lindahl *et al*., 2000; Hu *et al*., 2008), *in vivo* in wildtype and AD transgenic Tg2576 mice and validated in α7nAChR-knock-out mice, showed α7nAChR-selective activation reduced Tau phosphorylation (Bitner *et al*., 2009), through reduced GSK-3β activation (Cavallini *et al*., 2013). Conversely, data presented in this chapter highlighted α7nAChR activation in primary neurons had no effect on Tau phosphorylation. This contrasting effect may again be the result of a difference in α7nAChR expression level between cell types, especially following chronic *in vivo* activation of α7nAChR following a 2-week infusion of α7nAChR-selective agonist (Bitner *et al*., 2009). Chronic nAChR agonist treatment dramatically up-regulates nAChR receptor expression (Peng *et al*., 1994; Molinari *et al*., 1998; Liu *et al*., 2001; Vallejo *et al*., 2005; Fu *et al*., 2009; St John, 2009; Goriounova and Mansvelder, 2012; Mazzo *et al*., 2013), and subsequently leads to up-regulation of ionotropic glutamate receptor expression, following enhanced nAChR-mediated glutamate release both *in vitro* and *in vivo* (Risso *et al*., 2004; Wang *et al*., 2007; Lozada *et al*., 2012). Increased ionotropic glutamate receptor expression and activation thus modulates and attenuates Tau phosphorylation, indirect of subsequent nAChR activation.

4.3.2 NMDAR activation promoted non-amyloidogenic APP processing

Numerous previous studies have reported an NMDA-induced effect on APP processing, although whether NMDAR activation mediates non-amyloidogenic or pro-amyloidogenic APP processing remains somewhat controversial. Using SDS-PAGE and Western blot analyses; NMDAR activation was shown to reduce the levels of full length APP_{695}, indicative of cleavage, whilst also enhancing the production of α-CTF, thus promoting non-amyloidogenic APP processing. The findings presented here are in agreement with previous findings from our lab (Hoey *et al*., 2009), that NMDAR activation promotes non-amyloidogenic APP processing, and also in agreement with

independent findings (Tampellini *et al*., 2009; Bordji *et al*., 2010; Verges *et al*., 2011; Rush and Buisson, 2014).

Conversely, previous studies have reported functional APP processing and Aβ release from synaptosomes (Kim *et al*., 2010b), mediated by activation of metabotropic glutamate receptors. Given this study showed nerve terminal activation of ionotropic NMDA-type glutamate receptors had no effect on APP processing, this suggests NMDAR-mediated APP processing requires intact postsynaptic NMDAR-associated components (for downstream signalling cascades and/or direct modulation of postsynaptic APP cleavage); and further reinforces the previous evidence of postsynaptic NMDAR-mediated non-amyloidogenic APP processing (Hoey *et al*., 2009; Tampellini *et al*., 2009; Bordji *et al*., 2010; Verges *et al*., 2011; Rush and Buisson, 2014).

Furthermore, synaptic AMPAR and NMDAR activation both in this study and others in primary neurons indicate activation of ionotropic glutamate receptors modulates Tau phosphorylation (Mattson, 1990; Pooler *et al*., 2013) and cleavage (Garg *et al*., 2011). As with APP processing, memantine-mediated blockade of extrasynaptic NMDAR attenuates Aβ-induced tau hyperphosphorylation and toxicity (Song *et al*., 2008). This reinforces the protective effect of synaptic NMDAR activation, over the toxic repercussions of extrasynaptic NMDAR activation.

4.3.3 Non-amyloidogenic APP processing is not guaranteed following activity-dependent ERK phosphorylation

Given the data described in chapter 3, treatment with PNU-282987 and PNU-120596 selectively activates α7nAChR in primary cortical neurons, resulting in increased ERK phosphorylation. Thus, α7nAChR-induced cellular activation and resultant ERK phosphorylation is insufficient to induce APP processing, in contrast to ERK-dependent non-amyloidogenic APP processing following activation of other ligand-gated ion channels, such as NMDAR (Mills *et al*., 1997; Desdouits-Magnen *et al*., 1998; Kamenetz *et al*., 2003), AMPAR (Hoey *et al*., 2013) and P2X7 receptors (Delarasse *et al*., 2011); whereas mAChR-mediated non-amyloidogenic APP processing has been shown to be ERK phosphorylation-independent (Cissé *et al*., 2011). Furthermore, in accordance with the opposing effects of non-amyloidogenic versus pro-amyloidogenic APP processing following synaptic versus extrasynaptic NMDAR activation, a similar effect on ERK phosphorylation is also well documented. Synaptic NMDAR activation enhances ERK activation, whilst extrasynaptic NMDAR

activation inactivates ERK (Ivanov *et al*., 2006; Hoey *et al*., 2009). This further reinforces and validates the experimental conditions used in this thesis to characterise and investigate α7nAChR- and NMDAR-dependent ERK-mediated non-amyloidogenic APP processing.

4.3.4 Summary

When taken together, the findings of this chapter are relevant as contrary to published literature; activation of α7nAChR cannot promote APP processing. Furthermore, functional nerve terminal α7nAChR were spatially separated from the majority of neuronal APP, localised postsynaptically. Following activation of synaptosome-isolated nerve terminal α7nAChR, ERK phosphorylation resulted but could not directly promote APP processing. In whole-cell primary cortical neurons, α7nAChR activation was incapable of directly modulating APP processing, nor indirectly via a validated non-amyloidogenic APP processing mediator: activation of postsynaptic ionotropic glutamate receptors.

Chapter 5

5. α7nAChR modulation of microglial behaviour

5.1 Introduction

5.1.1 α7nAChR and modulation of microglial function

Microglia, derived from erythromyeloid precursors, are found uniformly distributed throughout the CNS and form the innate defence as the resident CNS immune cells (Ginhoux *et al*., 2010; Prinz and Priller, 2014). Microglia are highly versatile in assuming either a protective or neurotoxic state in response to environmental changes, through switching from their default 'resting' state of scanning the local environment, to a specialised 'activated' state in a diseased environment (Gordon, 2003; Mosser and Edwards, 2008; Kettenmann *et al*., 2013), where they proliferate to expand the population of immunoresponsive cells (Gómez-Nicola *et al*., 2013). Recent data suggests there are not merely two phenotypic states, as originally perceived, but a spectrum of microglial activation states (Xue *et al*., 2014). Activated microglia can immediately remove damaged cells and synapses by phagocytosis, termed 'phagoptosis' and 'synaptic stripping', respectively, along with foreign and infectious agents. A balance must be struck with immune cell phagocytic activity (Brown and Neher, 2014), with basal phagocytosis processes controlling debris and bacterial clearance, whilst overactive phagocytosis induces widespread neuron death (Neher *et al*., 2011; Emmrich *et al*., 2013). Neuron-secreted signalling molecules and downstream microglial cellular cascades result in neuron-microglia cellular contact and induction of phagocytosis, which can influence the pathological processes involved in disease onset and progression. Understanding the distinct microglial-neuronal communications involved in regulating CNS development during synaptogenesis (Parkhurst *et al*., 2013), synapse pruning (Kettenmann *et al*., 2013) and synapse maturation (Salter and Beggs, 2014) is crucial for targeting aberrant glia-neuron signalling observed in chronic disease (Zhan *et al*., 2014). A recent study highlighted early (24 h post-injury) microglia-neuron contact following CNS damage, whilst subsequent infiltrating macrophages were shown to persist (up to 42 d post-injury). This suggests microglia phagocytose initial damaged material, whilst infiltrating peripheral macrophages may contribute to the secondary CNS damage following injury (Greenhalgh and David, 2014). Using RNA sequencing, the microglial transcriptome was shown to change over the course of aging, with transcripts shifting from an initial endogenous ligand recognition phase to adopt a neuroprotective microbe recognition and host defence state (Hickman *et al*., 2013), thus indicating a heightened capacity for phagocytosis with age. Microglial phagocytosis controls CNS

homeostasis, through removal of cellular debris and neurotoxic foreign contaminants. Reduced *in vitro* and *in vivo* microglial phagocytosis results in enhanced inflammation and neurodegeneration, with impaired phagocytic capacity observed in AD patient brain samples (Lucin *et al*., 2013). Excessive release of microglial pro-inflammatory cytokines reduced Aβ phagocytosis (Koenigsknecht-Talboo and Landreth, 2005), further emphasising the need to understand and subsequently control microglial hyperactivation in chronic neurodegenerative disease states.

Activation of microglial α7nAChR has been shown to reduce cytotoxicity, mediated by various extracellular insults (Kawamata and Shimohama, 2011). Much of the initial literature to date has focussed on α7nAChR-mediated attenuation of Aβ toxicity, through enhanced microglial phagocytosis, to explain the anti-inflammatory properties of α7nAChR activation. Accordingly, excessive levels of Aβ result in microglial conversion to the 'activated' state. Microglial phenotype conversion results in production and release of neurotoxic cytokines, chemokines and reactive oxygen species, with deleterious effects on the CNS. Pro-inflammatory cytokine release triggers Tau hyperphosphorylation (Rojo *et al*., 2008), with implications for the etiology of AD, as previously discussed. Interestingly, α7nAChR immunoreactivity was observed to increase in glial cells throughout AD, representative of a compensatory mechanism to lower Aβ (Teaktong *et al*., 2003). Activation of α7nAChR prevented Aβ-induced reactive oxygen species secretion by microglia (Moon *et al*., 2008). Furthermore, the AChE inhibitor donepezil reduced pro-inflammatory microglial activation, with attenuated TNFα and reactive oxygen species production and release (Hwang *et al*., 2010). The α7nAChR-selective partial agonist GTS-21 restored the phagocytic activity of compromised macrophages; to enable enhanced bacterial clearance (Sitapara *et al*., 2014), whilst the AChE inhibitor galantamine has also shown enhanced microglial phagocytic activity, with increased Aβ clearance (Takata *et al*., 2010).

The current favoured signalling mechanism behind microglial phagocytosis involves the ligand-activated nuclear receptor peroxisome proliferator-activated receptor-γ (PPARγ, Heneka and Landreth, 2007), which acts in a metabolic cycle to increase brain apolipoprotein E (ApoE) levels (Mandrekar-Colucci *et al*., 2012), with ApoE promoting the clearance of unwanted cellular material, such as Aβ (Heneka *et al*., 2005). Both *in vitro* and *in vivo* PPARγ activation enhanced microglial phagocytosis and resulted in reduced soluble and insoluble Aβ in the cortex and hippocampus of

AD transgenic mice (Yamanaka *et al*., 2012), inhibited excessive pro-inflammatory cytokine gene expression and reduced Aβ- and cytokine-mediated neurotoxicity (Heneka and Landreth, 2007) and improved cognition (Cramer *et al*., 2012). *In vivo* application of a PPARγ agonist improved hippocampal-dependent cognitive deficits in humans and ameliorated cognitive deficits in AD transgenic mice. The mechanism of cognitive enhancement was purported to be through convergence of PPAR signalling and the MAPK-ERK cascade, strongly implicated in memory consolidation (section 1.4.2.3). PPAR agonism induced a PPARγ-phospho ERK complex, with PPAR activation facilitating recruitment of activated ERK (Jahrling *et al*., 2014).

Based on these published data, this chapter aims to show α7nAChR activation modulates microglial phagocytic behaviour. The results described within this chapter involve the characterisation of primary cortical microglia, analyses of functional expression of α7nAChR with respect to ERK phosphorylation and determination of microglial α7nAChR activation-induced phagocytosis.

5.2 Results

5.2.1 Primary cortical glia mature *in vitro,* with microglia adopting a basal 'resting' phenotype

Many studies attempting to understand CNS inflammation and the molecular mechanisms underlying neurodegeneration, use cell lines or microglia derived from embryonic tissue. As such, these *in vitro* models are less suitable in the study of aging and neurodegeneration (Stansley *et al*., 2012). In this study, we used neonatal P1-P2 CD1 mouse pups, to isolate primary mixed glia (astrocytes and microglia) from the cortex, which were grown and matured *in vitro* for 4-6 weeks (Saura *et al*., 2003). Photographed phase contrast microscopy of the mixed glial population revealed cellular maturation and proliferation *in vitro* over time (figure 5.1). The time-lapse sequence of images revealed significant cellular proliferation between 1 and 6 DIV (figure 5.1A and B, respectively), with a confluent monolayer by 14 DIV (figure 5.1C) that became dense by 22 DIV (figure 5.1E). Analysis of the surface characteristics of the culture revealed distinct morphologies at different microscopic focal planes. The top layer of cells possessed a round, flat and cobblestone morphology, typical of resting astrocytes (figure 5.1C and E), whilst the bottom layer of cells possessed the irregular, spiked and ramified morphology of resting microglia, (figure 5.1E) (Glenn *et al*., 1992) clearly visible at higher magnification (figure 5.1F).

5.2.2 Microglia are purified from a mixed glial population through mild trypsin incubation

Upon microglial cells reaching confluency, following 4-6 weeks *in vitro*, the contaminating astrocytes were removed from on top of the microglia through mild trypsin incubation. 0.0625% trypsin application onto mixed glia (figure 5.2A) resulted in the detachment of an intact layer of cells, starting at the periphery of the well and spread across the entire monolayer with time (figure 5.2B). The detached monolayer contained all the astrocytes and lifted away from the underlying microglia in one sheet (figure 5.2B, arrow). The trypsin isolation procedure was minimally invasive and resulted in a highly enriched and dense layer of microglia on the bottom of plastic wells or on glass coverslips (figure 5.2C).

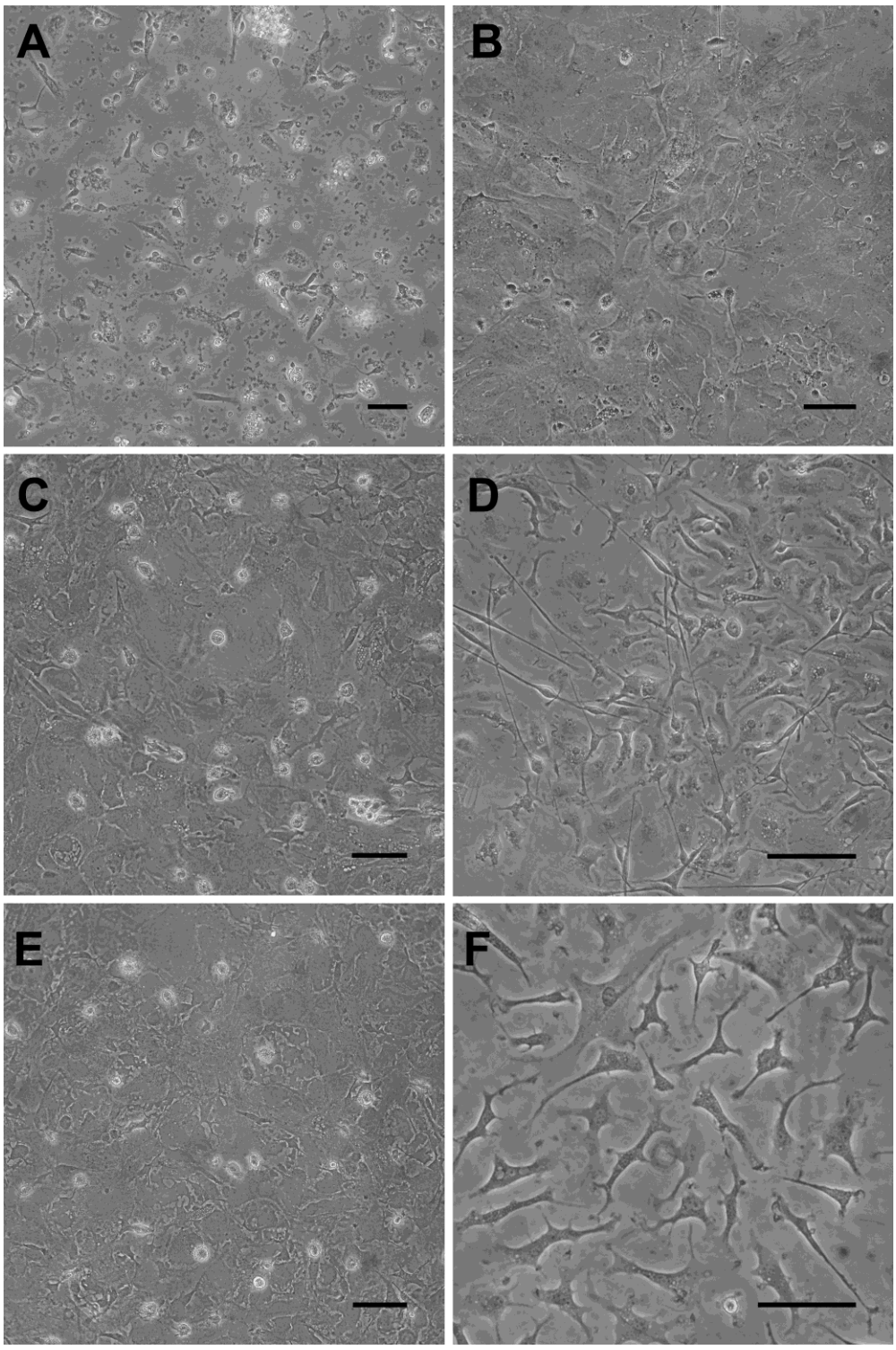

Figure 5.1: Morphological assessment of primary cortical mixed glia over time *in vitro.* A: Freshly isolated and plated glial cells following 1 DIV. B: Proliferation gives rise to a mixed glial monolayer by 6 DIV. C: Astrocyte confluency was reached by ~14 DIV, with a dense and uniform top layer of astrocytes visible. D: A bottom layer of microglia was clear by 14 DIV. E: With increasing time (22 DIV), the astrocyte layer became increasingly dense. F: High magnification of 22 DIV microglia, beginning to reach confluency. Scale bars represent 20μm.

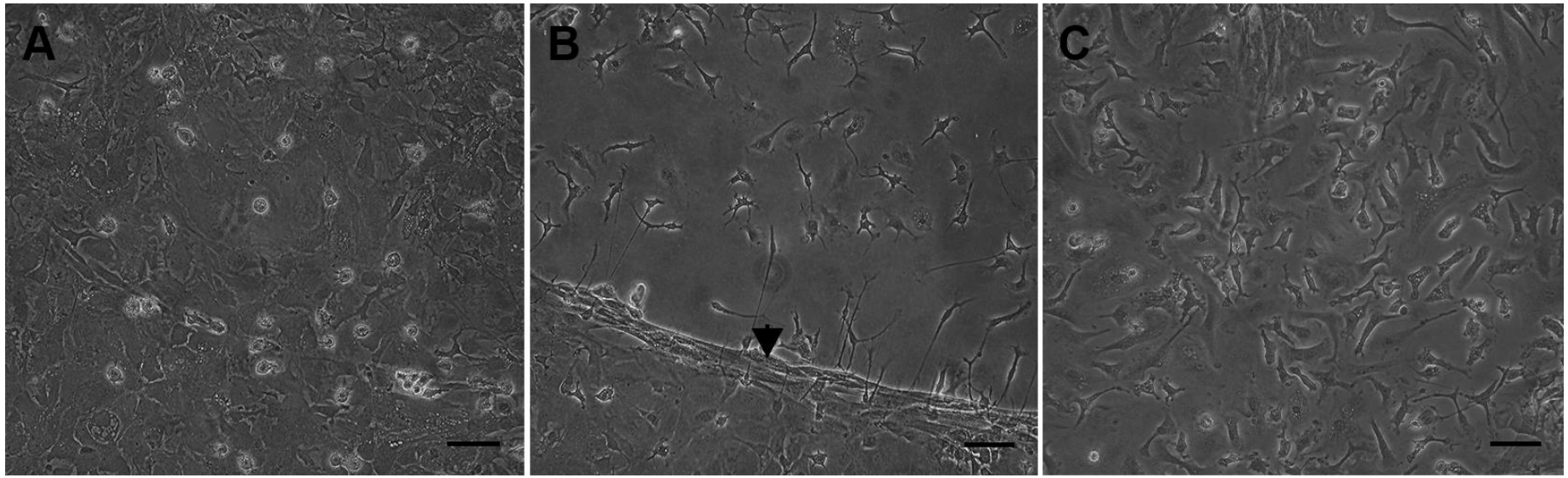

Figure 5.2: Purification of microglia from a mixed glial population. A: Confluent mixed glial cells following 35 DIV. B: Trypsin-EDTA (0.0625%) solution in DMEM-F12 medium was incubated on mixed glia for 15-25 min at 37°C, and the top astrocyte cell layer detached as a sheet (arrow). C: The remaining microglia monolayer was left in mixed glia-conditioned medium for 24 h, before use in immunofluorescence, biochemical assays or Western blotting.

5.2.3 Purified microglia are free from astrocytic contaminants and display microglia-specific protein expression

Both mixed glia and purified microglia were subjected to immunofluorescence staining, to determine expression of cell type-specific markers. Astrocytes are the major glial cell present within the CNS and selectively express glial fibrillary acidic protein (GFAP) (Brahmachari *et al*., 2006), figure 5.3A. Following trypsinisation of the mixed glial population, resulting in microglial purification and isolation, GFAP expression was completely abolished (figure 5.3B), indicating no contaminating astrocytes were present in the remaining microglial population. Microglia selectively express the β-integrin variant cluster of differentiation molecule 11B (CD11b) (Roy *et al*., 2006), figure 5.3C. Primary cortical microglia were positive for CD11b expression, which was localised to the cytoplasm and expressed throughout population of cells, indicating 100% microglial purity.

5.2.4 Primary microglia adopt a reactive 'activated' phenotype following exposure to LPS

To determine the reactive nature of the primary microglia, the cells were exposed to the bacterial endotoxin lipopolysaccharide (LPS, 100ng/ml) for 20 min. LPS is a widely used and powerful activator of microglial cells both *in vitro* and *in vivo* (Sun *et al*., 2008; Schmid *et al*., 2009; Chen *et al*., 2012), with LPS application triggering pro-inflammatory gene expression, signalling cascades, pro-inflammatory cytokine release and cell death. To establish the functional responsiveness of the primary cortical microglia, LPS was used to examine the reactive phenotype of the cells through their potential to undergo well-characterised shape changes from the 'resting' to 'activated' state (Pocock and Kettenmann, 2007). Under basal conditions, microglia appear classically ramified through both phase contrast microscopy (figure 5.4A) and confocal immunofluorescence (figure 5.4C), with microglial processes constantly surveying their surroundings. Following microglial activation with LPS, the cells undergo the characteristic shape change transformation and subsequently appear amoeboid (figure 5.4B and D), indicative of responsive and functional primary cortical microglia.

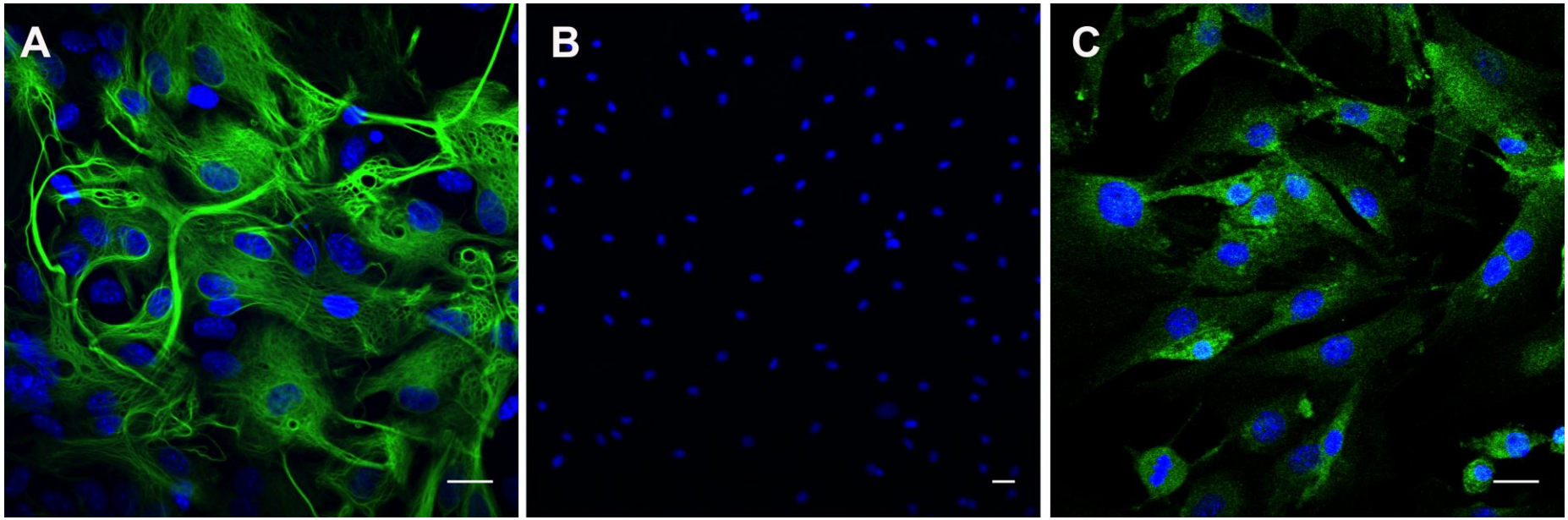

Figure 5.3: Purified primary microglia are free of astrocytic contaminants and express microglia-specific markers. A: 38 DIV mixed glial populations were subjected to single immunofluorescence staining, revealing GFAP (green) expression throughout the cytoplasm of approximately one third of the DAPI-positive total cell population. B: Purified microglia were negative for GFAP expression, indicating no astrocyte contamination post-purification. C: Immunofluorescence of 38 DIV purified microglia exhibited CD11b expression (green) throughout the cytoplasm of all DAPI-positive cells, indicating a pure microglial population. All glial cells were negative for the neuron-specific markers Tau and NeuN (data not shown). All nuclei were counter stained with DAPI (blue) and scale bars show 20μm.

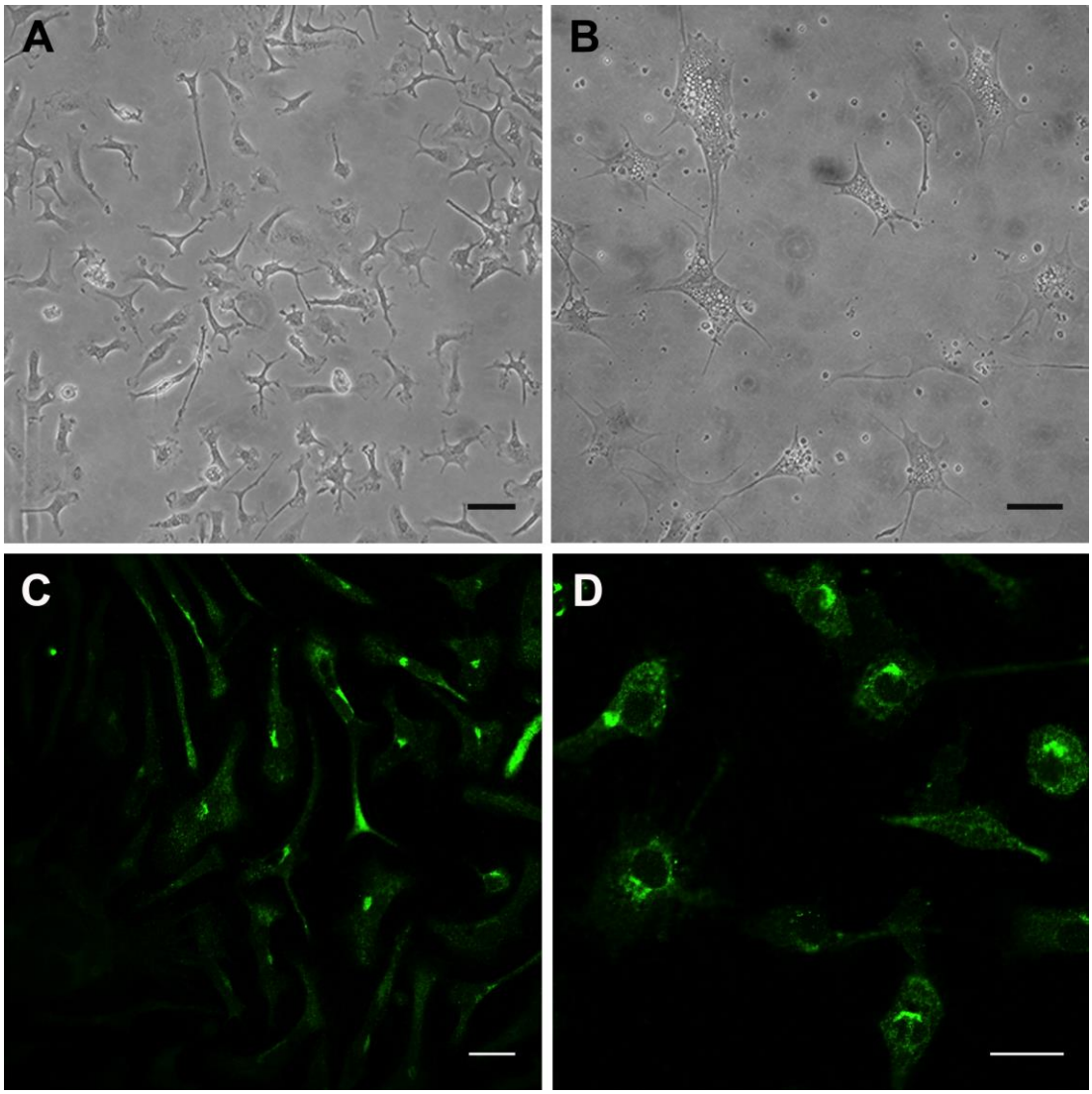

Figure 5.4: LPS exposure of primary microglia induces a reactive phenotype. A: Following purification and under homeostatic *in vitro* conditions, microglia appeared highly ramified with spiked processes by phase contrast microscopy. B: Following 100ng/ml LPS treatment for 20 min, microglia appeared to adopt a round and amoeboid morphology. C: Single immunofluorescence staining of untreated microglia revealed APP expression (green) throughout the cytoplasm, with an additional strong peri-nuclear localisation. D: LPS-induced cellular activation revealed the microglial cell body increases in roundness, indicative of an activated microglial phenotype. Scale bars show 20μm.

5.2.5 Primary microglia are functional and express α7nAChR that couple to ERK phosphorylation

To test the hypotheses that α7nAChR activation is capable of modulating microglial behaviour, demonstrating functional α7nAChR *in vitro* was essential. Changes in ERK phosphorylation status have been documented following glial cell activation, but its role is yet to be well defined in terms of microglial inflammatory cell behaviour. The effect of glial α7nAChR activation has been shown to both enhance (Koyama *et al*., 2004; Wang *et al*., 2013) and reduce (Shytle *et al*., 2004; Cui and Li, 2010) ERK phosphorylation, and is thus yet to be defined thoroughly. To establish the functional nature of the α7nAChR expressed by the primary cortical microglial model system, assessment of the ERK-coupling capacity of these receptors was carried out. 28-50 DIV microglia were subjected to combinatorial treatment with 10μM PNU-282987 for up to 1 h, following a 10 min pre-incubation with PNU-120596, and lysates immunoblotted for dual-phosphorylated (Thr202 and Tyr204) active pERK2 and total ERK2. Treatment with either the PAM (PNU-1) or agonist (PNU-2) alone had no significant effect over vehicle-treated control (figure 5.5A). However, PNU-1 potentiated α7nAChR activation with PNU-2 caused a rapid and significant ~18-fold increase in ERK2 phosphorylation, over vehicle-treated control samples (figure 5.5A). Over a time course of 1 h, ERK phosphorylation was significantly elevated following acute (3 min) PAM-potentiated α7nAChR activation, with phosphorylation status returning to baseline levels over longer periods of treatment (10-30 min). Interestingly, following 60 min α7nAChR activation, a trend towards an increase in ERK phosphorylation was observed (~10-fold), which can be attributed to a non-α7nAChR-mediated effect, as it is also observed following αBTX-mediated inhibition of α7nAChR (figure 5.5B). To establish the selectivity of the α7nAChR activation-dependent ERK phosphorylation, microglia were pre-treated for 20 min with αBTX (100nM), before application of PNU-120596 and PNU-282987 for up to 1 h (figure 5.5B). Application of αBTX alone had no effect on basal levels of ERK phosphorylation, indicating the functional population of α7nAChR were not modulating baseline microglial signalling and activation state. αBTX-mediated inhibition of α7nAChR currents significantly abolished PNU-282987-mediated ERK phosphorylation, returning phospho-ERK to baseline level, reinforcing the selectivity of α7nAChR-mediated microglial activation. Again, following 60 min α7nAChR

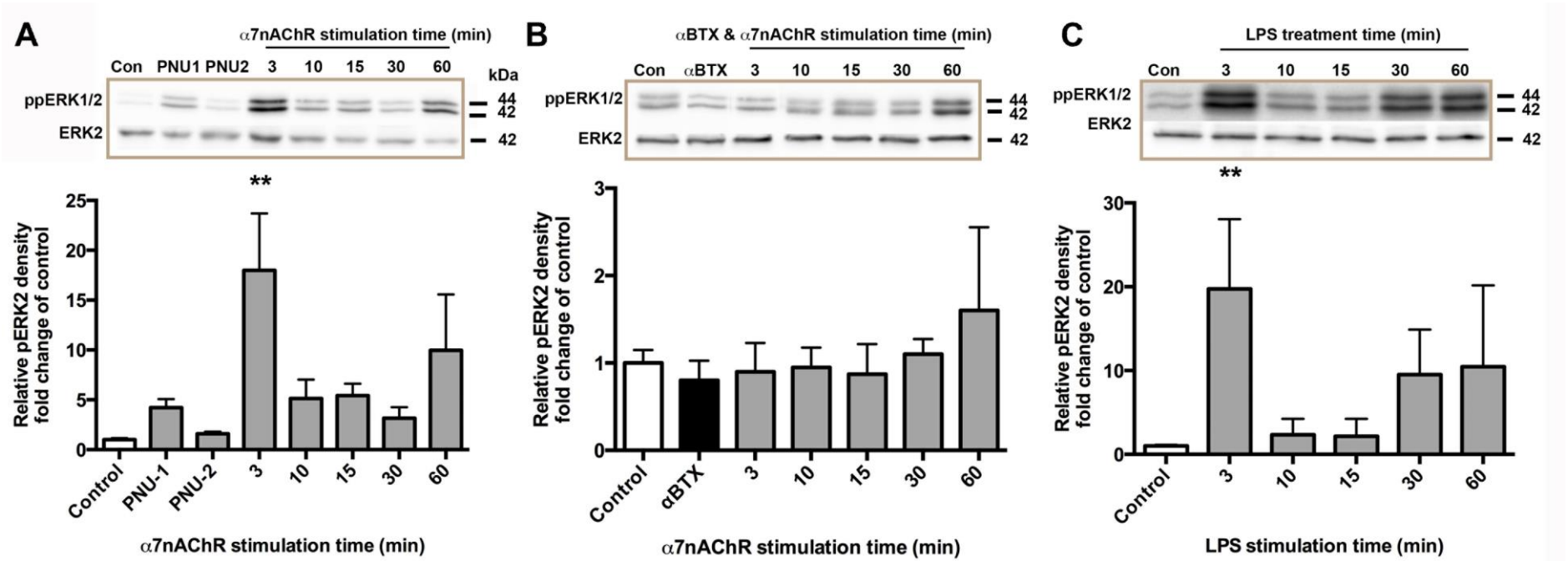

Figure 5.5: Cellular activation and stimulation of α7nAChR couples to ERK phosphorylation in 28-50 DIV primary microglia. A: PNU-282987 treatment in combination with PNU-120596 induces rapid ERK phosphorylation. B: PNU-mediated ERK phosphorylation is blocked by αBTX. C: Cellular activation with treatment with the bacterial endotoxin LPS induces rapid ERK phosphorylation. Protein band densitometry quantification expressed as the ratio of pERK2 to total ERK2 and indicates a significant time-dependent elevation in MAP kinase (ERK) activation. Data expressed as mean fold change of control pERK2:ERK2 ratio ± SEM, n=3 independent experiments. Representative ppERK1/2 and ERK2 blots for each experiment A-C are shown. ** indicates $p<0.01$, control (white bar) vs agonist/PAM treatment (grey bars) subjected to one-way ANOVA with Bonferroni post-test.

activation, even in the presence of αBTX, a trend towards a sight increase in ERK phosphorylation was observed, further reinforcing an α7nAChR-independent secondary effect of prolonged α7nAChR activation (figure 5.5B). To establish the selectivity of microglial activation and downstream ERK phosphorylation, 28-50 DIV microglia were subjected to treatment with 100ng/ml LPS for up to 1 h, and lysates immunoblotted for dual-phosphorylated (Thr202 and Tyr204) active pERK2 and total ERK2. LPS treatment is a well-characterised immune cell activator, but results in the release of pro-inflammatory cytokines. Acute LPS treatment for 3 min increased ERK phosphorylation ~20-fold over vehicle-treated control, whilst longer time points of 30-60 min displayed a trend towards increased ERK activation (figure 5.5C). Furthermore, 50μM NMDA treatment for up to 1 h had no effect (data not shown) on microglial ERK activation, consistent with a lack of functional NMDAR on microglia (Pocock and Kettenmann, 2007) and reinforcing the selectivity of the α7nAChR-mediated cellular activation.

5.2.6 α7nAChR activation promotes microglial phagocytosis

Phagocytosis is a specialised form of endocytosis by which large particles are ingested by specialised cell types (macrophages, neutrophils and microglia). Phagocytosis is a triggered process that requires activated receptors at the cell surface initiating a signalling cascade into the cell interior to start the process. The molecular mechanisms underlying phagocytosis are yet to be fully identified, but can occur by either a non-classical receptor-mediated mechanism via β_1-integrins, or by classical phagocytosis mechanisms via Ig receptors or complement receptors (Koenigsknecht and Landreth, 2004). The phagocytic capacity of primary microglia was assessed by ingestion of fluorescently labelled beads (Hassan *et al*., 2014) upon LPS-mediated cellular activation or stimulation of α7nAChR. Under basal vehicle-treated control conditions microglia phagocytosed 3 beads per cell, (figure 5.6A and 5.6B) whilst LPS treatment increased phagocytosis ~2.5-fold, indicative of responsive and activated microglia (figure 5.6A). Treatment with PNU-120596 or PNU-282987 alone had no significant effect on phagocytosis, reinforcing the previous observation for the requirement for PAM-potentiated α7nAChR activation to induce cellular activation and ERK phosphorylation. Combinatorial treatment with both PNU-1 and PNU-2 enhanced bead phagocytosis by 4-fold (figure 5.6A and 5.6C), in agreement with analogous published literature. For example, galantamine-mediated α7nAChR

activation enhanced microglial phagocytosis of Aβ, and depletion of the α7nAChR-selective agonist choline reduced Aβ phagocytosis (Takata *et al*., 2010). Furthermore, α7nAChR activation has previously been shown to enhance macrophage phagocytosis (Lee and Vazquez, 2013; Sitapara *et al*., 2014). Application of αBTX had no effect on basal levels of phagocytosis, when applied alone, but completely abolished the α7nAChR-mediated phagocytosis with PNU-120596 and PNU-282987, highlighting the specificity of the α7nAChR effect (figure 5.6A). The contribution of phagocytosis versus endocytosis was determined through blocking endocytosis with dynasore. Dynasore is a cell-permeable inhibitor of dynamin GTPase activity (Macia *et al*., 2006), which blocks both dynamin-1 and dynamin-2, required for clathrin-mediated endocytosis. Dynasore-mediated inhibition of endocytosis is well characterised (Macia *et al*., 2006; Hua *et al*., 2013; Xu *et al*., 2013). Pre-treatment with 100μM dynasore prior to bead and drug application was not sufficient to attenuate α7nAChR-mediated phagocytosis, suggestive that the bead uptake into microglia is not via endocytosis. Dynasore has previously been shown to reduce macrophage phagocytosis of parasitic protozoa (Barrias *et al*., 2010) and inhibits the formation of phagocytic cups in testicular Sertoli cells (Otsuka *et al*., 2009), but has not been tested as an inhibitor of microglial phagocytosis.

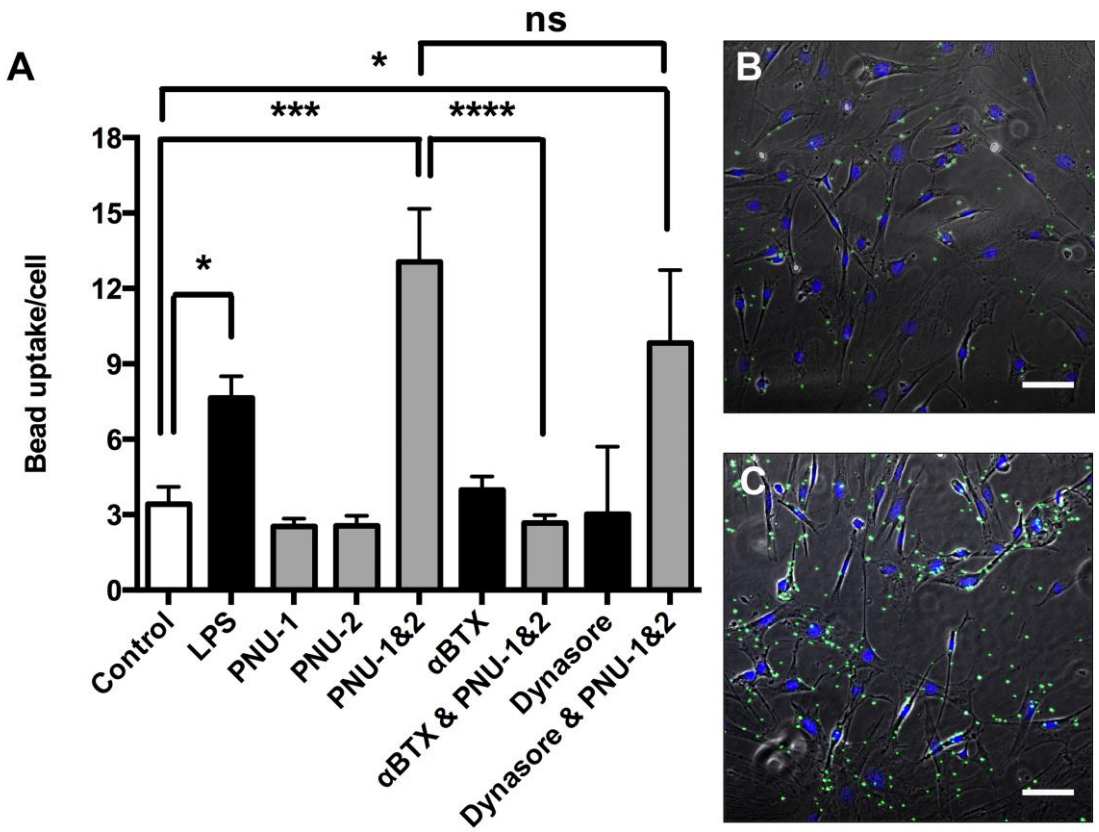

Figure 5.6: LPS-activated and α7nAChR-stimulated microglia display increased phagocytic behaviour. A: 28-60 DIV primary microglia were treated with fluorescently labelled latex beads for 2 h in 0.1% BSA in PBS, supplemented with vehicle (control), 100ng/ml LPS, 10μM PNU-120596, 10μM PNU-282987, 100nM αBTX or 100μM dynasore, followed by fixation and DAPI counter-staining. Data expressed as number of beads ingested per cell ± SEM, validated by z-stack image analysis, n=3-5 independent experiments with 40+ cells per field of view. * indicates $p<0.05$, ** $p<0.01$, *** $p<0.005$, **** $p<0.001$, control (white bar) vs LPS treatment (black bar) or vs PNU-1/2 ± inhibitor (grey bars), subjected to one-way ANOVA with Bonferroni post-test. B: Representative fluorescence microscopy image of vehicle-treated (control) primary microglial bead uptake. C: Representative fluorescence microscopy image of PNU-1/2-treated bead uptake into microglia.

5.3 Discussion

The previous results chapters of this thesis have shown that despite expression of α7nAChR at the glutamatergic synapse, neuronal α7nAChR activation had no effect on APP processing. Given the extensive literature on α7nAChR-mediated neuroprotective effects in cognitive decline, learning and memory, aging, AD and inflammation, understanding the functional effects of α7nAChR activation in all CNS cell types is important. Accordingly, this chapter aimed to show α7nAChR activation could modulate microglial behaviour and as such, assessment of α7nAChR-mediated microglial phagocytosis was undertaken. Characterisation of the primary microglial model system highlighted the specificity of the microglial cell type and the validity of the purification protocol in eliminating astrocyte contamination. Further analysis showed the model system was able to switch from a 'resting' to 'activated' morphological phenotype, which when coupled with α7nAChR-mediated ERK phosphorylation highlighted the presence of functional cell surface receptors on primary microglia. α7nAChR stimulation resulted in enhanced microglial phagocytosis, although the precise mechanism underling α7nAChR-mediated modulation of microglial behaviour is still unclear.

5.3.1 Trypsinisation of a primary cortical mixed glial population gives rise to pure microglia

Using conditions to promote a glial cell fate, both astrocytes and microglia were isolated from postnatal mouse cortex and sustained *in vitro* for long-term use. Cells proliferated in a time-dependent manner and by ~1 week *in vitro* a confluent layer of astrocytes was observed, with microglia reaching confluency by ~4 weeks *in vitro*. The cells adopted the classic morphology of round, flat and cobblestone shaped astrocytes and smaller irregular microglia with ramified processes, consistent with published glial culture morphometric characteristics (Alliot *et al*., 1991; Kettenmann and Hanisch, 2011; Torres-Platas *et al*., 2014). The purification protocol used (optimised from Saura *et al*., 2003) isolated and enriched primary cortical microglia, by using mild trypsin to detach astrocytes in one sheet from on top of the microglia. Commonly used alternative isolation procedures for primary microglia include density gradient centrifugation of mixed glial populations (Moussaud and Draheim, 2010) and shaking off and collecting loosely adherent microglia from mixed glial cultures (Ni and

Aschner, 2010), but result in a significantly lower yield of microglial cells (Saura *et al*., 2003), making these methods less favourable. Furthermore, the trypsin purification produced negligible astrocyte contamination, as judged by GFAP immunofluorescence, with retained residing cells shown to be microglia through expression of microglia-specific CD11b immunoreactivity, reinforcing the benefit of this culture method in producing high yields of pure primary microglia.

5.3.2 Primary cortical microglia are responsive and express functional α7nAChR

Primary microglia displayed a ramified morphology under resting conditions, and following an inflammatory activation signal, such as LPS, the cells adopted a round, large and flat amoeboid morphology, in accordance with previously published data (abd-el-Basset and Fedoroff, 1995), indicative of functional and responsive microglia. Upon inflammatory activation by LPS, microglia retracted and withdrew process branches, this process enables a transition to a motile state wherein the amoeboid shape aids locomotory actions required for CNS surveillance and tracking of pathogens (Stence *et al*., 2001). Transition from ramified to amoeboid morphology was not immediate, and an amoeboid state was not fully adopted following 20 min LPS treatment. Transition to a fully 'activated' state has been shown to require complete resorption of microglial cell processes before a fully motile amoeboid state can be adopted (Stence *et al*., 2001). Furthermore, LPS treatment induced acute ERK phosphorylation, further indicative of responsive microglia with functional cell surface receptors that are capable of transducing extracellular inflammatory signals to intracellular cell signalling cascades. Along with ERK activation, LPS treatment has also been shown to activate pro-inflammatory pathways, such as the p38 MAPK cascade (Pocock and Kettenmann, 2007; Bordji *et al*., 2010) that induce microglial hyperactivation, cytokine release and subsequent neuronal cell death. As both *in vitro* and *in vivo* microglia can adopt either pro-inflammatory or protective behaviours, mediated via activation of distinct cell surface expressed receptor populations, this highlights the critical need for further understanding of the functionality of α7nAChR in primary microglia, as α7nAChR activation has been shown to reduce microglial activation, cytokine release and inflammation. Having displayed the expression of functional α7nAChR that selectively couple to ERK phosphorylation, this reinforces the use of primary microglia as a model system to study the mechanisms underlying

heterogeneous cell population activation, inflammation and their roles in neurodegenerative disease onset and progression.

5.3.3 Primary cortical microglia are a good model system to study inflammatory cell phagocytic behaviour

Using a simple bead uptake assay, the phagocytic potential of primary microglial was defined and was significantly enhanced by 2 h exposure to LPS and activation of α7nAChR, blocked by the α7nAChR-selective antagonist αBTX. Preliminary data highlighted the phagocytosis was time-dependent (data not shown, as per Hassan *et al*., 2014) and an optimal 2 h time point was adopted to probe maximal microglial phagocytosis. Published literature has shown microglial phagocytosis required at least 30 min to form vacuoles before engulfment of foreign matter (Stence *et al*., 2001), in accordance with the 2 h timescale required for α7nAChR-mediated bead phagocytosis. The use of dynasore to block endocytosis is now a commonly used pharmacological tool in understanding cellular trafficking dynamics. The lack of a dynasore-mediated attenuating effect on phagocytosis highlights the distinct mechanisms underlying these cellular processes. Previous published data showed macrophage endocytosis required both clathrin and dynamin, whilst phagocytosis was unaffected by inhibition of dynamin or by reducing clathrin expression, conversely phagocytosis required actin assembly (Tse *et al*., 2003). This reinforces the relevance and selectivity of the observed α7nAChR-mediated bead uptake as a phagocytosis event.

5.3.4 Summary

When taken together, the findings of this chapter are relevant as selective activation of microglial α7nAChR enhanced both ERK phosphorylation and phagocytosis. Phagocytosis has previously been shown to be impaired in AD, through a loss of beclin-1 expression, which directly impaired phagocytic capacity (Lucin *et al*., 2013). Reduced phagocytosis results in increased cellular debris deposits, enhancing inflammation and resulting in neurodegeneration. Conversely, enhanced microglial phagocytosis, via PPARγ agonism, ERK activation and PPARγ-phospho ERK complex formation improved cognition in AD transgenic mice through enhanced Aβ phagocytic clearance (Cramer *et al*., 2012; Mandrekar-Colucci *et al*., 2012; Yamanaka *et al*., 2012; Jahrling *et al*., 2014). Therefore, having shown α7nAChR

activation can induce ERK phosphorylation and also enhance phagocytosis, this reinforces pharmacological activation of α7nAChR is an excellent clinical target for cognitive enhancement, memory consolidation and Aβ clearance in AD.

Chapter 6

6. General Discussion

6. Discussion

This thesis aimed to address the hypotheses that α7nAChR activation would both enhance non-amyloidogenic APP processing in primary cortical neurons and modulate inflammatory cellular behaviour of primary cortical microglia. Using a combination of immunofluorescence imaging, dual emission microfluorimetry and immunoblotting techniques, expression of APP and functional α7nAChR were demonstrated in primary cortical neurons. However, immunoblotting for full-length APP and APP C-terminal cleavage fragments, coupled with a highly sensitive APP cleavage luciferase reporter assay revealed that activation of α7nAChR with a subtype-selective agonist and PAM had no effect on APP processing, despite robust calcium influx and ERK phosphorylation. Stimulation of α7nAChR with a subtype-selective agonist and PAM also resulted in robust ERK phosphorylation in primary cortical microglia. Following α7nAChR activation and ERK phosphorylation, microglia displayed enhanced phagocytic behaviour, as determined through a bead-uptake assay, via a mechanism distinct from endocytosis. This suggests α7nAChR activation selectively regulates immunoresponsive behaviour in microglia. Together, these data provide no evidence to support the concept that targeting α7nAChR could be used to promote non-amyloidogenic APP processing in primary cortical neurons, but do support the ability of α7nAChR to promote neuroprotective phagocytic behaviour in microglial cells, figure 6.1.

6.1 α7nAChR-dependent regulation of APP processing

Over the last ~20 years, a number of research groups have shown activation of α7nAChR enhances non-amyloidogenic APP processing; resulting in increased sAPPα release (Kim *et al.*, 1997; Lahiri *et al.*, 2002; Mousavi and Hellström-Lindahl, 2009; Nie *et al.*, 2010), reduced Aβ release (Hellström-Lindahl *et al.*, 2004; Hedberg *et al.*, 2008; Nie *et al.*, 2010) and reduced plaque deposition (Nordberg *et al.*, 2002). The results from primary cortical neurons presented here conflict with these findings; by showing α7nAChR activation has no clear effect either at increasing α-secretase activity or reducing β-/γ-secretase activity. Due to the nature of the model system, primary cortical neurons can be considered more physiologically relevant than the 'neuron-like' cell lines and overexpressing transgenic models used in previous studies. For example, chronic treatment of PC12 cells with the non-selective agonist

nicotine, increased sAPPα levels, derived from cleavage of the APP_{770} isoform (Kim *et al*., 1997), whilst SH-SY5Y cells chronically treated with nicotine also enhanced secretion of sAPPα, which was not blocked by the α7-selective antagonists MLA and αBTX (Mousavi and Hellström-Lindahl, 2009), suggestive of a contribution of other nAChR subtypes. Furthermore, transfected SH-EP1 cells stably overexpressing α7nAChR and human APP_{695} were treated with nicotine for 24 h, increasing sAPPα and αCTF production and reducing Aβ secretion, suggesting overexpression of α7nAChR is sufficient to promote APP processing, but without nicotine-mediated increases in α- and β-secretase activity (Nie *et al*., 2010). *In vivo* studies of α7nAChR-mediated effects on APP processing have assessed physiological sAPP release following high dose and chronic 14 d (Lahiri *et al*., 2002) or 16 week (Srivareerat *et al*., 2011) non-selective agonist infusion, reporting nicotine-mediated attenuation of Aβ-induced behavioural deficits.

There exists a wealth of research showing Aβ accumulation alongside altered nAChR expression is significant in the progression of AD, as per the amyloid cascade and cholinergic hypotheses of AD (Parri *et al.*, 2011). Aβ-induced effects on α7nAChR may be mediated through direct Aβ-α7nAChR interactions (Wang *et al*., 2000a, 2000b; Dineley *et al*., 2001; Nagele *et al*., 2002) or secondary to activation of NMDAR (Snyder *et al.*, 2005; Abbott *et al.*, 2008). This interaction may play a physiological role, as low concentrations of Aβ peptide have been shown to enhance LTP via α7nAChR activation (Dineley *et al*., 2002a; Dougherty *et al*., 2003; Puzzo *et al*., 2008; Khan *et al*., 2010). However, increased soluble Aβ levels induce hyperexcitation of α7nAChR (Liu *et al.*, 2013) and in cognitively impaired AD transgenic mouse models and AD patient brain, the extent and affinity of Aβ-α7nAChR interaction is enhanced, resulting in desensitisation and functional inactivation of α7nAChR (Ren *et al.*, 2007; Wang *et al.*, 2009; Söderman *et al.*, 2010), reduced nicotine-evoked calcium influx (Wang *et al*., 2000b), disruption of synaptic signalling (Wang *et al*., 2000b; Lilja *et al*., 2011; Ni *et al*., 2013), and reduced ERK phosphorylation (Dineley *et al.*, 2001). Interestingly, chronic Aβ exposure (by exogenous Aβ application or in APP overexpressing AD model transgenic mice) up-regulates α3- and α7nAChR expression in both the cortex and hippocampus (Dineley *et al*., 2001, 2002a; Bednar *et al*., 2002; Jones *et al*., 2006; Mousavi and Nordberg, 2006), hypothesised to be due to an nAChR-Aβ interaction. Thus, AD-model transgenic mice are potentially endowed with the required nAChR expression level and thus the capability to mediate

nicotine-induced reductions in CSF Aβ level *in vivo* (Nordberg *et al*., 2002; Hellström-Lindahl *et al*., 2004; Unger *et al*., 2006). Given the on-going aim of both enhancing α7nAChR expression and reducing Aβ levels, agonist-mediated enhancement of α7nAChR expression and any resultant non-amyloidogenic APP processing would thus be highly beneficial, reinforcing targeting α7nAChR as an attractive and viable clinical strategy.

Given the low α7nAChR expression level coupled with the distinct spatial separation of presynaptic α7nAChR from the mainly postsynaptic APP, it is perhaps not unexpected that α7nAChR activation cannot couple directly to APP processing in these primary cortical neurons. Furthermore, the low level of natively expressed presynaptic α7nAChR appeared to be insufficient to promote indirect signalling through postsynaptic ionotropic glutamate receptors, to enhance ADAM-10 expression (Marcello *et al.*, 2007) and non-amyloidogenic APP processing (Hoey *et al.*, 2009, 2013). The neuroprotection (from NGF- and serum-deprivation) proffered by nicotine-mediated α7nAChR activation has already been shown to be proportional to the α7nAChR expression level in PC12 cells (Jonnala and Buccafusco, 2001). Previous studies in primary neurons reported 95% of primary hippocampal neurons were positive for α7nAChR, as detected by rhodamine-αBTX labelling, versus only 36% of primary cortical neurons, which expressed half the number of hippocampal αBTX binding sites per cell (Barrantes *et al*., 1995b). Results presented here support this finding; by showing primary cortical neurons do not express a sufficiently high level of α7nAChR (estimated at ~10-15% of neurons); thus 85-90% of cells were incapable of modulating α7nAChR-mediated APP processing.

Further data presented in this thesis, supports previous findings that direct activation of neuronal synaptic NMDAR promotes non-amyloidogenic APP processing (Hardingham, 2006; Marcello *et al.*, 2007; Léveillé *et al.*, 2008; Hoey *et al.*, 2009; Bordji *et al.*, 2010), although this remains controversial (Cirrito *et al*., 2003, 2005, 2008; Bero *et al*., 2011). The hypothesis that presynaptic α7nAChR activation would promote glutamate release and activate postsynaptic NMDAR and AMPAR, thus indirectly enhancing non-amyloidogenic APP processing has not been explored previously. Initially data from this thesis, highlighting α7nAChR plays no role even in indirect APP processing, seem difficult to reconcile, with numerous studies showing α7nAChR activation promotes nerve terminal glutamate release (Cheng and Yakel, 2014) and even glutamate synapse formation (Lozada *et al.*, 2012). However, given

the low expression of α7nAChR in this model system, and the fact that an overwhelming majority of the previous literature used cell lines expressing high levels of nAChR, activated by the non-selective agonist nicotine, the relative contribution to glutamate release of highly expressed non-α7 nAChR must be recognised. As such, increasing α7nAChR expression in primary cortical neurons might promote APP processing, through ionotropic glutamate receptor activation following α7nAChR-mediated glutamate release.

Activation of primary cortical neuronal α7nAChR directly induced ERK phosphorylation (observed in total neuronal lysates and nerve terminal synaptosome lysates), but did not modulate ERK-dependent transcription of Egr-1. Given that the MAPK pathway and ERK phosphorylation have been strongly linked to neuron activity-dependent APP processing (Mills *et al*., 1997; Desdouits-Magnen *et al*., 1998; Verges *et al*., 2011; Wan *et al*., 2012; Hoey *et al*., 2013), it was unexpected to observe no α7nAChR-mediated ERK-dependent APP processing. Expression of Egr-1 has been linked to NMDAR (Worley *et al*., 1991), AMPAR (Wang *et al*., 1994) and L-type voltage-gated calcium channel activity (Murphy *et al*., 1991); resulting in the hypothesis that Egr-1 expression is maintained by synaptic activity in response to physiological stimuli (Veyrac *et al*., 2014). Egr-1 expression plays a role in learning and memory induction and consolidation (Knapska and Kaczmarek, 2004). As such, one would expect α7nAChR activation to promote ERK-dependent transcription of Egr-1 in neurons, but data presented in this thesis indicate no α7nAChR-mediated effect. This again is likely to be due to the low expression level and spatial distribution of presynaptic α7nAChR in this model system, with previous literature highlighting gene expression changes require signalling above a threshold (Mann and Paulsen, 2007), through receptor populations situated postsynaptically, and are thus optimally situated for induction of gene expression changes. Accordingly, overexpression of α7nAChR in cell lines induces sustained ERK phosphorylation (Utsugisawa *et al*., 2002) and Egr-1 gene transcription (Dunckley and Lukas, 2003), suggestive of an α7nAChR-induced effect on ERK-dependent transcription with higher α7nAChR expression.

6.2 α7nAChR-dependent modulation of microglial behaviour

The primary cortical microglia characterised here were observed as being highly responsive and capable of adopting classical morphological phenotypes, switching

between ‘resting’ and ‘activated’ states. This is in accordance with both primary microglia and microglial cell line studies (Kettenmann and Hanisch, 2011). Having shown the functional expression of α7nAChR on primary cortical microglia, this reinforces the extensive published literature on microglial neurotransmitter receptor expression, known to play diverse roles in the modulation of microglial behaviour. Microglial neurotransmitter receptors are akin to extrasynaptic receptors on neurons, which are not used for synaptic transmission, but instead play a regulatory role in modulating cell behaviour (Pocock and Kettenmann, 2007). For example, activation of α7nAChR (Giunta *et al*., 2004; Shytle *et al*., 2004) and $GABA_B$ receptor (Kuhn *et al*., 2004) populations are neuroprotective, reducing pro-inflammatory cytokine release; activation of AMPAR is pro-inflammatory (Hide *et al*., 2000; Hagino *et al*., 2004); metabotropic glutamate receptors induce mitochondrial depolarisation and microglial apoptosis (Taylor *et al*., 2002, 2005) and P2Y (Davalos *et al*., 2005; Haynes *et al*., 2006) and dopamine receptors (Färber *et al*., 2005) enhance microglial migratory behaviour. Furthermore, data presented here extends current knowledge reinforcing α7nAChR activation in microglia is protective (Wang *et al.*, 2003; Cui and Li, 2010), through increased ERK phosphorylation and enhanced phagocytosis, in accordance with the α7nAChR-mediated ‘cholinergic anti-inflammation pathway’ (Giunta *et al.*, 2004; Shytle *et al.*, 2004; Moon *et al.*, 2008; Hwang *et al.*, 2010; Takata *et al.*, 2010; Kawamata and Shimohama, 2011; Thomsen and Mikkelsen, 2012; Parada *et al.*, 2013). Previous studies have shown α7nAChR-selective activation with PNU-282987 reduced TNFα release from an α7nAChR overexpressing immune cell line (Li *et al*., 2009) and enhanced anti-inflammatory gene expression in primary hippocampal microglia (Parada *et al*., 2013). The non-selective agonist nicotine also reduced TNFα release from primary microglia (Giunta *et al*., 2004; Shytle *et al*., 2004; Moon *et al*., 2008) and potentiation of α7nAChR on primary microglia and within AD transgenic mice with galantamine enhanced choline-mediated phagocytosis (Takata *et al*., 2010).

The Aβ phagocytosis capacity of microglia, has recently emerged as a topic of interest, with independent data showing Aβ phagocytosis is a tightly regulated process (Bamberger *et al.*, 2003; Koenigsknecht-Talboo and Landreth, 2005; Lee and Landreth, 2010; Mandrekar-Colucci *et al.*, 2012) that is impaired in AD patients and AD-model transgenic mice (Lucin *et al.*, 2013; Orre *et al.*, 2014). Enhanced phagocytic behaviour by microglia, through PPARγ activation has previously been shown to be neuroprotective and significantly lowers plaque burden in transgenic

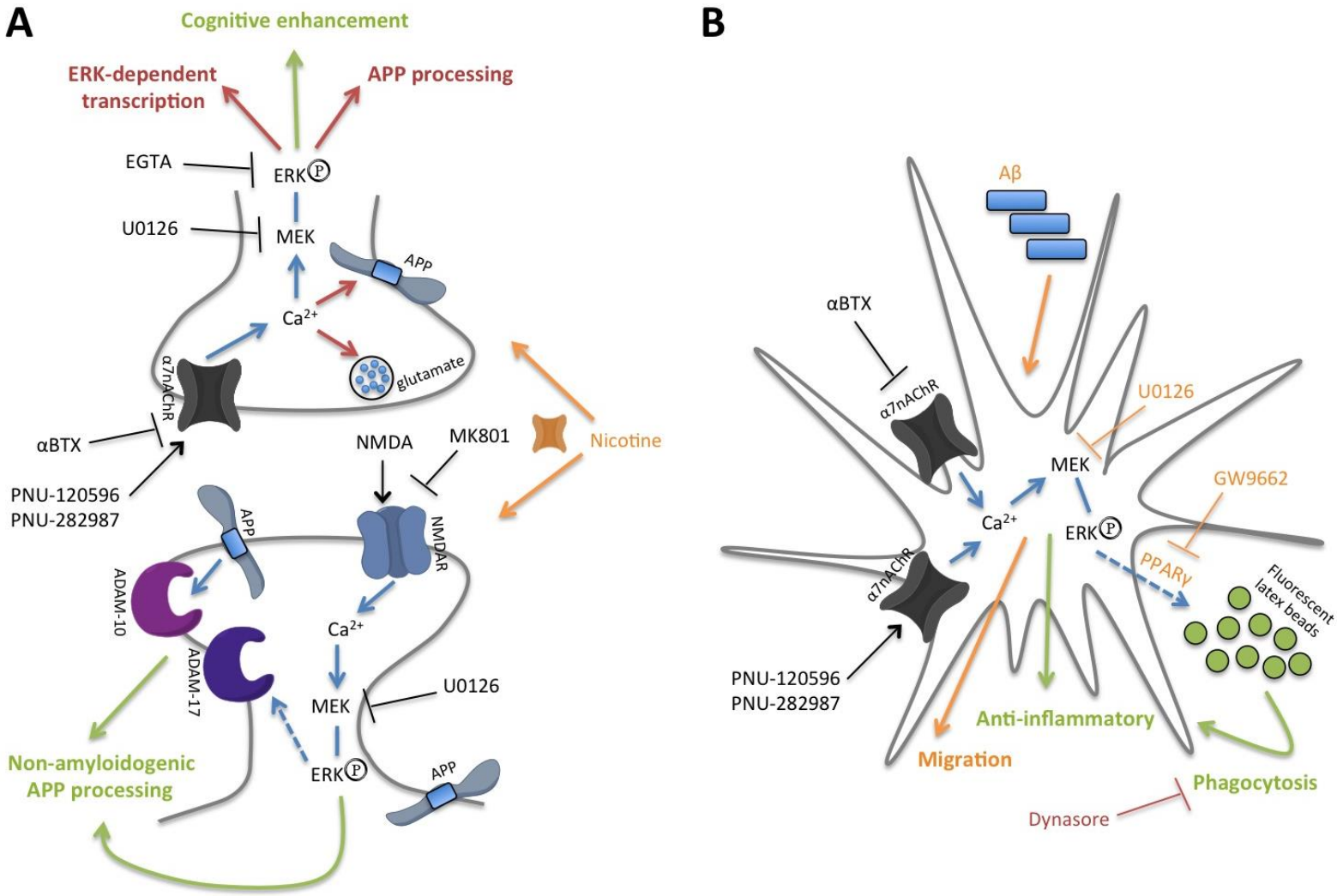
A
Cognitive enhancement
ERK-dependent transcription
APP processing
EGTA
ERK
U0126
MEK
APP
Ca2+
glutamate
α7nAChR
αBTX
PNU-120596
PNU-282987
NMDA
MK801
Nicotine
APP
NMDAR
ADAM-10
ADAM-17
Ca2+
MEK
U0126
ERK
APP
Non-amyloidogenic APP processing
B
Aβ
αBTX
α7nAChR
U0126
MEK
GW9662
Ca2+
ERK
PPARγ
Fluorescent latex beads
α7nAChR
PNU-120596
PNU-282987
Anti-inflammatory
Migration
Phagocytosis
Dynasore

Figure 6.1: Schematic of α7nAChR at the glutamatergic synapse. A: In primary cortical neurons α7nAChR are activated by the selective agonist PNU-282987, prevented from desensitising by the type II PAM PNU-120596 and antagonised by αBTX. Activation of α7nAChR induces calcium (Ca^{2+}) influx and MEK-dependent ERK phosphorylation (ERKP), which are inhibited by EGTA and U0126, respectively. Activation of α7nAChR does not drive ERK-dependent Egr-1 transcription or APP processing (red arrows, either directly or indirectly, via glutamate release and activation of postsynaptic NMDAR), but is sufficient for cognitive enhancement. NMDAR activation induces MEK-dependent ERK phosphorylation, enhanced α-secretase activity and promotes non-amyloidogenic APP processing (green arrows). Future experiments in primary neurons could probe the nicotine-mediated up-regulation of α7nAChR, with the aim of understanding whether nAChR expression level modulates APP processing (orange arrows). B: In primary cortical microglia α7nAChR activation with PNU-28987 and PNU-120596 is anti-inflammatory, enhancing ERK phosphorylation and phagocytosis of fluorescent latex beads. Phagocytosis is blocked by the α7nAChR-selective antagonist αBTX, but not blocked by the endocytosis inhibitor dynasore (red bar-headed line). Future experiments in primary microglia could establish the MEK- and PPARγ-dependence of phagocytosis (through U0126- and GW9662-mediated inhibition, respectively, orange bar-headed lines), whilst also characterising the physiologically relevant *in vitro* capacity of microglia to phagocytose Aβ peptide (orange arrow). Further behavioural paradigms could also be investigated, such as α7nAChR-mediated modulation of microglial migration (orange arrow).

mice (Cramer *et al.*, 2012). PPARγ activation also reverses AD-like cognitive deficits (Yamanaka *et al.*, 2012), but memory consolidation requires PPARγ-pERK complex formation (Jahrling *et al.*, 2014). Furthermore, nicotine has been shown to up-regulate PPARγ expression in monocyte-derived human dendritic cells (Yanagita *et al.*, 2012). Thus, data presented in this thesis corroborate with previous findings and extend our knowledge by showing α7nAChR-selective activation enhances ERK phosphorylation and promotes phagocytosis, which may be PPARγ-mediated.

Potential disadvantages and limitations of α7nAChR-mediated enhanced microglial phagocytosis exist. Aberrant and hyperactive phagocytosis can remove the synapses and processes of live neurons, termed 'phagoptosis' (Brown and Neher, 2014). Enhanced microglial phagoptosis has been implicated in the pathogenesis of Parkinson's disease (Emmrich *et al.*, 2013) and other neurological disorders, through release of microglial soluble pro-inflammatory mediators resulting in enhanced neuronal expression of cell-surface phagocytosis-promoting markers, such as phosphatidylserine (Neher *et al.*, 2011). Previous studies have shown inhibition of cellular phagocytosis prevents inflammation-induced neuronal death, following a 3-day LPS incubation (Neher *et al.*, 2011), however long-term damage through prolonged phagocytosis of CNS debris was recently shown to be induced by infiltrating macrophages and not resident microglia (Greenhalgh and David, 2014). Therefore in future investigations, characterising the neuroprotective potential of microglial phagocytosis would benefit from cell type-selective α7nAChR ligands or their local administration, to eliminate confounding results from other peripheral nervous system cell types.

Throughout this thesis, the α7nAChR-selective PAM PNU-120596 was used to reveal the effects of α7nAChR activity at the glutamatergic synapse. Given that the PAM alone had no effect on any cellular readout, such as ERK phosphorylation or microglial phagocytosis, this is found in contrast to *in vivo* examples of PAM use. For example, physiological concentrations of choline and PNU-120596 application activated α7nAChR-containing neurons within the hippocampus (Gusev and Uteshev, 2010; Kalappa *et al*., 2010) to facilitate action potentials and enhance cognition in rodents (Timmermann *et al*., 2007). In contrast, in these primary cortical neuronal and microglial model systems, under defined medium conditions, cells were plated into 20μM choline, a sub-maximal concentration for α7nAChR activation (Uteshev, 2014), given choline's low potency (Papke and Porter Papke, 2002). Over time *in vitro*, the

concentration of choline will reduce, as it is taken into cells as an essential component of cell membranes and as an ACh precursor. Nonetheless, extracellular choline failed to activate native primary cortical α7nAChR in the presence of PNU-120596, and required application of the α7nAChR-selective agonist PNU-282987 to activate neurons and microglia to bring about α7nAChR-mediated cellular responses.

6.3 Future work

Given the wealth of literature on chronic nAChR stimulation up-regulating neuronal α7nAChR expression in both *in vivo* and *in vitro* models (Peng *et al*., 1994; Barrantes *et al*., 1995b; Molinari *et al*., 1998; Kawai and Berg, 2001; Vallejo *et al*., 2005; Fu *et al*., 2009; St John, 2009; Goriounova and Mansvelder, 2012; Mazzo *et al*., 2013), further experiments could be conducted to definitively establish whether up-regulation of α7nAChR expression in primary neurons, previously shown to be enhanced by 40% (Barrantes *et al*., 1995b; Jonnala and Buccafusco, 2001), through chronic nicotine treatment, enhances the potential for α7nAChR to directly and/or indirectly modulate non-amyloidogenic APP processing, figure 6.1. Looking further into the future, a greater understanding of the physiological role of APP is required; with particular focus on why APP processing and formation of neurotrophic (sAPPα) and neurotoxic (Aβ) APP cleavage products are so closely related to neurotransmission. Furthermore, understanding the role of cortical layers in the nAChR-mediated onset of various pro-cognitive outcomes, such as improved attention and working memory, will require a deeper understanding and characterisation of α7nAChR-selective ligands at a molecular, cellular and neuronal network level.

Further minor experimental procedures, including characterising the ERK- and PPARγ-dependence of microglial phagocytosis with U0126-meditated MEK inhibition and GW9662- mediated PPARγ inhibition, respectively, would provide insight into the mechanism underlying microglial α7nAChR-induced phagocytosis. Of significant interest would be to establish whether Aβ phagocytosis is also affected by α7nAChR activation, through exogenous application of fluorescently-labelled Aβ into microglial culture medium, prior to α7nAChR stimulation. Such experiments could be coupled with characterisation of other microglial behavioural paradigms, such as α7nAChR-mediated modulation of microglial migration and pro-inflammatory cytokine release, figure 6.1. Looking further into the future, gaining a deeper understanding of the

cholinergic anti-inflammatory pathway is required. Until recently, glial cells were thought to be passive bystanders in the onset of neurodegenerative disorders, but the molecular mechanisms underlying chronic inflammation are yet to be discovered. Significant research efforts are required to characterise the anti-inflammatory signalling cascades in microglia with a view to targeting systemic inflammation in the treatment of neurodegenerative disorders.

6.4 Conclusion

Given the evidence supporting α7nAChR play a role in the pathophysiology of a number of neurological disorders, from AD to Parkinson's disease and schizophrenia, the use of α7nAChR-selective ligands as therapeutic agents presents an on-going research interest. Targeting the cholinergic system in the treatment of AD has proved to be the most successful strategy to date. Given the prolific clinical use of AChE inhibitors, which activate α7nAChR though boosting ACh levels and also through acting as α7nAChR PAMs, this highlights selective targeting of α7nAChR remains a viable clinical option in the treatment of neurological disorders. AChE inhibitors reduce pro-inflammatory cytokine release, boost microglial phagocytosis, reduce pro-amyloidogenic APP processing and Aβ production and enhance attention and working memory, reinforcing the multi-faceted benefits of enhanced α7nAChR expression and activation at the glutamatergic synapse.

The major novel findings from this thesis highlight that activating natively expressed α7nAChR with an α7nAChR-selective PAM and agonist cannot modulate ERK-dependent transcription nor direct and indirect APP processing in a primary neuronal model system, unlike stimulation of NMDAR that have been validated as coupling to non-amyloidogenic APP processing. Furthermore, activation of microglial α7nAChR increases ERK phosphorylation and promotes neuroprotective behaviour through selectively enhancing phagocytosis.

References

Abbott JJ, Howlett DR, Francis PT, Williams RJ (2008) Aβ1–42 modulation of Akt phosphorylation via α7 nAChR and NMDA receptors. Neurobiology of Aging 29:992–1001.

abd-el-Basset E, Fedoroff S (1995) Effect of bacterial wall lipopolysaccharide (LPS) on morphology, motility, and cytoskeletal organization of microglia in cultures. Journal of neuroscience research 41:222–237.

Abramov E, Dolev I, Fogel H, Ciccotosto GD, Ruff E, Slutsky I (2009) Amyloid-β as a positive endogenous regulator of release probability at hippocampal synapses. Nature neuroscience 12:1567–1576.

Alkondon M, Pereira EF, Barbosa CT, Albuquerque EX (1997) Neuronal nicotinic acetylcholine receptor activation modulates gamma-aminobutyric acid release from CA1 neurons of rat hippocampal slices. The Journal of pharmacology and experimental therapeutics 283:1396–1411.

Alkondon M, Pereira EFR, Albuquerque EX (2007) Age-dependent changes in the functional expression of two nicotinic receptor subtypes in CA1 stratum radiatum interneurons in the rat hippocampus. Biochemical pharmacology 74:1134–1144.

Alliot F, Lecain E, Grima B, Pessac B (1991) Microglial progenitors with a high proliferative potential in the embryonic and adult mouse brain. Proceedings of the National Academy of Sciences of the United States of America 88:1541–1545.

Alzheimer's Society (2014) Alzheimer's disease demography. Available at: http://goo.gl/wXIQY7 [Accessed July 7, 2014].

Andersen N, Corradi J, Bartos M, Sine SM, Bouzat C (2011) Functional relationships between agonist binding sites and coupling regions of homomeric Cys-loop receptors. The Journal of Neuroscience 31:3662–3669.

Andersen N, Corradi J, Sine SM, Bouzat C (2013) Stoichiometry for activation of neuronal α7 nicotinic receptors. Proceedings of the National Academy of Sciences of the United States of America 110:20819–20824.

Apelt J, Kumar A, Schliebs R (2002) Impairment of cholinergic neurotransmission in adult and aged transgenic Tg2576 mouse brain expressing the Swedish mutation of human beta-amyloid precursor protein. Brain research 953:17–30.

Back S, Haas P, Tschape J-A, Gruebl T, Kirsch J, Muller U, Beyreuther K, Kins S (2007) β-Amyloid Precursor Protein Can Be Transported Independent of Any Sorting Signal to the Axonal and Dendritic Compartment. Journal of neuroscience research 2590:2580–2590.

Bailey JA, Ray B, Greig NH, Lahiri DK (2011) Rivastigmine lowers Aβ and increases sAPPα levels, which parallel elevated synaptic markers and metabolic activity in degenerating primary rat neurons. PloS one 6:e21954.

Bamberger ME, Harris ME, McDonald DR, Husemann J, Landreth GE (2003) A cell surface receptor complex for fibrillar β-amyloid mediates microglial activation. The Journal of Neuroscience 23:2665–2674.

Barbagallo APM, Weldon R, Tamayev R, Zhou D, Giliberto L, Foreman O, D'Adamio L (2010) Tyr(682) in the intracellular domain of APP regulates amyloidogenic APP processing in vivo. PloS one 5:e15503.

Baroja-Mazo A, Martín-Sánchez F, Gomez AI, Martínez CM, Amores-Iniesta J, Compan V, Barberà-Cremades M, Yagüe J, Ruiz-Ortiz E, Antón J, Buján S, Couillin I, Brough D, Arostegui JI, Pelegrín P (2014) The NLRP3 inflammasome is released as a particulate danger signal that amplifies the inflammatory response. Nature immunology.

Barrantes G, Murphy C, Westwick J, Wonnacott S (1995a) Nicotine increases intracellular calcium in rat hippocampal neurons via voltage-gated calcium channels. Neuroscience letters 196:101–104.

Barrantes G, Rogers A, Lindstrom J, Wonnacott S (1995b) α-Bungarotoxin binding sites in rat hippocampal and cortical cultures: initial characterisation, colocalisation with α7 subunits and up-regulation by chronic nicotine treatment. Brain research 672:228–236.

Barrias ES, Reignault LC, De Souza W, Carvalho TMU (2010) Dynasore, a dynamin inhibitor, inhibits Trypanosoma cruzi entry into peritoneal macrophages. PloS one 5:e7764.

Barron SC, Mclaughlin JT, See JA, Richards VL, Rosenberg RL (2009) An Allosteric Modulator of α7 Nicotinic Receptors, N-(5-(PNU-120596), Causes Conformational Changes in the Extracellular Ligand Binding Domain Similar to Those Caused by Acetylcholine. Molecular Pharmacology 76:253–263.

Bartus RT, Dean RL, Beer B, Lippa a S (1982) The cholinergic hypothesis of geriatric memory dysfunction. Science 217:408–414.

Bednar I, Paterson D, Marutle A, Pham T, Svedberg M, Hellström-Lindahl E, Mousavi M, Court J, Morris C, Perry E, Mohammed A, Zhang X, Nordberg A (2002) Selective Nicotinic Receptor Consequences in APPswe Transgenic Mice. Molecular and Cellular Neuroscience 20:354–365.

Bencherif M, Lippiello PM, Lucas R, Marrero MB (2011) α7 nicotinic receptors as novel therapeutic targets for inflammation-based diseases. Cellular and molecular life sciences 68:931–949.

Berg DK, Conroy WG (2002) Nicotinic α7 receptors: synaptic options and downstream signaling in neurons. Journal of neurobiology 53:512–523.

Berg LK, Larsson M, Morland C, Gundersen V (2013) Pre- and postsynaptic localization of NMDA receptor subunits at hippocampal mossy fibre synapses. Neuroscience 230:139–150.

Bero AW, Yan P, Roh JH, Cirrito JR, Stewart FR, Raichle ME, Lee J-M, Holtzman DM (2011) Neuronal activity regulates the regional vulnerability to amyloid-β deposition. Nature neuroscience 14:750–756.

Bertrand D, Gopalakrishnan M (2007) Allosteric modulation of nicotinic acetylcholine receptors. Biochemical pharmacology 74:1155–1163.

Bettegazzi B, Mihailovich M, Di Cesare A, Consonni A, Macco R, Pelizzoni I, Codazzi F, Grohovaz F, Zacchetti D (2011) β-Secretase activity in rat astrocytes : translational block of BACE1 and modulation of BACE2 expression. European Journal of Neuroscience 33:236–243.

Bierer LM, Haroutunian V, Gabriel S, Knott PJ, Carlin LS, Purohit DP, Perl DP, Schmeidler J, Kanof P, Davis KL (1995) Neurochemical correlates of dementia severity in Alzheimer's disease: relative importance of the cholinergic deficits. Journal of neurochemistry 64:749–760.

Bitner RS *et al*. (2007) Broad-spectrum efficacy across cognitive domains by α7 nicotinic acetylcholine receptor agonism correlates with activation of ERK1/2 and CREB phosphorylation pathways. The Journal of Neuroscience 27:10578–10587.

Bitner RS, Nikkel AL, Markosyan S, Otte S, Puttfarcken P, Gopalakrishnan M (2009) Selective α7 nicotinic acetylcholine receptor activation regulates glycogen synthase kinase 3β and decreases tau phosphorylation in vivo. Brain research 1265:65–74.

Bodea L-G, Wang Y, Linnartz-Gerlach B, Kopatz J, Sinkkonen L, Musgrove R, Kaoma T, Muller A, Vallar L, Di Monte DA, Balling R, Neumann H (2014) Neurodegeneration by activation of the microglial complement-phagosome pathway. The Journal of Neuroscience 34:8546–8556.

Bodnar AL, Cortes-Burgos LA, Cook KK, Dinh DM, Groppi VE, Hajos M, Higdon NR, Hoffmann WE, Hurst RS, Myers JK, Rogers BN, Wall TM, Wolfe ML, Wong E (2005) Discovery and structure-activity relationship of quinuclidine benzamides as agonists of α7 nicotinic acetylcholine receptors. Journal of medicinal chemistry 48:905–908.

Bolkan BJ, Triphan T, Kretzschmar D (2012) β-Secretase Cleavage of the Fly Amyloid Precursor Protein Is Required for Glial Survival. The Journal of Neuroscience 32:16181–16192.

Bordji K, Becerril-Ortega J, Buisson A (2011) Synapses, NMDA receptor activity and neuronal Aβ production in Alzheimer's disease. Reviews in the neurosciences 22:285–294.

Bordji K, Becerril-Ortega J, Nicole O, Buisson A (2010) Activation of Extrasynaptic, But Not Synaptic, NMDA Receptors Modifies Amyloid Precursor Protein Expression Pattern and Increases Amyloid-β Production. Journal of Neuroscience 30:15927–15942.

Boulter J, Connolly J, Deneris E, Goldman D, Heinemann S, Patrick J (1987) Functional expression of two neuronal nicotinic acetylcholine receptors from cDNA clones identifies a gene family. Proceedings of the National Academy of Sciences of the United States of America 84:7763–7767.

Brady ST, Siegel GJ, Albers RW, Price DL (2012) Basic Neurochemistry, 8th ed. Academic Press.

Brahmachari S, Fung YK, Pahan K (2006) Induction of glial fibrillary acidic protein expression in astrocytes by nitric oxide. The Journal of neuroscience : the official journal of the Society for Neuroscience 26:4930–4939.

Breese CR, Adams C, Logel J, Drebing C, Rollins Y, Barnhart M, Sullivan B, Demasters BK, Freedman R, Leonard S (1997) Comparison of the regional expression of nicotinic acetylcholine receptor α7 mRNA and [125I]-α-bungarotoxin binding in human postmortem brain. The Journal of comparative neurology 387:385–398.

Brejc K, van Dijk WJ, Klaassen R V, Schuurmans M, van Der Oost J, Smit AB, Sixma TK (2001) Crystal structure of an ACh-binding protein reveals the ligand-binding domain of nicotinic receptors. Nature 411:269–276.

Brou C, Logeat F, Gupta N, Bessia C, LeBail O, Doedens JR, Cumano A, Roux P, Black RA, Israël A (2000) A novel proteolytic cleavage involved in Notch signaling: the role of the disintegrin-metalloprotease TACE. Molecular cell 5:207–216.

Brown GC, Neher JJ (2014) Microglial phagocytosis of live neurons. Nature reviews Neuroscience 15:209–216.

Brown JL, Wonnacott S (2014) Sazetidine-A Activates and Desensitizes Native α7 Nicotinic Acetylcholine Receptors. Neurochemical research.

Busche MA, Eichhoff G, Adelsberger H, Abramowski D, Wiederhold K-H, Haass C, Staufenbiel M, Konnerth A, Garaschuk O (2008) Clusters of hyperactive neurons near amyloid plaques in a mouse model of Alzheimer's disease. Science 321:1686–1689.

Buxbaum JD, Liu K-N, Luo Y, Slack JL, Stocking KL, Peschon JJ, Johnson RS, Castner BJ, Cerretti DP, Black RA (1998) Evidence That Tumor Necrosis Factor Converting Enzyme Is Involved in Regulated α-Secretase Cleavage of the Alzheimer Amyloid Protein Precursor. Journal of Biological Chemistry 273:27765–27767.

Buxbaum JD, Oishi M, Chen HI, Pinkas-Kramarski R, Jaffe EA, Gandy SE, Greengard P (1992) Cholinergic agonists and interleukin 1 regulate processing

and secretion of the Alzheimer β/A4 amyloid protein precursor. Proceedings of the National Academy of Sciences of the United States of America 89:10075–10078.

Cai G, Atzmon G, Naj AC, Beecham GW, Barzilai N, Haines JL, Sano M, Pericak-Vance M, Buxbaum JD (2012) Evidence against a role for rare ADAM10 mutations in sporadic Alzheimer disease. Neurobiology of aging 33:416–417.e3.

Cai H, Wang Y, McCarthy D, Wen H, Borchelt DR, Price DL, Wong PC (2001) BACE1 is the major β-secretase for generation of Abeta peptides by neurons. Nature neuroscience 4:233–234.

Camden JM, Schrader AM, Camden RE, González FA, Erb L, Seye CI, Weisman GA (2005) P2Y2 nucleotide receptors enhance alpha-secretase-dependent amyloid precursor protein processing. The Journal of biological chemistry 280:18696–18702.

Cao X, Südhof TC (2001) A transcriptionally active complex of APP with Fe65 and histone acetyltransferase Tip60. Science 293:115–120.

Caporaso GL, Gandy SE, Buxbaum JD, Ramabhadran T V, Greengard P (1992) Protein phosphorylation regulates secretion of Alzheimer β/A4 amyloid precursor protein. Proceedings of the National Academy of Sciences of the United States of America 89:3055–3059.

Caputi A, Barindelli S, Pastorino L, Cimino M, Buxbaum JD, Cattabeni F, Di Luca M (1997) Increased secretion of the amino-terminal fragment of amyloid precursor protein in brains of rats with a constitutive up-regulation of protein kinase C. Journal of neurochemistry 68:2523–2529.

Caunt CJ, Keyse SM (2013) Dual-specificity MAP kinase phosphatases (MKPs): shaping the outcome of MAP kinase signalling. The FEBS journal 280:489–504.

Cavallini A, Brewerton S, Bell A, Sargent S, Glover S, Hardy C, Moore R, Calley J, Ramachandran D, Poidinger M, Karran E, Davies P, Hutton M, Szekeres P, Bose S (2013) An unbiased approach to identifying tau kinases that phosphorylate tau at sites associated with Alzheimer disease. The Journal of biological chemistry 288:23331–23347.

Chang Q, Fischbach GD (2006) An Acute Effect of Neuregulin 1 to Suppress α7-Containing Nicotinic Acetylcholine Receptors in Hippocampal Interneurons. The Journal of Neuroscience 26:11295–11303.

Changeux J-P (2012) The Nicotinic Acetylcholine Receptor: The Founding Father of the Pentameric Ligand-gated Ion Channel Superfamily. Journal of Biological Chemistry 287:40207–40215.

Changeux J-P (2013a) The concept of allosteric interaction and its consequences for the chemistry of the brain. The Journal of biological chemistry 288:26969–26986.

Changeux J-P (2013b) The concept of allosteric modulation: an overview. Drug discovery today 10:e223–8.

Charpantier E, Wiesner A, Huh K-H, Ogier R, Hoda J-C, Allaman G, Raggenbass M, Feuerbach D, Bertrand D, Fuhrer C (2005) α7 neuronal nicotinic acetylcholine receptors are negatively regulated by tyrosine phosphorylation and Src-family kinases. The Journal of Neuroscience 25:9836–9849.

Chen D, Patrick JW (1997) The α-Bungarotoxin-binding Nicotinic Acetylcholine Receptor from Rat Brain Contains Only the α7 Subunit. Journal of Biological Chemistry 272:24024–24029.

Chen Z, Jalabi W, Shpargel KB, Farabaugh KT, Dutta R, Yin X, Kidd GJ, Bergmann CC, Stohlman SA, Trapp BD (2012) Lipopolysaccharide-induced microglial activation and neuroprotection against experimental brain injury is independent of hematogenous TLR4. The Journal of Neuroscience 32:11706–11715.

Cheng Q, Yakel JL (2014) Presynaptic α7 nicotinic acetylcholine receptors enhance hippocampal mossy fiber glutamatergic transmission via PKA activation. The Journal of Neuroscience 34:124–133.

Cheret C, Willem M, Fricker FR, Wende H, Wulf-Goldenberg A, Tahirovic S, Nave K-A, Saftig P, Haass C, Garratt AN, Bennett DL, Birchmeier C (2013) BACE1 and Neuregulin-1 cooperate to control formation and maintenance of muscle spindles. The EMBO journal 32:2015–2028.

Cirrito JR, Kang J-E, Lee J, Stewart FR, Verges DK, Silverio LM, Bu G, Mennerick S, Holtzman DM (2008) Endocytosis is required for synaptic activity-dependent release of amyloid-β in vivo. Neuron 58:42–51.

Cirrito JR, May PC, O'Dell MA, Taylor JW, Parsadanian M, Cramer JW, Audia JE, Nissen JS, Bales KR, Paul SM, DeMattos RB, Holtzman DM (2003) In vivo assessment of brain interstitial fluid with microdialysis reveals plaque-associated changes in amyloid-β metabolism and half-life. The Journal of Neuroscience 23:8844–8853.

Cirrito JR, Yamada KA, Finn MB, Sloviter RS, Bales KR, May PC, Schoepp DD, Paul SM, Mennerick S, Holtzman DM (2005) Synaptic activity regulates interstitial fluid amyloid-β levels in vivo. Neuron 48:913–922.

Cisse M, Braun U, Leitges M, Fisher A, Pages G, Checler F, Vincent B (2011) ERK1-independent α-secretase cut of β-amyloid precursor protein via M1 muscarinic receptors and PKCα/ε. Molecular and cellular neurosciences 47:223–232.

Cissé M, Halabisky B, Harris J, Devidze N, Dubal DB, Sun B, Orr A, Lotz G, Kim DH, Hamto P, Ho K, Yu G-Q, Mucke L (2011) Reversing EphB2 depletion rescues cognitive functions in Alzheimer model. Nature 469:47–52.

Cleary JP, Walsh DM, Hofmeister JJ, Shankar GM, Kuskowski MA, Selkoe DJ, Ashe KH (2005) Natural oligomers of the amyloid-β protein specifically disrupt cognitive function. Nature neuroscience 8:79–84.

Cole SL, Vassar R (2007) The Alzheimer's disease β-secretase enzyme, BACE1. Molecular neurodegeneration 15:22.

Colović MB, Krstić DZ, Lazarević-Pašti TD, Bondžić AM, Vasić VM (2013) Acetylcholinesterase inhibitors: pharmacology and toxicology. Current neuropharmacology 11:315–335.

Copanaki E, Chang S, Vlachos A, Tschäpe J-A, Müller UC, Kögel D, Deller T (2010) sAPPalpha antagonizes dendritic degeneration and neuron death triggered by proteasomal stress. Molecular and cellular neurosciences 44:386–393.

Cox CJ, Choudhry F, Peacey E, Perkinton MS, Richardson JC, Howlett DR, Lichtenthaler SF, Francis PT, Williams RJ (2014) Dietary (-) epicatechin as a potent inhibitor of βγ-secretase APP processing. Neurobiology of aging in press.

Coyle J, Price D, DeLong M (1983) Alzheimer's Disease: A Disorder of Cortical Cholinergic Innervation. Science 219:1184–1190.

Cramer PE, Cirrito JR, Wesson DW, Lee CYD, Karlo JC, Zinn AE, Casali BT, Restivo JL, Goebel WD, James MJ, Brunden KR, Wilson D a, Landreth GE (2012) ApoE-directed therapeutics rapidly clear β-amyloid and reverse deficits in AD mouse models. Science 335:1503–1506.

Croxson PL, Kyriazis DA, Baxter MG (2011) Cholinergic modulation of a specific memory function of prefrontal cortex. Nature neuroscience 14:1510–1512.

Cui W-Y, Li MD (2010) Nicotinic modulation of innate immune pathways via α7 nicotinic acetylcholine receptor. Journal of neuroimmune pharmacology : the official journal of the Society on NeuroImmune Pharmacology 5:479–488.

daCosta CJB, Free CR, Corradi J, Bouzat C, Sine SM (2011) Single-channel and structural foundations of neuronal α7 acetylcholine receptor potentiation. The Journal of Neuroscience 31:13870–13879.

Dajas-Bailador F, Heimala K, Wonnacott S (2003) The allosteric potentiation of nicotinic acetylcholine receptors by galantamine is transduced into cellular responses in neurons: Ca2+ signals and neurotransmitter release. Molecular pharmacology 64:1217–1226.

Dajas-Bailador F, Soliakov L, Wonnacott S (2002) Nicotine activates the extracellular signal-regulated kinase 1/2 via the α7 nicotinic acetylcholine

receptor and protein kinase A, in SH-SY5Y cells and hippocampal neurones. Journal of neurochemistry 80:520–530.

Dajas-Bailador F, Wonnacott S (2004) Nicotinic acetylcholine receptors and the regulation of neuronal signalling. Trends in pharmacological sciences 25:317–324.

Damme P Van (2002) GluR2-dependent properties of AMPA receptors determine the selective vulnerability of motor neurons to excitotoxicity. Journal of neurophysiology 88:1279–1287.

Dani JA, Bertrand D (2007) Nicotinic acetylcholine receptors and nicotinic cholinergic mechanisms of the central nervous system. Annual review of pharmacology and toxicology 47:699–729.

Dani JA, Radcliffe KA, Pidoplichko VI (2000) Variations in desensitization of nicotinic acetylcholine receptors from hippocampus and midbrain dopamine areas. European journal of pharmacology 393:31–38.

Das U, Scott DA, Ganguly A, Koo EH, Tang Y, Roy S (2013) Activity-induced convergence of APP and BACE-1 in acidic microdomains via an endocytosis-dependent pathway. Neuron 79:447–460.

Davalos D, Grutzendler J, Yang G, Kim J V, Zuo Y, Jung S, Littman DR, Dustin ML, Gan W-B (2005) ATP mediates rapid microglial response to local brain injury in vivo. Nature neuroscience 8:752–758.

Davis AA, Fritz JJ, Wess J, Lah JJ, Levey AI (2010) Deletion of M1 muscarinic acetylcholine receptors increases amyloid pathology in vitro and in vivo. The Journal of Neuroscience 30:4190–4196.

De Calignon A, Polydoro M, Suárez-Calvet M, William C, Adamowicz DH, Kopeikina KJ, Pitstick R, Sahara N, Ashe KH, Carlson GA, Spires-Jones TL, Hyman BT (2012) Propagation of tau pathology in a model of early Alzheimer's disease. Neuron 73:685–697.

De Strooper B (2003) Aph-1, Pen-2, and Nicastrin with Presenilin generate an active gamma-Secretase complex. Neuron 38:9–12.

De Strooper B, Annaert W (2000) Proteolytic processing and cell biological functions of the amyloid precursor protein. Journal of cell science 113 (Pt 1:1857–1870.

Dehmelt L, Halpain S (2004) The MAP2/Tau family of microtubule-associated proteins. Genome Biology 6:1–10.

Del Barrio L, Egea J, León R, Romero A, Ruiz A, Montero M, Alvarez J, López MG (2011) Calcium signalling mediated through α7 and non-α7 nAChR stimulation is differentially regulated in bovine chromaffin cells to induce catecholamine release. British journal of pharmacology 162:94–110.

Delarasse C, Auger R, Gonnord P, Fontaine B, Kanellopoulos JM (2011) The purinergic receptor P2X7 triggers α-secretase-dependent processing of the amyloid precursor protein. The Journal of biological chemistry 286:2596–2606.

Desdouits-Magnen J, Desdouits F, Takeda S, Syu LJ, Saltiel AR, Buxbaum JD, Czernik a J, Nairn a C, Greengard P (1998) Regulation of secretion of Alzheimer amyloid precursor protein by the mitogen-activated protein kinase cascade. Journal of neurochemistry 70:524–530.

Dickinson JA, Kew JNC, Wonnacott S (2008) Presynaptic α7- and β2-Containing Nicotinic Acetylcholine Receptors Modulate Excitatory Amino Acid Release from Rat Prefrontal Cortex Nerve Terminals via Distinct Cellular Mechanisms. Molecular Pharmacology 74:348–359.

Dineley KT, Bell KA, Bui D, Sweatt JD (2002a) β-Amyloid peptide activates α7 nicotinic acetylcholine receptors expressed in Xenopus oocytes. The Journal of biological chemistry 277:25056–25061.

Dineley KT, Westerman M, Bui D, Bell K, Ashe KH, Sweatt JD (2001) β-Amyloid Activates the Mitogen-Activated Protein Kinase Cascade via Hippocampal α7 Nicotinic Acetylcholine Receptors : In Vitro and In Vivo Mechanisms Related to Alzheimer's Disease. Journal of Neuroscience 21:4125–4133.

Dineley KT, Xia X, Bui D, Sweatt JD, Zheng H (2002b) Accelerated plaque accumulation, associative learning deficits, and up-regulation of α7 nicotinic receptor protein in transgenic mice co-expressing mutant human presenilin 1 and amyloid precursor proteins. The Journal of biological chemistry 277:22768–22780.

Dobrowolska J a *et al*. (2014) CNS Amyloid-β, Soluble APP-α and -β Kinetics during BACE Inhibition. The Journal of Neuroscience 34:8336–8346.

Domercq M, Alberdi E, Sánchez-Gómez MV, Ariz U, Pérez-Samartín A, Matute C (2011) Dual-specific phosphatase-6 (Dusp6) and ERK mediate AMPA receptor-induced oligodendrocyte death. The Journal of biological chemistry 286:11825–11836.

Dougherty JJ, Wu J, Nichols RA (2003) β-amyloid regulation of presynaptic nicotinic receptors in rat hippocampus and neocortex. The Journal of Neuroscience 23:6740–6747.

Duce JA *et al*. (2011) An iron-export ferroxidase activity of β-amyloid protein precursor is inhibited by zinc in Alzheimer's Disease. Cell 142:857–867.

Duffy AM, Fitzgerald ML, Chan J, Robinson DC, Milner T a, Mackie K, Pickel VM (2011) Acetylcholine α7 nicotinic and dopamine D2 receptors are targeted to many of the same postsynaptic dendrites and astrocytes in the rodent prefrontal cortex. Synapse 65:1350–1367.

Dunckley T, Lukas RJ (2003) Nicotine modulates the expression of a diverse set of genes in the neuronal SH-SY5Y cell line. The Journal of biological chemistry 278:15633–15640.

Dunkley PR, Jarvie PE, Robinson PJ (2008) A rapid Percoll gradient procedure for preparation of synaptosomes. Nature protocols 3:1718–1728.

Durand G, Kovalchuk Y, Konnerth A (1996) Long-term potentiation and functional synapse induction in developing hippocampus. Nature 381:71–75.

Eaton JB, Peng J-H, Schroeder KM, George AA, Fryer JD, Krishnan C, Buhlman L, Kuo Y-P, Steinlein O, Lukas RJ (2003) Characterization of human α4 β2-nicotinic acetylcholine receptors stably and heterologously expressed in native nicotinic receptor-null SH-EP1 human epithelial cells. Molecular pharmacology 64:1283–1294.

Ehrlich I, Malinow R (2004) Postsynaptic density 95 controls AMPA receptor incorporation during long-term potentiation and experience-driven synaptic plasticity. The Journal of Neuroscience 24:916–927.

El Kouhen R, Hu M, Anderson DJ, Li J, Gopalakrishnan M (2009) Pharmacology of α7 nicotinic acetylcholine receptor mediated extracellular signal-regulated kinase signalling in PC12 cells. British journal of pharmacology 156:638–648.

Emmrich J V, Hornik TC, Neher JJ, Brown GC (2013) Rotenone induces neuronal death by microglial phagocytosis of neurons. The FEBS journal 280:5030–5038.

Fabian-Fine R, Skehel P, Errington ML, Davies HA, Sher E, Stewart MG, Fine A (2001) Ultrastructural distribution of the α7 nicotinic acetylcholine receptor subunit in rat hippocampus. The Journal of Neuroscience 21:7993–8003.

Färber K, Pannasch U, Kettenmann H (2005) Dopamine and noradrenaline control distinct functions in rodent microglial cells. Molecular and cellular neurosciences 29:128–138.

Farzan M, Schnitzler CE, Vasilieva N, Leung D, Choe H (2000) BACE2, a β-secretase homolg, cleaves at the site and within the amyloid-β region of the amyloid-β precursor protein. Proceedings of the National Academy of Sciences 97:9712–9717.

Fenster CP, Rains MF, Noerager B, Quick MW, Lester RA (1997) Influence of subunit composition on desensitization of neuronal acetylcholine receptors at low concentrations of nicotine. The Journal of Neuroscience 17:5747–5759.

Ferrell JE, Bhatt RR (1997) Mechanistic Studies of the Dual Phosphorylation of Mitogen-activated Protein Kinase. Journal of Biological Chemistry 272:19008–19016.

Fisher A (2012) Cholinergic modulation of amyloid precursor protein processing with emphasis on M1 muscarinic receptor: perspectives and challenges in treatment of Alzheimer's disease. Journal of neurochemistry 120 Suppl :22–33.

Fowler SW, Chiang ACA, Savjani RR, Larson ME, Sherman MA, Schuler DR, Cirrito JR, Lesné SE, Jankowsky JL (2014) Genetic modulation of soluble Aβ rescues cognitive and synaptic impairment in a mouse model of Alzheimer's disease. The Journal of Neuroscience 34:7871–7885.

Francis PT, Palmer AM, Snape M, Wilcock GK (1999) The cholinergic hypothesis of Alzheimer's disease: a review of progress. Journal of Neurology, Neurosurgery and Psychiatry 66:137–147.

Frandemiche ML, De Seranno S, Rush T, Borel E, Elie A, Arnal I, Lanté F, Buisson A (2014) Activity-dependent tau protein translocation to excitatory synapse is disrupted by exposure to amyloid-β oligomers. The Journal of Neuroscience 34:6084–6097.

Frazier CJ, Buhler A V, Weiner JL, Dunwiddie T (1998a) Synaptic potentials mediated via alpha-bungarotoxin-sensitive nicotinic acetylcholine receptors in rat hippocampal interneurons. The Journal of Neuroscience 18:8228–8235.

Frazier CJ, Rollins YD, Breese CR, Leonard S, Freedman R, Dunwiddie T (1998b) Acetylcholine activates an alpha-bungarotoxin-sensitive nicotinic current in rat hippocampal interneurons, but not pyramidal cells. The Journal of Neuroscience 18:1187–1195.

Fu XW, Lindstrom J, Spindel ER (2009) Nicotine activates and up-regulates nicotinic acetylcholine receptors in bronchial epithelial cells. American journal of respiratory cell and molecular biology 41:93–99.

Fucile S (2004) Ca2+ permeability of nicotinic acetylcholine receptors. Cell Calcium 35:1–8.

Fukumoto H, Takahashi H, Tarui N, Matsui J, Tomita T, Hirode M, Sagayama M, Maeda R, Kawamoto M, Hirai K, Terauchi J, Sakura Y, Kakihana M, Kato K, Iwatsubo T, Miyamoto M (2010) A noncompetitive BACE1 inhibitor TAK-070 ameliorates Abeta pathology and behavioral deficits in a mouse model of Alzheimer's disease. The Journal of Neuroscience 30:11157–11166.

Galvin JE, Cornblatt B, Newhouse P, Ancoli-israel S, Wesnes K, Williamson JD, Zhu Y, Sorra K, Amatniek J (2008) Effects of Galantamine on Measures of Attention Results From 2 Clinical Trials in Alzheimer Disease Patients. Alzheimer's disease and associated disorders 22:30–38.

Garg S, Timm T, Mandelkow E-M, Mandelkow E, Wang Y (2011) Cleavage of Tau by calpain in Alzheimer's disease: the quest for the toxic 17 kD fragment. Neurobiology of aging 32:1–14.

Genzen JR, Cleve W Van, Mcgehee DS, Physiol AJ, Physiol C (2014) Dorsal Root Ganglion Neurons Express Multiple Nicotinic Acetylcholine Receptor Subtypes

nucleus of the solitary tract Dorsal Root Ganglion Neurons Express Multiple Nicotinic Acetylcholine Receptor Subtypes. Journal of neurophysiology 86:1773–1782.

Gill JK, Savolainen M, Young GT, Zwart R, Sher E, Millar NS (2011) Agonist activation of α7 nicotinic acetylcholine receptors via an allosteric transmembrane site. Proceedings of the National Academy of Sciences of the United States of America 108:5867–5872.

Ginhoux F, Greter M, Leboeuf M, Nandi S, See P, Gokhan S, Mehler MF, Conway SJ, Ng LG, Stanley ER, Samokhvalov IM, Merad M (2010) Fate mapping analysis reveals that adult microglia derive from primitive macrophages. Science 330:841–845.

Giunta B, Ehrhart J, Townsend K, Sun N, Vendrame M, Shytle D, Tan J, Fernandez F (2004) Galantamine and nicotine have a synergistic effect on inhibition of microglial activation induced by HIV-1 gp120. Brain research bulletin 64:165–170.

Glenn JA, Ward SA, Stone CR, Booth PL, Thomas WE (1992) Characterisation of ramified microglial cells: detailed morphology, morphological plasticity and proliferative capability. Journal of anatomy 180 (Pt 1:109–118.

Gómez-Nicola D, Fransen NL, Suzzi S, Perry VH (2013) Regulation of microglial proliferation during chronic neurodegeneration. The Journal of Neuroscience 33:2481–2493.

Gomez-Varela D, Berg DK (2013) Lateral mobility of presynaptic α7-containing nicotinic receptors and its relevance for glutamate release. The Journal of Neuroscience 33:17062–17071.

Gopalakrishnan M, Buisson B, Touma E, Giordano T, Campbell JE, Hu IC, Donnelly-Roberts D, Arneric SP, Bertrand D, Sullivan JP (1995) Stable expression and pharmacological properties of the human α7 nicotinic acetylcholine receptor. European journal of pharmacology 290:237–246.

Gordon S (2003) Alternative activation of macrophages. Nature reviews Immunology 3:23–35.

Goriounova NA, Mansvelder HD (2012) Short- and long-term consequences of nicotine exposure during adolescence for prefrontal cortex neuronal network function. Cold Spring Harbor perspectives in medicine 2:a012120.

Gray R, Rajan A, Radcliffe K, Yakehiro M, Dani J (1996) Hippocampal synaptic transmission enhanced by low concentrations of nicotine. Nature 383:713–716.

Greenberg ME, Ziff EB, Greene LA (1986) Stimulation of neuronal acetylcholine receptors induces rapid gene transcription. Science 234:80–83.

Greenhalgh AD, David S (2014) Differences in the phagocytic response of microglia and peripheral macrophages after spinal cord injury and its effects on cell death. The Journal of Neuroscience 34:6316–6322.

Grienberger C, Konnerth A (2012) Imaging calcium in neurons. Neuron 73:862–885.

Grilli M, Summa M, Salamone A, Olivero G, Zappettini S, Di Prisco S, Feligioni M, Usai C, Pittaluga A, Marchi M (2012) In vitro exposure to nicotine induces endocytosis of presynaptic AMPA receptors modulating dopamine release in rat nucleus accumbens nerve terminals. Neuropharmacology 63:916–926.

Grønlien JH, Håkerud M, Ween H, Thorin-hagene K, Briggs CA, Gopalakrishnan M, Malysz J (2007) Distinct Profiles of α7 nAChR Positive Allosteric Modulation Revealed by Structurally Diverse Chemotypes. Molecular Pharmacology 72:715–724.

Gusev A, Uteshev V (2010) Physiological concentrations of choline activate native α7-containing nicotinic acetylcholine receptors in the presence of PNU-120596 [1-(5-chloro-2, 4-dimethoxyphenyl)-3-(5-methylisoxazol-3-yl)-urea]. The Journal of pharmacology and experimental therapeutics 332:588–598.

Haapasalo A, Kovacs DM (2011) The many substrates of presenilin/γ-secretase. Journal of Alzheimer's Disease 25:3–28.

Haass C, Hung AY, Selkoe DJ (1991) Processing of β-Amyloid Precursor Protein in Microglia and Astrocytes Favors an Internal Localization over Constitutive Secretion. Journal of Neuroscience 11:3783–3793.

Haass C, Kaether C, Thinakaran G, Sisodia S (2012) Trafficking and proteolytic processing of APP. Cold Spring Harbor perspectives in medicine 2:a006270.

Hagino Y, Kariura Y, Manago Y, Amano T, Wang B, Sekiguchi M, Nishikawa K, Aoki S, Wada K, Noda M (2004) Heterogeneity and potentiation of AMPA type of glutamate receptors in rat cultured microglia. Glia 47:68–77.

Hajos M, Hurst RS, Hoffmann WE, Krause M, Wall TM, Higdon NR, Groppi VE (2005) The Selective α7 Nicotinic Acetylcholine Receptor Agonist chlorobenzamide Hydrochloride] Enhances GABAergic Synaptic Activity in Brain Slices and Restores Auditory Gating Deficits in Anesthetized Rats. Journal of Pharmacology and Experimental Therapeutics 312:1213–1222.

Halff AW, Gómez-Varela D, John D, Berg DK (2014) A novel mechanism for nicotinic potentiation of glutamatergic synapses. The Journal of Neuroscience 34:2051–2064.

Hardingham GE (2006) Pro-survival signalling from the NMDA receptor. Biochemical Society transactions 34:936–938.

Hardingham GE, Fukunaga Y, Bading H (2002) Extrasynaptic NMDARs oppose synaptic NMDARs by triggering CREB shut-off and cell death pathways. Nature neuroscience 5:405–414.

Hardy J, Allsop D (1991) Amyloid deposition as the central event in the aetiology of Alzheimer's disease. Trends in pharmacological sciences 12:383–388.

Hardy J, Selkoe DJ (2002) The amyloid hypothesis of Alzheimer's disease: progress and problems on the road to therapeutics. Science 297:353–356.

Hardy J, Selkoe DJ (2010) The Amyloid Hypothesis of Alzheimer's Disease: Progress and Problems on the Road to Therapeutics. Science 297:353–356.

Haring R, Fisher A, Marciano D (1998) Mitogen-activated protein kinase-dependent and protein kinase C-dependent pathways link the m1 muscarinic receptor to β-amyloid precursor protein secretion. Journal of neurochemistry 71:2094–2103.

Hartmann T, Bieger S, Brühl B, Tienari P (1997) Distinct sites of intracellular production for Alzheimer's disease Aβ40-42 amyloid peptides. Nature medicine 3:1016–1020.

Hassan S, Eldeeb K, Millns PJ, Bennett AJ, Alexander SPH, Kendall DA (2014) Cannabidiol enhances microglial phagocytosis via transient receptor potential (TRP) channel activation. British journal of pharmacology 171:2426–2439.

Haynes SE, Hollopeter G, Yang G, Kurpius D, Dailey ME, Gan W-B, Julius D (2006) The P2Y12 receptor regulates microglial activation by extracellular nucleotides. Nature neuroscience 9:1512–1519.

Hedberg MM, Svedberg MM, Mustafiz T, Yu WF, Mousavi M, Guan ZZ, Unger C, Nordberg a (2008) Transgenic mice overexpressing human acetylcholinesterase and the Swedish amyloid precursor protein mutation: effect of nicotine treatment. Neuroscience 152:223–233.

Heinemann S, Boulter J, Deneris E, Conolly J, Duvoisin R, Papke R, Patrick J (1990) The brain nicotinic acetylcholine receptor gene family. Progress in brain research 86:195–203.

Hellström-Lindahl E (2000) Modulation of β-amyloid precursor protein processing and tau phosphorylation by acetylcholine receptors. European journal of pharmacology 393:255–263.

Hellström-Lindahl E, Court J, Keverne J, Svedberg M, Lee M, Marutle A, Thomas A, Perry E, Bednar I, Nordberg A (2004) Nicotine reduces Aβ in the brain and cerebral vessels of APPsw mice. European Journal of Neuroscience 19:2703–2710.

Hellström-Lindahl E, Moore H, Nordberg a (2000) Increased levels of tau protein in SH-SY5Y cells after treatment with cholinesterase inhibitors and nicotinic agonists. Journal of neurochemistry 74:777–784.

Heneka MT, Kummer MP, Stutz A, Delekate A, Schwartz S, Vieira-Saecker A, Griep A, Axt D, Remus A, Tzeng T-C, Gelpi E, Halle A, Korte M, Latz E, Golenbock DT (2013) NLRP3 is activated in Alzheimer's disease and contributes to pathology in APP/PS1 mice. Nature 493:674–678.

Heneka MT, Landreth GE (2007) PPARs in the brain. Biochimica et biophysica acta 1771:1031–1045.

Heneka MT, Sastre M, Dumitrescu-Ozimek L, Hanke A, Dewachter I, Kuiperi C, O'Banion K, Klockgether T, Van Leuven F, Landreth GE (2005) Acute treatment with the PPARγ agonist pioglitazone and ibuprofen reduces glial inflammation and Aβ1-42 levels in APP V717I transgenic mice. Brain 128:1442–1453.

Herber DL, Severance EG, Cuevas J, Morgan D, Gordon MN (2004) Biochemical and histochemical evidence of nonspecific binding of α7nAChR antibodies to mouse brain tissue. The journal of histochemistry and cytochemistry 52:1367–1376.

Hernandez CM, Dineley KT (2012) α7 nicotinic acetylcholine receptors in Alzheimer's disease: neuroprotective, neurotrophic or both? Current drug targets 13:613–622.

Hickman SE, Kingery ND, Ohsumi TK, Borowsky ML, Wang L, Means TK, El Khoury J (2013) The microglial sensome revealed by direct RNA sequencing. Nature neuroscience 16:1896–1905.

Hide I, Tanaka M, Inoue A, Nakajima K, Kohsaka S, Inoue K, Nakata Y (2000) Extracellular ATP triggers tumor necrosis factor-alpha release from rat microglia. Journal of neurochemistry 75:965–972.

Hiraoka Y, Ohno M, Yoshida K, Okawa K, Tomimoto H, Kita T, Nishi E (2007) Enhancement of α-secretase cleavage of amyloid precursor protein by a metalloendopeptidase nardilysin. Journal of neurochemistry 102:1595–1605.

Hoe H-S, Fu Z, Makarova A, Lee J-Y, Lu C, Feng L, Pajoohesh-Ganji A, Matsuoka Y, Hyman BT, Ehlers MD, Vicini S, Pak DTS, Rebeck GW (2009) The effects of amyloid precursor protein on postsynaptic composition and activity. The Journal of biological chemistry 284:8495–8506.

Hoey SE, Buonocore F, Cox CJ, Hammond VJ, Perkinton MS, Williams RJ (2013) AMPA receptor activation promotes non-amyloidogenic amyloid precursor protein processing and suppresses neuronal amyloid-β production. PloS one 8:e78155.

Hoey SE, Williams RJ, Perkinton MS (2009) Synaptic NMDA receptor activation stimulates α-secretase amyloid precursor protein processing and inhibits amyloid-β production. The Journal of Neuroscience 29:4442–4460.

Hu M, Gopalakrishnan M, Li J (2009a) Positive allosteric modulation of α7 neuronal nicotinic acetylcholine receptors: lack of cytotoxicity in PC12 cells and rat primary cortical neurons. British Journal of Pharmacology 158:1857–1864.

Hu M, Schurdak ME, Puttfarcken PS, El Kouhen R, Gopalakrishnan M, Li J (2007) High content screen microscopy analysis of Aβ1-42-induced neurite outgrowth

reduction in rat primary cortical neurons: neuroprotective effects of α7 neuronal nicotinic acetylcholine receptor ligands. Brain research 1151:227–235.

Hu M, Waring JF, Gopalakrishnan M, Li J (2008) Role of GSK-3β activation and α7 nAChRs in Aβ(1-42)-induced tau phosphorylation in PC12 cells. Journal of neurochemistry 106:1371–1377.

Hu N-W, Klyubin I, Anwyl R, Anwy R, Rowan MJ (2009b) GluN2B subunit-containing NMDA receptor antagonists prevent Abeta-mediated synaptic plasticity disruption in vivo. Proceedings of the National Academy of Sciences of the United States of America 106:20504–20509.

Hua Y, Woehler A, Kahms M, Haucke V, Neher E, Klingauf J (2013) Blocking endocytosis enhances short-term synaptic depression under conditions of normal availability of vesicles. Neuron 80:343–349.

Huang L-T, Sherwood JL, Sun Y-J, Lodge D, Wang Y (2010) Activation of presynaptic α7 nicotinic receptors evokes an excitatory response in hippocampal CA3 neurones in anaesthetized rats: an in vivo iontophoretic study. British journal of pharmacology 159:554–565.

Hurst R, Rollema H, Bertrand D (2013) Nicotinic acetylcholine receptors: from basic science to therapeutics. Pharmacology and therapeutics 137:22–54.

Hurst RS, Hajós M, Raggenbass M, Wall TM, Higdon NR, Lawson JA, Rutherford-Root KL, Berkenpas MB, Hoffmann WE, Piotrowski DW, Groppi VE, Allaman G, Ogier R, Bertrand S, Bertrand D, Arneric SP (2005) A novel positive allosteric modulator of the α7 neuronal nicotinic acetylcholine receptor: in vitro and in vivo characterization. The Journal of Neuroscience 25:4396–4405.

Hwang J, Hwang H, Lee H-W, Suk K (2010) Microglia signaling as a target of donepezil. Neuropharmacology 58:1122–1129.

Innocent N, Evans N, Hille C, Wonnacott S (2010) Oligomerisation differentially affects the acute and chronic actions of amyloid-β in vitro. Neuropharmacology 59:343–352.

Ittner LM, Ke YD, Delerue F, Bi M, Gladbach A, van Eersel J, Wölfing H, Chieng BC, Christie MJ, Napier IA (2010) Dendritic Function of Tau Mediates Amyloid-β Toxicity in Alzheimer's Disease Mouse Models. Cell:387–397.

Ivanov A, Pellegrino C, Rama S, Dumalska I, Salyha Y, Ben-Ari Y, Medina I (2006) Opposing role of synaptic and extrasynaptic NMDA receptors in regulation of the extracellular signal-regulated kinases (ERK) activity in cultured rat hippocampal neurons. The Journal of physiology 572:789–798.

Jahrling JB, Hernandez CM, Denner L, Dineley KT (2014) PPARγ recruitment to active ERK during memory consolidation is required for Alzheimer's disease-related cognitive enhancement. The Journal of Neuroscience 34:4054–4063.

Jensen AA, Mikkelsen I, Frølund B, Bräuner-Osborne H, Falch E, Krogsgaard-Larsen P (2003) Carbamoylcholine homologs: novel and potent agonists at neuronal nicotinic acetylcholine receptors. Molecular pharmacology 64:865–875.

Jeon AHW, Böhm C, Chen F, Huo H, Ruan X, Ren CH, Ho K, Qamar S, Mathews PM, Fraser PE, Mount HTJ, St George-Hyslop P, Schmitt-Ulms G (2013) Interactome analyses of mature γ-secretase complexes reveal distinct molecular environments of presenilin (PS) paralogs and preferential binding of signal peptide peptidase to PS2. The Journal of biological chemistry 288:15352–15366.

Ji D, Lape R, Dani JA (2001) Timing and Location of Nicotinic Hippocampal Synaptic Plasticity. Neuron 31:131–141.

Jones IW, Westmacott A, Chan E, Jones RW, Dineley K, Neill MJO, Wonnacott S (2006) Nicotinic Acetylcholine Receptor Expression in Alzheimer's Disease. Journal of Molecular Neuroscience 30:83–84.

Jonnala RR, Buccafusco JJ (2001) Relationship between the increased cell surface α7 nicotinic receptor expression and neuroprotection induced by several nicotinic receptor agonists. Journal of neuroscience research 66:565–572.

Jucker M, Walker LC (2013) Self-propagation of pathogenic protein aggregates in neurodegenerative diseases. Nature 501:45–51.

Kalappa BI, Gusev AG, Uteshev V (2010) Activation of functional α7-containing nAChRs in hippocampal CA1 pyramidal neurons by physiological levels of choline in the presence of PNU-120596. PloS one 5:e13964.

Kallop DY, Meilandt WJ, Gogineni A, Easley-Neal C, Wu T, Jubb AM, Yaylaoglu M, Shamloo M, Tessier-Lavigne M, Scearce-Levie K, Weimer RM (2014) A death receptor 6-amyloid precursor protein pathway regulates synapse density in the mature CNS but does not contribute to Alzheimer's disease-related pathophysiology in murine models. The Journal of Neuroscience 34:6425–6437.

Kamenetz F, Tomita T, Hsieh H, Seabrook G, Borchelt D, Iwatsubo T, Sisodia S, Malinow R, Point W (2003) APP Processing and Synaptic Function. Neuron 37:925–937.

Karlin A (2002) Emerging structure of the nicotinic acetylcholine receptors. Nature reviews Neuroscience 3:102–114.

Karran E, Mercken M, De Strooper B (2011) The amyloid cascade hypothesis for Alzheimer's disease: an appraisal for the development of therapeutics. Nature reviews Drug discovery 10:698–712.

Kawai H, Berg DK (2001) Nicotinic acetylcholine receptors containing α7 subunits on rat cortical neurons do not undergo long-lasting inactivation even when up-

regulated by chronic nicotine exposure. Journal of neurochemistry 78:1367–1378.

Kawai H, Zago W, Berg DK (2002) Nicotinic α7 receptor clusters on hippocampal GABAergic neurons: regulation by synaptic activity and neurotrophins. Journal of Neuroscience 22:7903–7912.

Kawamata J, Shimohama S (2011) Stimulating nicotinic receptors trigger multiple pathways attenuating cytotoxicity in models of Alzheimer's and Parkinson's diseases. Journal of Alzheimer's disease 24 Suppl 2:95–109.

Kenney JW, Gould TJ (2008) Modulation of hippocampus-dependent learning and synaptic plasticity by nicotine. Molecular neurobiology 38:101–121.

Kettenmann H, Hanisch U (2011) Physiology of microglia. Physiological reviews 91:461–553.

Kettenmann H, Kirchhoff F, Verkhratsky A (2013) Microglia: new roles for the synaptic stripper. Neuron 77:10–18.

Khan GM, Tong M, Jhun M, Arora K, Nichols RA (2010) β-Amyloid activates presynaptic α7 nicotinic acetylcholine receptors reconstituted into a model nerve cell system: involvement of lipid rafts. The European journal of neuroscience 31:788–796.

Khan UA, Liu L, Provenzano FA, Berman DE, Profaci CP, Sloan R, Mayeux R, Duff KE, Small SA (2013) Molecular drivers and cortical spread of lateral entorhinal cortex dysfunction in preclinical Alzheimer's disease. Nature neuroscience 17:304–311.

Kierdorf K *et al*. (2013) Microglia emerge from erythromyeloid precursors via Pu.1- and Irf8-dependent pathways. Nature neuroscience 16:273–280.

Kihara T, Sawada H, Nakamizo T, Kanki R, Yamashita H, Maelicke A, Shimohama S (2004) Galantamine modulates nicotinic receptor and blocks Abeta-enhanced glutamate toxicity. Biochemical and biophysical research communications 325:976–982.

Kihara T, Shimohama S, Sawada H, Honda K, Nakamizo T, Shibasaki H, Kume T, Akaike a (2001) alpha 7 nicotinic receptor transduces signals to phosphatidylinositol 3-kinase to block A beta-amyloid-induced neurotoxicity. The Journal of biological chemistry 276:13541–13546.

Kim J, Lilliehook C, Dudak A, Prox J, Saftig P, Federoff HJ, Lim ST (2010a) Activity-dependent α-cleavage of nectin-1 is mediated by a disintegrin and metalloprotease 10 (ADAM10). The Journal of biological chemistry 285:22919–22926.

Kim ML, Zhang B, Mills IP, Milla ME, Brunden KR, Lee VM-Y (2008) Effects of TNFα-converting enzyme inhibition on amyloid-β production and APP processing in vitro and in vivo. The Journal of Neuroscience 28:12052–12061.

Kim S, Kim Y, Jeong S, Haass C, Kim Y, Suh Y (1997) Enhanced Release of Secreted Form of Alzheimer's Amyloid Precursor Protein from PC12 Cells by Nicotine. Molecular Pharmacology 436:430–436.

Kim SH, Fraser PE, Westaway D, St George-Hyslop PH, Ehrlich ME, Gandy S (2010b) Group II metabotropic glutamate receptor stimulation triggers production and release of Alzheimer's amyloid-β 1-42 from isolated intact nerve terminals. The Journal of Neuroscience 30:3870–3875.

Kimberly WT, Zheng JB, Guénette SY, Selkoe DJ (2001) The intracellular domain of the beta-amyloid precursor protein is stabilized by Fe65 and translocates to the nucleus in a notch-like manner. The Journal of biological chemistry 276:40288–40292.

Kirazov L, Löffler T, Schliebs R, Bigl V (1997) Glutamate-stimulated secretion of amyloid precursor protein from cortical rat brain slices. Neurochemistry international 30:557–563.

Knapska E, Kaczmarek L (2004) A gene for neuronal plasticity in the mammalian brain: Zif268/Egr-1/NGFI-A/Krox-24/TIS8/ZENK? Progress in neurobiology 74:183–211.

Knowles TPJ, Vendruscolo M, Dobson CM (2014) The amyloid state and its association with protein misfolding diseases. Nature reviews Molecular and cellular biology 15:384–396.

Koenigsknecht J, Landreth G (2004) Microglial phagocytosis of fibrillar β-amyloid through a β1 integrin-dependent mechanism. Journal of Neuroscience 24:9838–9846.

Koenigsknecht-Talboo J, Landreth GE (2005) Microglial phagocytosis induced by fibrillar β-amyloid and IgGs are differentially regulated by proinflammatory cytokines. Journal of Neuroscience 25:8240–8249.

Koike H, Tomioka S, Sorimachi H, Saido TC, Maruyama K, Okuyama A, Fujisawa-Sehara A, Ohno S, Suzuki K, Ishiura S (1999) Membrane-anchored metalloprotease MDC9 has an alpha-secretase activity responsible for processing the amyloid precursor protein. The Biochemical journal 343 Pt 2:371–375.

Koyama Y, Egawa H, Osakada M, Baba A, Matsuda T (2004) Increase by FK960, a novel cognitive enhancer, in glial cell line-derived neurotrophic factor production in cultured rat astrocytes. Biochemical pharmacology 68:275–282.

Kuhn P-H, Wang H, Dislich B, Colombo A, Zeitschel U, Ellwart JW, Kremmer E, Rossner S, Lichtenthaler SF (2010) ADAM10 is the physiologically relevant, constitutive α-secretase of the amyloid precursor protein in primary neurons. The EMBO journal 29:3020–3032.

Kuhn SA, van Landeghem FKH, Zacharias R, Färber K, Rappert A, Pavlovic S, Hoffmann A, Nolte C, Kettenmann H (2004) Microglia express GABA(B)

receptors to modulate interleukin release. Molecular and cellular neurosciences 25:312–322.

La Joie R, Perrotin A, Barre L, Hommet C, Me F, Camus V, Abbas A, Landeau B, Guilloteau D, De La Sayette V, Eustache F (2012) Region-Specific Hierarchy between Atrophy, Hypometabolism, and β-Amyloid (Aβ) Load in Alzheimer's Disease Dementia. Journal of Neuroscience 32:16265–16273.

Lahiri DK, Kotwal GJ, Farlow MR, Sima A, Kupsky W, Sarkar FH, Sambamurti K (2006) The role of the carboxy-terminal fragments of amyloid-precursor protein in Alzheimer's disease. Annals of the New York Academy of Sciences 973:334–339.

Lahiri DK, Utsuki T, Chen D, Farlow MR, Shoaib M, Ingram DK, Greig NH (2002) Nicotine Reduces the Secretion of Alzheimer's β-Amyloid Precursor Protein Containing β-Amyloid Peptide in the Rat without Altering Synaptic Proteins. Annals of the New York Academy of Sciences 965:364–372.

Lammich S, Kojro E, Postina R, Gilbert S, Pfeiffer R, Jasionowski M, Haass C, Fahrenholz F (1999) Constitutive and regulated α-secretase cleavage of Alzheimer's amyloid precursor protein by a disintegrin metalloprotease. Proceedings of the National Academy of Sciences 96:3922–3927.

Larson ME, Lesné SE (2012) Production of oligomeric Aβ assemblies. Journal of neurochemistry 120:125–139.

Lauritzen I, Pardossi-Piquard R, Bauer C, Brigham E, Abraham J-D, Ranaldi S, Fraser P, St-George-Hyslop P, Le Thuc O, Espin V, Chami L, Dunys J, Checler F (2012) The β-secretase-derived C-terminal fragment of βAPP, C99, but not Aβ, is a key contributor to early intraneuronal lesions in triple-transgenic mouse hippocampus. The Journal of Neuroscience 32:16243–55a.

Lazarov O, Robinson J, Tang Y-P, Hairston IS, Korade-Mirnics Z, Lee VM-Y, Hersh LB, Sapolsky RM, Mirnics K, Sisodia SS (2005) Environmental enrichment reduces Abeta levels and amyloid deposition in transgenic mice. Cell 120:701–713.

Lee CYD, Landreth GE (2010) The role of microglia in amyloid clearance from the AD brain. Journal of neural transmission 117:949–960.

Lee EB, Zhang B, Liu K, Greenbaum EA, Doms RW, Trojanowski JQ, Lee VM-Y (2005) BACE overexpression alters the subcellular processing of APP and inhibits Aβ deposition in vivo. The Journal of cell biology 168:291–302.

Lee H-M, Kang J, Lee SJ, Jo E-K (2013) Microglial activation of the NLRP3 inflammasome by the priming signals derived from macrophages infected with mycobacteria. Glia 61:441–452.

Lee RH, Vazquez G (2013) Evidence for a prosurvival role of alpha-7 nicotinic acetylcholine receptor in alternatively (M2)-activated macrophages. Physiological Reports 1:n/a–n/a.

Lee RK, Wurtman RJ, Cox AJ, Nitsch RM (1995) Amyloid precursor protein processing is stimulated by metabotropic glutamate receptors. Proceedings of the National Academy of Sciences of the United States of America 92:8083–8087.

Lee SH, Sharma M, Südhof TC, Shen J (2014) Synaptic function of nicastrin in hippocampal neurons. Proceedings of the National Academy of Sciences of the United States of America 111:8973–8978.

Lei P, Ayton S, Finkelstein DI, Spoerri L, Ciccotosto GD, Wright DK, Wong BXW, Adlard PA, Cherny RA, Lam LQ, Roberts BR, Volitakis I, Egan GF, McLean C a, Cappai R, Duce J a, Bush AI (2012) Tau deficiency induces parkinsonism with dementia by impairing APP-mediated iron export. Nature medicine 18:291–295.

Lendvai B, Kassai F, Szájli A, Némethy Z (2013) α7 Nicotinic Acetylcholine Receptors and Their Role in Cognition. Brain research bulletin 93:86–96.

Lesné S, Koh MT, Kotilinek L, Kayed R, Glabe CG, Yang A, Gallagher M, Ashe KH (2006) A specific amyloid-beta protein assembly in the brain impairs memory. Nature 440:352–357.

Léveillé F, El Gaamouch F, Gouix E, Lecocq M, Lobner D, Nicole O, Buisson A (2008) Neuronal viability is controlled by a functional relation between synaptic and extrasynaptic NMDA receptors. FASEB journal 22:4258–4271.

Levin ED (2013) Complex relationships of nicotinic receptor actions and cognitive functions. Biochemical pharmacology 86:1145–1152.

Levin ED, Rezvani AH (2000) Development of nicotinic drug therapy for cognitive disorders. European journal of pharmacology 393:141–146.

Lewis AS, Picciotto MR (2013) High-affinity nicotinic acetylcholine receptor expression and trafficking abnormalities in psychiatric illness. Psychopharmacology 229:477–485.

Lewis J, Dickson DW, Lin WL, Chisholm L, Corral A, Jones G, Yen SH, Sahara N, Skipper L, Yager D, Eckman C, Hardy J, Hutton M, McGowan E (2001) Enhanced neurofibrillary degeneration in transgenic mice expressing mutant tau and APP. Science 293:1487–1491.

Li D-J, Tang Q, Shen F-M, Su D-F, Duan J-L, Xi T (2009) Overexpressed alpha7 nicotinic acetylcholine receptor inhibited proinflammatory cytokine release in NIH3T3 cells. Journal of bioscience and bioengineering 108:85–91.

Li S-X, Huang S, Bren N, Noridomi K, Dellisanti CD, Sine SM, Chen L (2011) Ligand-binding domain of an α7-nicotinic receptor chimera and its complex with agonist. Nature neuroscience 14:1253–1259.

Lichtenthaler SF, Haass C (2004) Amyloid at the cutting edge : activation of α-secretase prevents amyloidogenesis in an Alzheimer disease mouse model. Journal of Clinical Investigation 113:1384–1387.

Lilja AM, Porras O, Storelli E, Nordberg A, Marutle A (2011) Functional interactions of fibrillar and oligomeric amyloid-β with α7 nicotinic receptors in Alzheimer's disease. Journal of Alzheimer's disease : JAD 23:335–347.

Lin H, Vicini S, Hsu F-C, Doshi S, Takano H, Coulter DA, Lynch DR (2010) Axonal α7 nicotinic ACh receptors modulate presynaptic NMDA receptor expression and structural plasticity of glutamatergic presynaptic boutons. Proceedings of the National Academy of Sciences of the United States of America.

Lipton SA (2007) Pathologically activated therapeutics for neuroprotection. Nature reviews Neuroscience 8:803–808.

Liu Q, Kawai H, Berg DK (2001) β-Amyloid peptide blocks the response of α7-containing nicotinic receptors on hippocampal neurons. Proceedings of the National Academy of Sciences 98:4734–4739.

Liu Q, Xie X, Lukas RJ, St John PA, Wu J (2013) A novel nicotinic mechanism underlies β-amyloid-induced neuronal hyperexcitation. Journal of Neuroscience 33:7253–7263.

Lozada AF, Wang X, Gounko N V, Massey KA, Duan J, Liu Z, Berg DK (2012) Glutamatergic synapse formation is promoted by α7-containing nicotinic acetylcholine receptors. Journal of Neuroscience 32:7651–7661.

Lu B, Kwan K, Levine YA, Olofsson PS, Li J, Joshi S, Wang H, Andersson U, Sangeeta S, Tracey KJ, Province H, Drive C (2014) α7 nicotinic acetylcholine receptor signaling inhibits inflammasome activation by preventing mitochondrial DNA release. Molecular Medicine.

Lubin M, Erisir A, Aoki C (1999) Ultrastructural Immunolocalization of the α7 nAChR Subunit in Guinea Pig Medial Prefronal Cortex. Annals of the New York Academy of Sciences 868:628–632.

Lucin KM, O'Brien CE, Bieri G, Czirr E, Mosher KI, Abbey RJ, Mastroeni DF, Rogers J, Spencer B, Masliah E, Wyss-Coray T (2013) Microglial beclin 1 regulates retromer trafficking and phagocytosis and is impaired in Alzheimer's disease. Neuron 79:873–886.

Macia E, Ehrlich M, Massol R, Boucrot E, Brunner C, Kirchhausen T (2006) Dynasore, a cell-permeable inhibitor of dynamin. Developmental cell 10:839–850.

Mackenzie IR, Miller LA (1994) Senile plaques in temporal lobe epilepsy. Acta neuropathologica 87:504–510.

Maelicke A (2000) Allosteric modulation of nicotinic acetylcholine receptors as a treatment strategy for Alzheimer's disease. European Journal of Pharmacology 393:165–170.

Maelicke A, Samochocki M, Jostock R, Fehrenbacher A, Ludwig J, Albuquerque EX, Zerlin M (2001) Allosteric sensitization of nicotinic receptors by galantamine, a new treatment strategy for Alzheimer's disease. Biological Psychiatry 49:279–288.

Mandrekar-Colucci S, Karlo JC, Landreth GE (2012) Mechanisms underlying the rapid peroxisome proliferator-activated receptor-γ-mediated amyloid clearance and reversal of cognitive deficits in a murine model of Alzheimer's disease. The Journal of Neuroscience 32:10117–10128.

Mann EO, Paulsen O (2007) Role of GABAergic inhibition in hippocampal network oscillations. Trends in neurosciences 30:343–349.

Mansvelder HD, Mcgehee DS (2000) Long-Term Potentiation of Excitatory Inputs to Brain Reward Areas by Nicotine. Neuron 27:349–357.

Mansvelder HD, Mertz M, Role LW (2009) Nicotinic modulation of synaptic transmission and plasticity in cortico-limbic circuits. Seminars in cell and developmental biology 20:432–440.

Marcello E, Gardoni F, Mauceri D, Romorini S, Jeromin A, Epis R, Borroni B, Cattabeni F, Sala C, Padovani A, Di Luca M (2007) Synapse-associated protein-97 mediates α-secretase ADAM10 trafficking and promotes its activity. Journal of Neuroscience 27:1682–1691.

Marks J, Stitzel A, Wehner M, Collins C (1986) Nicotinic Binding Sites in Rat and Mouse Brain : Comparison of Acetylcholine, Nicotine, and α-Bungarotoxin. Molecular Pharmacology 30:427–436.

Martin-Ruiz CM, Court JA, Molnar E, Lee M, Gotti C, Mamalaki A, Tsouloufis T, Tzartos S, Ballard C, Perry RH, Perry EK (2002) α4 but Not α3 and α7 Nicotinic Acetylcholine Receptor Subunits Are Lost from the Temporal Cortex in Alzheimer's Disease. Journal of Neurochemistry 73:1635–1640.

Marubio LM, Changeux J-P (2000) Nicotinic acetylcholine receptor knockout mice as animal models for studying receptor function. European journal of pharmacology 393:113–121.

Matrone C, Barbagallo APM, La Rosa LR, Florenzano F, Ciotti MT, Mercanti D, Chao M V, Calissano P, D'Adamio L (2011) APP is phosphorylated by TrkA and regulates NGF/TrkA signaling. Journal of Neuroscience 31:11756–11761.

Mattson MP (1990) Antigenic changes similar to those seen in neurofibrillary tangles are elicited by glutamate and Ca2+ influx in cultured hippocampal neurons. Neuron 4:105–117.

May PC *et al*. (2011) Robust central reduction of amyloid-β in humans with an orally available, non-peptidic β-secretase inhibitor. Journal of Neuroscience 31:16507–16516.

Mazzo F, Pistillo F, Grazioso G, Clementi F, Borgese N, Gotti C, Colombo SF (2013) Nicotine-modulated subunit stoichiometry affects stability and trafficking of α3β4 nicotinic receptor. Journal of Neuroscience 33:12316–12328.

McCarthy RC, Park Y-H, Kosman DJ (2014) sAPP modulates iron efflux from brain microvascular endothelial cells by stabilizing the ferrous iron exporter ferroportin. EMBO reports 15:809–815.

McKoy A, Chen J, Schupbach T, Hecht M (2012) A Novel Inhibitor of Amyloid-β (Aβ) Peptide Aggregation. Journal of Biological Chemistry 287:38992–39000.

Medeiros R, Castello NA, Cheng D, Kitazawa M, Baglietto-Vargas D, Green KN, Esbenshade TA, Bitner RS, Decker MW, LaFerla FM (2014) α7 nicotinic receptor agonist enhances cognition in aged 3xTg-AD mice with robust plaques and tangles. The American journal of pathology 184:520–529.

Meisl G, Yang X, Hellstrand E, Frohm B, Kirkegaard JB, Cohen SIA, Dobson CM, Linse S, Knowles TPJ (2014) Differences in nucleation behavior underlie the contrasting aggregation kinetics of the Aβ40 and Aβ42 peptides. Proceedings of the National Academy of Sciences of the United States of America 111:9384–9389.

Metherate R (2004) Nicotinic acetylcholine receptors in sensory cortex. Learning and memory 11:50–59.

Mills J, Laurent Charest D, Lam F, Beyreuther K, Ida N, Pelech SL, Reiner PB (1997) Regulation of amyloid precursor protein catabolism involves the mitogen-activated protein kinase signal transduction pathway. Journal of Neuroscience 17:9415–9422.

Mittelbronn M, Harter P, Warth A, Lupescu A, Schilbach K, Vollmann H, Capper D, Goeppert B, Frei K, Bertalanffy H, Weller M, Meyermann R, Lang F, Simon P (2009) EGR-1 is regulated by N-methyl-D-aspartate-receptor stimulation and associated with patient survival in human high grade astrocytomas. Brain pathology 19:195–204.

Miwa JM, Freedman R, Lester HA (2011) Neural systems governed by nicotinic acetylcholine receptors: emerging hypotheses. Neuron 70:20–33.

Miyazawa A, Fujiyoshi Y, Unwin N (2003) Structure and gating mechanism of the acetylcholine receptor pore. Nature 423:949–955.

Mizutari K, Fujioka M, Hosoya M, Bramhall N, Okano HJ, Okano H, Edge ASB (2013) Notch inhibition induces cochlear hair cell regeneration and recovery of hearing after acoustic trauma. Neuron 77:58–69.

Mokin M, Keifer J (n.d.) Expression of the immediate-early gene-encoded protein Egr-1 (zif268) during in vitro classical conditioning. Learning and memory 12:144–149.

Molinari EJ, Delbono O, Messi ML, Renganathan M, Arneric SP, Sullivan JP, Gopalakrishnan M (1998) Up-regulation of human α7 nicotinic receptors by chronic treatment with activator and antagonist ligands. European journal of pharmacology 347:131–139.

Moon JH, Kim SY, Lee HG, Kim SU, Lee YB (2008) Activation of nicotinic acetylcholine receptor prevents the production of reactive oxygen species in fibrillar β-amyloid peptide (1-42)-stimulated microglia. Experimental and molecular medicine 40:11–18.

Morioka N, Tokuhara M, Nakamura Y, Idenoshita Y, Harano S, Zhang FF, Hisaoka-Nakashima K, Nakata Y (2014) Primary cultures of rat cortical microglia treated with nicotine increases in the expression of excitatory amino acid transporter 1 (GLAST) via the activation of the α7 nicotinic acetylcholine receptor. Neuroscience 258:374–384.

Morris M, Maeda S, Vossel K, Mucke L (2011) The many faces of tau. Neuron 70:410–426.

Mosser DM, Edwards JP (2008) Exploring the full spectrum of macrophage activation. Nature reviews Immunology 8:958–969.

Mousavi M, Hellström-Lindahl E (2009) Nicotinic receptor agonists and antagonists increase sAPPalpha secretion and decrease Aβ levels in vitro. Neurochemistry international 54:237–244.

Mousavi M, Nordberg A (2006) Expression of the alpha7, alpha4 and alpha3 nicotinic receptor subtype in the brain and adrenal medulla of transgenic mice carrying genes coding for human AChE and beta-amyloid. International journal of developmental neuroscience 24:269–273.

Moussaud S, Draheim HJ (2010) A new method to isolate microglia from adult mice and culture them for an extended period of time. Journal of neuroscience methods 187:243–253.

Müller UC, Zheng H (2012) Physiological functions of APP family proteins. Cold Spring Harbor perspectives in medicine 2:a006288.

Murphy TH, Worley PF, Baraban JM (1991) L-type voltage-sensitive calcium channels mediate synaptic activation of immediate early genes. Neuron 7:625–635.

Nachmansohn D (1966) Role of acetylcholine in neuromuscular transmission. Annals of the New York Academy of Sciences 135:136–149.

Nagele R, D'Andrea MR, Anderson WJ, Wang H-Y (2002) Intracellular accumulation of β-amyloid 1–42 in neurons is facilitated by the α7 nicotinic acetylcholine receptor in Alzheimer's disease. Neuroscience 110:199–211.

Nakamura K, Greenwood A, Binder L, Bigio EH, Denial S, Nicholson L, Zhou XZ, Lu KP (2012) Proline isomer-specific antibodies reveal the early pathogenic tau conformation in Alzheimer's disease. Cell 149:232–244.

Nakayama H, Numakawa T, Ikeuchi T (2002) Nicotine-induced phosphorylation of Akt through epidermal growth factor receptor and Src in PC12h cells. Journal of neurochemistry 83:1372–1379.

Näslund J, Haroutunian V, Mohs R, Davis KL, Davies P, Greengard P, Buxbaum JD (2000) Correlation between elevated levels of amyloid beta-peptide in the brain and cognitive decline. JAMA : the journal of the American Medical Association 283:1571–1577.

Neher JJ, Neniskyte U, Zhao J-W, Bal-Price A, Tolkovsky AM, Brown GC (2011) Inhibition of microglial phagocytosis is sufficient to prevent inflammatory neuronal death. Journal of immunology 186:4973–4983.

Nery AA, Magdesian MH, Trujillo CA, Sathler LB, Juliano MA, Juliano L, Ulrich H, Ferreira ST (2013) Rescue of amyloid-β-induced inhibition of nicotinic acetylcholine receptors by a peptide homologous to the nicotine binding domain of the α7 subtype. PloS one 8:e67194.

Newhouse PA, Potter A, Singh A (2004) Effects of nicotinic stimulation on cognitive performance. Current opinion in pharmacology 4:36–46.

Ng HJ, Whittemore ER, Tran MB, Hogenkamp DJ, Broide RS, Johnstone TB, Zheng L, Stevens KE, Gee KW (2007) Nootropic α7 nicotinic receptor allosteric modulator derived from GABA-A receptor modulators. Proceedings of the National Academy of Sciences 104:8059–8064.

Ni M, Aschner M (2010) Neonatal rat primary microglia: isolation, culturing, and selected applications. Current Protocols in Toxicology:1–20.

Ni R, Marutle A, Nordberg A (2013) Modulation of α 7 nicotinic acetylcholine receptor and fibrillar amyloid-β interactions in Alzheimer brain. Journal of Alzheimer's Disease 33:841–851.

Nie HZ, Shi S, Lukas RJ, Zhao WJ, Sun YN, Yin M (2010) Activation of α7 nicotinic receptor affects APP processing by regulating secretase activity in SH-EP1-α7 nAChR-hAPP695 cells. Brain research 1356:112–120.

Nikolaev A, McLaughlin T, O'Leary DDM, Tessier-Lavigne M (2009) APP binds DR6 to trigger axon pruning and neuron death via distinct caspases. Nature 457:981–989.

Nitsch RM, Slack BE, Wurtman RJ, Growdon JH (1992) Release of Alzheimer amyloid precursor derivatives stimulated by activation of muscarinic acetylcholine receptors. Science 258:304–307.

Noh M-Y, Koh SH, Kim S-M, Maurice T, Ku S-K, Kim SH (2013) Neuroprotective effects of donepezil against Aβ42-induced neuronal toxicity are mediated through not only enhancing PP2A activity but also regulating GSK-3β and nAChRs activity. Journal of neurochemistry 127:562–574.

Nordberg A (2008) Amyloid imaging in Alzheimer's disease. Neuropsychologia 46:1636–1641.

Nordberg A, Hellström- Lindahl E, Lee M, Johnson M, Mousavi M, Hall R, Perry E, Bednar I, Court J (2002) Chronic nicotine treatment reduces β-amyloidosis in the brain of a mouse model of Alzheimer's disease (APPsw). Journal of neurochemistry 81:655–658.

Nordman JC, Phillips WS, Kodama N, Clark SG, Del Negro C a, Kabbani N (2014) Axon targeting of the alpha 7 nicotinic receptor in developing hippocampal neurons by Gprin1 regulates growth. Journal of neurochemistry 129:649–662.

Oddo S, Vasilevko V, Caccamo A (2006) Reduction of Soluble Aβ and Tau, but Not Soluble Aβ Alone, Ameliorates Cognitive Decline in Transgenic Mice with Plaques and Tangles. Journal of Biological Chemistry 281:39413–39423.

Ong KT, Villemagne VL, Bahar-fuchs A, Lamb F, Langdon N, Catafau AM, Stephens AW, Seibyl J, Dinkelborg LM, Reininger CB, Putz B, Rohde B, Masters CL, Rowe CC (2014) Aβ imaging with 18F-florbetaben in prodromal Alzheimer's disease : a prospective outcome study. Journal of Neurology, Neurosurgery and Psychiatry.

Orre M, Kamphuis W, Osborn LM, Jansen AHP, Kooijman L, Bossers K, Hol EM (2014) Isolation of glia from Alzheimer's mice reveals inflammation and dysfunction. Neurobiology of aging.

Otsuka A, Abe T, Watanabe M, Yagisawa H, Takei K, Yamada H (2009) Dynamin 2 is required for actin assembly in phagocytosis in Sertoli cells. Biochemical and biophysical research communications 378:478–482.

Oulès B, Del Prete D, Greco B, Zhang X, Lauritzen I, Sevalle J, Moreno S, Paterlini-Bréchot P, Trebak M, Checler F, Benfenati F, Chami M (2012) Ryanodine receptor blockade reduces amyloid-β load and memory impairments in Tg2576 mouse model of Alzheimer disease. The Journal of Neuroscience 32:11820–11834.

Page RM, Baumann K, Tomioka M, Pérez-Revuelta BI, Fukumori A, Jacobsen H, Flohr A, Luebbers T, Ozmen L, Steiner H, Haass C (2008) Generation of Aβ38 and Aβ42 is independently and differentially affected by familial Alzheimer disease-associated presenilin mutations and γ-secretase modulation. The Journal of biological chemistry 283:677–683.

Palacios G, Palacios J, Mengod G, Frey P (1992) β-Amyloid precursor protein localization in the Golgi apparatus in neurons and oligodendrocytes. An immunocytochemical structural and ultrastructural study in normal and axotomised neurons. Molecular Brain Research 15:195–206.

Palop JJ, Chin J, Roberson ED, Wang J, Thwin MT, Bien-Ly N, Yoo J, Ho KO, Yu G-Q, Kreitzer A, Finkbeiner S, Noebels JL, Mucke L (2007) Aberrant excitatory neuronal activity and compensatory remodeling of inhibitory hippocampal circuits in mouse models of Alzheimer's disease. Neuron 55:697–711.

Papke RL (2014) Merging old and new perspectives on nicotinic acetylcholine receptors. Biochemical pharmacology 89:1–11.

Papke RL, Kem WR, Soti F, Lo GY, Horenstein NA (2009) Activation and Desensitization of Nicotinic α7-type Acetylcholine Receptors by Benzylidene Anabaseines and Nicotine. Journal of Pharmacology and Experimental Therapeutics 329:791–807.

Papke RL, Porter Papke JK (2002) Comparative pharmacology of rat and human alpha7 nAChR conducted with net charge analysis. British journal of pharmacology 137:49–61.

Parada E, Egea J, Buendia I, Negredo P, Cunha AC, Cardoso S, Soares MP, López MG (2013) The microglial α7-acetylcholine nicotinic receptor is a key element in promoting neuroprotection by inducing heme oxygenase-1 via nuclear factor erythroid-2-related factor 2. Antioxidants and redox signaling 19:1135–1148.

Pardossi-Piquard R, Checler F (2012) The physiology of the β-amyloid precursor protein intracellular domain AICD. Journal of neurochemistry 120 Suppl :109–124.

Parkhurst CN, Yang G, Ninan I, Savas JN, Yates JR, Lafaille JJ, Hempstead BL, Littman DR, Gan W-B (2013) Microglia promote learning-dependent synapse formation through brain-derived neurotrophic factor. Cell 155:1596–1609.

Parri HR, Dineley TK (2010) Nicotinic acetylcholine receptor interaction with β-amyloid: molecular, cellular, and physiological consequences. Current Alzheimer research 7:27–39.

Parri HR, Hernandez CM, Dineley KT (2011) Research update: α7 nicotinic acetylcholine receptor mechanisms in Alzheimer's disease. Biochemical pharmacology 82:931–942.

Parsons MP, Raymond LA (2014) Extrasynaptic NMDA receptor involvement in central nervous system disorders. Neuron 82:279–293.

Peng X, Gerzanich V, Anand R, Whiting PJ, Lindstrom J (1994) Nicotine-induced increase in neuronal nicotinic receptors results from a decrease in the rate of receptor turnover. Molecular pharmacology 46:523–530.

Perry E *et al*. (2000) Nicotinic receptor subtypes in human brain ageing, Alzheimer and Lewy body diseases. European journal of pharmacology 393:215–222.

Perry EK (1986) THE CHOLINERGIC HYPOTHESIS — TEN YEARS ON. British Medical Journal 42:63–69.

Pesti K, Szabo AK, Mike A, Vizi ES (2014) Kinetic properties and open probability of α7 nicotinic acetylcholine receptors. Neuropharmacology 81:101–115.

Pettit DL, Shao Z, Yakel JL, Carolina N (2001) β-Amyloid 1–42 Peptide Directly Modulates Nicotinic Receptors in the Rat Hippocampal Slice. Journal of Neuroscience 21:1–5.

Picciotto MR (2003) Nicotine as a modulator of behavior: beyond the inverted U. Trends in pharmacological sciences 24:493–499.

Picciotto MR, Zoli M (2008) Neuroprotection via nAChRs: the role of nAChRs in neurodegenerative disorders such as Alzheimer's and Parkinson's disease. Frontiers in bioscience 13:492–504.

Pimplikar SW, Nixon RA, Robakis NK, Shen J, Tsai L-H (2010) Amyloid-Independent Mechanisms in Alzheimer's Disease Pathogenesis. Journal of Neuroscience 30:14946–14954.

Pocock JM, Kettenmann H (2007) Neurotransmitter receptors on microglia. Trends in neurosciences 30:527–535.

Poisik O V., Shen J-X, Jones S, Yakel JL (2008) Functional α7-containing nicotinic acetylcholine receptors localize to cell bodies and proximal dendrites in the rat substantia nigra pars reticulata. The Journal of Physiology 586:1365–1378.

Pooler AM, Phillips EC, Lau DHW, Noble W, Hanger DP (2013) Physiological release of endogenous tau is stimulated by neuronal activity. EMBO reports 14:389–394.

Poorthuis RB, Bloem B, Schak B, Wester J, de Kock CPJ, Mansvelder HD (2013) Layer-specific modulation of the prefrontal cortex by nicotinic acetylcholine receptors. Cerebral cortex 23:148–161.

Postina R (2012) Activation of α-secretase cleavage. Journal of neurochemistry 120 Suppl :46–54.

Postina R, Schroeder A, Dewachter I, Bohl J, Schmitt U, Kojro E, Prinzen C, Endres K, Hiemke C, Blessing M, Flamez P, Dequenne A, Godaux E, van Leuven F, Fahrenholz F (2004) A disintegrin-metalloproteinase prevents amyloid plaque formation and hippocampal defects in an Alzheimer disease mouse model. The Journal of clinical investigation 113:1456–1464.

Pratt KG, Zhu P, Watari H, Cook DG, Sullivan JM (2011) A novel role for γ-secretase: selective regulation of spontaneous neurotransmitter release from hippocampal neurons. Journal of Neuroscience 31:899–906.

Price DL, Sisodia SS (1998) Mutant genes in familial Alzheimer's disease and transgenic models. Annual review of neuroscience 21:479–505.

Prinz M, Priller J (2014) Microglia and brain macrophages in the molecular age: from origin to neuropsychiatric disease. Nature reviews Neuroscience 15:300–312.

Puzzo D, Arancio O (2013) Amyloid-β peptide: Dr. Jekyll or Mr. Hyde? Journal of Alzheimer's disease 33 Suppl 1:S111–20.

Puzzo D, Privitera L, Leznik E, Fa M, Staniszewski A, Palmeri A, Arancio O (2008) Picomolar amyloid-β positively modulates synaptic plasticity and memory in hippocampus. The Journal of Neuroscience 28:14537–14545.

Rainey-Smith SR, Andersson DA, Williams RJ, Rattray M (2010) Tumour necrosis factor-α induces rapid reduction in AMPA receptor-mediated calcium entry in motor neurones by increasing cell surface expression of the GluR2 subunit: relevance to neurodegeneration. Journal of neurochemistry 113:692–703.

Rayes D, De Rosa MJ, Sine SM, Bouzat C (2009) Number and locations of agonist binding sites required to activate homomeric Cys-loop receptors. The Journal of Neurosciencence 29:6022–6032.

Ren K, King MA, Liu J, Siemann J, Altman M, Meyers C, Hughes J a, Meyer EM (2007) The α7 nicotinic receptor agonist 4OH-GTS-21 protects axotomized septohippocampal cholinergic neurons in wild type but not amyloid-overexpressing transgenic mice. Neuroscience 148:230–237.

Ring S, Weyer SW, Kilian SB, Waldron E, Pietrzik CU, Filippov MA, Herms J, Buchholz C, Eckman CB, Korte M, Wolfer DP, Müller UC (2007) The secreted β-amyloid precursor protein ectodomain APPs-α is sufficient to rescue the anatomical, behavioral, and electrophysiological abnormalities of APP-deficient mice. Journal of Neuroscience 27:7817–7826.

Risso F, Parodi M, Grilli M, Molfino F, Raiteri M, Marchi M (2004) Chronic nicotine causes functional upregulation of ionotropic glutamate receptors mediating hippocampal noradrenaline and striatal dopamine release. Neurochemistry International 44:293–301.

Rockenstein E, Torrance M, Adame A, Mante M, Bar-on P, Rose JB, Crews L, Masliah E (2007) Neuroprotective Effects of Regulators of the Glycogen Synthase Kinase-3 Signaling Pathway in a Transgenic Model of Alzheimer's Disease Are Associated with Reduced Amyloid Precursor Protein Phosphorylation. Journal of Neuroscience 27:1981–1991.

Rojo LE, Fernández JA, Maccioni AA, Jimenez JM, Maccioni RB (2008) Neuroinflammation: implications for the pathogenesis and molecular diagnosis of Alzheimer's disease. Archives of medical research 39:1–16.

Rousseau SJ, Jones IW, Pullar IA, Wonnacott S (2005) Presynaptic α7 and non-α7 nicotinic acetylcholine receptors modulate [3H]d-aspartate release from rat frontal cortex in vitro. Neuropharmacology 49:59–72.

Roy A, Fung Y, Liu X, Pahan K (2006) Up-regulation of microglial CD11b expression by nitric oxide. Journal of Biological Chemistry 281:14971–14980.

Rush T, Buisson A (2014) Reciprocal disruption of neuronal signaling and Aβ production mediated by extrasynaptic NMDA receptors: a downward spiral. Cell and tissue research 356:279–286.

Rushworth J V, Griffiths HH, Watt T, Hooper NM, Watt NT (2013) Prion Protein-mediated Toxicity of Amyloid-b Oligomers Requires Lipid Rafts and the Transmembrane LRP1. Journal of Biological Chemistry 288:8935–9851.

Rushworth J V, Hooper NM (2011) Lipid Rafts : Linking Alzheimer's Amyloid-β Production, Aggregation, and Toxicity at Neuronal Membranes. International Journal of Alzheimer's Disease.

Sala C, Rudolph-Correia S, Sheng M (2000) Developmentally regulated NMDA receptor-dependent dephosphorylation of cAMP response element-binding protein (CREB) in hippocampal neurons. The Journal of Neuroscience 20:3529–3536.

Salter MW, Beggs S (2014) Sublime Microglia: Expanding Roles for the Guardians of the CNS. Cell 158:15–24.

Samson A, Scherf T, Eisenstein M, Chill J, Anglister J (2002) The mechanism for acetylcholine receptor inhibition by α-neurotoxins and species-specific resistance to α-bungarotoxin revealed by NMR. Neuron 35:319–332.

Samuel N, Wonnacott S, Lindstrom J, Futerman AH (1997) Parallel increases in [125I]-α-bungarotoxin binding and α7 nicotinic subunit immunoreactivity during the development of rat hippocampal neurons in culture. Neuroscience letters 222:179–182.

Sanders DW, Kaufman SK, DeVos SL, Sharma AM, Mirbaha H, Li A, Barker SJ, Foley AC, Thorpe JR, Serpell LC, Miller TM, Grinberg LT, Seeley WW, Diamond MI (2014) Distinct tau prion strains propagate in cells and mice and define different tauopathies. Neuron 82:1271–1288.

Sano Y, Nakaya T, Pedrini S, Takeda S, Iijima-Ando K, Iijima K, Mathews PM, Itohara S, Gandy S, Suzuki T (2006) Physiological mouse brain Abeta levels are not related to the phosphorylation state of threonine-668 of Alzheimer's APP. PloS one 1:e51.

Sauguet L, Poitevin F, Murail S, Van Renterghem C, Moraga-Cid G, Malherbe L, Thompson AW, Koehl P, Corringer P-J, Baaden M, Delarue M (2013) Structural basis for ion permeation mechanism in pentameric ligand-gated ion channels. The EMBO journal 32:728–741.

Saura J, Tusell JM, Serratosa J (2003) High-yield isolation of murine microglia by mild trypsinization. Glia 44:183–189.

Schafe GE, Atkins CM, Swank MW, Bauer EP, Sweatt JD, LeDoux JE (2000) Activation of ERK/MAP kinase in the amygdala is required for memory consolidation of pavlovian fear conditioning. Journal of Neuroscience 20:8177–8187.

Schafe GE, Swank MW, Rodrigues SM, Debiec J, Doyère V (2008) Phosphorylation of ERK/MAP kinase is required for long-term potentiation in anatomically restricted regions of the lateral amygdala in vivo. Learning and memory 15:55–62.

Schenk D *et al*. (1999) Immunization with amyloid- b attenuates Alzheimer- disease-like pathology in the PDAPP mouse. Nature 400:173–177.

Schettini G, Govoni S, Racchi M, Rodriguez G (2010) Phosphorylation of APP-CTF-AICD domains and interaction with adaptor proteins: signal transduction and/or transcriptional role--relevance for Alzheimer pathology. Journal of neurochemistry 115:1299–1308.

Schliebs R, Arendt T (2011) The cholinergic system in aging and neuronal degeneration. Behavioural brain research 221:555–563.

Schmid CD, Melchior B, Masek K, Puntambekar SS, Danielson PE, Lo DD, Sutcliffe JG, Carson MJ (2009) Differential gene expression in LPS/IFNgamma activated microglia and macrophages: in vitro versus in vivo. Journal of neurochemistry 109 Suppl :117–125.

Schrenk-Siemens K, Perez-Alcala S, Richter J, Lacroix E, Rahuel J, Korte M, Müller U, Barde Y-A, Bibel M (2008) Embryonic stem cell-derived neurons as a cellular system to study gene function: lack of amyloid precursor proteins APP and APLP2 leads to defective synaptic transmission. Stem cells 26:2153–2163.

Schroeder B, Koo E (2005) To Think or Not to Think: Synaptic Activity and Aβ Release. Neuron 48:873–875.

Séguéla P, Wadiche J, Dineley-Miller K, Dani JA, Patrick JW (1993) Molecular cloning, functional properties, and distribution of rat brain α7: a nicotinic cation channel highly permeable to calcium. The Journal of Neuroscience 13:596–604.

Selkoe DJ, Wolfe MS (2007) Presenilin: running with scissors in the membrane. Cell 131:215–221.

Shah P, Lal N, Leung E, Traul DE, Gonzalo-Ruiz A, Geula C (2010) Neuronal and axonal loss are selectively linked to fibrillar amyloid-β within plaques of the aged primate cerebral cortex. The American journal of pathology 177:325–333.

Shankar GM, Bloodgood BL, Townsend M, Walsh DM, Selkoe DJ, Sabatini BL (2007) Natural oligomers of the Alzheimer amyloid-β protein induce reversible

synapse loss by modulating an NMDA-type glutamate receptor-dependent signaling pathway. Journal of Neuroscience 27:2866–2875.

Sharma G, Vijayaraghavan S (2002) Nicotinic receptor signaling in nonexcitable cells. Journal of neurobiology 53:524–534.

Shaw S, Bencherif M, Marrero MB (2002) Janus kinase 2, an early target of α7 nicotinic acetylcholine receptor-mediated neuroprotection against Aβ1-42 amyloid. The Journal of biological chemistry 277:44920–44924.

Shelukhina I V, Kryukova E V, Lips KS, Tsetlin VI, Kummer W (2009) Presence of α7 nicotinic acetylcholine receptors on dorsal root ganglion neurons proved using knockout mice and selective α-neurotoxins in histochemistry. Journal of neurochemistry 109:1087–1095.

Shimohama S, Kihara T (2001) Nicotinic receptor-mediated protection against beta-amyloid neurotoxicity. Biological psychiatry 49:233–239.

Shytle RD, Mori T, Townsend K, Vendrame M, Sun N, Zeng J, Ehrhart J, Silver AA, Sanberg PR, Tan J (2004) Cholinergic modulation of microglial activation by α7 nicotinic receptors. Journal of neurochemistry 89:337–343.

Sine SM, Engel AG (2006) Recent advances in Cys-loop receptor structure and function. Nature 440:448–455.

Sisodia SS, Kim SH, Thinakaran G (1999) Function and Dysfunction of the Presenilins. American Journal of Human Genetics 65:7–12.

Sitapara RA, Antoine DJ, Sharma L, Patel VS, Ashby CR, Gorasiya S, Yang H, Zur M, Mantell LL (2014) The α7 Nicotinic Acetylcholine Receptor Agonist GTS-21 Improves Bacterial Clearance in Mice by Restoring Hyperoxia-Compromised Macrophage Function. Molecular medicine 20:238–247.

Slack BE, Ma LK, Seah CC (2001) Constitutive shedding of the amyloid precursor protein ectodomain is up-regulated by tumour necrosis factor-α converting enzyme. Biochemical Journal 794:787–794.

Small DH, Maksel D, Kerr ML, Ng J, Hou X, Chu C, Mehrani H, Unabia S, Azari MF, Loiacono R, Aguilar M-I, Chebib M (2007) The β-amyloid protein of Alzheimer's disease binds to membrane lipids but does not bind to the α7 nicotinic acetylcholine receptor. Journal of neurochemistry 101:1527–1538.

Snyder EM, Nong Y, Almeida CG, Paul S, Moran T, Choi EY, Nairn AC, Salter MW, Lombroso PJ, Gouras GK, Greengard P (2005) Regulation of NMDA receptor trafficking by amyloid-β. Nature neuroscience 8:1051–1058.

Söderman A, Mikkelsen JD, West MJ, Christensen DZ, Jensen MS (2010) Activation of nicotinic α7 acetylcholine receptor enhances long term potentation in wild type mice but not in APP(swe)/PS1ΔE9 mice. Neuroscience letters 487:5–9.

Song MS, Rauw G, Baker GB, Kar S (2008) Memantine protects rat cortical cultured neurons against β-amyloid-induced toxicity by attenuating tau phosphorylation. The European journal of neuroscience 28:1989–2002.

Sosa LJ, Bergman J, Estrada-Bernal A, Glorioso TJ, Kittelson JM, Pfenninger KH (2013) Amyloid precursor protein is an autonomous growth cone adhesion molecule engaged in contact guidance. PloS one 8:e64521.

Srivareerat M, Tran TT, Salim S, Aleisa AM, Alkadhi KA (2011) Chronic nicotine restores normal Aβ levels and prevents short-term memory and E-LTP impairment in Aβ rat model of Alzheimer's disease. Neurobiology of aging 32:834–844.

St John PA (2009) Cellular trafficking of nicotinic acetylcholine receptors. Acta pharmacologica Sinica 30:656–662.

Stansley B, Post J, Hensley K (2012) A comparative review of cell culture systems for the study of microglial biology in Alzheimer's disease. Journal of neuroinflammation 9:115.

Steiner RC, Heath CJ, Picciotto MR (2007) Nicotine-induced phosphorylation of ERK in mouse primary cortical neurons: evidence for involvement of glutamatergic signaling and CaMKII. Journal of neurochemistry 103:666–678.

Stence N, Waite M, Dailey ME (2001) Dynamics of microglial activation: a confocal time-lapse analysis in hippocampal slices. Glia 33:256–266.

Stern Y (2006) Cognitive reserve and Alzheimer disease. Alzheimer disease and associated disorders 20:112–117.

Suh J, Choi SH, Romano DM, Gannon MA, Lesinski AN, Kim DY, Tanzi RE, Andrea N (2013) ADAM10 missense mutations potentiate β-amyloid accumulation by impairing prodomain chaperone function. Neuron 80:385–401.

Sun J, Zheng JH, Zhao M, Lee S, Goldstein H (2008) Increased in vivo activation of microglia and astrocytes in the brains of mice transgenic for an infectious R5 human immunodeficiency virus type 1 provirus and for CD4-specific expression of human cyclin T1 in response to stimulation by lipopolysaccharide. Journal of virology 82:5562–5572.

Sweatt JD (2004) Mitogen-activated protein kinases in synaptic plasticity and memory. Current opinion in neurobiology 14:311–317.

Szabo AK, Pesti K, Mike A, Vizi ES (2014) Mode of action of the positive modulator PNU-120596 on α7 nicotinic acetylcholine receptors. Neuropharmacology 81:42–54.

Takata K, Kitamura Y, Saeki M, Terada M, Kagitani S, Kitamura R, Fujikawa Y, Maelicke A, Tomimoto H, Taniguchi T, Shimohama S (2010) Galantamine-induced amyloid-β clearance mediated via stimulation of microglial nicotinic acetylcholine receptors. The Journal of biological chemistry 285:40180–40191.

Talantova M *et al*. (2013) Aβ induces astrocytic glutamate release, extrasynaptic NMDA receptor activation, and synaptic loss. Proceedings of the National Academy of Sciences 110:E2518–E2527.

Taly A, Corringer P-J, Guedin D, Lestage P, Changeux J-P (2009) Nicotinic receptors: allosteric transitions and therapeutic targets in the nervous system. Nature reviews Drug discovery 8:733–750.

Tampellini D, Gouras GK (2010) Synapses, synaptic activity and intraneuronal abeta in Alzheimer's disease. Frontiers in aging neuroscience 2:1–5.

Tampellini D, Rahman N, Gallo EF, Huang Z, Dumont M, Capetillo-Zarate E, Ma T, Zheng R, Lu B, Nanus DM, Lin MT, Gouras GK (2009) Synaptic activity reduces intraneuronal Aβ, promotes APP transport to synapses, and protects against Aβ-related synaptic alterations. Journal of Neuroscience 29:9704–9713.

Taylor DL, Diemel LT, Cuzner ML, Pocock JM (2002) Activation of group II metabotropic glutamate receptors underlies microglial reactivity and neurotoxicity following stimulation with chromogranin A, a peptide up-regulated in Alzheimer's disease. Journal of neurochemistry 82:1179–1191.

Taylor DL, Jones F, Kubota ESFCS, Pocock JM (2005) Stimulation of microglial metabotropic glutamate receptor mGlu2 triggers tumor necrosis factor alpha-induced neurotoxicity in concert with microglial-derived Fas ligand. The Journal of Neuroscience 25:2952–2964.

Teaktong T, Graham A, Court J, Perry R, Jaros E, Johnson M, Hall ROS, Perry E (2003) Alzheimer's Disease Is Associated With a Selective Increase in α7 Nicotinic Acetylcholine Receptor Immunoreactivity in Astrocytes. Glia 211:207–211.

Terry RD, Masliah E, Salmon DP, Butters N, DeTeresa R, Hill R, Hansen LA, Katzman R (1991) Physical basis of cognitive alterations in Alzheimer's disease: synapse loss is the major correlate of cognitive impairment. Annals of neurology 30:572–580.

Thomsen MS, Mikkelsen JD (2012) The α7 nicotinic acetylcholine receptor ligands methyllycaconitine, NS6740 and GTS-21 reduce lipopolysaccharide-induced TNF-α release from microglia. Journal of Neuroimmunology 251:65–72.

Timmermann DB, Grønlien JH, Kohlhaas KL, Nielsen EØ, Dam E, Jørgensen TD, Ahring PK, Peters D, Holst D, Chrsitensen JK, Malysz J, Briggs CA, Gopalakrishnan M, Olsen GM (2007) An Allosteric Modulator of the α7 Nicotinic Acetylcholine Receptor Possessing Cognition-Enhancing Properties in Vivo. Pharmacology 323:294–307.

Tong M, Arora K, White MM, Nichols R a (2011) Role of key aromatic residues in the ligand-binding domain of α7 nicotinic receptors in the agonist action of β-amyloid. The Journal of biological chemistry 286:34373–34381.

Torres-Platas SG, Comeau S, Rachalski A, Bo GD, Cruceanu C, Turecki G, Giros B, Mechawar N (2014) Morphometric characterization of microglial phenotypes in human cerebral cortex. Journal of neuroinflammation 11:12.

Toyohara J, Hashimoto K (2010) α7 Nicotinic Receptor Agonists: Potential Therapeutic Drugs for Treatment of Cognitive Impairments in Schizophrenia and Alzheimer's Disease. The open medicinal chemistry journal 4:37–56.

Tse SML, Furuya W, Gold E, Schreiber AD, Sandvig K, Inman RD, Grinstein S (2003) Differential role of actin, clathrin, and dynamin in Fcγ receptor-mediated endocytosis and phagocytosis. The Journal of biological chemistry 278:3331–3338.

Ulloa L (2005) The vagus nerve and the nicotinic anti-inflammatory pathway. Nature reviews Drug discovery 4:673–684.

Unger C, Svedberg MM, Yu W-F, Hedberg MM, Nordberg A (2006) Effect of subchronic treatment of memantine, galantamine, and nicotine in the brain of Tg2576 (APPswe) transgenic mice. The Journal of pharmacology and experimental therapeutics 317:30–36.

Unwin N (2005) Refined structure of the nicotinic acetylcholine receptor at 4A resolution. Journal of molecular biology 346:967–989.

Uteshev V (2014) The therapeutic promise of positive allosteric modulation of nicotinic receptors. European journal of pharmacology 727:181–185.

Utsugisawa K, Nagane Y, Obara D, Tohgi H (2002) Over-expression of α7 nicotinic acetylcholine receptor induces sustained ERK phosphorylation and N-cadherin expression in PC12 cells. Brain research Molecular brain research 106:88–93.

Vallejo YF, Buisson B, Bertrand D, Green WN (2005) Chronic nicotine exposure upregulates nicotinic receptors by a novel mechanism. The Journal of Neuroscience 25:5563–5572.

Vassar R (1999) β-Secretase Cleavage of Alzheimer's Amyloid Precursor Protein by the Transmembrane Aspartic Protease BACE. Science 286:735–741.

Vassar R (2004) BACE1: the beta-secretase enzyme in Alzheimer's disease. Journal of molecular neuroscience 23:105–114.

Vassar R (2013) ADAM10 prodomain mutations cause late-ons*et al*zheimer's disease: not just the latest FAD. Neuron 80:250–253.

Verges DK, Restivo JL, Goebel WD, Holtzman DM, Cirrito JR (2011) Opposing synaptic regulation of amyloid-β metabolism by NMDA receptors in vivo. Journal of Neuroscience 31:11328–11337.

Veyrac A, Besnard A, Caboche J, Davis S, Laroche S (2014) The transcription factor Zif268/Egr1, brain plasticity, and memory. Progress in molecular biology and translational science 122:89–129.

Vingtdeux V, Marambaud P (2012) Identification and biology of α-secretase. Journal of neurochemistry 120 Suppl :34–45.

Walker JR, Pacoma R, Watson J, Ou W, Alves J, Mason DE, Peters EC, Urbina HD, Welzel G, Althage A, Liu B, Tuntland T, Jacobson LH, Harris JL, Schumacher AM (2013) Enhanced proteolytic clearance of plasma Aβ by peripherally administered neprilysin does not result in reduced levels of brain Aβ in mice. Journal of Neuroscience 33:2457–2464.

Walker LC, Jucker M (2011) Amyloid by default. Nature neuroscience 14:669–670.

Wallace TL, Porter RHP (2011) Targeting the nicotinic α7 acetylcholine receptor to enhance cognition in disease. Biochemical pharmacology 82:891–903.

Walsh DM, Klyubin I, Fadeeva J V, Cullen WK, Anwyl R, Wolfe MS, Rowan MJ, Selkoe DJ (2002) Naturally secreted oligomers of amyloid-β protein potently inhibit hippocampal long-term potentiation in vivo. Nature 416:535–539.

Walsh DM, Selkoe DJ (2007) Aβ oligomers - a decade of discovery. Journal of neurochemistry 101:1172–1184.

Wan X-Z, Li B, Li Y-C, Yang X-L, Zhang W, Zhong L, Tang S-J (2012) Activation of NMDA receptors upregulates a disintegrin and metalloproteinase 10 via a Wnt/MAPK signaling pathway. Journal of Neuroscience 32:3910–3916.

Wang B, Wang Z, Sun L, Yang L, Li H, Cole a. L, Rodriguez-Rivera J, Lu H-C, Zheng H (2014) The Amyloid Precursor Protein Controls Adult Hippocampal Neurogenesis through GABAergic Interneurons. Journal of Neuroscience 34:13314–13325.

Wang DD, Kriegstein AR (2008) GABA regulates excitatory synapse formation in the neocortex via NMDA receptor activation. Journal of Neuroscience 28:5547–5558.

Wang F, Chen H, Steketee JD, Sharp BM (2007) Upregulation of ionotropic glutamate receptor subunits within specific mesocorticolimbic regions during chronic nicotine self-administration. Neuropsychopharmacology 32:103–109.

Wang H, Lee DHS, Andrea MRD, Peterson PA, Shank RP, Reitz AB (2000a) β-Amyloid 1–42 Binds to α7 Nicotinic Acetylcholine Receptor with High Affinity. Biochemistry 275:5626 –5632.

Wang H, Song L, Lee A, Laird F, Wong PC, Lee H-K (2010a) Mossy fiber long-term potentiation deficits in BACE1 knock-outs can be rescued by activation of α7 nicotinic acetylcholine receptors. Journal of Neuroscience 30:13808–13813.

Wang H, Yu M, Ochani M, Amella CA (2003) Nicotinic acetylcholine receptor a 7 subunit is an essential regulator of inflammation. Nature 421:384–388.

Wang H-W, Pasternak JF, Kuo H, Ristic H, Lambert MP, Chromy B, Viola KL, Klein WL, Stine WB, Krafft G a, Trommer BL (2002) Soluble oligomers of β-amyloid

(1-42) inhibit long-term potentiation but not long-term depression in rat dentate gyrus. Brain research 924:133–140.

Wang H-Y, Bakshi K, Shen C, Frankfurt M, Trocmé-Thibierge C, Morain P (2010b) S 24795 limits beta-amyloid-alpha7 nicotinic receptor interaction and reduces Alzheimer's disease-like pathologies. Biological psychiatry 67:522–530.

Wang H-Y, Stucky A, Liu J, Shen C, Trocme-Thibierge C, Morain P (2009) Dissociating β-amyloid from α7 nicotinic acetylcholine receptor by a novel therapeutic agent, S 24795, normalizes α7 nicotinic acetylcholine and NMDA receptor function in Alzheimer's disease brain. Journal of Neuroscience 29:10961–10973.

Wang HY, Lee DH, Davis CB, Shank RP (2000b) Amyloid peptide Aβ1-42 binds selectively and with picomolar affinity to α7 nicotinic acetylcholine receptors. Journal of neurochemistry 75:1155–1161.

Wang JQ, Daunais JB, McGinty JF (1994) Role of kainate/AMPA receptors in induction of striatal zif/268 and preprodynorphin mRNA by a single injection of amphetamine. Molecular Brain Research 27:118–126.

Wang R, Dineley KT, Sweatt JD, Zheng H (2004) Presenilin 1 familial Alzheimer's disease mutation leads to defective associative learning and impaired adult neurogenesis. Neuroscience 126:305–312.

Wang X, Lippi G, Carlson DM, Berg DK (2013) Activation of α7-containing nicotinic receptors on astrocytes triggers AMPA receptor recruitment to glutamatergic synapses. Journal of neurochemistry 127:632–643.

Wei W, Nguyen LN, Kessels HW, Hagiwara H, Sisodia S, Malinow R (2010) Amyloid-β from axons and dendrites reduces local spine number and plasticity. Nature neuroscience 13:190–196.

Wessler I, Kirkpatrick CJ (2008) Acetylcholine beyond neurons: the non-neuronal cholinergic system in humans. British journal of pharmacology 154:1558–1571.

West AE, Greenberg ME (2011) Neuronal activity-regulated gene transcription in synapse development and cognitive function. Cold Spring Harbor perspectives in biology 3.

Whitehouse P, Price D, Struble R (1982) Alzheimer's disease and senile dementia: loss of neurons in the basal forebrain. Science 215:1237–1239.

Williams DK, Peng C, Kimbrell MR, Papke RL (2012) Intrinsically low open probability of α7 nicotinic acetylcholine receptors can be overcome by positive allosteric modulation and serum factors leading to the generation of excitotoxic currents at physiological temperatures. Molecular pharmacology 82:746–759.

Williams DK, Stokes C, Horenstein NA, Papke RL (2011a) The effective opening of nicotinic acetylcholine receptors with single agonist binding sites. The Journal of general physiology 137:369–384.

Williams DK, Wang J, Papke RL (2011b) Positive allosteric modulators as an approach to nicotinic acetylcholine receptor-targeted therapeutics: advantages and limitations. Biochemical pharmacology 82:915–930.

Wolfe MS (2012) γ-Secretase inhibitors and modulators for Alzheimer's disease. Journal of neurochemistry 120 Suppl :89–98.

Wonnacott S (1997) Presynaptic nicotinic ACh receptors. Trends in neurosciences 20:92–98.

Wonnacott S, Barik J, Dickinson J, Jones IW (2006) Nicotinic Receptors Modulate Transmitter Cross Talk in the CNS Nicotinic Modulation of Transmitters Nicotinic Modulation of Striatal. Journal of Molecular Neuroscience 30:137–140.

Worley PF, Christy BA, Nakabeppu Y, Bhat R V., Cole AJ, Baraban JM (1991) Constitutive expression of zif268 in neocortex is regulated by synaptic activity. Proceedings of the National Academy of Sciences 88:5106–5110.

Wu B, Yamaguchi H, Lai FA, Shen J (2013) Presenilins regulate calcium homeostasis and presynaptic function via ryanodine receptors in hippocampal neurons. Proceedings of the National Academy of Sciences of the United States of America 110:15091–15096.

Wu G, Malinow R, Cline HT (1996) Maturation of a central glutamatergic synapse. Science 274:972–976.

Wu J, Lukas R (2011) Naturally-expressed nicotinic acetylcholine receptor subtypes. Biochemical pharmacology 82:800–807.

Xia P, Chen HV, Zhang D, Lipton SA (2010) Memantine preferentially blocks extrasynaptic over synaptic NMDA receptor currents in hippocampal autapses. The Journal of Neuroscience 30:11246–11250.

Xia W, Zhang J, Ostaszewski BL, Kimberly WT, Seubert P, Koo EH, Shen J, Selkoe DJ (1998) Presenilin 1 Regulates the Processing of β-Amyloid Precursor Protein C-Terminal Fragments and the Generation of Amyloid β-Protein in Endoplasmic Reticulum and Golgi. Biochemistry 37:16465–16471.

Xie T, Yan C, Zhou R, Zhao Y, Sun L, Yang G, Lu P, Ma D, Shi Y (2014) Crystal structure of the γ-secretase component nicastrin. Proceedings of the National Academy of Sciences of the United States of America 111:13349–13354.

Xiu J, Nordberg A, Shan K-R, Yu W-F, Olsson JM, Nordman T, Mousavi M, Guan Z-Z (2005) Lovastatin stimulates up-regulation of α7 nicotinic receptors in cultured neurons without cholesterol dependency, a mechanism involving production of the α-form of secreted amyloid precursor protein. Journal of neuroscience research 82:531–541.

Xu J, Chen Q, Zen K, Zhang C, Zhang Q (2013) Synaptosomes secrete and uptake functionally active microRNAs via exocytosis and endocytosis pathways. Journal of neurochemistry 124:15–25.

Xue J *et al*. (2014) Transcriptome-based network analysis reveals a spectrum model of human macrophage activation. Immunity 40:274–288.

Yamada K, Holth JK, Liao F, Stewart FR, Mahan TE, Jiang H, Cirrito JR, Patel TK, Hochgräfe K, Mandelkow E-M, Holtzman DM (2014) Neuronal activity regulates extracellular tau in vivo. The Journal of experimental medicine 211:387–393.

Yamanaka M, Ishikawa T, Griep A, Axt D, Kummer MP, Heneka MT (2012) PPARγ/RXRα-induced and CD36-mediated microglial amyloid-β phagocytosis results in cognitive improvement in amyloid precursor protein/presenilin 1 mice. The Journal of Neuroscience 32:17321–17331.

Yanagita M, Kobayashi R, Kojima Y, Mori K, Murakami S (2012) Nicotine modulates the immunological function of dendritic cells through peroxisome proliferator-activated receptor-γ upregulation. Cellular immunology 274:26–33.

Yang Y, Paspalas CD, Jin LE, Picciotto MR, Arnsten AFT, Wang M (2013) Nicotinic α7 receptors enhance NMDA cognitive circuits in dorsolateral prefrontal cortex. Proceedings of the National Academy of Sciences of the United States of America 110:12078–12083.

Young JW, Crawford N, Kelly JS, Kerr LE, Marston HM, Spratt C, Finlayson K, Sharkey J (2007) Impaired attention is central to the cognitive deficits observed in α7 deficient mice. European Neurophyschopharmacology 17:145–155.

Yu W, Mechawar N, Krantic S, Quirion R (2011) α7 Nicotinic receptor activation reduces β-amyloid-induced apoptosis by inhibiting caspase-independent death through phosphatidylinositol 3-kinase signaling. Journal of neurochemistry 119:848–858.

Zamani MR, Allen YS, Owen GP, Gray JA (1997) Nicotine modulates the neurotoxic effect of beta-amyloid protein(25-35)) in hippocampal cultures. Neuroreport 8:513–517.

Zhan Y, Paolicelli RC, Sforazzini F, Weinhard L, Bolasco G, Pagani F, Vyssotski AL, Bifone A, Gozzi A, Ragozzino D, Gross CT (2014) Deficient neuron-microglia signaling results in impaired functional brain connectivity and social behavior. Nature neuroscience 17:400–406.

Zhang C, Wu B, Beglopoulos V, Wines-Samuelson M, Zhang D, Dragatsis I, Shen J, Su TC, Südhof TC (2009) Activation of nicotinic α7 acetylcholine receptor enhances long term potentation in wild type mice but not in APP(swe)/PS1ΔE9 mice. Nature 460:632–636.

Zhang H, Gao Y, Dai Z (2010) IGF-1 Reduces BACE-1 Expression in PC12 Cells via Activation of PI3-K/Akt and MAPK/ERK1/2 Signaling Pathways. Neurobiology of Disease 36:49–57.

Zhang H, Ma Q, Zhang Y, Xu H (2012) Proteolytic processing of Alzheimer's β-amyloid precursor protein. Journal of neurochemistry 120 Suppl :9–21.

Zhang J, Xue F, Liu Y, Yang H, Wang X (2013) The structural mechanism of the Cys-loop receptor desensitization. Molecular neurobiology 48:97–108.

Zhang Y, Thompson R, Zhang H, Xu H (2011) APP processing in Alzheimer's disease. Molecular brain 4:3.

Zheng H, Jiang M, Trumbauer ME, Sirinathsinghji DJ, Hopkins R, Smith DW, Heavens RP, Dawson GR, Boyce S, Conner MW, Stevens K a, Slunt HH, Sisoda SS, Chen HY, Van der Ploeg LH (1995) β-Amyloid precursor protein-deficient mice show reactive gliosis and decreased locomotor activity. Cell 81:525–531.

Zhou L, Chávez-Gutiérrez L, Bockstael K, Sannerud R, Annaert W, May PC, Karran E, De Strooper B (2011) Inhibition of β-secretase in vivo via antibody binding to unique loops (D and F) of BACE1. The Journal of biological chemistry 286:8677–8687.

Zolles G, Wagner E, Lampert A, Sutor B (2009) Functional expression of nicotinic acetylcholine receptors in rat neocortical layer 5 pyramidal cells. Cerebral cortex 19:1079–1091.